

# Assessing The Role of the Rodent Prefrontal Cortex In Anxiety During Reward Seeking

Probing mechanisms and neural underpinnings for behavioral adaptation to threat

**David S. Jacobs**

Bachelor of Arts, Skidmore College, 2014

A thesis presented for partial fulfillment for the degree of Doctor of Philosophy



Behavioral and Systems Neuroscience Graduate Program

Oregon Health & Science University

Portland, OR USA

October 2021

© David S. Jacobs

**School of Medicine**  
**Oregon Health & Science University**

This dissertation was presented  
by  
David S. Jacobs

It was defended on  
October 13, 2021  
and approved by  
Atheir Abbas, MD, PhD, Assistant Professor, Behavioral Neuroscience  
K. Matthew Lattal, PhD, Professor, Behavioral Neuroscience  
Susan Ingram, PhD, Professor, Neurological Surgery  
Alicia Izquierdo, PhD, Professor, Psychiatry, Neuroscience  
Dissertation Advisor: Bitá Moghaddam, PhD, Professor, Behavioral  
Neuroscience

# Acknowledgements

First, I would like to thank my mentor, Dr. Bita Moghaddam. Bita has been an amazing mentor, pushing me to think more critically and to move out of my comfort zone. I've learned so much in my time in the lab and now find myself doing experiments I didn't know I was capable of. Bita is an amazing scientist. She has an unrivaled dedication to what she does and to her lab. Whether it was answering my weekend emails or putting up with my stubbornness, her patience and guidance sets her apart. This year was nothing short of difficult for many reasons. Bita was an incredible and selfless leader who always looked out for me and gave me the support I needed to not only navigate a global pandemic but also my PhD.

I also would like to acknowledge the many members of the Moghaddam lab who supported me over the years by listening to my near-daily rants about science, helping me trouble shoot experiments, or helping me out when I bit off more than I could chew. Both Alina Bogachuk and Michelle Kielhold deserve a special mention for helping me with troubleshooting and being worthy opponents in a game of Dominoes. I also need to thank Maddie Allen who put in a ton of work in helping with fiber photometry and collecting much of the data in Chapter 4.

I'd also like to thank my dissertation committee members. My conversations with Dr. Matt Lattal, both when I interviewed and later after joining the program and rotating in his lab, were formative for helping me develop the behavioral task. To Dr. Susie Ingram and Dr. Atheir Abbas, your thoughtful and productive feedback not only made me a better scientist but fostered an excellent environment for scientific discussion. I appreciate all of the thoughtful feedback and conversations that pushed me to think more critically about my work. To Dr. Alicia Izquierdo, hopefully I will get to meet you one day in person. It is an honor to have you join this dissertation committee after reading so much of your work over the years as I made sense of these data.

I also need to thank many other mentors before graduate school. To Dr. Flip Phillips, I can't thank you enough for taking me in as a random freshman into your lab. You were and continue to be a huge influence in the way I approach science and without you I would not be in neuroscience to begin with. To Dr. Stephen Kohut and Dr. Jack Bergman, you took a chance on a naive college grad and taught me so much about thinking critically about behavioral data and being careful and metered with scientific interpretation. Steve went above and beyond to mentor me not only on how to do science but also the zen of making graphs. There were also so many people in the preclinical pharmacology program, Dr. Carol Paronis, Dr. Brian Kangas, and Dr. Rajeev Desai, who gave me the support and feedback I needed to hit the ground running when I moved on to graduate school.

To my friends both from childhood, college, Portland, and all things in between, you know who you are. I feel incredibly lucky to have you all. Thanks for all the good times that kept me sane in grad school. Grabbing drinks, playing cards, biking, talking about the NBA, or just chatting over the phone, your friendship means so much.

To Jackie, I can't thank you enough for your support throughout grad school. Your patience and selflessness was so important in giving me a rock during graduate school and giving me a partner to take on the world with. Whether it was exploring new places or trying out every food cart possible, I cherish all my time with you and our cat daughter, Fili H. Bili.

Finally I need to thank my family. Mom and Dad (Lyn and Barry) you always put me first

and were there to support me in growing up and adulting. I know it's not easy to have your son move to the other side of the country. You're constant support in letting me pursue my own passions and helping me when I need it was everything. And Carla thank you for being the best sister. You gave me a role model that pushed me to be my best self.

# List of Abbreviations

ACC - Anterior Cingulate Cortex (dACC- dorsal anterior cingulate cortex)	NE - Norepinephrine
ADHD - Attention-Deficit/Hyperactivity Disorder	NIH - National Institute of Health
AMY - Amygdala	NPM - Neurophotometrics
AIC - Agranular insular cortex	NS - No Shock
ANOVA - Analysis of Variance	OFC - Orbitofrontal Cortex (MO - medial orbital, VO - ventral orbital, LO - Lateral orbital)
AUC - Area Under the Curve	OHSU - Oregon Health & Science University
BAS - Behavioral Activation System	PAG - Periaqueductal Grey
BLA - Basal Lateral Amygdala	PBS - Phosphate Buffered Saline
BNST - Bed nucleus of the Stria Terminalis	PND - Postnatal day
BIS - Behavioral Inhibition System	PPT - Probabilistic Punishment Task
BOLD - Blood Oxygen Level Dependent	PR - Progressive Ratio
CR - Conditioned Response	PRT - Punishment Risk Task
CS - Conditioned Stimulus	PVN - Paraventricular Nucleus of the Hypothalamus
D2 - Dopamine Receptor 2	RDoC - Research Domain Criteria
DA - Dopamine	RI - Random Interval
DR - Dorsal Raphe	R → O - Response - Outcome
DREADDs - Designer Receptors Exclusively Activated by Designer Drugs	S → R - Stimulus - Response
DS - Dorsal Striatum	SABV - Sex as a Biological Variable
FFFS - Fight, flight, freeze system	STNS - Seek-take no shock
FR - Fixed Ratio	TDT - Tucker-Davis Technologies
GFP - Green Fluorescent Protein	Thal - Thalamus
HC - Hippocampus	TO - Time-Out
HPA - Hypothalamic-Pituitary Axis	TTL - Transistor-transistor logic
HyTh - Hypothalamus	US - Unconditioned Stimulus
ITI - Intertrial interval	VTA - Ventral Tegmental Area
LC - Locus Coeruleus	VI - Variable Interval
LFP - Local Field Potential	4PLR - Four-parameter logistic regression
mPFC - Medial Prefrontal Cortex (PL - pre- limbic, IL - infralimbic)	5HT - Serotonin
NAc - Nucleus Accumbens	5HT <sub>2a</sub> - Serotonin 2a Receptor

# List of Figures

1.1	Publication trends for models of approach-avoidance . . . . .	3
1.2	Role of the behavioral inhibition system in approach-avoidance models . . . . .	5
1.3	PFC pathways implicated in approach and avoidance systems during reward seeking . . . . .	11
2.1	Outline and characterization of learning in the probabilistic punishment task . . .	32
2.2	Assessing the effects of probabilistic punishment on task behaviors after learning	34
2.3	Behavioral effects of manipulation of reinforcer and punisher value . . . . .	36
2.4	Effects of systemic diazepam treatment on PPT Behavior . . . . .	37
2.5	Assessment of sex differences in the probabilistic punishment task . . . . .	41
2.6	Titration of behavior using shock intensity and modeling for males and females .	42
3.1	Recording neuronal calcium activity with GCaMP6 in PL-mPFC during the probabilistic punishment task . . . . .	53
3.2	Behavior in a PPT optimized for fiber photometry . . . . .	55
3.3	Phasic increases in PL-mPFC neural calcium activity following action contingent footshock . . . . .	56
3.4	Changes in PL-mPFC neural calcium activity following seek action execution before and after PPT learning . . . . .	57
3.5	Neural calcium activity in the PL-mPFC for the take action and reward delivery	58
3.6	Individual differences in punishment resistance are associated with risky, unpunished action encoding changes . . . . .	59
3.7	Phasic decreases during FR1 action execution emerge with learning in the PL-mPFC . . . . .	60
3.8	Phasic decreases during seek action execution are recovered by extinction . . . .	61
4.1	Schematic of experimental design and behavior on the PRT . . . . .	70
4.2	Encoding of punishment by VTA and PL-mPFC . . . . .	71
4.3	Encoding of punishment anticipation by VTA and PL-mPFC during the first three sessions of PRT learning . . . . .	72
4.4	Effects of diazepam on PRT behavior and punishment encoding . . . . .	73
4.5	Effects of diazepam on action encoding in the PRT in the PL-mPFC and VTA .	74
4.6	Effects of diazepam on correlated activity between the PL-mPFC and VTA during action and food epochs . . . . .	75
5.1	Fiber placements and representative coexpression of GCaMP and tdTomato for OFC . . . . .	84
5.2	Encoding of footshock punishment by the LO-OFC . . . . .	85
5.3	LO-OFC response to non-contingent, unsignaled footshock . . . . .	86
5.4	Encoding of risky actions by LO-OFC during PPT learning . . . . .	87
5.5	Encoding of safe actions and reward delivery by LO-OFC during PPT learning .	88
5.6	Individual differences in learned suppression of behavior are not associated with LO-OFC encoding . . . . .	89

5.7	Correlated activity of the PL-mPFC and LO-OFC during risky action encoding is disrupted by probabilistic punishment . . . . .	90
5.8	Correlated activity of the PL-mPFC and LO-OFC during safe action encoding not influenced by probabilistic punishment . . . . .	90
5.9	Extinction of probabilistic punishment attenuates phasic increases in safe action encoding after punishment learning . . . . .	91
5.10	Extinction of probabilistic punishment recovers correlated activity during seek action execution . . . . .	92
5.11	Extinction of probabilistic punishment does not alter correlated activity during take action execution . . . . .	92
A.1	Demonstration of stable PPT performance over learning . . . . .	118
A.2	Pro-conflict effects of dopamine D2-ergic drugs . . . . .	119
A.3	Effects of psilocybin and $\pm$ -DOI treatment on PPT behavior . . . . .	120
A.4	Female trial completion after PPT learning . . . . .	120
A.5	Sex differences in PPT optimized for fiber photometry . . . . .	121
A.6	mPFC Activity of borderline IL-mPFC subject . . . . .	121
A.7	Sex differences in punishment encoding in the PPT . . . . .	122
A.8	Recording from GFP control rats in the PL-mPFC during PPT performance . .	122
A.9	Sex differences are not seen in PPT PL-mPFC seek action encoding . . . . .	123
A.10	Action encoding of FR1 over learning does not differ between sexes . . . . .	123
A.11	Location of fiber placements for FR1 learning studies . . . . .	124
A.12	PL-mPFC Activity in the take epoch before and during probabilistic punishment extinction . . . . .	124
A.13	Correlated activity between the PL-mPFC and VTA during footshock after diazepam treatment . . . . .	125
A.14	PPT behavior for the LO-OFC cohort alone . . . . .	126
A.15	LO-OFC activity changes over blocks in the absence of probabilistic punishment	127
A.16	LO-OFC activity in the seek epoch before and during punishment extinction . .	128
A.17	PL-mPFC time to reach peak does not change with learning . . . . .	128
A.18	Response to non-contingent footshock was less than action contingent footshock	129
B.1	Schematic of operant box For behavioral experiments . . . . .	130
B.2	Schematic of equipment for recording neural activity during operant behavior . .	131

# List of Tables

2.1	Pearson correlation values of open field behavior with probabilistic punishment task measures . . . . .	34
2.2	Effects of systemic treatment of dopaminergic, GABAergic, and serotonergic drugs on probabilistic punishment task behavior . . . . .	38
A.1	Subject Ages through fiber photometry experiments with PPT . . . . .	125
A.2	Subjects utilized in fiber photometry experiments with FR1 and PRT . . . . .	127

# Contents

<b>Acknowledgements</b>	<b>i</b>
<b>List of Abbreviations</b>	<b>iii</b>
<b>List of Figures</b>	<b>iii</b>
<b>List of Tables</b>	<b>v</b>
<b>1 Introduction</b>	<b>1</b>
Overview . . . . .	1
Stimulus and outcome associated responding . . . . .	2
Issues in models for approach-avoidance behavior . . . . .	2
Alternative approaches for motivated behavior in conflict situations . . . . .	5
Neural systems underlying anxiety and motivated behavior . . . . .	8
Prefrontal cortex involvement in reward motivated action . . . . .	12
Prefrontal cortex involvement in fear states and fear learning . . . . .	17
Prefrontal cortex involvement in anxiety . . . . .	20
Prefrontal cortex manipulation of goal-directed action under anxiety states . . . . .	21
Purpose of the dissertation . . . . .	23
<b>2 Behavioral Characterization of a Probabilistic Punishment Task to Assess Action Under Anxiety</b>	<b>25</b>
Abstract . . . . .	25
Introduction . . . . .	25
Methods . . . . .	26
Subjects . . . . .	26
Overview of Experimental Design . . . . .	27
Apparatus . . . . .	27
Training . . . . .	27
Probabilistic Punishment Task (PPT) Procedures . . . . .	28
Task Characterization . . . . .	28
Behavioral Pharmacology . . . . .	29
Data Analysis . . . . .	30
Results . . . . .	32
Learning of the probabilistic punishment task . . . . .	32
Behavioral and pharmacological manipulations of probabilistic punishment task behavior . . . . .	34
Sex as a biological variable in probabilistic punishment resistance . . . . .	38
Integration of probabilistic punishment in males and females after titrating shock intensity . . . . .	40
Discussion . . . . .	43
Punishment probability learning during reward-guided actions . . . . .	43

Diverse mechanisms underlying punishment resistance . . . . .	44
Sex as a biological variable in probabilistic punishment resistance . . . . .	44
Conclusion . . . . .	44
<b>3 PL-mPFC Encoding During Probabilistic Punishment Task Learning</b>	<b>46</b>
Abstract . . . . .	46
Introduction . . . . .	46
Methods . . . . .	47
Subjects . . . . .	47
Surgery for Fiber Photometry . . . . .	47
Apparatus . . . . .	48
Fixed Ratio One (FR1) Training and Recording . . . . .	48
Punishment Punishment Task (PPT) for Fiber Photometry . . . . .	48
Extinction of Probabilistic Punishment . . . . .	49
Shock Probe Test . . . . .	49
Fiber Photometry Systems and Recording Procedures . . . . .	49
Data and Statistical Analysis . . . . .	50
Histology and Imaging . . . . .	52
Results . . . . .	52
Histology and photometry overview . . . . .	52
Behavioral suppression in the PPT . . . . .	53
Footshock punishment is uniformly encoded by the PL-mPFC . . . . .	54
Prefrontal cortex encoding of risky action changes with task learning . . . . .	54
Prefrontal cortex encoding of safe action does not change with learning . . . . .	56
Risky action encoding changes are associated with punishment sensitivity . . . . .	56
Emergence of phasic decreases during action encoding in the PL-mPFC during instrumental action learning . . . . .	60
Phasic decreases are recovered by extinction of probabilistic punishment after PPT learning . . . . .	61
Discussion . . . . .	62
A PPT for fiber photometry recording . . . . .	62
The PL-mPFC adapts its response to learning action-outcome contingencies . . . . .	62
PL-mPFC response to footshock is learning independent . . . . .	63
Conclusions . . . . .	64
<b>4 PL-mPFC and VTA Encoding During Probabilistic Punishment: Diazepam   Treatment and Comparison to Electrophysiology</b>	<b>65</b>
Abstract . . . . .	65
Introduction . . . . .	65
Methods . . . . .	67
Subjects . . . . .	67
Surgery . . . . .	67
Initial Training & Punishment Risk Task (PRT) . . . . .	67
Diazepam Treatment . . . . .	68
Fiber Photometry Analysis . . . . .	68
Statistical Analysis . . . . .	69
Histology and Imaging . . . . .	69
Results . . . . .	69
Modeling learned anxiety using the probabilistic risk task (PRT) . . . . .	69
Punishment is encoded by the VTA and mPFC over Learning . . . . .	70
The PL-mPFC and VTA dynamically encode actions in PRT learning . . . . .	71

Diazepam does not alter punishment encoding by the VTA or PL-mPFC . . . . .	71
Diazepam changes VTA but not PL-mPFC encoding during action execution . .	73
Diazepam enhances correlated activity of the PL-mPFC and VTA . . . . .	74
Discussion . . . . .	76
Relation to electrophysiological findings . . . . .	76
Uniform punishment encoding in mPFC and VTA . . . . .	76
Diazepam does not alter PL-mPFC action or punishment encoding . . . . .	77
Diazepam enhances VTA action encoding and VTA-mPFC coactivity . . . . .	77
Conclusion . . . . .	78
<b>5 LO-OFC Encoding During Probabilistic Punishment Task Learning</b>	<b>79</b>
Abstract . . . . .	79
Introduction . . . . .	79
Methods . . . . .	80
Subjects . . . . .	80
Surgery . . . . .	81
Apparatus . . . . .	81
Probabilistic Punishment Task (PPT) . . . . .	82
Extinction of Probabilistic Punishment . . . . .	82
Shock Probe Test . . . . .	82
Fiber Photometry System and Recording Procedures . . . . .	82
Fiber Photometry Analysis . . . . .	83
Statistical Analysis . . . . .	83
Results . . . . .	84
Histology and Behavioral Analysis . . . . .	84
LO-OFC Response to Punishment Changes with Learning . . . . .	85
LO-OFC encoding of risky actions does not change after probabilistic punishment learning . . . . .	85
LO-OFC encoding of safe actions changes after probabilistic punishment learning	86
LO-OFC related changes are not correlated with sensitivity to punishment . . .	89
LO-OFC and PL-mPFC correlated activity during risky actions, but not safe actions, decreases with punishment risk . . . . .	89
Probabilistic punishment extinction normalizes LO-OFC activity . . . . .	91
Discussion . . . . .	93
A role for the LO-OFC in Approach-Avoidance Conflict . . . . .	93
Correlated activity between PL-mPFC and LO-OFC is disrupted by approach-avoidance conflict . . . . .	94
Conclusions . . . . .	95
<b>6 General Discussion</b>	<b>96</b>
Main Findings . . . . .	96
Limitations . . . . .	99
Future Directions . . . . .	99
<b>Bibliography</b>	<b>101</b>
<b>Appendix A</b>	<b>118</b>
Supplemental Figures . . . . .	118
<b>Appendix B</b>	<b>130</b>
Instrument Setup . . . . .	130
Software . . . . .	132

# Chapter 1

## Introduction

Parts of this chapter are adapted from: **Jacobs, D. S., & Moghaddam, B. (2021). Chapter two - medial prefrontal cortex encoding of stress and anxiety.** In A. T. Brockett, L. M. Amarante, M. Laubach, & M. R. Roesch (Eds.), *What does medial frontal cortex signal during behavior? insights from behavioral neurophysiology* (pp. 29–55). Academic Press. <https://doi.org/doi.org/10.1016/bs.irn.2020.11.014>

### Overview

In a basic sense, action is driven by the need to acquire resources, or rewards, and the desire to avoid harm, or punishments. These drives are supported by interconnected behavioral processes which allow one to decide the best course of action based on individual goals and expectations. Thus action is the result of conflict between reward and punishment mechanisms, also termed approach-avoidance conflict. Neural differences in systems that control approach-avoidance conflict are believed to produce individual differences in expression of behaviors and, ultimately, psychopathologies. The balance between reward and punishment sensitivity is implicated in several mental health disorders such as generalized anxiety disorder, obsessive compulsive disorder, addiction, depression, and attention deficit/hyper-activity disorder (ADHD; Bechara et al., 2002; Hartley & Phelps, 2012; Milad & Rauch, 2007; Torregrossa et al., 2008). Thus disruptions in resolving conflicts between reward and punishment processes may be a common feature of many mental health disorders, making understanding the neural underpinnings a critical area for investigation.

In neuroscience research, reward and punishment mechanisms are typically assessed, or are assumed to be assessed, in isolation. While the researcher assumes the paradigm tightly controls the animals behavior, this is not always the case. For example, even in tasks of impulsive reward seeking, like the 5-choice serial reaction time task, the occurrence of punishment is concurrently present in the form of reward omission. Thus the measure of impulsive reward seeking is really up to the animal's own sensitivity to either reward or punishment or both. Furthermore, while investigating reward and punishment mechanisms in isolation aids interpretation of complex behavior, it is less relatable to how the brain adapts to real-world scenarios where any action towards some reward carries some, however small, risk of punishment.

The primary focus of this dissertation was to develop methods to model learning to adjust action as a function of risk using rats to assess neural representations of actions in a state of learned approach-avoidance conflict. Once the appropriate behavioral model was developed, I focused on involvement of the prefrontal cortex (PFC) in encoding key events in behaving male and female rats in part because: 1) conflict is believed to engage higher level control processes which are a key function of the PFC, and 2) PFC dysfunction is a common observation across

psychopathologies mentioned above (Balderston, Vytal, et al., 2017; Goldstein & Volkow, 2011; Han et al., 2016; Milad & Rauch, 2007).

This dissertation is organized as follows: 1) an introduction (below) reviewing relevant behavioral and neuronal literature related to action-guided reward and punishment processing 2) design and characterization of a probabilistic punishment task (PPT) that provided the basis of my work (Chapter 2), 3) characterization of how the prelimbic medial prefrontal cortex (PL-mPFC) encodes action and punishment using fiber photometry before and after learning the PPT (Chapter 3), 4) characterization of the role of the PL-mPFC in encoding a single action conflict task to allow for comparison of PL-mPFC signal across tasks and to electrophysiological data (Chapter 4), and 5) characterization of how the lateral orbitofrontal cortex (LO-OFC) encodes action and punishment using fiber photometry in the PPT to further investigate PFC involvement in learned approach-avoidance conflict (Chapter 5). I then provide a general discussion of the key findings for these studies and how they inform our understanding of the roles for the PFC in approach-avoidance behavior.

## Stimulus and outcome associated responding

Animal behavioral responses are typically divided into two types: Pavlovian responses, where a particular stimulus (S) elicits a particular behavioral response (R; i.e.  $S \rightarrow R$ ), and instrumental responses in which a particular response or action becomes associated with an outcome (O; i.e.  $R \rightarrow O$ ). Both processes are fundamental to learning and decision making. Pavlovian responding is constrained in that responses are driven by conditioned stimuli that are not typically within the animal's control. This form of conditioning, however, is useful for assessing learning because the experimenter controls the nature of the stimulus. In instrumental responding the response itself is under the control of the animal, making the interpretation of the learning process more difficult.

Pavlovian and instrumental processes are also not independent of one another, as action execution also utilizes  $S \rightarrow R$  relationships. The stimulus complex as a whole provides the animal with relevant information to inform its internal affective or motivational state and orients the animal to possible outcomes. In other words, learned conditioned stimuli which inform behavioral action provide a mechanism by which instrumental action can be enhanced.

In this dissertation, action will largely refer to an instrumental action, which is a behavioral response performed by an organism that is learned to produce a particular outcome. This is not to discount that contextual or other associated stimuli may have important impacts on instrumental behavior. The nature of conditioned stimuli on responding will be considered but the main goal of this dissertation will be to understand specifically how actions themselves and their corresponding outcomes are represented in the brain in the absence or presence of approach-avoidance conflict.

## Issues in models for approach-avoidance behavior

Behavioral models for approach-avoidance behavior involve an interplay of reinforcement and punishment. In these models reinforcement is typically defined as stimuli or outcomes which elicit approach. This need not be valence specific. Reward itself (e.g. food) or the omission of a punishment (e.g. responding to prevent footshock) can elicit approach behavior. This further extends to punishment, which elicits avoidance and can be produced by an undesirable stimulus (footshock) or a lack/removal of a reward (non-reward). These four possibilities

make up reinforced behavior and can also be described using positive/negative and reinforcement/punishment nomenclature.

Animal models of approach-avoidance conflict classically involve innate measures of exploration in novel contexts (e.g. elevated plus maze, open field, and light-dark boxes; Lezak et al., 2017). While these models contain some face validity, they are quite limited. Such approaches contain ambiguity in terms of reward and punishment, and in reality contain neither. It is only inferred that the animal wants to explore as a form of “reward”. It is also possible that the ambiguous context itself is perceived as an immediate threat which would engage fear systems rather than conflict systems. Lastly, innate anxiety tests are usually given once and thus do not assess how contingencies of reward and punishment are learned over time. This is critical because the learning of such contingencies involves changes in neural activity that may ultimately drive behavior and symptoms of mental health disorders. These issues will become more apparent when we highlight models for behavioral systems which resolve conflict in goal-motivate behavior. Nevertheless, these procedures have seen great attention compared to instrumental action procedures for approach-avoidance conflict such as the Vogel or Geiller-Seifter tasks Figure 1.1.

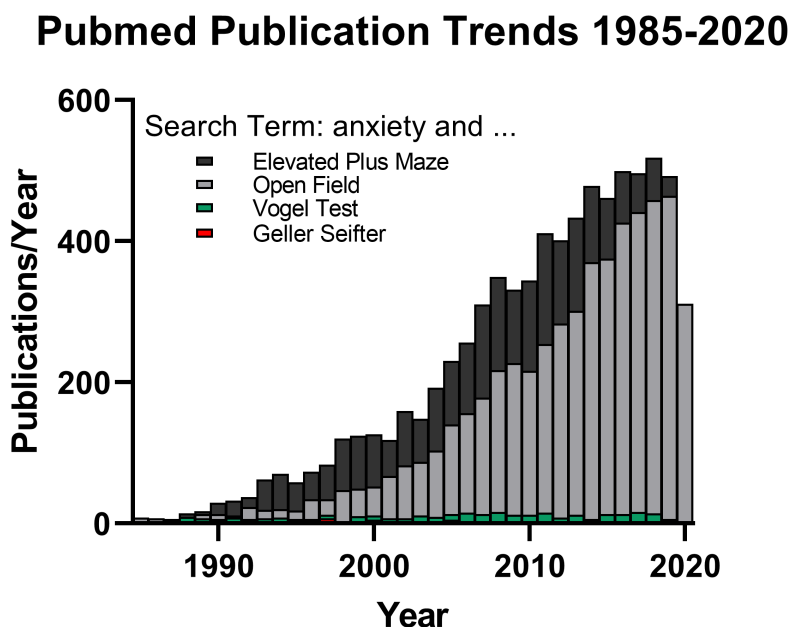


Figure 1.1: Publication trends for models of approach-avoidance from 1985-mid 2020. Both innate anxiety measures (open field and elevated plus maze) have seen considerable use, while conflict procedures involving instrumental behavior have been considerably less utilized (Vogel Test and Geller-Seifter Task). Data were sourced from Pubmed with search terms outlined in the legend.

### Psychological frameworks for approach-avoidance conflict

A predominant, and continually evolving, framework for understanding approach-avoidance conflict is Jeffery Gray’s reinforcement sensitivity theory, which has also been utilized to understand multiple facets of psychopathology including impulsivity and excessive anxiety (Gray & McNaughton, 2000; Gray, 1987). Reinforcement sensitivity theory describes three systems which work in parallel: the behavioral activation system for approach to rewards, the fight-flight-freeze system for defensive avoidance, and the behavioral inhibition system which serves

a complex role to interface the behavioral activation and fight-flight-freeze systems, and facilitate conflict resolution through defensive approach (McNaughton & Corr, 2004).

Together actions under approach-avoidance conflict can be perceived as a collective interaction of these systems to produce a decision on how an animal should proceed. The interaction of mechanisms for this process is nicely provided by the Gray and Smith, 1969 model for selecting action during approach-avoidance conflict (Figure 1.2A). In this model reward and punishment mechanisms both inhibit one another and enhance arousal when decision processes are required. These mechanisms ultimately feed into a “decision mechanism” to determine the appropriate command for the motor system. Motor actions then lead to some consequence. This action consequence aspect of the model is particularly important and reflects the lines extending from action consequences to comparators for reward and punishment. These processes emphasize that behavior is shaped according to experienced consequences of decisions to execute or withhold action. These comparators thus allow the animal to learn and adapt its approach-avoidance behavior in a dynamic world by comparing expectations to outcomes for both mechanisms and utilizing information from previous experience.

This theory was further revised by Gray and McNaughton, 2000 and by the McNaughton and Corr, 2004 two dimensional system of defense (Figure 1.2B). In this theory, defense can be broken into defensive avoidance, such as fleeing or freezing, and defensive approach, such as risk assessment and hesitancy. This is an important distinction because it not only creates a basis for behavior/neural differences from fear and anxiety but also would differentially involve the fight-flight-freeze system and behavioral inhibition system, respectively.

This clarification of the behavioral inhibition system has created a significant extension of the model outlined in Figure 1.2A. The behavioral inhibition system serves as a “conflict detector” based on incoming information about reward and punishment as the animal interacts with and learns about the world (Figure 1.2C). This emphasizes a higher order role for the behavioral inhibition system in approach-avoidance by negatively biasing information related to the behavioral activation system and fight-flight-freeze system, producing enhancements in arousal and attention through risk assessment, and utilization of previous memories of contingencies of a given context (Corr, 2010, 2013).

The behavioral activation system, fight-flight-freeze system, and behavioral inhibition system are generally considered systems of reward, fear, and anxiety, respectively, with an important distinction between fear and anxiety being the perceived imminence of the threat as well as the the direction of the defensive behavior (McNaughton & Corr, 2004). Again, this differentiation is an important one, even though such terms are incorrectly interchanged in neuroscience research. Clinically, and as described in NIH’s Research Domain Criteria (RDoC), anxiety is defined as an affective state characterized by sustained dread and risk assessment when there is a perceived probability of a distant harmful outcome (Grillon, 2008).

In a natural setting anxiety is commonly learned through experience. An animal foraging for food encounters a predator and consequently retreats to a safe location. The initial reaction to the predator is fear, but the animal must eventually attempt to forage again to acquire basic needs. When the animal forages again, after learning from this experience, it will likely be in a sustained state of uneasiness, heightened risk assessment, and high vigilance even if no predator is present, a state more reflective of anxiety. Thus an ideal model for approach-avoidance across these systems would allow for assessment of learning about reward and punishment under changing probabilistic contingencies that produce conflict. Furthermore, the punishment contingencies should be under the control of the subjects (i.e. they are avoidable), but should be probabilistic in nature (Corr, 2013).

Laboratory animal models of innate anxiety are not well suited for this more ethologically relevant mode of anxiety. For this reason, and because treatment of anxiety remains suboptimal

with benzodiazepines, novel models for anxiety related to the behavioral inhibition system have been called for (Daviu et al., 2019; Park & Moghaddam, 2017a).

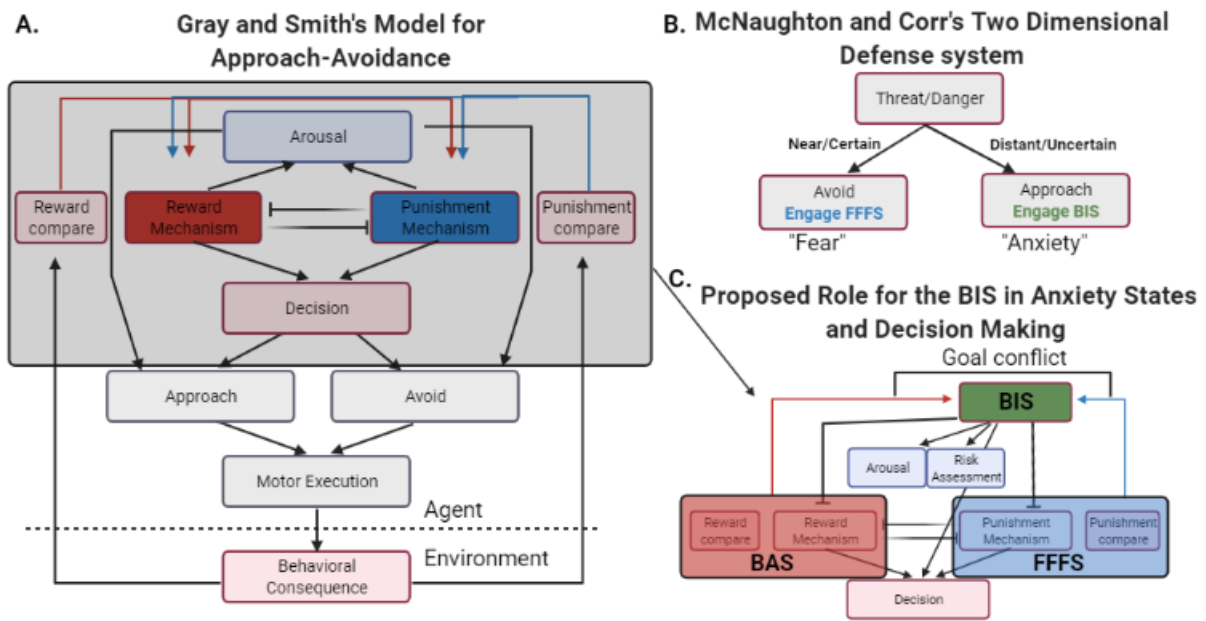


Figure 1.2: Role of the behavioral inhibition system in approach-avoidance models proposed by Jeffrey Gray. **A.** A simplified earlier model for approach-avoidance behavior proposed by Gray and Smith (1969). Reward and punishment mechanisms serve opposite roles in decisions to approach or avoid. Both mechanisms receive input from the environment to update approach/avoid decisions. **B.** McNaughton and Corr's two dimensional defense system proposed to disambiguate defense mechanisms based on the proximity of danger and the behavior they evoke. **C.** An extension of the behavioral inhibition system in the control of approach-avoidance processes. When activated by goal conflict the behavioral inhibition system promotes risk assessment and interacts with the behavioral activation and fight-flight-freeze systems to bias behavior. BAS = behavioral activation system, BIS = behavioral inhibition system, FFFS = fight-flight-freeze system. Schematic created with Biorender.com

## Alternative approaches for motivated behavior in conflict situations

The approach to assess learned anxiety from conflict between true rewards and punishments as outlined in this dissertation provides a significant deviation from typical innate procedures used to assess anxiety in rodents. There have been several protocols developed for assessing how punishment influences reward seeking, which I will briefly describe below.

**Vogel and Geller Seifter Conflict Tasks** These are some of the earliest works establishing paradigms for assessing anxiety from action conflict between reward and punishment, (also see pioneering work from Neil Miller and Nate Azrin; Azrin et al., 1963; Miller, 1944). In the Vogel conflict test (Vogel et al., 1971) subjects are trained to seek rewards through a simple appetitive response such as licking a sipper. Later a punishment contingency is introduced in a probe sessions at a fixed ratio (FR, i.e. a fixed number of licks produces punishment) and the amount of licking in the face of punishment is assessed.

The Geller-Seifter task uses a similar approach (Geller & Seifter, 1960) except that a stimulus cue is used to signal a favorable reinforcement schedule compared to what the animal was originally trained on (e.g. variable interval (VI) versus FR1). Responding during the cue then becomes conflicted when an additional contingency is added where each response will also produce a footshock (i.e. punishment is avoidable but predictable). Both these procedures are sensitive to treatment with benzodiazepines at doses that produce anxiolytic effects in startle paradigms (Brodkin et al., 2002; Dalterio et al., 1988; Liljequist & Engel, 1984; Shimizu et al., 1992), supporting their validity in assessing anxiety.

**Simultaneous Reward and Punishment Learning Task** A recent task developed by Jean-Richard-dit-Bressel et al., 2019 proposes to assess the learning of punishment and reward contingencies simultaneously. Briefly subjects are placed in an operant box with two operanda. Initially an action on either operandum which completes the VI schedule results in food reinforcement. After learning, a punishment contingency is added to one of the responses whereby action completion on a separate VI schedule produces a conditioned stimulus (tone or light; i.e. the CS<sup>+</sup>) that co-terminates with footshock. An action on the other operandum continues to produce reward and a neutral stimulus (i.e. the CS<sup>-</sup>). Animals are then allowed to learn these contingencies and the overall response rate for each operandum is determined.

Such a design is clever in that it uses the same metric for both reward and punishment-associated actions and learning curves can be determined by comparing the changes in response rate after punishment introduction. It also allows for determination of fear-related behavior by quantification of behavioral suppression during the CS<sup>+</sup> itself. However, there is uncertainty about how punishment contingencies are perceived. Utilization of a VI schedule means each action is uncertain in its own right. Thus there are multiple “punishments” at play, the punishment of the CS<sup>+</sup> and the punishment of no reward after action.

**Seek-Take Compulsive Reward Seeking Task** This task developed by Pelloux et al., 2007 assesses actions with and without punishment but instead utilizes a two-response “chained” schedule of reinforcement, where a response completes one link of the chain and a second response after the first response completes the second link of the chain and results in reinforcement. There are multiple ways to chain reinforcement schedules. This procedure utilizes a random interval schedule (RI, i.e. actions performed after a random amount of time are reinforced) for response one and a FR1 for response two. The first action is uncertain and leads to reward taking and is called a “seeking” response. The second action is more directed and allows for reward consumption and is therefore called the “taking” response. After learning the task, a response on one of the links in the chain is punished with a fixed probability by mild footshock and does not result in reward (typically the seek link). After probabilistic punishment contingencies are introduced, behavioral suppression and hesitation can be seen across both food and drug reinforcers and across punishment contingencies on either response in the chain (Pelloux et al., 2015).

The use of the chained schedule nicely allows for the assessment of actions with and without punishment. However, the RI schedule can complicate interpretation when it is the punished link in the chain because each action in this context itself carries a level of uncertainty with it. Thus because reward and non-reward outcomes are possible, both the probability of reward and punishment are variable. This design was intentional because the study was specifically focused on assessing compulsive responding under punishment. However, such a design may not be optimal if the goal of the study is to assess how punishment uncertainty itself impacts reward seeking.

**Loss (or Probability) Discounting Tasks** This task originally developed by Cardinal and Howes, 2005, and further expanded on by Floresco and Whelan, 2009, is based on delay discounting procedures from the lab of Dr. Trevor Robbins. In loss discounting tasks, animals must decide between two action choices, one of which produces a small amount of reward with 100% probability, and another that produces a large amount of reward but probabilistically results in non-reward. While not an explicit punishment, reward omission itself is technically a form of punishment in an operant sense, in that it reduces the likelihood of the associated action occurring again in the future. Loss discounting tasks are broken into blocks, with each block carrying an ascending probability of non-reward for choosing the risky option. Thus, as blocks increase it becomes less favorable to take risks. These progressive increases in risk typically cause subjects to shift behavior from the risky action to the safe action. The percentage of times the risky action is chosen for each block is the main metric of behavior.

Due to its relation to delay discounting, results from this type of task are typically interpreted in the context of impulsive choice, though one can conceptualize from the models proposed earlier that choices in this task could be from either sensitivity to the value (i.e. magnitude) of the reward or from sensitivity to non-reward. Some additional considerations should be addressed. Alternative reinforcing outcomes are possible which is not always the case in the real world nor in appetitive disorders where alternative reinforcers may not be perceived as viable (Volkow et al., 2003). The trial design of this task also requires subjects to respond in under 10 seconds or the trial is scored as an omission. Such a design doesn't permit longer-term deliberation and anticipation, which is a critical factor in anxiety.

**Risky Decision Making Task** The risky decision making task designed by Simon et al., 2009 has a similar design to loss discounting, and behavior between the two tasks is positively correlated (Simon et al., 2009). Using the same choice procedures, this task allows for safe actions for small amounts of reward that carry no risk of footshock or risky actions that produce more reward but also probabilistically result in explicit punishment in the form of mild footshock. The probability of footshock for the risky action begins at 0% and progressively increases to 100% throughout the session. Animals typically show preference for the risky lever when risk of shock is 0% and then progressively shift their actions to the safe option as punishment risk increases. Thus increased selection of the risky option even in the face of high shock risk is an indicator of punishment resistance that may relate to compulsive or impulsive reward seeking. Alternatively, some rats also become hypersensitive to the risk of shock and avoid the risky action even when probability is low, which may have roots in enhanced risk assessment and behavioral suppression seen with anxiety (Gabriel et al., 2019).

This task uses a similar timed trial structure to loss discounting; actions are performed quickly or they are scored as omissions, which also increase with punishment risk. Thus while data is commonly reported as percentage of risky choices it is also complicated by the percentage of lack of choices even though alternative safe options are present. Lastly, the use of large versus small reward choice can raise issues with satiety. A total of 46 pellets may be earned in each block, which across 5 blocks results in 230 pellets. It is worth noting, however, that this task has not been consistently affected by switching the order of risk (ascending versus descending, though ascending is more commonly utilized) which argues that rodents do not simply maximize pellet intake quickly but rather adjust according to the punishment risk.

**Punishment Risk Task** As noted, choice based tasks which utilize punishment risk have great power in modeling behavior under probabilistic punishment. However alternative reinforcement in the form of less valued reinforcement is not always possible, i.e. sometimes the "choice" is to seek the reinforcer or get nothing. For example, in the case of an animal foraging

for food the animal must perform this action to acquire resources (and take on some risk) or forgo eating altogether. In the case of psychopathologies this is also observed. A person may need to acquire a job but is afraid of performing poorly in the interview, the options are to take on the risk or forgo the job altogether.

To assess this process Park and Moghaddam, 2017b developed a task where a single FR1 instrumental action taken to obtain food reward carries a probability of footshock punishment which increases in each block of the session. Blocks are broken up into 50 trials, and completion of all 50 trials in one block permits subject to enter the next block. Thus the probability of an action producing shock increases from 0% to 10% over the three blocks and subjects have three hours to complete the task. This task carries the advantage of being self-timed which allows subjects to display sustained hesitation to perform actions when risk is present. The main outcome is consequently the increases in latency to perform the risky action.

While this task contains a “safe” block it has no safe action which raises the question of what the locus of behavioral suppression is, which is a point of interest in punished behavior (Jean-Richard-Dit-Bressel et al., 2018). Is it the context in general? Or is it specifically the action itself that engenders suppression? Further the risks utilized in this task do not typically get high enough to suppress reward seeking itself, only enough to slow behavior, which may mask individual differences in punishment sensitivity that could be related to psychopathologies. Lastly the three hour length of the task can be problematic when paired with other techniques such as behavioral pharmacology or optical recordings due to drug pharmacokinetics and photobleaching, respectively.

## Conclusions on Approaches to Studying Reward Seeking and Anxiety

The above section highlighted a burgeoning area of instrumental tasks which inform our understanding of reward motivated action under approach-avoidance conflict. Furthermore, I hope considerations of each approach highlight that for specific questions, there are alterations that may be made and validated. For the aims of this dissertation this is namely understanding how learned probabilistic punishment affects reward seeking. Additionally, understanding explicit probabilistic punishment itself requires a task which assesses both safe and risky actions and holds reward likelihood itself constant, as this prevents complications in interpreting the effects of probabilistic punishment because of concurrent reward uncertainty effects (i.e. sensitivity to non-reward). These ideas form the motivation for the first set of experiments in this dissertation. It is from this base we can then interpret neural data during specific epochs to speculate what changes in neural signals during learned approach avoidance “represent”. Next, I will provide background into the neural systems in reward and punishment processes and highlight the PFC as a key node in networks which subserve behavior under risk.

## Neural systems underlying anxiety and motivated behavior

Neural systems which subserve the behavioral activation, fight-flight-freeze, and behavioral inhibition systems are densely interconnected, and share multiple roles for behavior (Gray, 1982; McNaughton & Corr, 2004). The complex and interconnected nature of these systems, and corresponding brain regions, stresses a need for careful assessment of these processes simultaneously.

For the behavioral activation system, dopaminergic (DA) regions like the ventral tegmental area (VTA) and substantia nigra have been proposed to be involved, as well as the dorsal

striatum (DS) and nucleus accumbens (NAc). A sizable amount of work has demonstrated DA VTA afferents to the NAc are involved in prediction error signaling, a process where organisms learn based on outcomes being greater, worse, or the same according to the subjects' expectations (Schultz, 2016). The NAc has also long been a site for the mediation of reward motivated behavior, signaling the value of rewards and incentive motivation of conditioned stimuli to guide behavior (Hart et al., 2014).

The fight-flight-freeze system and behavioral inhibition system likely involves some overlap in mechanisms, as these systems respond to or bias information related to avoidance states. The hippocampal formation has received considerable attention (Gray & McNaughton, 2000), forming connections with the thalamus and cortex, as well as having important roles in contextual fear memory. Other limbic structures are also implicated such as the amygdala and bed nucleus of the stria terminalis (BNST), cingulate cortex, and brainstem structures for pain and avoidance such as the periaqueductal grey (PAG). Stressful information and avoidance responses related to fear are also processed through the basal and central nuclei of the amygdala and have been implicated in action under punishment risk, fear conditioning, and discriminating signals related to threat and safety (Bishop et al., 2004; McEwen et al., 2016; Orsini et al., 2015). Relatedly, anxiety processing has also implicated the amygdala and the BNST (Walker et al., 2003).

Unlike the behavioral activation system, neuromodulation in these systems has been proposed to be mediated by serotonergic (5-HT) and norepinephrine (NE) mechanisms (McNaughton & Corr, 2004). Such specific roles for neuromodulators in each system is questionable, however, as these systems are interconnected and each neuromodulator can be utilized in approach and avoid processes (Rygula et al., 2015; Verharen, Luijendijk, et al., 2020; Weinshenker & Schroeder, 2007). For example, a core function of DA in prediction error signaling could also carry over to punishment from non-reward, and circuit level work has confirmed VTA DA neuron involvement in both aversion and appetitive processes (Cohen et al., 2012).

An additional level of complexity is added from the hierarchical organization of the behavioral inhibition, fight-flight-freeze, and behavioral activation systems. Higher levels reflect higher order processes like cognitive processes and anticipatory anxiety, and result in enhanced engagement of cortical brain regions. Lower levels reflect more basic motor processes centered in lower brain regions such as the PAG. However as acknowledged by its authors, neural mechanisms can span several systems and hierarchical levels, with significant cross-talk. Thus assuming a specific one behavioral mechanism to one brain region relationship is unlikely. Rather, a more informative approach may be to assess how each brain region responds to different aspects of approach-avoidance conflict to parse out roles for neural subregions.

Of the neural systems proposed in reinforcement sensitivity theory, the PFC is a critical region for the multiple dimensions of behavior emphasized in this dissertation. The PFC is implicated in complex scenarios where different outcomes for different responses must be monitored and utilized. Neural models for reinforcement sensitivity theory suggest the PFC sits at the top of the hierarchy, spanning across the behavioral activation, behavioral inhibition, and fight-flight-freeze systems, though the role of the PFC in the behavioral inhibition system is described as "tentative" (McNaughton & Corr, 2004). The PFC may be critical for more recent proposals for the behavioral inhibition system; notably its role in risk assessment, the comparison of received outcomes with predictions, and control of the behavioral activation and fight-flight-freeze systems (Corr, 2013). For this reason the remainder of this introduction and this dissertation will be centered on understanding how two regions of the prefrontal cortex, the mPFC and OFC, adapt to reward and punishment contingencies.

## Prefrontal cortex as a hub for the processing of affective information

The behavioral inhibition and fight-flight-freeze systems are engaged through exposure to stressful stimuli or adverse experiences. Several brain regions respond acutely and adaptively to stressful manipulations and are often grouped as “stress circuitry.” These include, but are not limited to, the amygdala (particularly the basal lateral nucleus), BNST, hippocampus, and hypothalamus (McEwen et al., 2015; McEwen et al., 2016; Walker et al., 2003). The PFC, both mPFC and OFC, are connected to each of these regions (Hoover & Vertes, 2007; Hoover & Vertes, 2011; Murphy & Deutch, 2018; Vertes, 2004). It is therefore not surprising that PFC is exquisitely sensitive to stressful manipulations (Arnsten, 2015; Mychasiuk et al., 2016). Stress increases the expression of neural activity markers such as c-Fos, glutamate and monoamine release; elevates blood oxygen level dependent signal (BOLD) in the mPFC and OFC (Abercrombie et al., 1989; Campeau et al., 2002; Han et al., 2016; Holmes & Wellman, 2009; Moghaddam, 1993; Morrow et al., 2000; Olson et al., 2019; Ostrander et al., 2003; Pizzagalli et al., 2004; Porcelli et al., 2008); and alters neuronal signaling and morphology in both pyramidal neurons and  $\gamma$ -aminobutyric acid (GABA) interneurons (Cook & Wellman, 2004; McKlveen et al., 2019; McKlveen et al., 2016; Radley et al., 2006; Yuen et al., 2012).

Disruptions in PFC activity may reduce top-down control of brain regions involved in the both the behavioral activation system and fight-flight-freeze system and has been tied to behavioral disruption and negative affective states at the preclinical and clinical level (Balderston, Vytal, et al., 2017; Cerqueira et al., 2007; Friedman et al., 2017; Kim et al., 2007; Liston et al., 2006; Mizoguchi et al., 2000; Murphy et al., 1996; Schwabe & Wolf, 2011). Such a central role is outlined in Figure 1.3, which demonstrates some of the brain regions connected with the PFC and their predominant involvement in each system. The memory of contexts, particularly fear and threat related contexts, is in part mediated by the hippocampus, which displays strong connectivity with the PFC, and synchrony between the two has also been implicated in mediating anxiety-related behavior (Adhikari et al., 2010; Padilla-Coreano et al., 2016). The amygdala is also reciprocally connected to the PFC and these projections have been deemed important for discriminating fear stimuli and value judgement (Likhtik et al., 2014; Sotres-Bayon et al., 2012). There is also more recent but convincing evidence of PFC interfacing with the BNST during uncertain threat, which has long been a hub for anxious approach behavior (Glover et al., 2020; Goode et al., 2019).

The PFC is also connected to key regions involved in reward approach such as the VTA, NAc, and DS (Friedman et al., 2015; Kim et al., 2017; Lodge, 2011). These connections however do not simply produce reward signals. OFC-NAc signaling, in connection with the amygdala, reflects outcome value during probabilistic learning (Groman et al., 2019). Further, mPFC-NAc activity is implicated in reward processing, and more recently, shock responsive mPFC-NAc projections have been shown to control reward seeking behavior when there is a fixed risk of punishment (Kim et al., 2017). The DS receives innervation from both the mPFC and OFC and these connections have been directly implicated in the execution of action under concurrent reward and punishment schedules (Friedman et al., 2017; Friedman et al., 2015; Pascoli et al., 2018).

Lastly the impact of monoamines cannot be ignored in the context of the PFC. The PFC receives projections from several key brainstem nuclei for monoamines; the dorsal raphe (DR), locus coeruleus (LC), and VTA. Neurotransmitters such as DA and 5-HT have been implicated in the processing of reward and punishment in both mPFC and OFC (Rygula et al., 2015; Schoenbaum et al., 2009; Verharen, Luijendijk, et al., 2020), while the LC is a key node for stress responsivity and NE activity in the PFC and has been linked to stress related reinstatement and cognitive flexibility deficits (Jett & Morilak, 2013; Weinshenker & Schroeder, 2007).

The PFC sits within a hierarchy that takes multidimensional information into account

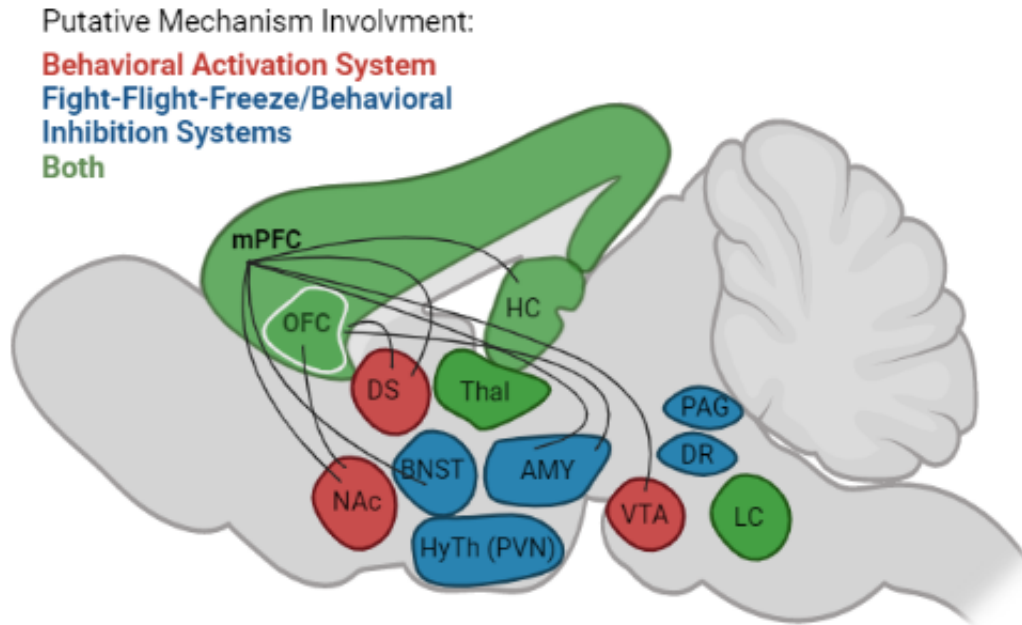


Figure 1.3: PFC pathways implicated in approach and avoidance systems during reward seeking. Each brain region is color-coded according to its predominant role in reward seeking (red), avoidance defense systems (blue), or both (green). These distinctions are putative and simplified. In reality each region could be involved in each system. Each region displays some level of connectivity with the PFC in reward or punishment situations. Lines denote connections where the PFC has been implicated in approach-avoidance conflict specifically. Image created with BioRender.com

from multiple brain regions, including sensory, motor, and limbic systems (Fuster, 2001; Fuster, 2015). Ultimately these processes allow the PFC to flexibly plan and adapt behavior in accordance with the demands of the environment, internal affective states, and motivational states (Compton, 2003; Naqvi et al., 2006). This section just began to highlight the PFC's central role in the encoding and processing of reward and punishment. Landmark papers for reinforcement sensitivity theory, and specifically the behavioral inhibition system, have implicated the PFC (including the anterior cingulate cortex) in these processes. These claims were, in the words of the authors, tentative (Gray & McNaughton, 2000; McNaughton & Corr, 2004), highlighting that there is much to be done to understand the role of the PFC in approach-avoidance conflict. Next, I will outline the anatomy of the rodent PFC and its relation to primates. This will be followed by a more detailed description the role of these PFC subregions in reward-motivated processes, fear and anxiety alone, and when anxiety is present during reward seeking.

## Brief review of rodent prefrontal cortex subdivisions

Rodent models have been instrumental in increasing our understanding of the neural basis of behaviors dependent on the PFC. Because the present work and much of the literature studying the neural processes of reward seeking when conflicted with punishment has been performed in rodents, which have a less developed PFC compared to primates, a brief overview of functional and anatomical properties of rodent PFC is provided before reviewing the current literature.

**Medial Prefrontal Cortex** The rodent mPFC comprises the medial wall of the PFC and has two primary subregions: the dorsal prelimbic (PL) region (which can sometimes include the anterior cingulate cortex (ACC)) and the ventral infralimbic (IL) region. The exact boundaries

of these regions is still a matter of debate (see Carlén, 2017; Laubach et al., 2018). Where possible, subregions will be denoted in this introduction (e.g. PL-mPFC). While broad outlines of the contributions of mPFC subregions to behavior have emerged, considerable debate still remains about the exact functions of each of these cortical domains. Also, because the rodent mPFC is agranular, strict functional-anatomical homologues between primate and rodent PFC is a matter of debate (Laubach et al., 2018; Preuss, 1995; Rushworth & Owen, 1998). Early studies suggested that the rodent mPFC is homologous to the primate dorsolateral PFC, citing that this region shares similar projections from the mediodorsal thalamic nucleus and performs similar functions (Carlén, 2017; Rose & Woolsey, 1948). This belief, and the entire idea of a homologous rodent mPFC compared to primate, is still uncertain as later studies established the mediodorsal thalamus does not solely project to PFC and its functional similarities in the context of working memory are complicated (Laubach et al., 2018; Preuss, 1995). More recent accounts posit that rodent mPFC may represent the anterior midcingulate cortex, pregenual ACC, and subgenual ACC for rodent ACC, PL, and IL regions, respectively (see Laubach et al., 2018). Regardless, there is general agreement that the mPFC in rodents is involved in several analogous functions of the dorsolateral, medial, and cingulate cortical regions in humans and monkeys such as working memory, response control, updating, and affective regulation including sensitivity to stressors (Arnsten, 2015; Floresco et al., 2006; Miller, 2000; Wager et al., 2008). This makes rodents a valuable organism for assessing neural underpinnings of these PFC-dependent constructs.

**Orbitofrontal Cortex** The OFC is studied extensively in both rodents and primates (Izquierdo, 2017; Stalnaker et al., 2015). The OFC makes up the ventral portion of frontal cortex above the rhinal sulcus of the rat and is characterized by several subregions: the medial orbital (MO), ventral orbital (VO), ventrolateral orbital (VLO), lateral orbital (LO), and agranular insular (AI) regions, each with distinct and shared functions and neurological connectivity to which there are a number of exceptional reviews (see Barreiros et al., 2021; Hoover & Vertes, 2011; Izquierdo, 2017; Murphy & Deutch, 2018). Of the most interest to the work presented in this dissertation are the LO-OFC and AI-OFC, though it is worth noting the MO-OFC and VO-OFC appear lesser studied and will be important for future work. Similar to other PFC regions, homology between the rodent and primate OFC has been debated because the rodent OFC lacks a granular layer, and its diversity of function complicates direct homology comparisons (Roberts & Clarke, 2019; Wallis, 2012). Similar to primates, however, the rodent OFC is posited to contain a medial and orbital subdivision, whereby the LO and AI comprise the orbital network and MO and mPFC subregions may characterize the medial network (Öngür & Price, 2000; Wallis, 2012). Overlapping connectivity patterns have also been observed and some functional aspects of rodent OFC mirror primate OFC, particularly in regard to value encoding and adaptive behavior (Izquierdo, 2017). Thus while rodent OFC shares some general functions with the primate OFC, debate remains about the extent of functional similarity between the two.

## Prefrontal cortex involvement in reward motivated action

### Prefrontal cortex and goal-directed action

Pioneering work by Balleine and Dickinson, 1998, established a role of the prelimbic region of the mPFC (PL-mPFC) in goal-directed actions through contingency degradation procedures. In these procedures animals learn two instrumental contingencies and one contingency is eventually degraded by being reinforced at the same rate as before independent of instrumental action execution. While animals with PL-mPFC lesions were able to learn action-outcome associations at the same rate as control rats, PL-mPFC lesions were found to block discrimination between

the degraded and non-degraded contingencies. Additional studies involving the mPFC in goal-directed action are seen with outcome devaluation procedures. Here, a reinforcer is devalued by allowing the animal to become satiated with the particular reinforcer prior to an instrumental action session. If behavior is goal-directed, this should selectively decrease action associated with the devalued reinforcer. Sham subjects responded less for the devalued outcome, as expected, but mPFC lesion animals were insensitive to devaluation (Balleine & Dickinson, 1998). Also, insensitivity to devaluation was only observed in animals where the mPFC was lesioned before training in instrumental action contingencies. If the lesion was performed after the contingencies were learned, reinforcer devaluation was observed. These results suggest the mPFC plays a role in the acquisition (i.e. learning) of goal-directed action, while expression of learned goal-directed action does not depend on the mPFC (Ostlund & Balleine, 2005). Electrophysiology has further supported a role of PL-mPFC in goal-directed behavior. Single unit activity in animals trained to perform instrumental actions for a food reward has demonstrated that subpopulations of neurons significantly modulate firing rate at the time of action execution and outcome expectation in the PL-mPFC. PL-mPFC neurons also adapt to changes in the number of actions required for reinforcement and to the learning of instrumental contingencies and contexts (Mulder et al., 2003; Simon et al., 2015).

The OFC also is implicated in goal-directed behavioral processes (Schoenbaum et al., 2009), particularly in encoding of outcomes (Schoenbaum & Roesch, 2005). Single units in the OFC demonstrate diverse responses to action execution and unique responsivity to various aspects of outcome value such as outcome identity, location, magnitude, and valence (McDannald et al., 2014; Schoenbaum et al., 1998; Simon et al., 2015). However the role of OFC in goal-directed action is complicated by work from Ostlund and Balleine, 2007. Lesions of the OFC, particularly the LO-OFC, do not affect outcome devaluation in instrumental procedures but disrupt Pavlovian-instrumental transfer and Pavlovian contingency degradation. This led the authors to conclude the OFC mediates outcome encoding in Pavlovian rather than instrumental settings. However, electrophysiological studies argued against this interpretation, as one year later, work from Furuyashiki et al., 2008 discovered that distinct populations of neurons encode both specific outcomes and goal-directed instrumental actions in animals performing an odor discrimination task (also see Furuyashiki & Gallagher, 2007, for review). A lack of OFC involvement in goal-directed instrumental action also produces a point of divergence between primate and rodent OFC. Lesions of the OFC alter the ability of subjects to make accurate instrumental responses based on changing reward value or reinforcement contingencies in primates (Izquierdo & Murray, 2005; Izquierdo et al., 2004).

In summary, these findings indicate the PFC plays a role in encoding outcome and action associations to aid instrumental action learning and the adaptation of behavior when learned action contingencies change. They also give one an appreciation for the complexity and nuance when understanding how the PFC serves motivated action even when  $R \rightarrow O$  contingencies are reasonably straightforward. Next I will touch upon habitual responding, as it is critical to understanding overall action execution and because habitual patterns of responding are seen when PFC integrity is compromised.

## **Prefrontal cortex and habitual action**

Instrumental actions are initially goal-directed and influenced by outcomes. Actions can become more insensitive to outcome, often termed habitual, after animals become overtrained to static  $R \rightarrow O$  contingencies. Habitual responding need not be interpreted in a negative light, as its emergence allows for actions that have well predicted outcomes to be executed quickly and efficiently. Habitual behavior can be assessed through overtraining of a  $R \rightarrow O$  contingency prior to reward devaluation. In these studies subjects are either overtrained or limited in training in

a  $R \rightarrow O$  contingency, where a lever press results in food reward. In the limited training condition, actions should be goal directed and sensitive to devaluation. Whereas in the overtraining condition actions should be habitual and insensitive to devaluation.

Involvement of the mPFC in habitual responding was first reported in lesions studies. Lesions of the PL-mPFC did not block actions from becoming habitual but rather generally prevented goal-directed behavior. However, lesions of the IL-mPFC spared goal-directed behavior after limited training, but blocked behavior from becoming habitual after overtraining (Killcross & Coutureau, 2003). A follow up study used temporary inactivation of the IL-mPFC using similar procedures to assess whether the shift from goal-directed to habitual action came from the degradation in  $R \rightarrow O$  associations or the influence of  $R \rightarrow O$  associations. Evidence was found for the latter, as inactivation of the IL-mPFC cortex in overtrained subjects reestablished sensitivity to reward devaluation. This findings indicates that goal-directed processing is intact but inhibited by the IL-mPFC during habit (Coutureau & Killcross, 2003).

Single unit recordings of neural activity have supported a role for IL-mPFC in habitual responding. In a recent study, animals were overtrained using two reinforcement schedules: random ratio which commonly engenders goal-directed responding, and random interval which commonly engenders habitual response strategies. IL-mPFC neural excitability in response to reinforcer delivery (outcome) was similar across schedules early in training. After extended training neural response to action execution and outcome became blunted in the random interval (habit) condition but not the random ratio condition (Barker et al., 2017). Importantly promoting inhibition of the IL-mPFC specifically after action execution was sufficient to reinstate goal-directed behavior, showing that the IL-mPFC involvement, much like the PL-mPFC, is particularly pivotal in influencing response strategy.

The OFC has also been implicated in habitual behavior in rodents and primates (Izquierdo, 2017; Rhodes & Murray, 2013; Zimmermann et al., 2017). Many of these studies in rodents have only implicated a role of the OFC (particularly the LO subregion) in habitual responding using Pavlovian conditioning, whereby inactivation and lesions promote habitual behavior (Gallagher et al., 1999; Pickens et al., 2005; Pickens et al., 2003). Primate studies, however, indicate an anti-habit role for the OFC in instrumental devaluations (Baxter et al., 2000). One study by Panayi and Killcross, 2018 investigated this directly by lesioning the LO-OFC and training animals in either Pavlovian or instrumental outcome devaluation procedures. Again, instrumental devaluation was insensitive to lesions of LO-OFC, while Pavlovian devaluation was blocked by LO-OFC lesion. Follow up experiments clarified this effect by showing that these LO-OFC lesions are likely due to disruptions in attributing motivational value to stimuli because sign-tracking, a canonical measure of incentive value where animals attend to learned reinforcer-associated stimuli, was disrupted (Panayi & Killcross, 2018).

Thus it seems that in the context of habitual behavior, and perhaps specifically lesion studies, the LO-OFC is particularly sensitive to cue and outcome changes but not to action related changes. This interpretation comes into question due to the OFC's role in behavioral flexibility. An elegant study by Gremel and Costa, 2013 used random ratio and random interval schedules of reinforcement, combined with outcome revaluation procedures, to understand how OFC neurons alter firing rate during goal-directed and habitual behavior. Subjects reliably learned to shift between habitual and goal-directed strategies, and lesions of the OFC disrupted proper shifts in behavior when outcome value changed. The authors also observed lever-press selective neurons which increased activity in both random ratio and random interval schedules. Furthermore, units with higher levels of discrimination between ratio and interval schedules were positively correlated with higher levels of sensitivity to outcome value changes. Thus the role of the rodent OFC in instrumental behavior is complex, as it appears to play a role when animals must shift behavior between different strategies (as is common in the real world) but not when one strategy is selected as in devaluation procedures.

## To go or not to go: PFC role in behavioral flexibility during reward motivated action

Conventional theories of PFC function in action control, particularly the mPFC, have proposed a dichotomous Go/No-go framework (see Gourley & Taylor, 2016). Several decades of research have added some support to the idea that the PL-mPFC serves a facilitative role (Go signal) for actions while the IL-mPFC serves an inhibitory role (No-go signal). Much evidence for Go signaling in the PL-mPFC have involved reinstatement paradigms, in which an instrumental response is extinguished and reinstated by non-contingent delivery of the primary reinforcer or reinforcer-associated stimuli. PL-mPFC lesions have been shown to decrease reinstatement induced responding across a wide range of natural and unnatural reinforcers (Capriles et al., 2003; McFarland et al., 2004; Ostlund & Balleine, 2005). Alternatively, stimulation of the IL-mPFC produces opposing effects in such reinstatement procedures by inhibiting reinstatement and/or enhancing extinction retention in reinstatement tests (Peters et al., 2008). The OFC's role in this framework has also been considered. Overall the LO-OFC role in these behaviors seems most similar to the PL-mPFC, that is, facilitating action execution (Arinze & Moorman, 2020). In the 5-choice serial reaction time task, lesions of the OFC lead to deficits in action execution as evidenced by increased omissions (Chudasama et al., 2003) and optogenetic inhibition of the MO-OFC, VO-OFC, or LO-OFC slowed behavior in a reactive motor control task (Hardung et al., 2017). Recently subregion specificity has been documented in a few studies. In a task designed to assess punishment-motivated inhibition of reward retrieval, inactivation of the LO-OFC resulted in increased omissions and slower reaction times while MO-OFC inactivation in this task led to increased failures of inhibition during trials where early reward port entries were punished with footshock (Verharen et al., 2019).

While this Go/No-go dichotomy has been useful in understanding roles of PFC subregions in motivated action, it has become clear that the framework is not without flaws. Recent work in the mPFC has failed to replicate some of these roles of mPFC subregions in instrumental responding and even found contradictory results (Caballero et al., 2019). In this study, inactivation of the PL-mPFC resulted in increased reward seeking actions while inactivation of the IL-PFC attenuated cue-induced reinstatement. Further using a response preparation task where subjects had to release a lever in response to a cue, photoinhibition of the PL or IL mPFC resulted in more or less premature responding, respectively, which is opposite to what one would anticipate from the PL-Go, IL-No-go dichotomy (Hardung et al., 2017). These findings would thus implicate a PL-No-go, IL-Go dichotomy in action control when motivated by reward/non-reward. Furthermore, in tasks with reward and punishment conflict, stimulation of the PL-mPFC inhibits rather than promotes responding (Chen, Yau, et al., 2013), and a recent impulsivity task developed by Verharen et al., 2019 found that inactivation of PL, AC, or IL mPFC all resulted in the same impairments in abilities to inhibit reward-motivated actions.

Inconsistent findings also extend to the OFC. In the 5-choice serial reaction time task, where OFC lesions (largely LO) increased omissions, lesions also attenuate behavioral inhibition as indicated by increased impulsive and compulsive-like responding (Chudasama et al., 2003). This suggests LO-OFC inactivation through lesions impacts *both* action execution and inhibition depending on the construct being assessed. In a Go/No-go odor discrimination task, single unit studies in the OFC have found differential activity depending on whether or not responses were correctly inhibited, suggesting a broader role of the OFC in expectations of outcomes (Schoenbaum et al., 1998). These findings are difficult to reconcile with later studies which used large scale OFC lesion to demonstrate that OFC is not necessary for the acquisition of Go/No-go behavior (Schoenbaum et al., 2002). When the Go/No-go discriminative stimuli were reversed, however, OFC lesioned animals showed deficits. Whether such deficits in reversal are a failure of inhibition is also difficult to interpret. Later work in primates which used a three

stimuli to determine if errors were generally due to flexibility or from inhibitory deficits, found that LO-OFC damage did not result in inhibitory failures but rather general failures at flexibly adapting behavior (Walton et al., 2010). Thus while the OFC shows documented importance in tests of behavioral action, its role is more nuanced than control of action execution or inhibition (also see Stalnaker et al., 2015, for review).

Though addressing this dichotomy is useful in highlighting important functions of the PFC, it oversimplifies the complex neural basis of action execution. In reality these actions are also supported by the motivational states and the external context from which they are derived (i.e. the learned associations between actions and outcomes from basic stimulus detection to cognitive processes). Such demands may also implicate the PFC in attention processes to activate volitional and/or well learned behavior, as proposed in other theories of PFC function (see Sharpe & Killcross, 2018). The diverse involvement of the PFC in different aspects of reward motivated behavior stresses the importance of investigating not just whether removal of the PFC affects behavior but also how neurons in the PFC respond to actions and outcomes during motivated behavior. To aid in this we can look at time-locked recording of the PFC during behavior flexibility tasks to inform our common theories of PFC function.

## Encoding of action and outcomes in behavioral flexibility tasks

PFC subregions may be better understood in the context of the information they convey to permit behavioral adaptation rather than a sole controller of action execution or inhibition *per se*. This idea supports the complimentary approach of *recording* rather than inactivating PFC activity to aid in understand roles for the PFC in motivated behavior. One approach has been to record PFC activity during set-shifting tasks which require subjects to learn and switch between distinct rules (or sets). Successful performance of these tasks requires subjects to encode actions and outcomes as well as inhibit and execute the appropriate responses (Birrell & Brown, 2000; Floresco et al., 2008; Stefani & Moghaddam, 2005).

Previous studies have shown that PL-mPFC neurons show time-locked activity changes at the time of action execution and the corresponding outcome period (Del Arco et al., 2017; Park et al., 2016; Spellman et al., 2021). These neural activity patterns likely reflect real-time encoding of actions because (1) most of these neurons display a peak correlation with current trial actions and outcomes and (2) neural population signals during encoding periods (i.e., the post-action period) can discriminate between rules and be used to predict the current rule (Del Arco et al., 2017; Park et al., 2016). Finally, in a version of a set shifting task where actions are randomly reinforced (i.e., no rule is “correct” and there is no cognitive demand), significant levels of neural encoding of the post action period are not observed, while outcome responsivity of mPFC neurons is preserved (Del Arco et al., 2017). These studies provide evidence that mPFC neurons are of particular importance for action encoding during situations in which flexible behavior is required.

In the LO-OFC task responsive units after learning of set-shifting contingencies are also observed. However, the largest percentages of responsive units in the OFC were observed during the response outcomes (Park et al., 2016). While some units were also responsive to task rules and previous responses, they generally made up less of the population compared to mPFC units. Thus under these contingencies the mPFC and OFC play important but possibly distinct roles in encoding action contingencies and outcomes.

Similar overlap and divergence of multiple signals relevant to behavioral flexibility have been documented in bandit tasks, where animals choose between different options (actions) which have unique probabilities of reinforcement. Thus different actions purportedly have different subjective values and animals must update action strategy based on outcome proba-

bilities. This approach was used by Sul et al., 2010, who trained animals to traverse a maze where each arm contained a unique probability of reinforcement that changed throughout the session. As the animals adapted behavior to these contingencies the investigators concurrently recorded single units in the ACC, PL-mPFC and IL-mPFC (combined due to similarities in response), and LO-OFC. Neural signals for animal choices were seen in all regions, but were highest in the ACC and began earlier in the approach period in the mPFC compared to the LO-OFC. A similar responsiveness to outcomes was also observed across regions, particularly in the approach and reward stage, but the LO-OFC generally showed the highest responsiveness for this measure. Using a reinforcement learning model the authors extrapolated the value of actions over the task, which revealed that small but significant percentages of value responsive units were present across the mPFC and OFC with distinct temporal patterns across regions. The OFC also showed the highest level of value encoding. Taken together these studies demonstrate that the PFC processes a multitude of signals important for adapting behavior under reward/non-reward contingencies. These signals are importantly time-locked to action execution and reward related periods, a level of resolution not afforded by lesion or pharmacological approaches. These studies also indicate that OFC neurons encode distinct information compared to the mPFC, and highlight characterization of such similarities and differences as a key area for future research (Moghaddam & Homayoun, 2008).

## Prefrontal cortex involvement in fear states and fear learning

Fear is generally defined as distressing emotions caused by the presence of impending danger (Grillon, 2008). mPFC encoding of fear is commonly assessed using Pavlovian fear conditioning. This procedure applies an aversive unconditioned stimulus (US), such as a footshock, paired with a conditioned stimulus (CS), such as a tone, that elicits a conditioned behavioral fear response (CR) such as freezing or darting (Gruene et al., 2015; Johansen et al., 2011). Thus, the main measure in these and similar paradigms is the strength of the association between the CS and US through the CR.

It is well documented that expression of freezing behavior in Pavlovian fear conditioning requires the PL-mPFC. Inactivation of the PL-mPFC after fear learning prevents conditioned freezing (Corcoran & Quirk, 2007). However, when this region is inactivated during the acquisition of fear learning and the subject is tested for fear expression later, the fear expression remains intact (Corcoran & Quirk, 2007). Furthermore, fear responses to predator odor and in a novel open field, where learned associations are not required, remain intact following inactivation of the PL-mPFC. Thus, mPFC circuitry is critical for expression of learned fear responses but not necessary for the acquisition of fear learning itself nor for innate fear expression. However, some studies using lesion approaches have argued against this interpretation, suggesting the main role of the PL-mPFC in fear, and appetitive, learning is due to a PL-mPFC control of attentional processes when stimuli are in conflict with one another (Sharpe & Killcross, 2018). Support for this idea comes from data showing that in fear conditioning preparations where the context has low levels of competition for attention with the CS, the mPFC is not necessary for fear expression (Sharpe & Killcross, 2015).

Nevertheless, at the neural level, single unit recordings of putative excitatory and inhibitory neurons in PL-mPFC show heterogeneous but time-locked changes in firing rate when fear associated stimuli are presented and during freezing (Baeg et al., 2001; Courtin et al., 2014). In addition, the excitatory PL-mPFC response to a CS is associated with higher levels of fear expression across all phases of fear learning (i.e., habituation, conditioning, and extinction; Burgos-Robles et al., 2009). IL-mPFC neuron inactivation, however, does not influence fear

learning (Sierra-Mercado et al., 2011) and IL-mPFC neurons fail to show time-locked responses to CS during the acquisition phase of fear learning (Milad & Quirk, 2002). These findings suggest that for the development of associations between CS and US, the PL-mPFC shows high involvement, while the IL-mPFC does not.

The OFC has similarly been involved in fear conditioning, though less is known compared to mPFC (see Shiba et al., 2016, for review). Stimulation of LO and AIC-OFC using microinjections of NMDA attenuates the expression of fear the day after learning (Chang et al., 2018). Lesions of the LO-OFC enhance fear expression during initial learning, an effect which can also be seen through context overgeneralization and CS<sup>+</sup> presentation tests after acquisition (Lacroix et al., 2000; Zelinski et al., 2010). Take together these results suggest the OFC may facilitate the inhibition of fear expression.

One outstanding question is whether OFC facilitates the learning of fear signals or is more generally involved in behavioral flexibility by mediating fear responses based on context or cues. To assess this Sarlitto et al., 2018 used temporary inactivation of the LO/VLO to see if this would effect acquisition or recall of conditioned fear discrimination. While fear discrimination was normal both in acquisition and recall when OFC activity was inhibited during initial learning, fear cue discrimination was disrupted when the LO-OFC was inhibited before recall. In another study utilizing cues with unique probabilities of footshock lesions of the LO-OFC did not impact discrimination of fear and safety signals. Rather, enhancement of fear was observed when the probabilities of fear changed (Ray et al., 2018). These findings suggest the OFC may play a role in behavioral flexibility in the context of fear but not necessarily in the learning of fear itself (Sarlitto et al., 2018).

Fear conditioning paradigms can also assess behavioral flexibility by a process known as fear extinction. The extinction procedure involves extinguishing the CS-US association, after freezing in response to the CS is learned, by presenting the CS while omitting the US. Animals' ability to learn the change in contingencies is measured by a reduction (or extinction) in CR after the CS. While extinction of freezing is unchanged by lesions in the PL-mPFC, it is impaired by lesions of IL-mPFC (Quirk et al., 2000). Consistent with lesion studies, single unit recording from IL-mPFC and PL-mPFC neurons showed that IL-mPFC responses correlate with the extinguishing of fear behavior (Chang et al., 2010). Moreover, animals that displayed a large IL-mPFC neural response to the CS showed deficits in an extinction retention test (Chang et al., 2010). This is intriguing because earlier studies showed that larger phasic responses of IL-mPFC neurons in response to the CS in extinction was associated with improved learning (Milad & Quirk, 2002). To resolve this, a recent study used optogenetics to selectively stimulate or inhibit IL-mPFC neurons at the time of CS delivery during extinction training (Do-Monte et al., 2015). Optogenetic stimulation produced a dramatic effect, nearly abolishing freezing during training and enhancing extinction learning in a later recall test in the absence of optogenetic stimulation. Surprisingly, inhibition of these neurons during extinction training had no effects on extinction *per se*, but produced deficits in extinction memory because freezing was elevated in the retrieval test the following day.

Other recent studies have begun to characterize the role of the OFC in fear extinction learning. Activation of the LO-OFC with NMDA microinjection potentiated freezing during the end of extinction training (Chang et al., 2018). In a retention test the following day these same animals showed normal responses to fear conditioned tones but animals who were injected just prior to retention showed a hyper-reduction in freezing that gradually recovered over the session. This finding also extends to the MO region of the OFC (albeit the more anterior MO) as extinction learning and recall was disrupted by MO stimulation during extinction training (Hsieh & Chang, 2020). Using designer receptors exclusively activated by designer drugs (DREADDs) it has also been demonstrated that inhibition of mouse VLO excitatory neurons during extinction training results in normal extinction behavior but excessive levels of

freezing in later recall tests (Zimmermann et al., 2018).

Contextual discrimination is also part of the extinction process which can be directly assessed through renewal procedures. Using ABA renewal procedures, subjects are fear conditioned to stimuli in context A, trained in extinction in context B, and tested for recall in contexts A and B, whereby heightened fear in context A represents renewal. LO-OFC stimulation in extinction led to a potentiation of freezing in extinction and a subsequent lack of renewal (though there was a modest, non-significant, increase in the A-renewal context compared to the B-renewal context). MO-OFC stimulation also enhanced freezing late in extinction and completely blocked renewal (Shih & Chang, 2021). Though more work is required, these results indicate that the OFC plays a role in the proper recall of extinction. Like fear conditioning studies these effects may also be from general deficits in behavioral flexibility. For example in the study where DREADDs disrupted extinction recall, the same inactivations also produced deficits in reward devaluation of instrumental contingencies by disrupting outcome memory (Zimmermann et al., 2018).

While fear conditioning paradigms lack explicit goal-directed actions, other procedures such as active avoidance can measure how the PFC is involved in planning and encoding actions that are executed after cued footshock threat. In active avoidance paradigms, subjects learn to move to a safe location or execute an action (such as pressing a lever) with the goal of avoiding an imminent aversive outcome signaled by a cue. Thus the latency to escape the aversive stimulus is the main measure of how well a subject learns this action-outcome association. A recent comprehensive study recording from PL-mPFC found that these neurons encode cues that signal avoidance, and that inhibiting the phasic response of mPFC neurons (through excitation) increases the latency to actively avoid the footshock (Diehl et al., 2018). Thus, PL-mPFC is believed to be necessary for facilitating actions toward the goal of avoiding an aversive outcome. This is similar to previous studies where IL-mPFC lesions before avoidance resulted in impaired active avoidance (Moscarello & LeDoux, 2013). While the results of the IL-mPFC study may be due to enhancement of freezing behavior seen after the lesion, facilitatory roles for PL and IL-mPFC in avoidance have been shown in more recent studies which required animals to discriminate active and inhibitory avoidance cues (Capuzzo & Floresco, 2020). However, when the active avoidance task was simple, requiring no discrimination, this study failed to show an effect of PL-mPFC lesion even though IL-mPFC lesions continued to perturb avoidance responses. This is interesting because the avoidance study outlined earlier (Diehl et al., 2018) also had a food reinforcement contingency in the task to coax animals away from the safety platform. Taken together these findings suggest that PL-mPFC may be involved in avoidance actions when discriminating multiple contingencies is required.

There has been considerably less research in the OFC in regards to active avoidance learning. In one study, Rodriguez-Romaguera et al., 2016 trained rats in a cued active avoidance task and then required these subjects to extinguish the avoidance response. Muscimol was injected into the LO-OFC to temporarily inactivate the OFC when tested for extinction recall. Inactivation during conditioning was not investigated. LO inactivation bidirectionally influenced avoidance in extinction recall, such that low fear rats (which put low value on the avoidance response) showed increases and high fear rats (which put high value on the avoidance response) showed decreases in avoidance following inactivation. These findings suggest that the OFC may not have been critical for affective response *per se* but rather is important in assigning and recalling value to actions, a finding which extends its role in decision making and reward motivated behaviors outlined earlier.

Collectively fear learning literature suggests that PL-mPFC activity subserves the expression of fear whereas the IL-mPFC activity exhibits greater involvement in promoting the extinction of fear. These regions, however, are also important for execution of actions motivated by the goal of avoiding stressors in active avoidance procedures. Results of the OFC in fear

learning and extinction are more recent and have not received as much attention as the mPFC. While these studies have implicated the LO-OFC in the processing of fear it is possible these effects have more to do with the OFC's roles in value attribution and behavioral flexibility. Thus while the computational and functional processes of neural activity in the PFC in response to fear learning and avoidance remain to be fully determined, subregions in the mPFC and OFC appear involved in encoding fear related information and behavior.

## Prefrontal cortex involvement in anxiety

While fear and anxiety are related, they are distinct constructs. Anxiety results from the perceived potential of an uncertain threatening event whereas fear is a response to imminent threat. Consistent with the literature establishing that PFC neurons encode internalized information in service of distant/future actions (Fuster, 2000; Kesner & Churchwell, 2011; Schoenbaum et al., 1998), the major body of preclinical and clinical work has implicated disruption of PFC function in animal models of anxiety and in most forms of anxiety disorders (Balderston, Liu, et al., 2017; Balderston, Vytal, et al., 2017; Basten et al., 2011, 2012; Calhoun & Tye, 2015; Han et al., 2016; Lammel et al., 2014; Milad & Rauch, 2007; Roberts, 2020). For example, in the N-back working memory task generalized anxiety disorder patients show impairments in the speed of responding, and high trait anxiety is associated with problems in the ability to shift strategies and disregard irrelevant information (Balderston, Vytal, et al., 2017; Basten et al., 2011, 2012). PFC activity, as measured by BOLD activity, is perturbed in patients with generalized anxiety disorder compared to controls during working memory task performance. Specifically, generalized anxiety disorder patients show decreased working memory load related activation of the PFC, particularly in the frontal gyrus and the dorsolateral and cingulate regions (Balderston, Vytal, et al., 2017). Similarly, high trait anxiety is associated with reduced dorsolateral PFC activity during attentional control and conflict processing (Bishop, 2009). Anxiety from threat of shock also elicited robust changes in PFC activation during working memory task performance in both generalized anxiety disorder patients and controls, though these changes did not interact with diagnosis. Taken together these studies demonstrate that longstanding anxiety phenotypes or a transient state of anxiety are associated with decreased PFC activity, and anxiety phenotypes appear to be associated with altered PFC engagement during cognitive performance.

To behaviorally induce anxiety in rodents, canonical models include the open field and the elevated plus maze, whereby animals are placed in a novel context that has "safe" areas like enclosed arms and "threatening" areas like open arms (Lezak et al., 2017). These models have some face validity for assessing anxiety states, but they can be difficult to interpret because the impetus for behavior in these tasks is ambiguous. These limitations are possibly reflected in the variability that has been seen in studies investigating the role of the PFC using these models (see Roberts, 2020, for review). For example, lesions and pharmacological manipulations of the PL-mPFC subregion, and even the ACC, suggest PL-mPFC activity is necessary for anxiety-like behavior in the open field and elevated plus maze, but other studies have shown either contradictory or null effects from lesions of these regions (Bissiere et al., 2006; Lacroix et al., 1998; Pati et al., 2018; Stern et al., 2010). Inconsistencies have also been reported after manipulation of the IL-mPFC, though some studies which compared PL-mPFC vs. IL-mPFC excitation demonstrated anxiogenic effects of PL-mPFC stimulation with no effect of IL-mPFC stimulation (Bi et al., 2013; Shah & Treit, 2003; Sierra-Mercado et al., 2011; Suzuki et al., 2016). In the OFC less work has been done and some inconsistencies, at least in the LO/AIC subregions, have been observed. Lesions and muscimol inactivation of the LO-OFC have failed to produce an effect on behavior in the elevated plus maze (Green et al., 2020; Lacroix et al., 2000; Orsini et al., 2015) while chronic inactivation increased anxiety in the open field and

decreased distance traveled (Kuniishi et al., 2017).

PFC neurons encode the location of rodents in these innate anxiety paradigms. One study which recorded single unit activity in the PL-mPFC in the elevated plus maze demonstrated increases in PL-mPFC neural firing rate when animals entered closed or open arms and these changes typically preceded transitions from safe to risky areas (Adhikari et al., 2011). This pattern of activity was replicated in recent work which recorded population neural calcium activity in the PL-mPFC in the elevated zero maze (Loewke et al., 2021), suggesting that the mPFC tracks the entry and exit from anxiogenic contexts. At the behavioral level, firing patterns appear to have some relation to anxiety-like behavior. Animals with higher anxiety on the elevated plus maze show lesser mPFC neuron discrimination of closed and open arms (Adhikari et al., 2011). This would argue that mPFC neurons have direct involvement in behavioral strategies under innate anxiety. However, optogenetic stimulation of the PL-PFC and PL-PFC  $\rightarrow$  amygdala projection neurons have not supported this idea as stimulation had no effect on open field or elevated plus maze behavior (Adhikari et al., 2015; Kumar et al., 2013). However, IL-mPFC  $\rightarrow$  amygdala projection neuron stimulation has been shown to produce anxiolytic effects in the elevated plus maze (Adhikari et al., 2015). It may also be the case that the mPFC role in innate anxiety may depend more on changes in inputs it receives. This is supported by work which has shown that anxiety in the elevated plus maze can be bidirectionally controlled through optogenetic manipulation of ventral hippocampal terminals in the mPFC (Padilla-Coreano et al., 2016; Padilla-Coreano et al., 2019).

The role of the mPFC in innate models of anxiety is nuanced, though evidence for mPFC encoding of behavior in the such models seems apparent the functional role of the mPFC may be based on specific inputs or outputs. It is also possible some of the variability in the effects of mPFC inactivation is a reflection of diverse strategies and levels of anxiety states in these tasks or that such effects can only be seen in certain contexts. For example, Kumar et al., 2013 showed that PL-mPFC stimulation had anxiolytic effects when subjects were exposed to chronic stress earlier in life. There is scant evidence for neural encoding by the OFC in innate anxiety using single-unit or calcium imaging based approaches. Burgeoning evidence has demonstrated a role for the OFC in neurons tracking spatial location in an open field (Wikenheiser et al., 2021). This study, however, was not designed to assess if such signaling was related to anxiety. This highlights the OFC's role in anxiety-like behavior as an important avenue for future research.

## Prefrontal cortex manipulation of goal-directed action under anxiety states

The innate anxiety models, while contributing a great deal to our knowledge of the nature of PFC involvement, do not inform us about the nature of cortical encoding of ongoing behavior in anxiety states. In a real-life situation, the impact of anxiety extends beyond its general aversive quality and engages the behavioral inhibition system to influence ongoing goal-directed actions that utilize cognitive and affective processing. Thus understanding how PFC encoding of motivated actions changes with anxiety is a crucial area of interest, though addressing this has not been trivial (Park & Moghaddam, 2017a). One approach is to record from PFC neurons during goal-guided behavior after administering the anxiogenic GABA inverse agonist FG-7142 (Park et al., 2016). This approach is reinforced by several studies in rodents, monkeys, and humans, demonstrating that ligands which decrease GABA<sub>a</sub> receptor function produce anxiety (Crawley et al., 1985; Dorow, 1987; Pellow & File, 1986). Additionally, FG-7142 produces a robust and consistent reduction in the spontaneous firing rate of a population of putative excitatory neurons in the rat PL-mPFC and LO-OFC (Park et al., 2016). These findings corroborate the population level BOLD signal decreases in human fMRI studies, and further support the idea

of modulation of the PFC during anxiety states (Balderston, Liu, et al., 2017).

Using a PFC-dependent set-shifting task, Park et al., 2016 assessed the impact of the anxiogenic treatment on performance and encoding of behavioral events. Behaviorally, FG-7142-induced anxiety modestly affected set-shifting performance. Animals treated with FG-7142 completed the task, but took longer than vehicle treated animals. Moreover, FG-7142 treatment increased the number of errors following rule switches, suggesting disrupted cognitive flexibility. The population response of PL-mPFC neurons across all trials did not reveal an effect of anxiety on action encoding or neural activity after correct or incorrect outcomes, suggesting outcome encoding is also not influenced by FG-7142-induced anxiety. The response of neurons that encoded the rules, particularly in the peri-action period, were attenuated by anxiogenic treatment. These “rule-sensitive” neurons under control conditions developed rule selective response in later periods of rule learning (i.e., after several trials of exposure to the rule change). FG-7142 attenuated this rule-sensitive response by disrupting the phasic response of neurons. Finally, some trials in the set shifting task were further classified as “conflict” trials. These were instances where the incorrect rule conflicted with the correct rule, requiring increased attention and discrimination. Treatment with FG-7142 had a stronger disruptive effect on behavioral performance in these conflict trials compared to non-conflict trials and decreased the percentage of rule encoding neurons in conflict trials. This suggested that anxiety, at least using this model, disrupts cognitive function by decreasing PL-mPFC responsivity to discriminate between rules when stimuli for a past rule is present and must be ignored. Such disruptions ultimately decrease animals’ ability to make the correct choice because the presence of conflicting stimuli are either not properly processed under anxiety, or such rules and stimuli are not properly integrated to optimize action selection. Additionally, it is of note that recording LO-OFC neurons in this task did not yield the same effects of anxiety. While LO-OFC neurons were sensitive to the task itself, FG-7142-induced anxiety did not change encoding of task related actions or outcomes. Thus the effects of this mode of anxiety on motivated behavior may preferentially effect the PFC in a region specific manner.

The approach of pharmacological induction of anxiety clearly has limitations. While it provides the advantage of studying ongoing behavior under an extended state of anxiety, the drug could be producing brain-wide effects that are unrelated to anxiety. Further in such an approach, anxiety is not “learned” nor is it produced through conflict between the behavioral activation system and fight-flight-freeze system, which could result in different processes from those proposed in models of approach-avoidance conflict. This highlights the need for studies which perform neural recordings during the ongoing learning of operant conflict tasks, which serves as the impetus for much of this dissertation.

A role for the mPFC in the Geller-Seifter task has been demonstrated by local pharmacological manipulation of neuronal activity. Inactivating the PL and IL-mPFC with lidocaine resulted in anti-conflict (i.e. anxiolytic) effects in rats in this task. This indicates that mPFC activity supports anxiety and/or sensitivity to anxiogenic conditions (Resstel et al., 2008). Also, pharmacologically blocking DA receptors in the PL-mPFC similarly reduced anxiety (by promoting action under conflict) in a variation of the Geller-Seifter task (Broersen et al., 1995), suggesting a facilitory role of DA in the mPFC for learned anxiety. This finding is intriguing because increases in monoamines, such as DA, in the mPFC are a common observation in response to stressful and aversive stimuli and are generally attenuated by anxiolytic treatment (Finlay et al., 1995). Further, very recent research in more complex conflict tasks like the risky decision making task have demonstrated that mPFC lesions disrupt proper adjustments of behavior in response to probabilistic punishment, while OFC inactivation results in hypersensitivity to risk of punishment *after* learning (Orsini et al., 2018; Orsini et al., 2015).

While we have ample reason to assume involvement of both the mPFC and OFC in such behaviors, we still have considerable work to do with respect to understanding time-locked

neural activity during learning of approach-avoidance conflict contingencies. Only recently have tasks which measure approach-avoidance conflict during action execution been combined with recording techniques. Using the punishment risk task, Park and Moghaddam, 2017b assessed if PL-mPFC neuron spiking activity during the trial initiation cue, the action encoding period, and reward delivery changed with anxiety. This analysis revealed that the largest anxiety-related neural activity change occurred during the action encoding period rather than reward delivery or the trial initiation cue. Population level activity in the PL-mPFC was also influenced by anxiety. The population level state derived from single units was predictive of anxiety-like action suppression on a trial by trial basis. Furthermore, assessing oscillatory population activity through local field potentials (LFP) revealed anxiety-related changes in theta activity and synchrony between the PL-mPFC and the VTA. Thus PL-mPFC neurons and network coordination are exquisitely sensitive to this model of anxiety particularly during the encoding of motivated actions.

In another study, neural calcium activity in PL-mPFC projections to the NAc or the VTA were recorded using fiber photometry in a task where one action was reinforced with probabilistic reward (water) or punishment (footshock). PL-mPFC  $\rightarrow$  NAc or VTA projections displayed discriminate encoding between rewarded and punished (shocked) outcomes for the same action, but greater changes in PL-mPFC  $\rightarrow$  NAc projections just before the time of action execution were correlated with increased suppression of reward seeking (Kim et al., 2017). Another recent study by Halladay et al., 2020 punished ethanol seeking for every other trial to elicit conflict. These contingencies produced both behavioral suppression and increased “aborts” of lever approaches in a probe sessions one day later. Single unit recording in the mPFC revealed that both ventro-medial (IL) and dorso-medial (PL) neurons showed enhanced responding to lever presses and aborts in the probe session, but such changes were more robust in the IL. Finally, using a task where punishment is predictable but contingent on reward seeking, Pascoli and colleagues discovered enhanced c-fos activity and action encoding differences in the LO-OFC using fiber photometry that were associated with punishment resistance (Pascoli et al., 2015; Pascoli et al., 2018). In summary, findings of conflict during reward seeking indicate that actions and outcomes are encoded at the single neuron and population levels across multiple regions of PFC. However there is much work to be done as none of these studies assessed PFC action encoding before and after the learning of punishment contingencies.

## Purpose of the dissertation

Novel animal models for symptoms of brain disorders are needed to gain a better understanding of the neural basis of these illnesses (Bale et al., 2019; Park & Moghaddam, 2017a). As outlined there are a number of tasks that model the process of reward seeking when conflicted by punishment. These tasks, however, hold limitations in the context of this dissertation. Specifically, they have not addressed the extent to which anxiety is specific to risky action itself and how conflict is learned and represented in the brain in probabilistic punishment situations.

How resistant will subjects be to probabilistic punishment when alternative options are not possible? How do actions change with the learning of these contingencies? To what extent do PFC neurons adapt their responses to safe or risky actions, as well as to rewards and punishment itself? And how do different PFC regions support the critical processes of the behavioral inhibition system? The overarching premise of the work outlined in this dissertation is to better understand the neural basis of how anxiety from approach-avoidance conflict is learned and impacts ongoing reward-guided action.

To this end I designed and validated a novel probabilistic punishment task (PPT) based on different facets of tasks outlined above to allow for assessment of safe and risky actions

under probabilistic conditions that promote anxiety in male and female rats. This is an important consideration given sex differences in mood and addictive disorders and the fact that an overwhelming amount of work in the tasks outlined above was performed only in male subjects (Orsini & Setlow, 2017). I then measure neural calcium activity using fiber photometry to record activity in the PL-mPFC during the learning of the PPT, and a related punishment risk task, to understand how action and outcome encoding changes with the learning of anxietyogenic contingencies. The use of fiber photometry critically serves these goals by permitting long term recording and the recording of population neural activity during punishment itself. Lastly I used the same approach in the LO-OFC to understand how different regions of the PFC uniquely contribute to encoding of probabilistic punishment contingencies and to understand how anxiety alters neural encoding and reward motivated behavior. These results have important implications for our understanding of the neurobiology of brain disorders.

## Chapter 2

# Behavioral Characterization of a Probabilistic Punishment Task to Assess Action Under Anxiety

Adapted from: Jacobs, D. S., & Moghaddam, B. (2020). Prefrontal cortex representation of learning of punishment probability during reward-motivated actions. *J Neurosci*, 40(26), 5063–5077. <https://doi.org/10.1523/jneurosci.0310-20.2020>

### Abstract

Actions executed toward obtaining a reward are frequently associated with the probability of harm occurring. Learning this probability allows for appropriate computation of future harm to guide action selection. Impaired learning of this probability may be critical for the pathogenesis of anxiety or reckless and impulsive behavior. Here we designed a task for punishment probability learning during reward-guided actions to begin to understand the neuronal basis of this form of learning, and the biological or environmental variables that influence action selection after learning. Male and female Long-Evans rats were trained in a seek-take behavioral paradigm where the seek action was associated with varying probability of punishment. The take action remained safe and was followed by reward delivery. Learning was evident as subjects selectively adapted seek action behavior as a function of punishment probability. After learning, the variables that influenced behavior included reinforcer and punisher value, pretreatment with the anxiolytic diazepam, and sex. In particular, females were more sensitive to probabilistic punishment than males. These studies provide a novel behavioral approach for studying the pathogenesis of anxiety and reckless behavior with inclusion of sex as a biological variable.

**Key Abbreviations:** PPT-Probabilistic punishment task, NS-No shock, S-shock, SABV - Sex as a biological variable

### Introduction

Actions executed toward obtaining a desired outcome are often associated with varying risk of harmful consequences. For example, driving a car to go to a restaurant for dinner (reward) is associated with the probability of getting into a car accident (punishment). This probability increases if driving in a blizzard and increases even further if the driver is drunk. In these contexts, the desired outcome (or reward) is certain after the successful execution of the action. What changes is the probability that a punishment may occur during action execution. Importantly, the punishment probability associated with an action is often learned. In the above

example, one is either taught, or learns by experience, the hazards of driving in bad weather or while drunk. After learning, computation of this probability is fundamental to making the optimal decision to execute, or to inhibit, reward-guided actions. Abnormalities in this computation may lead to an exaggerated assessment of punishment risk, which is a hallmark of anxiety disorders, or to attenuated calculation of this risk, which may be associated with reckless behavior or impulsivity (Bechara et al., 2002; Ersche et al., 2016; Hartley & Phelps, 2012; Jean-Richard-Dit-Bressel et al., 2018; Vanderschuren et al., 2017).

When learned reward and punishment contingencies conflict in the context of achieving a goal they engage anxiety mechanisms such as the behavioral inhibition system to resolve approach and avoidance drives (Corr, 2004; Gray, 1982). Two lines of previous work have provided behavioral models that assess this mode of anxiety on reward seeking behavior. First are conflict paradigms demonstrating that punishment under a fixed probability suppresses reward motivated actions (Azrin et al., 1963; Geller & Seifter, 1960; Pelloux et al., 2015; Vogel et al., 1971). These models, however, do not assess situations where the risk of punishment occurs at differing probabilities for a given expected reward. Second are studies that assess risk aversion through choice procedures. In these tasks different actions can lead to a large reward with a high probability of punishment or small reward delivered with little probability of punishment (Friedman et al., 2015; Simon et al., 2009; St Onge & Floresco, 2010). However, shifting action options to different quantities of reward is different than risk assessment when only one reinforcement option is possible. In the real world choosing different reinforcing outcomes is not always an option and, in the case of addiction, may no longer be salient or perceived as viable (Volkow et al., 2003).

Guided by this, we sought to design a model for punishment probability learning during reward-guided actions with several aims in mind: 1) to characterize the behavioral changes seen in this form of learning, 2) to characterize the biological and environmental variables that influence the decision to execute, or to resist, reward-directed actions after punishment learning, and 3) to assess both safe and risky actions performed under punishment risk. Rats performed a task where actions taken toward obtaining the same reward were associated with changes in the risk of punishment. The task used a chained schedule of reinforcement where an initial “seek” action preceded a “take” action, which then led to reward delivery. Seek and take actions were operationally similar but punishment (mild footshock) probability was introduced, using an ascending design, only contingent on the seek action. Initial learning was quantified by changes in trial completion and action latencies over twelve sessions of training. After learning, the variables that influenced behavior included reinforcer and punisher value, pretreatment with the common anxiolytic diazepam, and sex. The influence of sex as a biological variable (SABV) was explored in detail to reveal critical similarities and differences on how risk of punishment is integrated into reward-guided actions.

## Methods

### Subjects

Adult Long-Evans rats, pair-housed on a reverse 12 h:12 h light/dark cycle, were used. All experimental procedures were performed during the rodents’ dark (active) cycle. For task characterization, 28 adult rats (14 male, 14 female) were obtained from Charles River at postnatal day (PND) 50-55. Separate cohorts with equal male-female representation were used to ensure replicability of performance (n=12-16 per cohort). About a week after arrival, rats were handled and food restricted to 14 g/day. The food restriction was monitored throughout the study to maintain their weight at 90% of free feeding weight, with the target weight increasing by 5 g

per week. Behavioral training began at PND 65-69 at which time males and females on average weighed, 278 g and 208 g, respectively. A third cohort of 17 adult rats (13 male, 4 female) were used to characterize the effects of psilocybin on initial task learning and after learning. Due to the timing of drug treatment this group is not included in the characterization figures for this chapter but make up the psilocybin and  $\pm$ -DOI data in [Figure A.3](#) and [Table 2.2](#). All experimental procedures were approved by the Oregon Health & Science University (OHSU) Institutional Animal Use and Care Committee and were conducted in accordance with National Institutes of Health Guide for the Care and Use of Laboratory Animals.

## Overview of Experimental Design

The probabilistic punishment task is depicted in [Figure 2.1A-B](#). All cohorts were trained to learn the task similarly. After learning, two of the cohorts used for task characterization were treated differently as follows: one cohort (n=16) was tested with shock intensity adjusted for body weight (1 mA/kg, 300 ms) followed by dopamine D2 ligand treatment, and another cohort (n=12) was tested in the task after diazepam treatment followed by satiation, behavior titrated shock intensity, shock extinction, and progressive ratio after a washout period ([see below](#)).

## Apparatus

Operant chambers (Coulbourn Instruments, PA) were used for behavioral testing. They included two nose poke holes, which could be illuminated, on one wall located 2 cm above a grid floor. The grid floor was connected to a shock generator which delivered foot shocks. The food trough was on the opposite wall and was used to dispense 45 mg sucrose pellets (Bio-Serv) and detect food trough entries. Chambers contained infrared activity monitors (Coulbourn Instruments, PA) located on the roof of the chamber which detected rodent body movements in arbitrary units. Graphic State software (version 3.03 and 4, Coulbourn Instruments) running on a windows computer was used for programming the task.

## Training

### Chain schedule training

After 1 d of habituation to the operant box and food trough (60 min, pellet dispensed every 45 s on average), subjects began chained schedule training. Subjects were first trained to respond on the “take” nose poke under a fixed ratio 1 (FR1) for 45 mg sucrose pellets. Daily sessions lasted until 90 pellets were delivered or 90 min elapsed. This phase of training lasted 6 days. Subjects were then trained to respond on the “seek” nose poke. A FR1 response on the seek nose poke (first link of the chain) resulted in extinguishing of the seek nose poke light concurrent with a 750 ms delay. After this delay, the take nose poke was illuminated and completion of an FR1 on the illuminated take nose poke (second link of the chain) resulted in extinguishing of the take nose poke light concurrent with food delivery and food trough illumination. Subjects were required to retrieve the pellet to initiate the 10 s inter-trial interval (ITI). After the ITI, the seek nose poke was illuminated and a new trial began. Responding during the ITI was recorded but had no scheduled consequences. The side of seek and take nose pokes were counterbalanced across subjects. After the completion of 90 trials or 90 min the session was terminated. All subjects were given 4 d of training and were moved to no-shock baseline procedures.

## No-Shock Baseline Procedures

This procedure began after subjects reliably learned the chained reinforcement schedule. The schedule of reinforcement was identical to that in previous training with the exception that the 90 trials were broken into six 15 trial blocks that were 15 min in length. Each block began by a 3 min time-out (TO) period, where all lights were extinguished, followed by a 12 min response period where subjects could earn up to 15 pellets. The nose poke light remained on until the subject made a response on the illuminated nose poke or until the end of the 12 min response period. If the 12 min response period ended before completion of the 15 possible trials, then lights were extinguished, and the subject moved to the next block. If subjects completed 15 trials before the 12 min response period elapsed, all lights were extinguished and responding produced no programmed consequences for the duration of the 12 min response period. Thus, these sessions served as a control to verify that subjects learned and could complete the sequential actions in a block-wise manner without punishment. These control sessions are hereafter referred to as “no-shock” sessions. After subjects performed this procedure for 4 d, they began the probabilistic punishment task.

## Probabilistic Punishment Task (PPT) Procedures

After no-shock baseline procedures, footshock contingencies were introduced for the PPT. The reinforcement schedule was identical to that used in the no-shock baseline procedure but now each block was accompanied by an increase in probability of a mild footshock (0.25 mA, 300-ms) immediately after the seek action. As was the case in no-shock procedures, subjects could complete up to 15 trials in a block. A trial ended upon reward retrieval after completion of the seek and take action sequence or after the 12 min response period elapsed in the absence of action execution. To prevent generalization of the shock to other blocks, the risk of the seek action contingent footshock increased with each successive block in the same ascending order for each session (0%, 6%, 10%, 18%, 30%, 60%). To assess learning of probabilistic punishment we performed the task for 12-consecutive sessions and monitored subject behavior. The task was considered learned when stable behavior was achieved for trial completion. We considered performance stable when two-way ANOVA for trial completion in the last 5 consecutive sessions in either sex revealed no main effect of session or interaction. This is a similar approach to that used in previous studies (Simon et al., 2009).

## Task Characterization

### Body Weight and Behavior Titrated Shock

Subjects in one cohort (n=16) were required to achieve stable performance (as indicated above) using a footshock which was titrated based on body weight (1.0 mA/kg, 300-ms; Cooper et al., 2014; Orsini et al., 2016). In another cohort (n=12), shock intensity was later titrated for each subject until animals showed comparable levels of action suppression of about 50% trial completion for the session (behavior titrated shock). This was done by increasing or decreasing the shock intensity by about 0.05 mA until stable behavior was acquired (three consecutive sessions within 25% of the session mean). This procedure allowed for comparisons of how punishment probability effects reward seeking when the shock intensity produced action suppression in all subjects.

## Satiety Testing

Subjects had 22 h of unlimited access to standard lab chow before a PPT session.

## Shock Threshold Testing

Procedures were performed similar to previously published methods (Söderpalm & Engel, 1988). Subjects were placed in the chamber under red light for 15 min with no scheduled consequences on day 1. On day 2, after 3 min of acclimation to the operant chamber, a footshock was applied about every 40 s (contingent on all 4 paws being on the shock grid). An ascending intensity (0, 0.05, 0.06, 0.08, 0.1, 0.13, 0.16, 0.2, 0.3 mA) was used until the subject responded to the stimulus with a flinch, defined as a sudden rearward jerk immediately after shock administration.

## Extinction of Shock Suppressed Behavior

After a 3 week break, animals were tested for three sessions on the PPT using the behavior titrated shock intensities to ensure that behavior remained stable. They were then tested in extinction sessions where no footshock punishment was administered during the task.

## Progressive Ratio Behavior

Progressive ratio (PR) procedures were performed after extinction of shock suppressed behavior in accordance to previously published methods (Richardson & Roberts, 1996). Briefly, completion of a fixed ratio on what was previously the take nose poke resulted in a food pellet. The response ratio increased according to the following algorithm:

$$\text{Response ratio} = [5 * e^{0.2n}] - 5 \quad (2.1)$$

Where n is the number of reinforcers earned for a given session. PR sessions ran for 5 h or until 45 min elapsed without the completion of a ratio. The last completed ratio was considered the subjects' break point. PR sessions were run for 6 d and all subjects reached a stability criterion of two consecutive sessions with a break point within two step sizes.

## Open Field Testing

In cohort one, animals were tested on the open field 3 d after food restriction but before any operant training. The open field consisted of a gray box (36" x 36") with grey walls (16" height). Sessions were performed during the rodent dark cycle under constant red-light conditions. Subjects were placed in the center of the open field and allowed 10 min to explore the field. Zone entries as well as total distance traveled was monitored by camera and analyzed using Smart software (Version 3.0, Harvard Apparatus). Dependent measures were percent time in the inner region, percent time in the outer region, and locomotor activity (total distance traveled) and were correlated with PPT performance using Pearson correlations.

## Behavioral Pharmacology

### Diazepam Testing

Injectable diazepam (Pfizer/Hospira, Lake Forest, Il.) at a concentration of 5 mg/mL was used. Sterile saline (0.9% NaCl) was used for control injections. Diazepam (1.0 and 2.0 mg/kg) or

saline was administered intraperitoneal 10 min prior to operant sessions with all injections given at a volume of 0.5 mL/kg or less. Doses were separated by at least one day contingent on subjects performing within 25% of baseline (pre-diazepam) levels or after reestablishment of stable behavior (mean overall trials completed for three consecutive sessions within 25%). These doses of diazepam have been shown to produce anxiolytic effects on rats in the elevated plus maze (Pellow et al., 1985).

## Dopaminergic Drug Testing

Quinpirole (Tocris Biosciences) was dissolved in sterile saline and administered intraperitoneally, while eticlopride (Tocris Biosciences) was administered subcutaneously with all injections given at a volume of 1 ml/kg or less. Doses were calculated as salt weights.

Following stable PPT performance subjects from cohort one received D2/D3 agonist Quinpirole (0.03-0.1 mg/kg) or D2 antagonist Eticlopride (0.01-0.03 mg/kg) 15-min prior to PPT sessions with 1 mA/kg footshock in counterbalanced order. These doses were chosen based on previous behavioral studies in rats (Collins & Woods, 2007; Simon et al., 2011). Doses of the same drug were separated by one day contingent on subjects performing within 25% of baseline levels or three consecutive sessions within 25% of the overall mean.

## Psilocybin and $\pm$ -DOI Drug Testing

Psilocybin (a gift from the National Institute of Drug Abuse) and racemic DOI (Sigma-Aldrich) were dissolved in sterile saline and administered intraperitoneally (i.p.) 15 min before the PPT. All injections were given at a volume of 1 ml/kg or less and doses were calculated as salt weights.

Groups were divided into two groups who received psilocybin (1.0 mg/kg) either in the first PPT session or after PPT behavior was stable. After this, shock intensity was titrated to produce comparable suppression of behavior across subjects. The groups were divided into psilocybin and  $\pm$ -DOI groups (counterbalanced for sex and prior psilocybin exposure) and the effects of psilocybin and  $\pm$ -DOI (1.0 mg/kg) were tested using the titrated shock procedures outlined above. A small subset of subjects were tested with a dose of 3.2 mg/kg for each drug after the 1.0 mg/kg dose. Doses were determined by previous behavioral studies in rats (Fox et al., 2010; Winter et al., 2007).

## Data Analysis

### Task Measures

We assessed both no-shock and PPT sessions. Trial completion was measured as the percentage of completed trials (of the 15 possible) for each block, while action latencies were defined as time from nose poke cue onset to action execution. Group mean values for each risk block or comparing risk and no-risk blocks are presented as mean  $\pm$  SEM in all figures. In addition to assessing trial completion over each punishment risk we also analyzed overall trial completion to determine if subgroups emerged that were differentially sensitive to punishment based on an 80/30% trial completion split where  $>80\%$  completion was resistant, 30-80% completion was moderate, and  $<30\%$  completion was sensitive to punishment (Gabriel et al., 2019). For action latency measures an exclusion criteria was utilized where data were only included in analyses if the subjects completed two or more trials for a given block. Further non-complete actions were not included in latency analysis. This was done to prevent errant data points from

skewing the data. Because the lack of some latency data from subjects not completing any trials complicates the ability to perform repeated measures ANOVA, latency behavior in risk associated trials was collapsed across the five blocks with risk of shock (6%-60%) to yield values for behavioral indices of action latency changes when punishment risk was present versus the no risk (0% risk) block.

## Behavioral Modeling

Behavioral modeling of punishment probability dependent changes in trial completion was performed by fitting a sigmoid using a four-parameter logistic regression equation (4PLR) with the least squares method to the three stability days when shock was titrated for behavioral output. The 4PLR utilized the following equation:

$$Y = d + (a - d)/(1 + 10^{((c-X)*b)}) \quad (2.2)$$

Where Y is the percent of trials completed, X is the log risk of shock, a is the top of the asymptote, constrained to be less than or equal to 100, d is the bottom asymptote, c is the X value associated with a 50% decrease in behavior, and b is the measurement of steepness of the curve. To assess the integration of increasing probabilistic punishment, we quantified the slope of the linear portion of the sigmoid between high and low action by fitting a linear trendline to the bend points of the sigmoid. Briefly, we used the estimates for the top and bottom asymptote (a and d, respectively) and applied the following formula:

$$Upper = (a - d)/(1 + k) + d \quad (2.3)$$

$$Lower = (a - d)/(1 + 1/k) + d \quad (2.4)$$

Where k is a constant equal to 4.6805 (Sebaugh & McCray, 2003). A linear trendline was then fit to the upper and lower values to yield a slope for the linear portion of the sigmoid. Modeling was performed in GraphPad Prism (Version 8).

## Statistical Analysis

Statistical procedures utilized either an ANOVA or mixed-effects model. Three-way ANOVA was used with factors of Risk Blocks, Sex, and Session type and followed up with two-way or one-way ANOVA where appropriate. Because of smaller sample sizes in pharmacological, extinction, titration, and satiety procedures, we assessed these manipulations with two-way ANOVA using factors of Risk Block and Manipulation or Treatment. Tests were done with the Greenhouse-Geisser correction for sphericity violation where appropriate. Activity counts during the ITI and during the shock period (i.e. the 300-ms period during which the shock was administered) were also quantified and activity during blocks was collapsed and compared using two-tailed t-tests. Post-hoc comparisons were performed using the bonferroni correction. An  $\alpha$  level of .05 was used for all tests. Behavior data files were processed using custom written scripts in Python (version 2.7 and 3.0) and all statistical analyses were performed in GraphPad Prism (Version 8, San Diego, CA) or R (Version 3.6.1, ez package).

## Excluded Data

Behavioral data from four individual subjects' sessions were excluded due to feeder malfunctions.

# Results

## Learning of the probabilistic punishment task

Guided by other tasks (Pelloux et al., 2015) we utilized a procedure where an instrumental “seek” action in one nose poke was followed by a “take” instrumental action in a second nose poke, which then led to reward delivery (Figure 2.1A). The “seek” action was punished by delivering of a mild footshock after rats completed the action. The probability of the “seek” action being punished escalated in a blockwise manner throughout a single session (Figure 2.1B).

Rats first learned to perform the sequential actions without punishment, which are designated as no-shock sessions, for at least four sessions. To validate task learning and to further mirror other procedures assessing risky choice, we determined stable PPT behavior by identifying when five consecutive sessions produced no significant effect of session nor session by risk interaction in a two-way ANOVA for each cohort (Simon et al., 2009). These methods determined that stable behavior was observed in sessions 4-11 (range for all cohorts; main effect of session or session by risk block interaction:  $F$  values  $>1.97$ ,  $p$  values  $>.13$ ). Trial completion and seek action latency for the first 12 sessions can be seen in Figure A.1. After assessing the first 11 PPT sessions, we noted that task behavior differed in Session 1, when animals were first learning of the shock contingency, compared to Sessions 4-11 where the task was learned. In Session 1, there was an overall resistance to probabilistic punishment in the 6%-18% risk blocks that decreased after subjects learned the task in Sessions 4-11 (session by risk block interaction:  $F(3.07, 83.05)=18.04$ ,  $p <.01$ ; post hoc  $p$  values  $<.021$ ; Figure 2.1C).

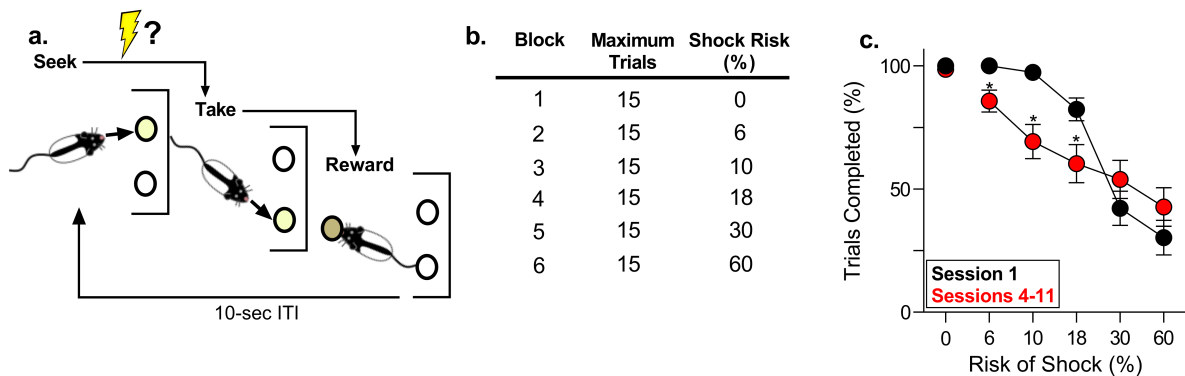


Figure 2.1: Outline and characterization of learning in the probabilistic punishment task. **a.** A schematic demonstrating a given trial and **(b.)** structure of a given session for the probabilistic punishment task. **c.** Probabilistic punishment related decreases in task behavior differed before learning (Session 1, black) compared to after animals had learned the task (Sessions 4-11, red) as trial completion perseverated for the first 3 risk blocks in Session 1 compared to Sessions 4-11. \*  $p <.05$  vs Session 1,  $n=28$ .

## Characterization of probabilistic punishment task after learning

Collapsed data for the last two no-shock sessions and the PPT sessions when performance under shock risk was stable as determined by ANOVA are shown in Figure 2.2A-E. As noted earlier, trial completion decreased as a function of punishment probability (risk block by session type interaction:  $F(2.3, 60.04)=32.27$ ,  $p >.0001$ ), with significant decreases for all risk blocks in PPT (i.e. shock) sessions compared to the corresponding block in the no-shock sessions (post hoc  $p$  values  $<.029$ ). Inspection of these data at the individual level revealed considerable between-subject variability in punishment resistance, with subjects showing anywhere from complete

punishment resistance to little. Dividing subjects based on trial completion into punishment resistant ( $> 80\%$  trial completion), moderate (30-80% trial completion), and sensitive ( $<30\%$  trial completion) subgroups resulted in 15/28 resistant, 8/28 moderate, and 5/28 sensitive subjects (Figure 2.2A).

The suppressive effects of probabilistic punishment were observed during the latency to complete the seek action, i.e. the risky action (risk by session type interaction:  $F(1,26)=27.9$ ,  $p < .001$ , Figure 2.2B). Increased seek action latency was observed in the risk blocks of PPT sessions compared to the corresponding blocks in no-shock sessions (post hoc  $p < .001$ , Figure 2.2B). Overgeneralization of shock risk to the 0% risk block, i.e. first block, was not observed (post hoc  $p = .99$  vs. no-shock). Of note, variability increased at higher risk blocks because fewer subjects completed more than one trial (21/28 subjects). Subjects also demonstrated anticipation of footshock as the latency to complete the first seek action of a block increased with punishment risk compared to no-shock sessions (risk by session type interaction:  $F(1,26)=29.08$ ,  $p < .001$ ; Figure 2.2C) and was also specific to blocks with a risk of shock (post hoc  $p < .01$ ).

Seek actions were followed by a small ( $<1$  s) but significant increase in latency to complete the take action in PPT sessions (risk by session type interaction:  $F(1,26)=9.45$ ,  $p = .005$ , Figure 2.2D). Because in some trials, the take action is operationally preceded by footshock, we further investigated if the increase in take action latency is related to receiving a footshock. A one-way ANOVA was used to compare take action latency for take actions preceded by footshock (punished) and no footshock (unpunished) in PPT sessions with take actions from the corresponding blocks (i.e. blocks 2-6) in no-shock sessions. This analysis revealed take action latency increases seen in PPT sessions were related to receiving the footshock punishment (main effect of trial type:  $F(1,07, 29.1 = 17.3$ ,  $p < .01$ ). Take action latency in punished trials was increased compared to the no-shock sessions and the unpunished trials of punished sessions (post-hoc  $p$  values  $\leq .001$ ) while unpunished trial latencies were comparable to that of the no-shock sessions (post hoc  $p = .99$ , Figure 2.2D).

Reward retrieval latency was not influenced by risk of shock (risk by session type interaction:  $F(1,26)=0.31$ ,  $p = .58$ ; Figure 2.2E) but modestly increased in later blocks compared to earlier blocks regardless of whether shock risk was present (main effect of block:  $F(1,26)=27.6$ ,  $p < .001$ ). This suggests a lack of overgeneralization of punishment to the context.

According to theories of the behavioral inhibition system, it is also worth noting that behavioral inhibition system activation is believed to increase arousal, which could manifest as behavioral displacement under states of anxiety (McNaughton & Corr, 2004). To assess this we also asked if displacement actions were present in the form of responding on the take nosepoke when the the seek light was illuminated (i.e. when take actions were not appropriate). We found support for increased arousal from conflict in our task, as displacement actions were significantly increased in risk blocks (risk block by session type interaction:  $F(3.33, 91.59)=13.2$ ,  $p < .001$ , all *post-hoc*  $p$  values  $< .043$  for risk blocks; Figure 2.2F).

In one cohort we also assessed innate anxiety in the open field before task training to assess if individual patterns exploratory behavior would be associated with learned punishment related behavior in the PPT ( $n=16$ ; Table 2.1). Individual variability in punishment resistance was not associated with exploratory behavior in the inner or outer zones of the open field or overall locomotor activity. Similarly, increases in seek latency during risk blocks were not associated with increased time spent in the inner or outer zones of the open field, nor with activity as assessed through locomotor activity (all  $p$  values  $> .06$ , uncorrected).

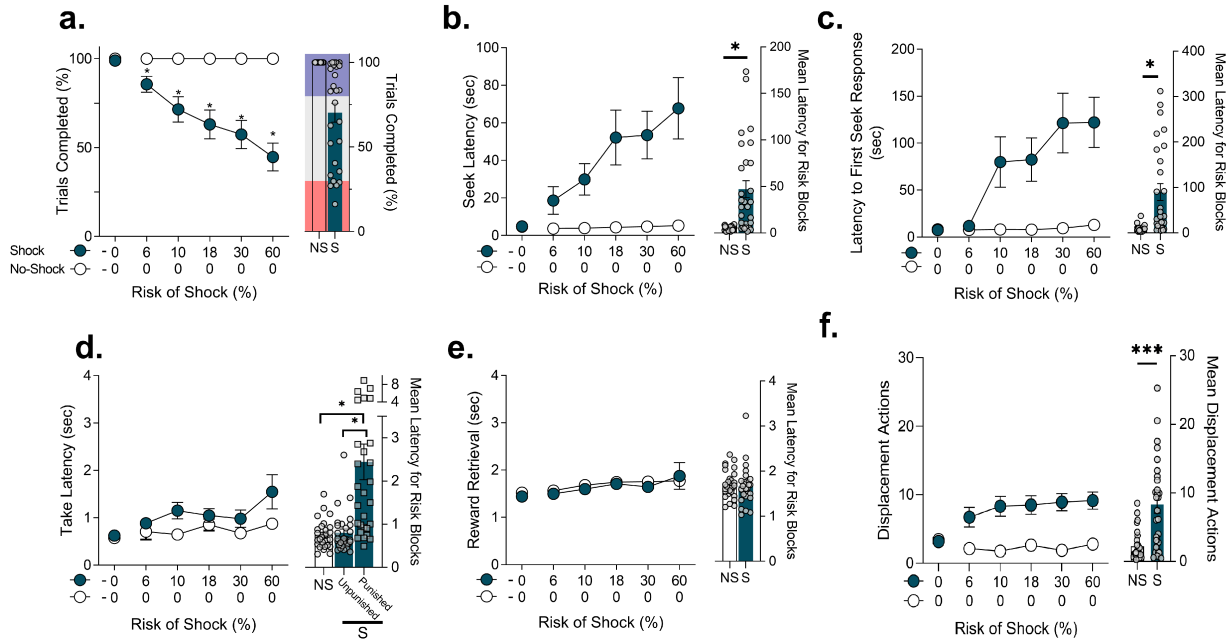


Figure 2.2: Assessing the effects of probabilistic punishment on task behaviors after learning. **a.** The number of trials completed in each block decreased on average in the probabilistic punishment task sessions where shock risk was present (S-blue) but not in no-shock sessions (NS-white). Subgroups with differing levels of punishment resistance emerged, blue area= punishment resistant, grey area = moderate, red area=punishment sensitive (**a-right**). **b-c.** Increasing risk of shock was also associated with an increase in latency to complete the risky “seek” action during and at the start of risk blocks. **d.** The take action latency modestly but significantly increased under shock risk. **e.** Latency to retrieve the food reward was not affected by shock risk. **f.** Displacement behavior increased in blocks with shock risk. NS= no-shock, S=shock.\*  $p < .05$  vs no-shock.  $n=28$  for trials completed and for mean risk block latencies. Individual data points are depicted as grey circles.

Table 2.1: Pearson correlation ( $r$ ) values of open field (OF) behavior with probabilistic punishment task measures

	Trial Completion	Seek Latency	Take Latency	Reward Retrieval
OF Inner	-.17	.19	-.06	-.21
OF Outer	.03	-.09	.01	.24
OF Activity	.48	.39	.32	.38

## Behavioral and pharmacological manipulations of probabilistic punishment task behavior

### Reinforcer and punisher value manipulations

Value of reward or punishment may change even after action-punishment contingencies are learned. Thus, animals must appropriately adapt their behavior to such changes. To assess if the current task is sensitive to shifting reward or punishment contingencies, we did three additional behavioral experiments to manipulate reinforcement and punishment values after task learning.

To decrease the reinforcing value of the food reward, subjects were given 22 h of ad libitum access to standard chow in the home cage before the task. This manipulation decreased

punishment resistance when there was 30%-60% risk of shock (risk block by satiety interaction:  $F(2.9,32.4)=3.02$ ,  $p=.045$ ; post hoc  $p$  values  $< .046$ ; [Figure 2.3A](#)) but not during the 0%-18% risk blocks (post hoc  $p$  values  $> .24$ ). Satiation also increased latency to complete the seek action (risk by satiety interaction:  $F(1,10)=24.04$ ,  $p<.01$ ; [Figure 2.3B](#)) an effect seen more profoundly in risk blocks (post hoc  $p<.01$ ) but also in the 0% risk block (post hoc  $p=.045$ ).

To assess if the task was sensitive to the value of punishment, and to help produce comparable behavioral levels across subjects, we adjusted the shock intensity until levels of action suppression were similar between subjects. Stable behavior was acquired after 3-12 d of adjustment of shock intensity in approximately 0.05 mA increments. Subjects reliably responded to manipulation in the intensity of punishment which overall decreased punishment resistance (titration by risk block interaction:  $F(2.2,24.4)=22.8$ ,  $p<.001$ ; [Figure 2.3C](#)). Post hoc analyses revealed that, overall, task completion decreased after shock adjustment in 30-60% risk blocks ( $p<.01$ ). Seek action latency during risk blocks also increased after titration of shock intensity (titration by risk interaction:  $F(1,11)=32.2$ ,  $p<.01$ ; [Figure 2.3D](#)), but no effect of titration was observed on seek latency in the 0% risk block (post hoc  $p=.21$ ).

To assess if subjects could flexibly adapt to the omission of punishment, subjects underwent extinction sessions in which the probabilistic footshock was no longer presented after the seek action. Extinction of shock risk increased task completion in risk blocks (extinction day by risk block interaction:  $F(3.1,33.6)=24.95$ ,  $p<.001$ ; [Figure 2.3E](#)). This was apparent for blocks with previous shock risk of 10% or greater for the first and second extinction session. Further, increases in trial completion were observed in the second extinction day compared to the first extinction day (main effect of session:  $F(1.47,16.1)=134.5$ ,  $p$  values  $< .005$ ). Extinction of probabilistic punishment also resulted in decreases in seek latency (extinction day by risk block interaction:  $F(1.5,16.4)=15.46$ ,  $p < .001$ ; [Figure 2.3F](#)). As early as the first extinction session, seek latency in risk blocks decreased non-significantly from 66 s to 26 s (post hoc  $p=.078$  vs shock). However a continued significant decreases in seek latency to 4 s was observed in Extinction 2 (post hoc  $p<.001$  Extinction 2 vs Shock). No changes were seen in the 0% risk block for seek latency between the shock risk sessions and either of the extinction sessions (all  $p$  values  $>.11$ ).

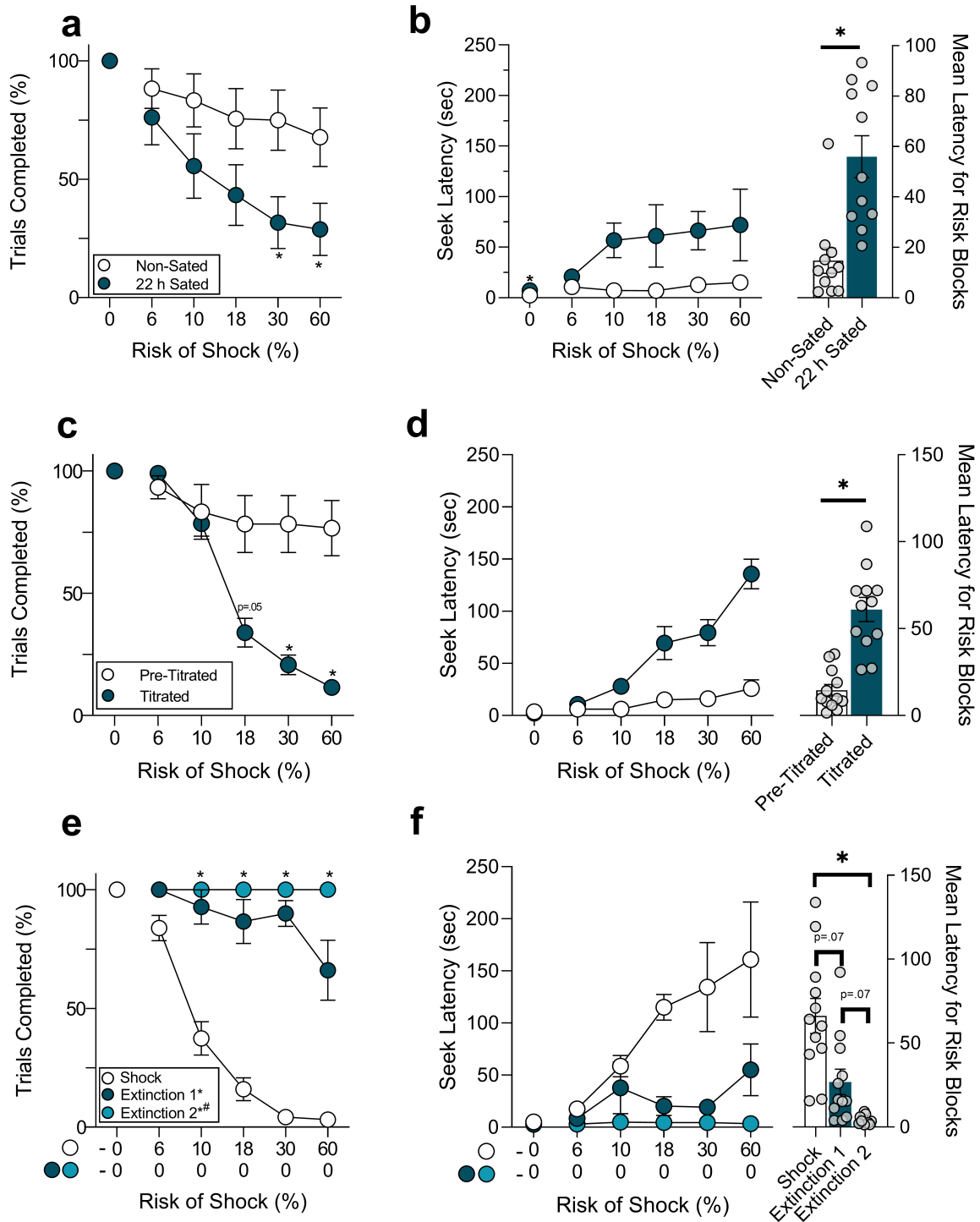


Figure 2.3: Behavioral effects of manipulation of reinforcer and punisher value. **a.** Decreasing reward value with 22 h of home cage access to ad libitum food prior to a session (blue) decreased trial completion under probabilistic punishment and **(b.)** potentiated increases in latency to complete the punished seek action compared to the session prior (white). One subject (female) was excluded from seek latency analysis in panel b due to inability to complete more than one trial in any of the risk blocks. **c.-d.** Adjusting the subjective value of the footshock punishment by changing shock intensity (blue) resulted in changes in trial completion under probabilistic punishment and seek action latency. **e.** Extinguishing the risk of punishment by omission of the footshock presentation resulted in increase in trial completion and **(f.)** decreased seek action latency over the two extinction sessions (blue/light-blue). \* $p < .05$  vs. white symbols, # $p < .05$  extinction 1 vs extinction 2.  $n = 12$  except where noted otherwise. Individual data points are depicted as grey circles.

## Treatment with diazepam

We asked if the behavioral responses to probabilistic punishment have relevance to anxiety states by testing the impact of the anxiolytic drug and GABA<sub>a</sub> receptor positive allosteric modulator diazepam (1 and 2 mg/kg) on the PPT. These low doses of diazepam were chosen so that motor behavior would not be impacted to the degree that animals could not complete the task. 1.0 mg/kg diazepam was first tested when all subjects were given the same 0.25 mA shock intensity and did not change trial completion or seek action latency (main effect of treatment:  $F(1,11)=0.14$ ,  $p=.71$ ,  $F(1,11)=.23$ ,  $p=.64$ ; **Figure 2.4A-B**). However, it was possible that a ceiling effect precluded detection of significant changes for many of the subjects. We, therefore, tested diazepam after action suppression was titrated using shock intensity (as shown in **Figure 2.3C**). To control for the ascending dose order or additive effects we also analyzed an additional saline injection session that was at least 48 h after the last diazepam test. Diazepam produced increases in trial completion under probabilistic punishment (main effect of treatment:  $F(2.1,22.93)=6.9$ ,  $p<.01$ ) for both doses (post hoc  $p$  values  $<.022$ ; **Figure 2.4C**). These anti-conflict effects of diazepam complicated interpretation of seek action latency changes, as subjects were completing trials at higher risk blocks than at baseline. Consequently, we assessed seek latency up to the 10% risk block as this was the risk block where all subjects were completing more than two trials (i.e. did not meet exclusion criteria) on the first saline day. Diazepam attenuated seek latency increases (risk by treatment interaction:  $F(1.57,17.3)=7.76$ ,  $p=.02$ ; **Figure 2.4D**) at the 6% risk block (post hoc  $p$  values  $<.04$ ) and non-significantly at the 10% risk block for 2 mg/kg diazepam (post hoc  $p$  values = .07 1 mg/kg and .051 2 mg/kg). These effects were not observed at higher risk blocks, though there were increased amounts of variability (data not shown). Importantly, these low doses of diazepam had no effect on locomotor reactivity to the shock with comparable activity levels seen on the saline day (mean<sub>Diazepam</sub>  $\pm$  SEM:  $2.3\pm 0.24$ , mean<sub>Saline</sub>  $\pm$  SEM:  $2.13\pm 0.23$ ; paired  $t$ -test:  $t(10)=0.52$ ,  $p=.62$ ).

### Diazepam Treatment

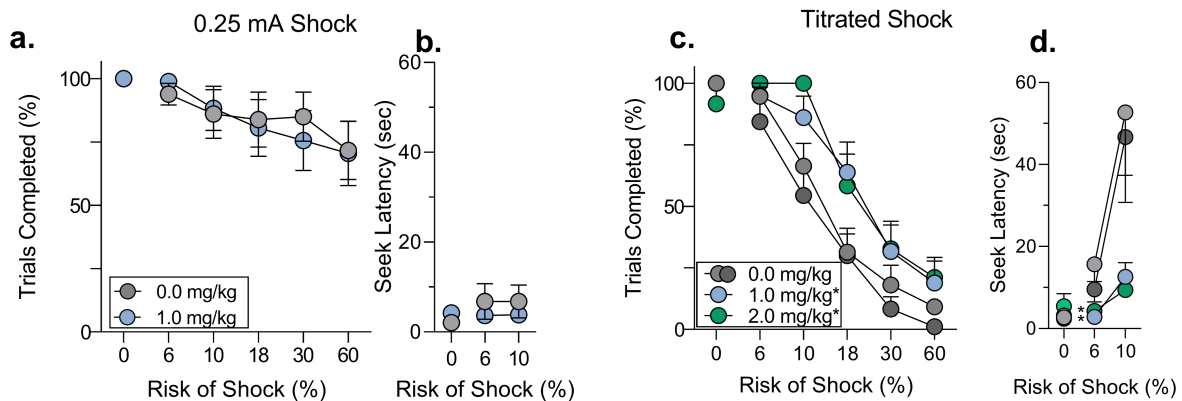


Figure 2.4: Effects of systemic diazepam treatment on PPT Behavior. **a.-b.** Under conditions where the shock intensity was fixed at 0.25 mA for all subjects no effects of 1.0 mg/kg diazepam (light blue) were observed on trial completion nor seek action latency compared to saline (light grey). **c.** After behavior was titrated such that all subjects showed sensitivity to probabilistic punishment, 1.0 and 2.0 mg/kg diazepam increased resistance to punishment and **(d.)** attenuated increases in seek action latency at lower risks. Importantly task behavior returned to saline levels after diazepam testing (dark grey). \* $p<.05$  1.0 and 2.0 vs 0.0 mg/kg.  $n=12$ .

## Treatment with dopamine D2-ergic drugs

Dopamine D2 receptor drugs produced dose dependent downward shifts in the PPT risk effect curves. D2/D3 receptor agonist quinpirole significantly decreased punishment resistance at both doses tested (effect of dose:  $F(1.73,26.07)=17.14$ ,  $p<.001$ ; see [Figure A.2A](#)), an effect which was observed at doses which produced general locomotor disruption and slowed action latency in the 0% risk block. However, it is of note that such disruptive locomotor-suppressing effects were highest when actual task performance was greatest (i.e. the 0% risk block). As such, the fact that the general shape of the risk effect curves was maintained when peak disruptive effects occurred may suggest the punishment resistive effects are not entirely due to non-selective behavioral disruption. Eticlopride produced a similar suppressive effect on behavior at the highest dose tested (effect of dose:  $F(1.25,18.82)=15.31$ ,  $p<.001$ ; see [Figure A.2B](#)), again this dose of drug generally disrupted behavior.

Surprisingly, there was a sex by treatment interaction (sex by dose interaction:  $F(2,28)=8.93$ ,  $p<.01$ ) which revealed that females were less sensitive to the effects of quinpirole on punishment resistance, but were equally susceptible to quinpirole’s locomotor suppressing effects compared to males (sex by dose interaction:  $F(2,28)=2.3$ ,  $p>.11$ ; data not shown). The effects of eticlopride did not vary by sex (sex by dose interaction:  $F(2,28)=.05$ ,  $p=.95$ ).

## Treatment with 5HT<sub>2a</sub> agonists psilocybin and $\pm$ DOI

We failed to observe any affect of psilocybin treatment on punishment resistance in the first punishment session nor after the PPT was learned [Figure A.3A-B](#). Additionally, psilocybin treatment in the first session did not influence the punishment resistance of stable behavior ( $F$  values  $< 1.0$ ,  $p$  values  $>.34$ ).

To prevent the occlusion of anxiolytic effects due to ceiling effects (as seen with diazepam, [Figure 2.4](#)), we reassessed psilocybin and, as a comparison, an alternative 5HT<sub>2a</sub> agonist  $\pm$ DOI after titrating shock intensity. We observed a marginally significant (effect of drug:  $F(1,8)=5.18$ ,  $p = .052$ ) increase in punishment resistance following psilocybin treatment, while  $\pm$ DOI surprisingly produced no effect (Effect of drug:  $F(1,7)=0.47$ ,  $p=.52$ ; see [Figure A.3C-D](#) and [Table 2.2](#)). Higher doses of both drugs produced behavioral suppression in the safe 0% risk block and later.

Table 2.2: Effects of systemic treatment of dopaminergic, GABAergic, and serotonergic drugs on probabilistic punishment task behavior

Drug	Dose (mg/kg)	Mechanism	Effect
Diazepam	1.0, 2.0	GABA PAM	Anti-Conflict
Eticlopride	0.01, 0.03	D2 Antagonist	Pro-Conflict
Quinpirole	0.03, 0.1	D2/D3 Agonist	Pro-Conflict
Psilocybin	1.0, 3.2	5HT <sub>2a</sub> Agonist	Weakly Anti-Conflict
$\pm$ -DOI	1.0, 3.2	5HT <sub>2a</sub> Agonist	No Effect

## Sex as a biological variable in probabilistic punishment resistance

The work above was done in both male and female rats. After the completion of data collection, without *a priori* hypothesis, we analyzed behavioral data with sex as a factor. Although the aim of this study at the beginning was not to study sex differences, the constructs of anxiety and impulsive reward seeking relevant to this task show sex differences in prevalence. Overall the learning pattern of the task was similar between sexes, with stabilization of both male

and female behavior after about 4-5 sessions as seen in [Figure 2.5A](#) (main effect of session:  $F(3.27, 84.8)=9.98$ ,  $p<.001$ ) which did not interact with sex (sex by session interaction:  $F(11,285)=1.67$ ,  $p=.08$ ).

Once behavior was stable, however, females displayed increased sensitivity to probabilistic punishment compared to males with greater blockwise decreases in trial completion for females compared to males (sex by risk block by session interaction:  $F(5,130)=7.2$ ,  $p<.001$ ; [Figure 2.5B](#)). This difference was only present when the risk of shock was 10% or greater (post hoc  $p$  values  $<.03$ ) and not during 0% or 6% risk blocks (post hoc  $p$  values  $>.07$ ). Interestingly, the ‘sensitive’ subgroup observed in [Figure 2.2A](#) exclusively included female subjects, whereas moderate and resistant subgroups contained both males and females albeit in different proportions ([Figure 2.5C](#)).

Other task behaviors were also significantly different between males and females. While latencies to complete the punished seek action increased during risk blocks compared to no-shock conditions, females showed heightened increases in seek latency during risk blocks in PPT sessions (sex by risk block by session interaction:  $F(1,26)=5.7$ ,  $p=.02$ , post hoc  $p<.01$ ; [Figure 2.5D](#)). No differences were observed for seek action latencies at the 0% risk block when no shocks were given (post hoc  $p=.99$ ). Females were slower to complete the take action compared to males (main effect of sex:  $F(1,26)=7.03$ ,  $p=.014$ ). While these differences appeared to depend on receiving punishment (sex by trial type interaction:  $F(2,52)=3.34$ ,  $p=.043$ ; [Figure 2.5E](#)), post hoc testing indicated no significant differences between males and females in the 0% risk block, and between unpunished or punished trials in risk blocks (post hoc  $p$  values  $>.088$ ). Importantly, both males and females showed similar latencies to retrieve the food reward, suggesting comparable motivation to acquire the reward (main effect of sex or sex by risk block by session interaction: all  $F$  values  $< 1.1$ ,  $p$  values  $>.29$ ; [Figure 2.5F](#)). To more directly assess underlying reward motivation differences, a cohort was also tested with a PR task following extinction of probabilistic punishment. Males and females displayed comparable motivation, as measured through PR break point, to obtain the food reward (unpaired  $t$ -test:  $t(10)=0.72$ ,  $p=.48$ ; [Figure 2.5G](#)).

To determine if these effects were due to differences in body size, in one cohort we tested performance after adjusting shock intensity for body weight (1 mA/kg). For males it was observed that trial completion decreased when the risk of shock was 30% or higher (effect of risk block:  $F(1.6,11)=6.45$ ,  $p$  values  $<.04$ ). Females however showed significant decreases at 10% or higher shock risks (effect of risk block:  $F(1.6,11.4)=11.6$ ,  $p$  values  $< 0.001$ ). Importantly body weight adjusted shock intensity had no effect on the amount of trial completion under probabilistic punishment for either sex (effect of shock intensity:  $F$  values  $<.1$ ,  $p$  values  $>.7$ ; [Figure 2.5H](#)), suggesting body weight is not a critical factor in punishment resistance. This was further supported by a second cohort exposed to a shock threshold procedure where no differences between sexes were seen in shock intensity required to elicit a flinch response (unpaired  $t$ -test:  $t(10)=.71$ ,  $p=.49$ ; [Figure 2.5I](#)). These data suggest differences in punishment resistance were not due to general sensory differences between males and females. Finally, both sexes showed similar activity in response to the shock and during ITI periods suggesting similar reactivity to the shock despite body weight differences (unpaired  $t$ -tests:  $t$  values  $< 2.06$ ,  $p$  values  $>.05$ ; [Figure 2.5J](#)).

While estrous cycle was not systematically investigated in the present study, analysis of female subject data during the 5 consecutive stability sessions (the length of the estrous cycle) did not reveal any consistent fluctuations on a day to day basis ([Figure A.4](#)). To assess if overall trial completion or seek latency were differentially affected by sex in other tasks manipulations such as shock extinction, satiety tests, and diazepam treatment, we performed additional two-way ANOVAs using sex and manipulation or treatment as factors. No significant sex-by-treatment or sex-by-manipulation interactions were observed for overall trial completion ( $F$  values  $< 2.1$ ,

p values  $>.12$ ) or mean seek latency in risk blocks (F values  $< 1$ , p values  $>.46$ ).

## **Integration of probabilistic punishment in males and females after titrating shock intensity**

Both males and females showed changes in task behavior when we adjusted shock intensity to produce similar overall levels of trial completion (Figure 2.6A). These procedures produced nearly identical probabilistic punishment resistance and seek latency increases between sexes (effect of sex or sex by risk block interaction: F values  $< 1.5$ , p values  $> .26$ ; Figure 2.6B-C). However, the intensity of shock needed to achieve these comparable behavioral results was significantly higher in males compared to females (unpaired t-test:  $t(10)=3.47$ ,  $p<.01$ ; Figure 2.6b insert). To better understand if males and females integrate risk of punishment into reward guided actions differently, we modeled action suppression by risk of punishment using a 4 parameter logistic regression (4PLR) similar to that used to assess cost-benefit decision making (Friedman et al., 2017). We fit a sigmoid to individual data from titrated shock trials, when presumably the subjective suppressive effects of the shock were equal, and revealed three distinct phases; a high action phase, a transition phase, and a low action phase (Figure 2.6D-F). Effects of probabilistic punishment on action suppression (trial completion) was well predicted by the model ( $R^2=0.64-0.97$ ) and comparison of small sample size corrected akaike information criteria values between the 4PLR model and a linear regression revealed the 4PLR was the preferred model (paired t-test:  $t(11)=2.4$ ,  $p=.03$ ). The use of the 4PLR model allowed us to assess whether the integration of punishment risk into behavioral actions differed between sexes. This was achieved by fitting a straight line to the transition from high to low action (i.e. the linear portion of the sigmoid; Figure 2.6D). The similar slope steepness (unpaired t-test:  $t(10)=0.30$ ,  $p=.76$ ; Figure 2.6G) revealed that males and females demonstrated comparable patterns of integrating punishment risk when transitioning from high to low action.

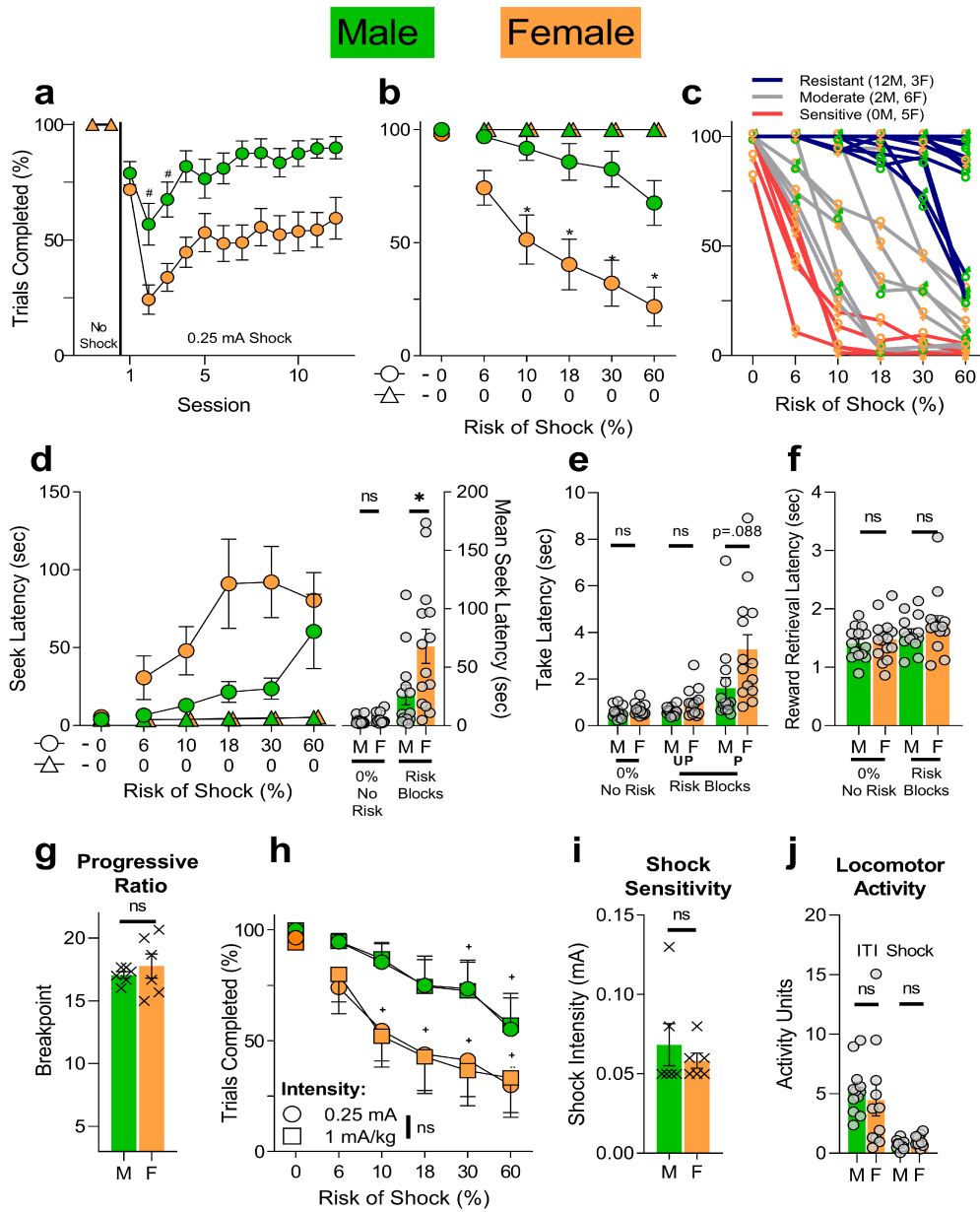


Figure 2.5: Assessment of sex differences in the probabilistic punishment task. Male data are shown in green while female data are shown in orange. **a**. Patterns of task acquisition were similar between males and females, both of which showed stable behavior after about session 4-5. **b**. Generally, males were less sensitive to punishment compared to females, i.e. males completed more trials than females after task behavior stabilized (circles) though they did not differ when no footshock risk was present (triangles) **c**. Individual data demonstrating punishment resistant (blue lines) and moderate (grey lines) subcategorized males were observed but only females were observed to be resistant, moderate, and sensitive (red lines) to punishment. **d**. Females showed increased latencies to complete the seek action compared to males when the risk of shock was present. **e**. Take action latency was also increased in females compared to males, though this effect was not uniquely attributed to risk nor if the take action was preceded by a punished (P) or unpunished outcome (UP). **f**. Latency to retrieve the reward did not differ between sexes. **g**. Motivation for sucrose pellets was similar as assessed through a progressive ratio task. **h**. Titrating shock intensity based on body weight failed to exert a significant effect in males or females. **i**. Flinch sensitivity to the shock did not differ between sexes. **j**. Sex differences did not appear to be related to general locomotor activity nor shock reactivity during the task. \* $p < .05$  male vs. female, # $p < .05$  vs Session 1, + $p < .05$  vs 0% risk block, ns= non-significant,  $n=12-28$ . M=male, F=female. Individual data points are depicted as grey symbols and x's.

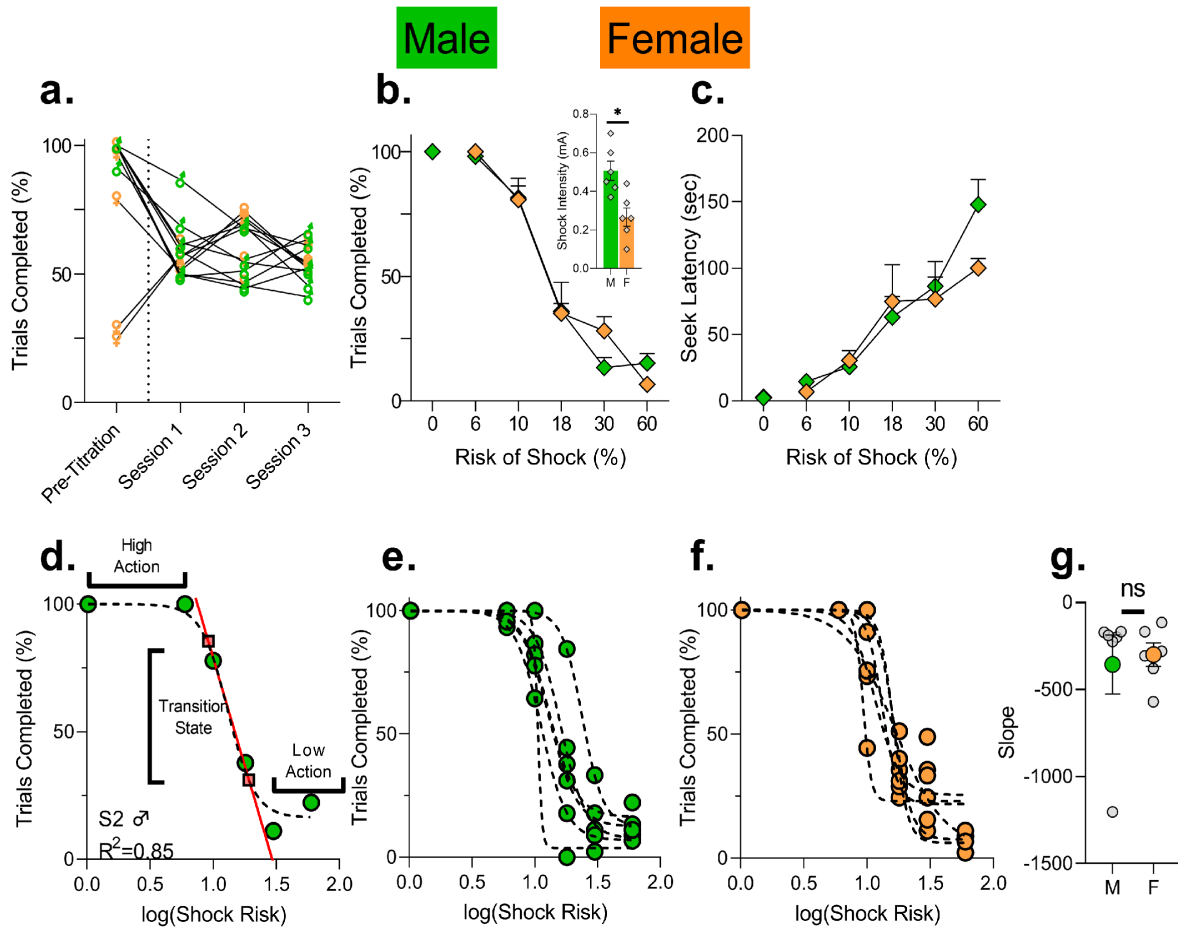


Figure 2.6: Titration of behavior using shock intensity and modeling for males and females. **a.** Altering shock intensities produced increases or decreases in task completion to result in near 50% suppression of task completion. **b-c.** These procedures produced near identical changes in trial completion and seek action latency in males and females. **b-insert.** Higher shock intensity for males was required to produce comparable male and female behavior. **d.** A representative subject's data showing high, low, and transition states and the fit of the 4PLR model (dashed line). The linear portion of the sigmoid was determined by fitting a linear line (red line) to the bend points of the sigmoid (red squares). **e-f.** Individual risk effect curves revealed that task behavior was well captured using a 4PLR to assess high action, low action and transition states for behavior during risk of punishment for both males and females. **g.** The steepness of the transition state (i.e. the linear portion of the sigmoid) was not different between males and females. M=male, F=female. Individual points are depicted as grey symbols.  $n=6/\text{sex}$ ,  $*p<.05$ , ns = not significant.

# Discussion

Actions we execute to obtain a reward are often associated with the probability of harm occurring. Learning about this probability allows for appropriate computation of risk and guides future action by weighting that risk against the value of obtaining a reward. Impaired learning of this probability may be critical for the pathogenesis of anxiety or reckless and impulsive behavior. To investigate this mode of learned anxiety, we developed a seek-take instrumental task. Animals learned to adapt to probabilistic punishment and exhibited a stable but individualized pattern for inhibiting reward-guided actions as a function of punishment probability. The task was further characterized by establishing that sex is a critical biological variable and that inhibition of behavior as a function of punishment probability is sensitive to manipulations in reinforcer and punisher value, and anxiolytic treatment.

## Punishment probability learning during reward-guided actions

Our task provides a tool to measure probabilistic punishment learning. During the first session where animals were exposed to the risk of punishment during the seek action, their behavior remained unchanged until the risk increased to 18%. In subsequent sessions, animals adjusted their behavior earlier. A critical aspect of this learning process was that a robust change in behavior was only seen for the risky seek actions, and not for risk-free take actions or reward retrieval actions. This supports the notion that changes in behavior as training progressed were not due to reduced motivation or general motor effects, and were due to punishment probability learning.

The stability of performance after learning allowed us to examine the effect of several manipulations on performance. This led to several key observations on how reward-guided actions are impacted by punishment probability. First, although behavior stabilized, there was a high level of individual variability, in particular with respect to when subjects stopped responding. Some subjects displayed complete resistance to the risk of punishment while others were more sensitive. Open field behavior, a traditional method of assessing anxiety, was not associated with these individual differences. This indicates that individual differences observed in our task are not due to innate anxiety but relate to learning and expression of punishment probability. Behavioral differences were also absent in the no-shock trials indicating that motivation to work for reward, in the absence of punishment risk, was not a factor in differences to risk of punishment. Thus, the present task provides a valuable behavioral tool for future investigation of individual differences in the emergence of phenotypes related to anxiety and impulsivity.

Second, after learning, behavior was flexibly influenced by changes in the value of the reinforcer or punisher. The sensitivity of behavior in the current task to value manipulation is consistent with human behavior providing a valid clinical model for assessing physiological or maladaptive reward and punishment valuation or risk depreciation (Bechara et al., 2002; Hartley & Phelps, 2012).

Third, the increases in the latency of the seek action may provide a novel model for the anxious apprehension state commonly associated with some anxiety disorders. Anticipation of, and adaptation to, potential harm are fundamental features of anxiety (Grillon et al., 2009). Consistent with this notion, the anxiolytic diazepam reduced the impact of punishment risk on seek action execution and latency. In the context of anxiety, another interesting and clinically relevant observation was that when the risk of shock was removed after learning, seek action latency remained elevated until the second extinction session. The sustained anxiety-like behavior despite extinction of punishment may provide a useful model for assessing normal or pathological coping with changes in punishment risk over time.

## Diverse mechanisms underlying punishment resistance

Using behavioral pharmacology we show that several receptor/neurotransmitter systems may be involved in the resistance of behavior to probabilistic punishment. While exact circuit level predictions are difficult to make with systemic approaches, the current studies implicate GABA, 5HT, and DA systems in these conditions. The DA system, particularly through the D2 receptor, has been strongly implicated in decision making under conflict (Floresco et al., 2006; Simon et al., 2011). Also, GABA agonists and dopamine releasers exert bidirectional effects on behavior in the risky decision making task that mirror those observed here (Mitchell et al., 2011). Thus these results stress continued investigation of GABA and DA mechanisms and will be considered more in Chapter 4 through benzodiazepine treatment and VTA recordings, respectively.

The effects of serotonergic mechanisms particularly the 5HT<sub>2a</sub> receptor are novel and of pressing interest due to the increased usage of psilocybin for treatment in anxiety, depressive, and addictive disorders (Johnson & Griffiths, 2017). The finding of a weakly anti-conflict effect with psilocybin while an absent to weakly pro-conflict effect of  $\pm$ DOI is also puzzling due to their comparable mechanism of action (Nichols, 2016). Both drugs have differing potency ratios in relation to other serotonin receptors however, and the necessity of the 2A receptor in psilocybin's therapeutic-like effects have begun to be questioned in animal models (Hesselgrave et al., 2021; Nichols, 2016). Thus these findings also illuminate some key opportunities in more novel anxiolytics.

## Sex as a biological variable in probabilistic punishment resistance

Male and female rats learned the PPT at the same rate, but after learning, sex differences indicated greater risky action apprehension and sensitivity to punishment in females. This effect was not related to motivation to obtain reward, body size differences or basic shock reactivity as adjusting shock for body weight failed to alter punishment resistance. These findings are consistent with, and complement, the emerging data involving sex related differences in risk taking during reward seeking behavior (Becker & Chartoff, 2019; Orsini et al., 2016; van den Bos et al., 2013). The sex differences in seek action latency, however, dissipated when shock intensity was individually adjusted to produce comparable levels of overall trial completion. This suggested that if the subjective value of the punishment is normalized, there is no sex difference in transition from resisting punishment to inhibiting behavioral responding. This concept was verified using a 4PLR model, where we observed that the transition from high to low action states had a similar steepness in both sexes. The sigmoidal pattern revealed in this model is similar to that reported in choice-based decision making tasks (Friedman et al., 2017). Given the sexual dimorphisms seen in symptoms of psychiatric illnesses, including impulsivity and anxiety, our overall observation on sex differences in punishment resistant behavior highlights the importance of using SABV to inform our understanding of the neuronal basis of reward-motivated actions.

## Conclusion

The present study provides a powerful model for determining biological and environmental factors that influence the resistance of reward seeking behavior to probabilistic punishment and that such conditions may partially be related to learned anxiety states. Our data further emphasize the importance of studying the impact of SABV, particularly in the context of mental health disorders where prevalence is known to be sexually dimorphic. Future work into neural processes which underlie learning of this form of probabilistic contingencies will be informative

towards our understanding of processes related to anxious avoidant or punishment resistant behavior.

To begin to illuminate neural processes which support these behaviors, the next chapter will present work performed using this task to clarify how activity in the PL-mPFC relates to probabilistic punishment learning. Specifically we will combine the recording of neural calcium activity using fiber photometry both before and after animals have learned the probabilistic punishment task to assess time-locked activity of the PL-mPFC. This approach will permit us to assess if unique aspects of reward driven behavior under punishment (e.g. action execution and punishment) are encoded by the mPFC.

# Chapter 3

## PL-mPFC Encoding During Probabilistic Punishment Task Learning

Adapted from: Jacobs, D. S., & Moghaddam, B. (2020). Prefrontal cortex representation of learning of punishment probability during reward-motivated actions. *J Neurosci*, 40(26), 5063–5077. <https://doi.org/10.1523/jneurosci.0310-20.2020>

### Abstract

An important outstanding question is how the brain encodes the learning of reward seeking under punishment as it may highlight targets for instances where action execution becomes maladaptive. Male and female Long-Evans rats were injected with a virus to permit real-time measure of population level neural calcium activity in the prelimbic medial prefrontal cortex (PL-mPFC) while they learned the probabilistic punishment task. Again, subjects learned to adapt responding based on learning of risk of punishment. Recording of neural activity in the PL-mPFC during learning revealed changes in phasic PL-mPFC neuronal activity during risky seek actions, but not during the safe take actions, suggesting that this region is involved in learning of probabilistic punishment. While punishment itself was encoded by the PL-mPFC, the response of PL-mPFC to punishment did not change with learning. Lastly, on an individual level, changes in behavior over learning were correlated with risky action encoding changes but not with changes in punishment encoding. These data suggest an important role for the PL-mPFC in the flexible encoding of risky actions as probabilistic punishment contingencies are learned.

**Key Abbreviations:** PPT-Probabilistic Punishment Task, PL-mPFC-prelimbic medial prefrontal cortex, GFP= green fluorescent protein

### Introduction

Anxiety disorders, and related mental health disorders, are commonly associated with PFC dysfunction (Balderston, Liu, et al., 2017; Balderston, Vytal, et al., 2017; Goldstein & Volkow, 2011; Han et al., 2016; Mochcovitch et al., 2014; Volkow et al., 2003). In rodents, the mPFC is believed to be analogous to some of these PFC regions and is similarly implicated in anxiety and maladaptive behavior (Cerqueira et al., 2007; Park & Moghaddam, 2017a). In the context of the probabilistic punishment task (PPT) outlined in the previous chapter, mPFC neurons encode many aspects of goal-directed behavior and decision making (Balleine & Dickinson, 1998; Hong et al., 2019; Simon et al., 2015; St Onge & Floresco, 2010), internalized information

at the service of future actions (Del Arco et al., 2017; Mulder et al., 2003), and are involved in neuronal encoding of behavioral events when anxiety is present (Park et al., 2016). These functions indicate the mPFC may be important for adapting motivated action under anxiogenic contingencies.

The mPFC is reciprocally connected with brain regions implicated in motivated action, fear, and anxiety, making it a prime location for approach-avoidance conflict related anxiety (Hoover & Vertes, 2011; Vertes, 2004). A large literature implicating subregions of mPFC in fear conditioning (Baeg et al., 2001; Corcoran & Quirk, 2007; Courtin et al., 2014) or tasks that assess the impact of punishment on rewarded action when alternative outcomes are possible for instrumental actions (Chen, Yau, et al., 2013; Friedman et al., 2015) has begun to develop. Moreover, suppression of mPFC activity is associated with perturbed punishment processing, impulsive-like inflexible behavior, and disrupted anxiety responses (Chen, Yau, et al., 2013; Orsini et al., 2018; Park & Moghaddam, 2017a; Pascoli et al., 2015; Verharen et al., 2019). Studies which have investigated neural encoding of motivated action under probabilistic punishment, however, are scarce (Park & Moghaddam, 2017b), and in regards to learning were previously non-existent.

We posited that neuronal ensembles in the rodent mPFC are dynamically involved in punishment probability learning. To understand these processes, the aim of the current studies was to characterize neural responses of PL-mPFC to actions performed with and with out probabilistic punishment. Using our understanding of behavior from Chapter 2, we adopted our PPT to make it more amenable to fiber photometric recording by increasing the length between task events and utilizing only four blocks (0-18% risk). *In vivo* fiber photometry permitted multi-day measurement of real time changes in neuronal calcium activity and, critically, allowed for assessment of whether punishment reception versus expectation were differentially encoded over PPT learning. We find that PPT learning is associated with changes in the phasic response of PL-mPFC neuronal activity during the seek action but not during the take action. While shock elicited robust calcium activity in PL-mPFC neurons, this response did not change with learning of probabilistic punishment contingencies. The removal of punishment risk through extinction returned PL-mPFC risky action encoding to pre-punishment states. These findings suggest the PL-mPFC selectively adapts responding to learned contingencies that support anxiety.

## Methods

### Subjects

Subjects for the PPT were 18 adult Long-Evans rats (12 ♂, 6 ♀) bred in house and were > PND 86 at the time of recording. Subjects for fixed ratio one (FR1) experiments were 13 adult Long Evans and Sprague-Dawley rats (8 ♂, 5 ♀). All experimental procedures were approved by the OHSU Institutional Animal Care and Use Committee and were conducted in accordance with NIH Guide for the Care and Use of Laboratory Animals.

### Surgery for Fiber Photometry

**Viral Infusion Surgery:** Prior to task training, subjects were injected with AAV8-hSyn-GCaMP6s-P2A-tdTomato (OHSU Vector Core,  $5 \times 10^{13}$  ng/mL) to allow for pan-neuronal expression of fluorescent calcium indicator GCaMP6s in the PL-mPFC as well as a non-calcium dependent fluorophore tdTomato. The coexpression of tdTomato allows for a motion artifact control signal to be used to correct GCaMP signals in noisy environments with rodents (Babayan

et al., 2018; Matias et al., 2017; Menegas et al., 2018; Soares et al., 2016). Another subset of rats ( $n=2$ ) were injected with a control virus (AAV8-hSyn-GFP) in the PL-mPFC to assess the extent of motion artifact that was not properly corrected. Rats were anesthetized with isoflurane and placed in a stereotaxic apparatus. Following an incision and topical application of lidocaine, craniotomy was performed to lower a 10  $\mu$ L syringe (Hamilton) for virus infusion into the PL-mPFC. Two injections were made (325 nL/site @ 50 nL/min) at the coordinates AP +2.7, ML  $\pm$  0.65, DV -2.5 and -3.5 mm (from dura) with the most ventral injection always performed first. A microcontroller (World Precision Instruments) was used for the injections. Virus was allowed to diffuse for 5 min after the most ventral injection. The needle was slowly raised and the second injection was performed and allowed 12 min to diffuse. After this the needle was removed, the incision was stapled, and animals were given a 5 mg/kg injection of carprofen subcutaneously.

**Fiber Implant Surgery:** After allowing at least four weeks for virus expression and stabilization, subjects were implanted with an optical fiber (400  $\mu$ m core) aimed at the PL-mPFC (AP +2.7, ML  $\pm$  0.65, DV -3.3 mm from dura) using the surgical procedures outlined above, with the exception that three additional bore holes were made for three skull screws which surrounded the craniotomy of the mPFC. The optical fiber was slowly lowered and was glued to the skull with light-curing epoxy (Tetric N-flow, Ivoclar Vivadent). Subjects were given 5 mg/kg of carprofen after this procedure and returned to ad libitum food for 5 d before returning to food restriction. Subjects were given 1 week to recover from surgery before behavioral testing and were handled every other day to habituate them to being connected to the recording patchcord.

## Apparatus

An operant chamber (Coulbourn Instruments, PA) was used for behavioral testing. The chamber included two nose poke holes, which could be illuminated, on one wall located 2 cm above a grid floor. The grid floor was connected to a shock generator which delivered foot shocks. The food trough was on the opposite wall and was used to dispense 45 mg sucrose pellets (Bio-Serv) and detect food trough entries. The operant chamber had an opening in the top of the box to permit entry for the recording patchcord. Graphic State software (version 3 or 4, Coulbourn Instruments) running on a windows computer was used for programming the task.

## Fixed Ratio One (FR1) Training and Recording

A separate group of subjects were trained to perform a simple FR1 schedule of reinforcement and recording of PL-mPFC was performed during the learning process. Rats were trained to make an instrumental nosepoke response to receive a 45-mg sugar pellet under FR1 schedule of reinforcement. The availability of the nosepoke for reinforcement was signaled by a 5-s tone and cue light onset. Animals received at least three FR1 training sessions which consisted of 90 trials or 1 hr, whichever came first, and were recorded for all sessions (see below).

## Punishment Punishment Task (PPT) for Fiber Photometry

The PPT was based off of procedures outlined elsewhere (see Jacobs & Moghaddam, 2020) and optimized for fiber photometry recording (see Figure 3.1A). This was done by 1) increasing the delay between the “seek” action and “take” cue illumination to 1.5 s to account for the relatively slow offset of GCaMP6s activity (Decay Time  $t_{1/2}=1$  s for 1 action potential; Chen,

Wardill, et al., 2013), 2) increasing the delay between take action and reward delivery to 1 s, 3) increasing the inter-trial interval to 15 s to allow for increased samples for normalizing the control signal, 4) increasing the risk of shock from 0% to 18% in quarter log units (i.e. 4 blocks) to allow for increased signal to noise ratio for each block by allowing for 20 trials per block rather than 15, and 5) shorter inter-block intervals of 2 min and less blocks decreased the task length down to 56 min, to prevent photobleaching of fluorophores that can occur of continuous exposure to light. We focused on the risk blocks that deviated between Session 1 and after learning as seen in earlier behavior studies (see Figure 2.1). Behavior was considered stable after a minimum of 4 sessions and when individual trial completion was within 25% of a 3 d mean for 3-consecutive sessions.

## Extinction of Probabilistic Punishment

A subset of the subjects (n=8) were exposed to probabilistic punishment extinction. Following learning of the PPT, extinction was performed by removing the probabilistic punishment (i.e. shock) contingency and keeping all other contingencies (see Jacobs & Moghaddam, 2020). If subjects were completely resistant to shock, we increased shock intensity (up to 0.5 mA) to achieve suppression of behavior. Neural activity was recorded in a session prior to extinction and in two successive extinction sessions.

## Shock Probe Test

To determine if any learning related changes in shock responsivity were products of shock exposure we applied the same footshock (0.25 mA, 300 msec) in a different context (operant box with no nosepokes or feeder) with a variable 90 sec (60-120 sec) inter-stimulus interval. Shock probe tests were performed after extinction procedures. Subjects were given one session to acclimate to the new context for 10-min. In the next session subjects received seven unsignaled footshocks after a 5-min habituation period while PL-mPFC activity was monitored.

## Fiber Photometry Systems and Recording Procedures

Two commercially available fiber photometry systems, Neurophotometrics Model: FP3001 (NPM) and Tucker-Davis Technologies RZ5 (TDT) were used. For NPM (n=13 for FR1; n= 2 for PPT), recording was accomplished by providing both 470 nm and 560 nm excitation light through the 400- $\mu$ m core patchcord to the mPFC for GCaMP6 and tdTomato signals, respectively. LEDs were reflected through a dichroic mirror and onto a 20X Olympus objective. Excitation power was measured at 240-260  $\mu$ w at the tip of the patch cord. Emission at 510-530 and 630-660 nm, from 470 and 560 nm excitation light, respectively, were split with an image splitting filter and captured via a high quantum efficiency CMOS Pointgrey camera. Recordings were performed using bonsai open source software (Lopes et al., 2015) and recorded at 41 Hz.

For TDT recording (n=16), excitation light was emitted from 465 and 560 nm LEDs (Doric Instruments), sinusoidally modulated at 220 and 310-Hz, respectively, and controlled through an LED driver interfacing with the TDT RZ5 processor running Synapse software. Excitation light was passed through a 400  $\mu$ m core patchcord connected to a dual fluorescence mini-cube (Doric Instruments). Light intensity at the tip of the patchcord was started at 10  $\mu$ w but adjusted on an individual basis to optimize comparable levels of GCaMP and tdTomato and prevent photodetector clipping. This resulted in a range of 1-10  $\mu$ w for light intensity for these subjects. GCaMP and tdTomato emission (500-540 nm and 580-680 nm, respectively) were collected back through the patchcord to dichroic mirrors and bandpass filters within the Doric

minicube. For the GFP-only group the TDT recording system was used but 470 nm (GCaMP6) and 405 (Isosbestic Control) nm excitation light was provide through the patchcord and were collected back through the patchcord to dichroic mirrors and bandpass filters within the Doric minicube (500-540 nm). Fluorescence was converted to voltage through two femtowatt detectors (Newport 2151). Synapse software demodulated fluorescence signals in real time at 1 kHz with a 6-Hz low pass filter.

For both systems, timestamps of behavioral events were collected by 5V TTL pulses that were read into an Arduino interfaced with bonsai software or the same RZ5 processor in the NPM and TDT systems, respectively, to allow for aligning calcium activity with specific behavioral events in the task. Following behavioral training, but prior to shock contingency exposure, subjects were well acclimated to connection of the recording patchcord to assure changes in behavior were not due to distraction from the recording setup. The recording fiber was prebleached once over 12 h and for 30 min prior to recording sessions.

To prevent slippage of patchcord connector from the implant the ADAL3 connector (Thorlabs) was used instead of a standard ceramic ferrule. Subjects were connected to a dummy fiber for non-recording days which mirrored the recording fiber but did not emit any light. Recording was performed at 2-3 timepoints: in the third no-shock session before probabilistic punishment (n=13), at the first PPT session when subjects first experience the footshock contingencies (Session 1; n=15), and after PPT behavior had stabilized, i.e. the PPT was learned (Session 5-8; n=15). For the GFP only rats, we only assessed the first PPT session.

## Data and Statistical Analysis

**Fiber Photometry Pre-processing:** Signals from the 465 (GCaMP6) and 560 (tdTomato) streams were processed in Python (Version 3) using custom written scripts. 465 and control 560 or 405 streams were broken up based on the start and end of a given trial (for a given trial  $n$ : start of the ITI of trial $_{n-1}$  to end of the ITI of trial $_n$ ). This was done to fit the control signal to the 465 signal on a trial by trial basis using a least squares linear fit (numpy polyfit function in Python), as fitting the control signal to the entire session recording can be difficult when high amounts of motion are present as in the current task or if bleaching rates are different between fluorophores (Matias et al., 2017; Soares et al., 2016). The fitted control signal was then subtracted from the corresponding 465 signal to yield the change in fluorescent activity ( $\Delta F/F = 465 \text{ signal} - \text{fitted control signal} / \text{fitted control signal}$ ) that is corrected for non-calcium dependent motion artifact and photobleaching from extended light exposure. Data were low-pass filtered at 3 Hz.

To normalize activity changes based on basal fluorescence, peri-event z-scores were computed by comparing the  $\Delta F/F$  after the behavioral action to the 4-2 s baseline  $\Delta F/F$  prior to the behavioral action. For example, the changes in  $\Delta F/F$  following the seek action was compared to mean of the  $\Delta F/F$  4-2 s prior to the seek action. This window was chosen to allow us to see if neural activity changes happened before or after action execution. Because data from the NPM was sampled at 41 Hz, we downsampled the TDT signals to 41 Hz as well for graphical purposes using Fourier method (scipy library in Python).

## PPT Experiments

We combined our data from [Chapter 5](#) to permit more thorough analysis of behavior and individual and sex differences using this version of the PPT. Data are shown as combined across sexes, but data separated by sex can be found in [Appendix A](#) (see [Figure A.7](#)).

**Behavior Data:** For behavior we utilized a repeated measures ANOVA or mixed effects model with factors risk block and session to assess if action completion or latency to complete actions or retrieve rewards was impacted by punishment. Tests were done with the Greenhouse-Geisser correction for sphericity violation where appropriate. Post-hoc comparisons were performed using the bonferroni correction. An  $\alpha$  level of .05 was used for all tests. Behavior data files were processed using custom written scripts in Python (version 2.7 and 3.0) and all statistical analyses were performed in GraphPad Prism (Version 8, San Diego, CA).

**Fiber Photometry Data:** To assess the timing of changes in neural activity, we utilized a permutation based approach as outlined in (Jean-Richard-dit-Bressel et al., 2020) using Python (Version 3). The average z-scored response for each subject for a given time point in the action epoch or punishment delivery period for a risk block was compared to the 0% risk block. For each time point a null distribution was generated by shuffling the data and randomly selecting the data into two groups. This was done 1,000 times for each timepoint and a two-sided p-value was obtained by determining the percentage of times a value in the null distribution of mean differences was greater than or equal to the observed difference in the unshuffled data. To control for multiple comparisons we utilized a consecutive threshold approach based on the 3 Hz lowpass filter window (Jean-Richard-dit-Bressel et al., 2020; Pascoli et al., 2018), where a p value  $< .05$  was required for 13 consecutive samples (i.e.  $>$  the low-pass filter window, 300 msec) to be considered significant. We further separated punished (i.e. shock) trials from unpunished trials, to investigate differential activity that was seen during punishment administration and during anticipation of, but no actual administration of, punishment.

We complimented the permutation analysis with area under the curve (AUC) analysis to better understand the individual responses of PL-mPFC activity during PPT learning. We took pre and post AUC values to calculate change scores for the seek action or take action and for the 2 s after reward delivery. We quantified responsiveness to footshock by calculating the post footshock AUC as well as the time to peak of the response. These values were analyzed using mixed effects model with the factor of risk block for each session. Post-hoc bonferroni corrections were used when comparing to the 0% risk block.

We also performed correlation analyses between behavioral and PL-mPFC activity changes before and after learning (i.e. between Session 1 and Session 5-8). For behavior, more negative values reflect subjects who showed greater increases in sensitivity to probabilistic punishment after learning. For PL-mPFC activity we took the difference between risk block z-score AUCs for risky seek actions or punishment in the corresponding sessions ( $AUC_{\text{Session 5-8}} - AUC_{\text{Session 1}}$ ). After checking for violations in normality with the Shapiro-Wilk test, we performed either two-tailed Pearson correlations or Spearman rank tests for these punished and unpunished trials. All statistical tests were performed with an  $\alpha$  level of .05 in GraphPad Prism (Version 8).

## FR1 Experiments

**Behavior Data:** Trial completion was measured as the number of completed nose pokes (of the 90 possible) for each block, while action latencies were defined as time from cue onset to action execution. Retrieval latency was defined as the time until pellet retrieval after delivery. Group mean values are presented as mean  $\pm$  SEM in all figures.

**Fiber Photometry Data:** To assess the development of phasic decreases in neural activity, area under the curve (AUC) values were converted to peri-event change scores and assessed with mixed-effects model for FR1 sessions in GraphPad Prism (version 8). Post-hoc tests were performed using a bonferroni correction where appropriate. An  $\alpha$  level of .05 was used for all

tests.

## Excluded Data

Fiber photometry data from one male was excluded from fiber photometry experiments due to injection of a differing GCaMP6 expressing viral construct from the other subjects, complicating his comparison to other subjects. For one session of another subject, the mPFC data were excluded because the fiber was not properly coupled to the patchcord. These subjects were included for behavioral analysis. FR1 data for one session for a subject was excluded due to LED malfunction. Trials where the optical fiber patch cord fell off during action periods and needed to be reconnected were also excluded.

## Histology and Imaging

Viral expression and fiber placements were verified after behavioral testing. Subjects were transcardially perfused with 0.01 M phosphate buffered saline (PBS) followed by 4% paraformaldehyde (PFA). Brains were removed and post-fixed in PFA for 36 h before being placed in 20% sucrose solution and stored at 4°C. Forty- $\mu$ m brain slices were collected on a cryostat (Leica Microsystems) and preserved in 0.05% phosphate buffered azide. Brain slices were mounted to slides and cover slipped with Vectashield anti-fade mounting medium (Vector Labs). A Zeiss Apotome.2 microscope was used to image brain slices for GFP (Zeiss Filter set 38: 470-nm excitation/525-nm emission) and tdTomato (Zeiss Filter Set 43: 545-nm excitation/605-nm emission) to validate expression of both fluorophores in cells near the fiber tip. Rat brain atlases (Paxinos & Watson, 1998) were overlaid onto brain slices to determine the location of viral expression and fiber placement. Fiber placement was determined by the brain slice demonstrating the most ventral fiber damage.

While immunohistochemical techniques were not typically required to see viral expression, we utilized immunohistochemistry with a GFP antibody if a subject lacked virus expression to confirm the presence or absence of GCaMP. Brain slices were permeabilized in 3% BSA, 0.5% Triton X, and 5% Tween 80 dissolved in PBS + 0.05% sodium azide for 2 hr at room temperature. Slices were then incubated with rabbit antiserum against GFP (Abcam, Catalogue# 6556, 1:500) diluted in PBS + Azide, 3% BSA + 0.1% Triton, and 1% Tween for 48 hr at 4° C. Slices were then washed in PBS + Azide, 3% BSA + 0.1% Triton + 1% Tween, three times for five minutes each. After this, slices were incubated with goat-anti-rabbit Alexa-488 (Abcam, Catalogue# 1051G, 1:2000) diluted in PBS + Azide, 3% BSA + 0.1% Triton, and 1% Tween for 24 hr at 4° C and subsequently washed again as outlined above. Slices were then mounted to slides with Vectashield and imaged using the same procedures outlined above.

## Results

### Histology and photometry overview

The mPFC is implicated in risky choice, the representation of aversive stimuli, and action inhibition (Chen, Yau, et al., 2013; Friedman et al., 2015; Orsini et al., 2018; Pascoli et al., 2015; Verharen et al., 2019). Importantly, neurons in mPFC are sensitive to punishment risk as well as to the experience of a stressor or punisher (McEwen & Morrison, 2013; Park & Moghaddam, 2017b). Little is known, however, if the mPFC flexibly encodes probabilistic punishment during learning. We hypothesized that, in the PPT, the PL-mPFC processes risky action differently

when probabilistic punishment is a factor. Fiber photometry, compared to spike recording, provided the advantage of being able to record the mPFC response during footshock (i.e. punished trials) and we adapted the PPT to better suit this recording technique (Figure 3.1A).

Fibers were generally located within the PL-mPFC. Fiber placement in one subject was on the borderline of the prelimbic/infralimbic region (Figure 3.1B). Inspection of the data, however, revealed that the patterns of activity for this subject was similar to the rest of the group (Figure A.6). After z-scoring calcium activity based on behavioral action, we noticed robust elevations in the PL-mPFC following shock administration (Figure 3.1C-D). This led us to divide trials into punished and unpunished trials focused around the seek action (i.e. the action with a risk of shock).

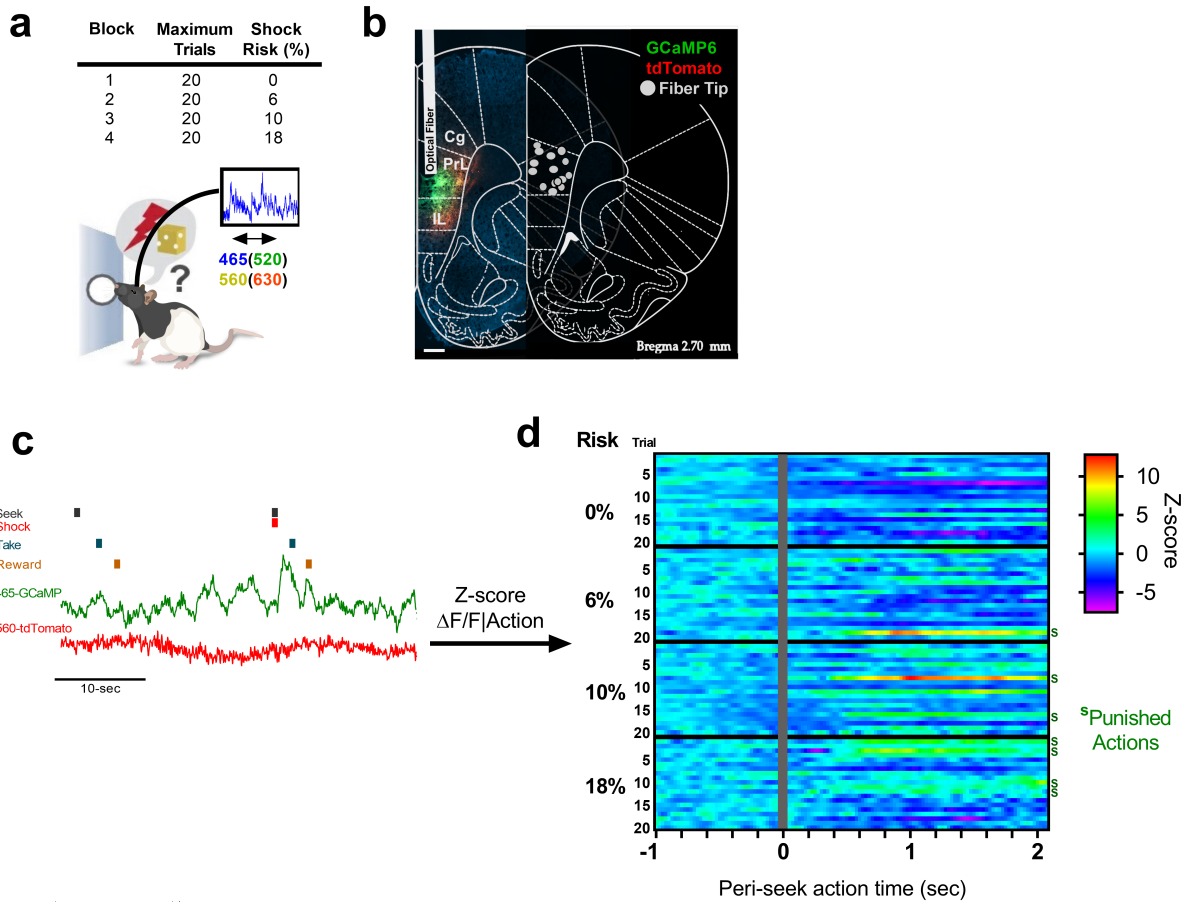


Figure 3.1: Recording neuronal calcium activity with GCaMP6 in PL-mPFC during the probabilistic punishment task. **a**. Subjects performing a modified version of the probabilistic punishment task while neuronal calcium activity in the PL-mPFC was recorded via GCaMP6s. **b**. GCaMP6s (green) and tdTomato (red) was readily expressed in the mPFC, with optical fibers (grey dots) targeting the prelimbic region (scale bar: 500  $\mu$ m). **c**. A representative raw trace depicting GCaMP6s and tdTomato signals and **d**. representative z-score calculations surrounding the seek action. Each row is a trial with time 0 being the seek action time. Green 's' indicates punished (i.e. shocked) trials.

## Behavioral suppression in the PPT

Using an individualized method of determine task learning (see methods), we found that performance was stable (i.e. learned) by Sessions 5-8. After learning, punishment resistance decreased in Sessions 5-8 compared to Session 1 (Figure 3.2A, risk by session interaction:  $F(2.7,40.2)=13.1$ ,

$p < .001$ ) and mirrored the behavior seen in the full version of the PPT in [Chapter 2](#) at the corresponding 0-18% risk blocks ([Figure 2.1A](#)). That is, increasing shock risk resulted in decreases in trial completion at both 10 and 18% risk after the task was learned, while only 18% risk of shock suppressed behavior significantly for Session 1 when compared with the no-shock sessions. We also replicated findings of individual variability in punishment resistance, with some subjects demonstrating complete resistance and some enhanced sensitivity to punishment risk ([Figure 3.2A](#)).

We also observed similar latency increases to perform the risky action as those seen in the full version of the task ([Figure 3.2B](#), risk by session interaction:  $F(1.7, 25.3) = 5.9$ ,  $p < .01$ ). Post-hoc tests indicated that increased latency was non-significantly elevated by the 10% risk block after task learning, and significantly elevated in the 18% risk block before and after learning. Importantly, the latency to perform the safe take action or retrieve the reward were not impacted after the task was learned. Rather a transient elevation in take action latency was observed in session 1 at the 10 and 18% risk blocks (risk by session interaction:  $F(3.8, 50.7) = 7.7$ ,  $p < .001$ ) but these over generalizations dissipated after animals learned the task ([Figure 3.2C](#)).

Lastly, similar to our observations in the previous chapter, sex differences in behavior were observed in these studies. No significant sex differences were observed in the first PPT session (Effect of sex or sex by risk interaction:  $F$  values  $< 2.9$ ,  $p$  values  $> .07$ ). However after task learning it was observed that females were more sensitive to punishment risk ( $F_{\text{sex}}(1, 13) = 19.4$ ,  $p < .001$ ,  $F_{\text{interaction}}(3, 39) = 7.03$ ,  $p < .001$ ; [Figure A.5A](#)). These differences began when risk was present and became significant at the 18% risk block. No difference in completion of the corresponding blocks was observed in no shock sessions (Welch t-test:  $t(5) = 1.55$ ;  $p > .09$ , one-tailed; [Figure A.5B](#)). Because we had different amounts of trial completion between males and females we assessed if seek latency for females during risk blocks was generally higher than males. Females showed higher latencies to perform the risk action though this effect was just short of significance (Welch t-test:  $t(6.3) = 1.69$ ;  $p = .069$ , one-tailed; [Figure A.5C](#)).

## Footshock punishment is uniformly encoded by the PL-mPFC

When seek actions resulted in footshock, a large increase in PL-mPFC activity was observed immediately after shock onset ([Figure 3.3A](#)). However this robust increase did not change after animals had continued exposure to shocks and learned the PPT contingencies (paired t-test:  $t(13) = 1.78$ ,  $p = .09$ , [Figure 3.3B](#)). In a subset of animals ( $n = 8$ ) we assessed mPFC response to the same footshock but in a non-contingent manner. We observed the response to footshock was still present in this context but weaker in magnitude (paired t-test:  $t(7) = 2.8$ ,  $p = .0264$ , two-tailed; [Figure A.18](#)). Responses to footshock were not observed in the GFP control subjects ([Figure A.8](#)).

While females appeared to show a larger response to footshock, assessing the AUC values revealed this effect was likely driven by a few subjects and consequently did not achieve significance (effect of sex or interaction:  $F$  values  $< 2.7$ ,  $p$  values  $> .13$ ; [Figure A.7C](#)).

## Prefrontal cortex encoding of risky action changes with task learning

Unpunished seek actions revealed a different response depending on session. We observed a phasic decrease in activity during seek action execution across blocks in the no shock session. Session 1 was similar to those observed in the no-shock session although attenuation of the phasic decrease was seen in the last block of the session ([Figure 3.4A-B](#)). After learning (Session 5-8) the phasic decrease during seek action execution was attenuated across all risk blocks

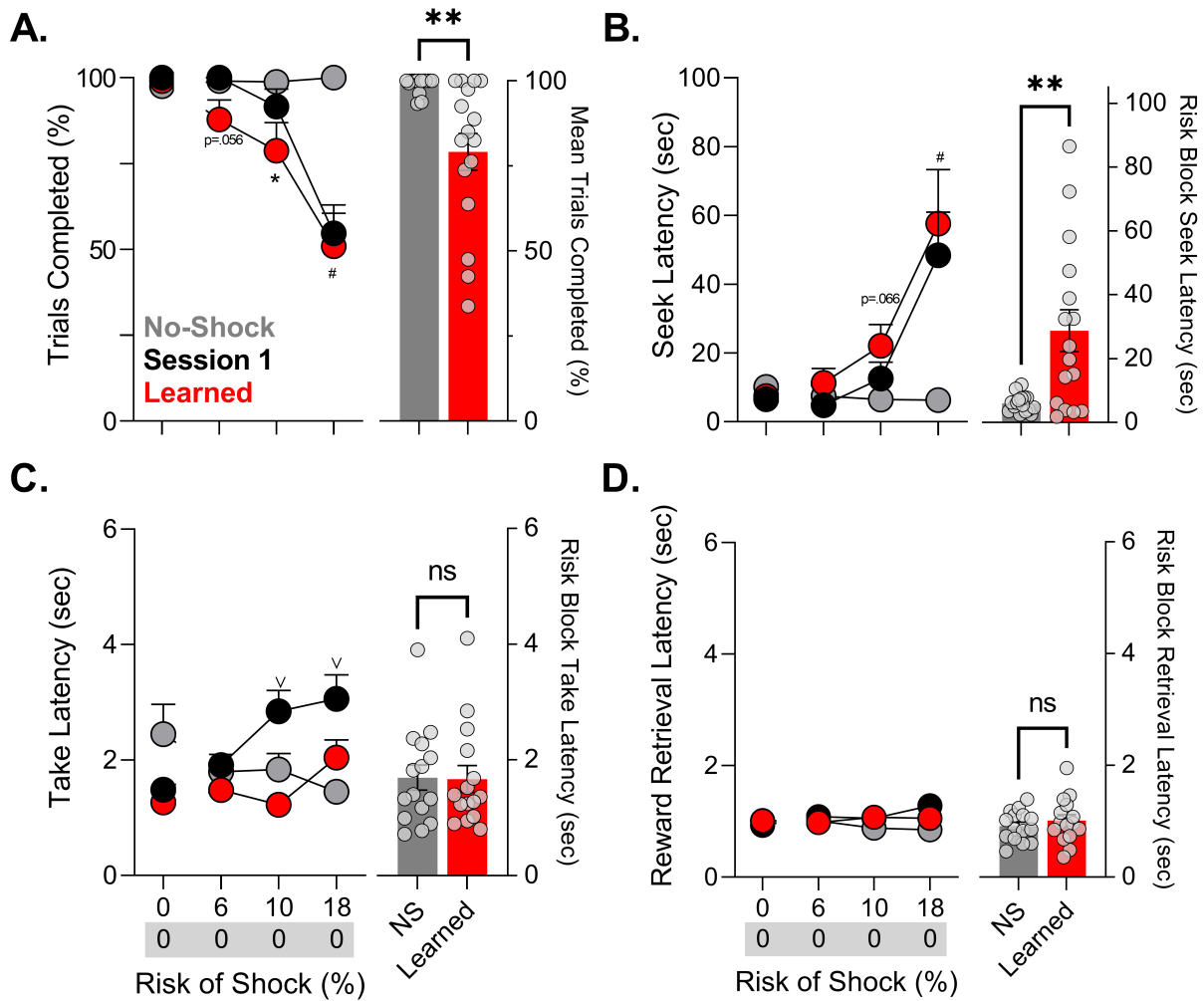


Figure 3.2: PPT behavior in fiber photometry experiments. **A.** Trial completion was suppressed by probabilistic punishment, an effect that was observed earlier after task learning. **B.** Seek latency increases were also observed specifically when probabilistic punishment was present. **C.** Take action was initially suppressed by probabilistic punishment but these overgeneralization effects disappeared after learning. **D.** Reward retrieval was not impacted by probabilistic punishment. Bar graphs represent average trial completion (**A**) or mean latency in risk blocks (**B-D**). Grey circles are individual data points.  $\vee$   $p < .05$  session 1 vs. no shock,  $*$   $p < .05$  learned vs. no shock,  $\#$   $p < .05$  both PPT sessions vs. no shock.  $n = 16$ .

(Figure 3.4C). These changes were restricted to just after seek action execution rather than before execution. Finally, AUC analysis reinforced the idea that phasic decreases did not change with block in the no-shock sessions (effect of risk:  $F(2.3, 27.2) = 1.75$ ,  $p = .19$ ) but that phasic decreases were significantly attenuated after learning (effect of risk:  $F(2.25, 28.5) = 4.56$ ,  $p = .016$ ) across all risk blocks.

Lastly, no sex differences were observed in PL-mPFC risky action encoding after learning (Figure A.9). Both males and females demonstrated a progressive attenuation of the phasic response during risk blocks as the PPT was learned (effect of session:  $F(1.7, 19.9) = 6.82$ ,  $p < .01$ ) but this did not interact with sex (effect of sex or interaction:  $F$  values  $< 1.1$ ,  $p$  values  $> .37$ ).

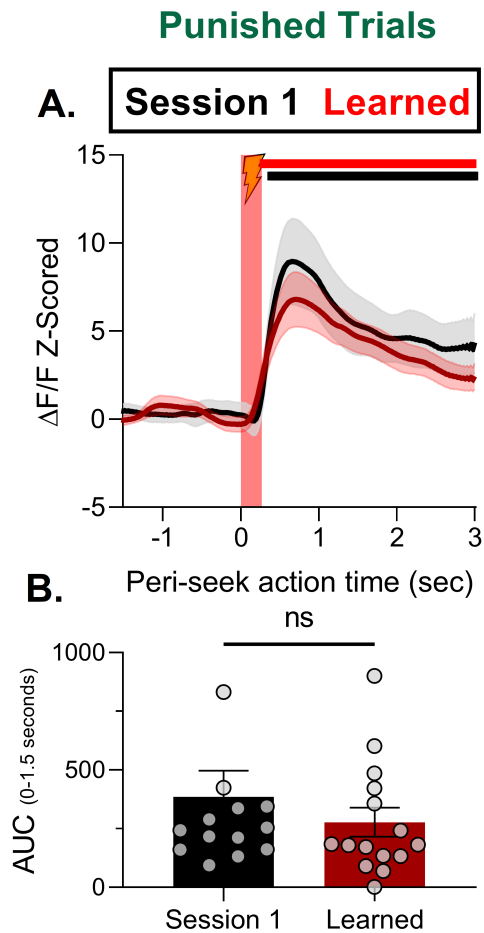


Figure 3.3: Phasic increases in PL-mPFC neural calcium activity following action contingent footshock. **A.** Footshock punishment administration (red bar) for a seek action produced robust increases in calcium activity in the PL-mPFC in Session 1 and Session 5-8 that was significantly greater than the 0% risk block. **B.** PL-mPFC responses to punishment did not change after learning of the probabilistic punishment task. Solid lines in upper plots indicate timepoints that are significantly different from 0% risk. ns = not significant,  $n = 14-15$ . Individual data points are depicted as grey circles. One data point for Session 1 is omitted from the plot as it is above axis limits.

## Prefrontal cortex encoding of safe action does not change with learning

We examined whether learning related changes in PL-mPFC calcium activity during seek action generalizes to execution of safe actions. The advantage of the seek-take task structure is that the take response has the same mechanics but carries no punishment risk.

Unlike seek actions, PL-mPFC activity in unpunished trials did not change in Session 1 compared to Session 5-8 during take action or reward delivery (Figure 3.5A-C). This was supported by a lack of significant effect using both permutation and AUC analysis for take epochs (effect of block or risk:  $F$  values  $< 1.3$ ,  $p$  values  $> .29$ ) and reward delivery (effect of block or risk:  $F$  values  $< 2.81$ ,  $p$  values  $> .08$ ).

## Risky action encoding changes are associated with punishment sensitivity

Analysis of individual differences in behavioral and neural activity changes before and after task learning (i.e. Session 1 and Session 5-8) revealed a significant negative correlation (Pearson  $r = -.64$ ,  $p = .013$ , two-tailed) between the magnitude of decrease in punishment resistance (behavioral change) with increases in the seek action PL-mPFC activity state for risky, unpunished trials (Figure 3.6A). While individual differences in PL-mPFC responsivity to punishment were observed, these differences were not associated with behavioral changes (Pearson  $r = -.29$ ,  $p = .30$ , two-tailed; Figure 3.6B).

## Unpunished Trials

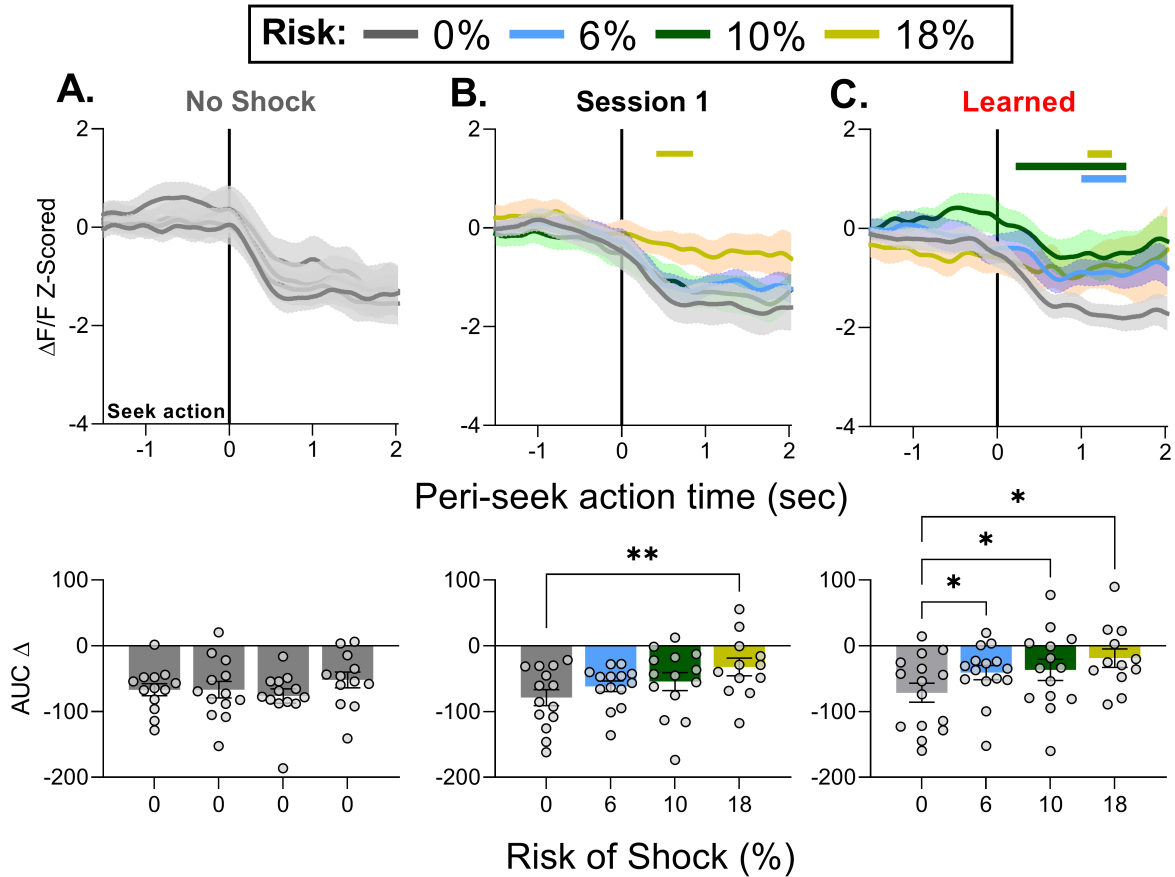


Figure 3.4: Changes in PL-mPFC neural calcium activity following seek action execution before and after PPT learning. **A-B.** Seek actions that were unpunished resulted in decreases in calcium activity at the time of action execution both before introduction of probabilistic punishment (no-shock, grey), and in the Session 1 (black) before probabilistic punishment was learned. **C.** These decreases were attenuated across risk blocks following stabilization (learning) of the PPT (red). Solid lines in upper plots indicate timepoints that are different from the first block. \* $p < .05$  vs 0% risk of shock,  $n = 13-15$ . Individual data points are depicted as grey circles.

## Unpunished Trials

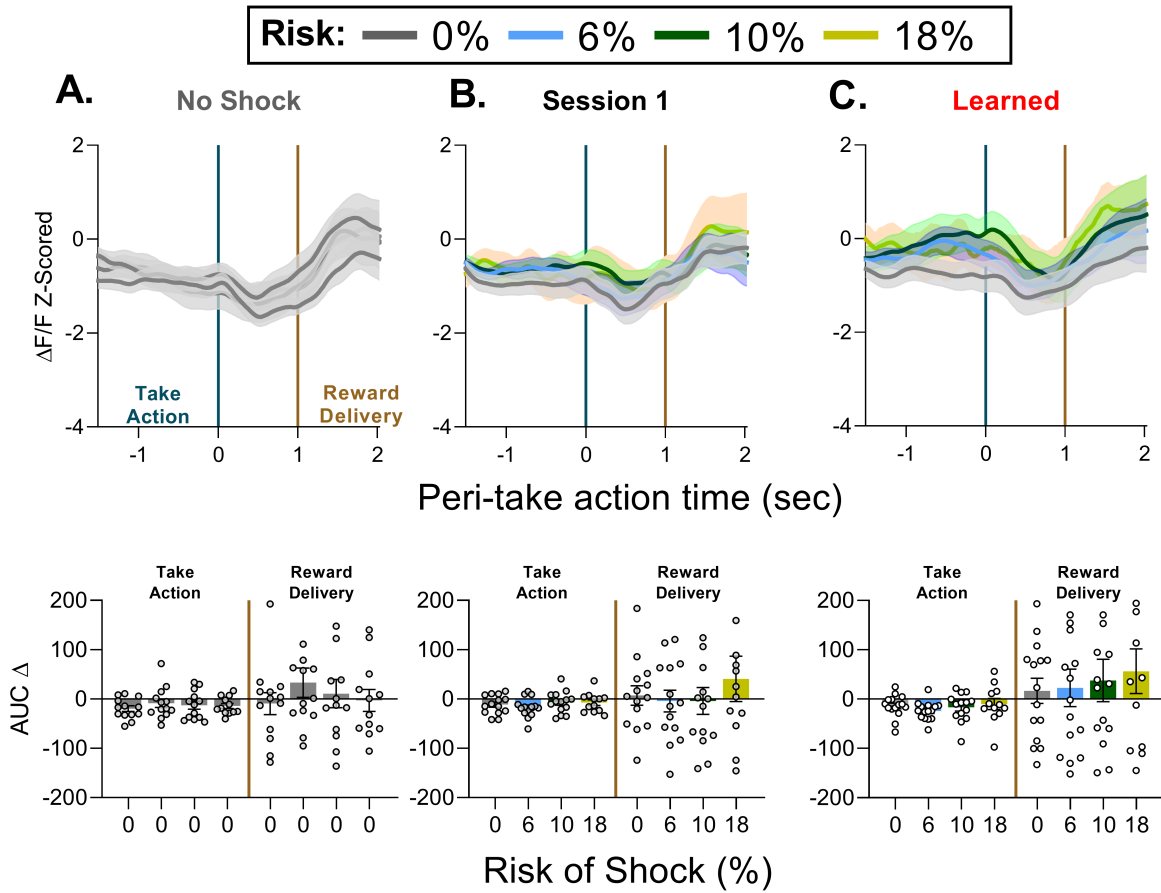


Figure 3.5: Neural calcium activity in the PL-mPFC for the take action and reward delivery. **A-C.** Take actions (blue vertical line) and reward delivery (brown vertical line) produced little effect on mPFC calcium activity and were not influenced by task learning.  $n=13-15$ . Individual data points are depicted as grey circles.

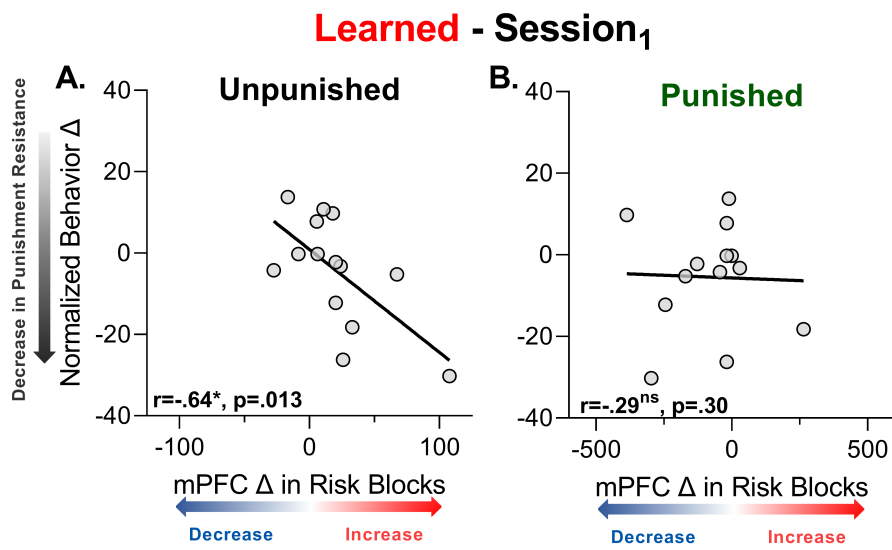


Figure 3.6: Individual differences in punishment resistance are associated with risky, unpunished action encoding changes. **A.** Individual changes between Session 5-8 and Session 1 revealed that greater decreases in punishment resistance (shaded black arrow) were associated with greater learning related increases in PL-mPFC activity for risky, unpunished seek actions. **B.** Individual differences in behavior were not associated with changes in PL-mPFC response to the footshock after punished seek actions. Black line represents the linear trendline for the data. \* $p < .05$ ,  $n = 14$ . Individual data points are depicted as grey circles.

## Emergence of phasic decreases during action encoding in the PL-mPFC during instrumental action learning

We further asked if the phasic decreases in peri-action activity may be an indicator of well learned, stable contingencies. Thus we assessed neural activity while animals learned to nose-poke for sucrose pellets under an FR1 schedule of reinforcement (Figure 3.7A). Fiber placements were similar to those attained in the PPT experiments, with a majority of fibers targeting the PL-mPFC (see Figure A.11). Nose poking behavior for sucrose became asymptotic by approximately day three of training. Subjects earned approximately 75/90 pellets and cue to action latencies were under 10-seconds. Further the latency to retrieve the reward decreased dramatically by session three (Figure 3.7B-D). Thus the FR1 was well learned by the fourth session.

The PL-mPFC showed unique patterns of activity during the learning of the FR1. While the PL-mPFC did not show a response to the tone cue which signaled the initiation of the trial, the PL-mPFC developed a phasic negative response to action execution as FR1 contingencies were well learned ( $F_{\text{session}}(3,45)=3.66$ ,  $p=.019$ ; Figure 3.7E-G). Reward delivery was accompanied by a weak phasic increase in the PL-mPFC, which also decreased with learning ( $F_{\text{session}}(3,45)=4.98$ ,  $p=.005$ ; Figure 3.7H). We further separated the data according to sex and did not observe any difference in the neural activity changes for the given epochs, as both males and females showed phasic reductions in peri-action activity after the FR1 was learned (Figure A.10).

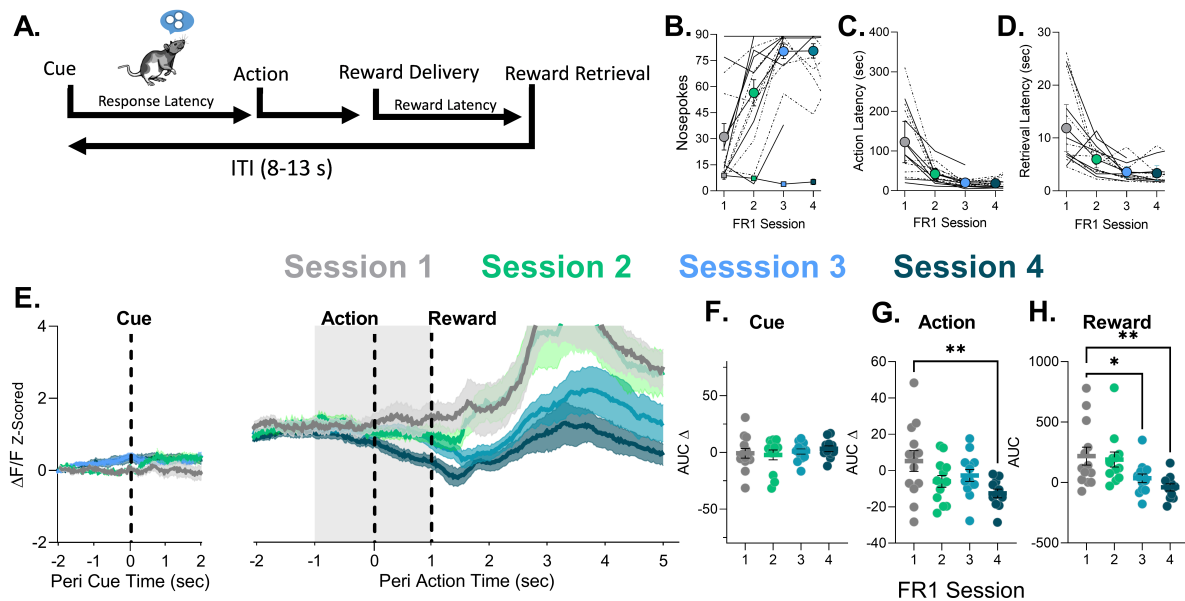


Figure 3.7: Phasic decreases during action execution emerge with FR1 learning in the PL-mPFC. **A.** Trial structure for FR1. **B.** Number of pellets earned for each session, with lines denoting individual subjects and green squares denoting inactive nosepokes. **C.** Latency to perform the FR1 over the first four sessions. **D.** Latency to retrieve the food pellet over the first four sessions. **E.** Peri-event activity of the PL-mPFC for cue onset, action execution, and food delivery. Line colors indicate each of the four successive sessions. **F-H.** AUC values for each epoch over the sessions. \*  $p < .05$ ,  $n=11-13$ .

## Phasic decreases are recovered by extinction of probabilistic punishment after PPT learning

To investigate if changes in seek action encoding were specific to probabilistic punishment and not time on task, we removed the punishment contingency until behavior returned to baseline levels of trial completion for a subset of the subjects. Attenuation in phasic decreases during seek actions under probabilistic punishment was observed with this subset of subjects through permutation tests and with AUC approaches (effect of risk:  $F(1.7,10.3)=4.56$ ,  $p = .04$ ; Figure 3.8A), albeit with more variability than the full data set. When punishment risk was removed, these attenuations of peri-action phasic decreases dissipated. Phasic decreases re-emerged and only some pre-action changes were identified by permutation tests when comparing to the first block. Furthermore no significant effect of AUC change scores over blocks was observed in either extinction session (effect of block:  $F$  values  $< 2.7$ ,  $p$  values  $> .11$ ; Figure 3.8B-C). No change for the take action or reward delivery were observed before or after probabilistic punishment extinction through the permutation based approach (Figure A.12). For this reason AUC values were not calculated.

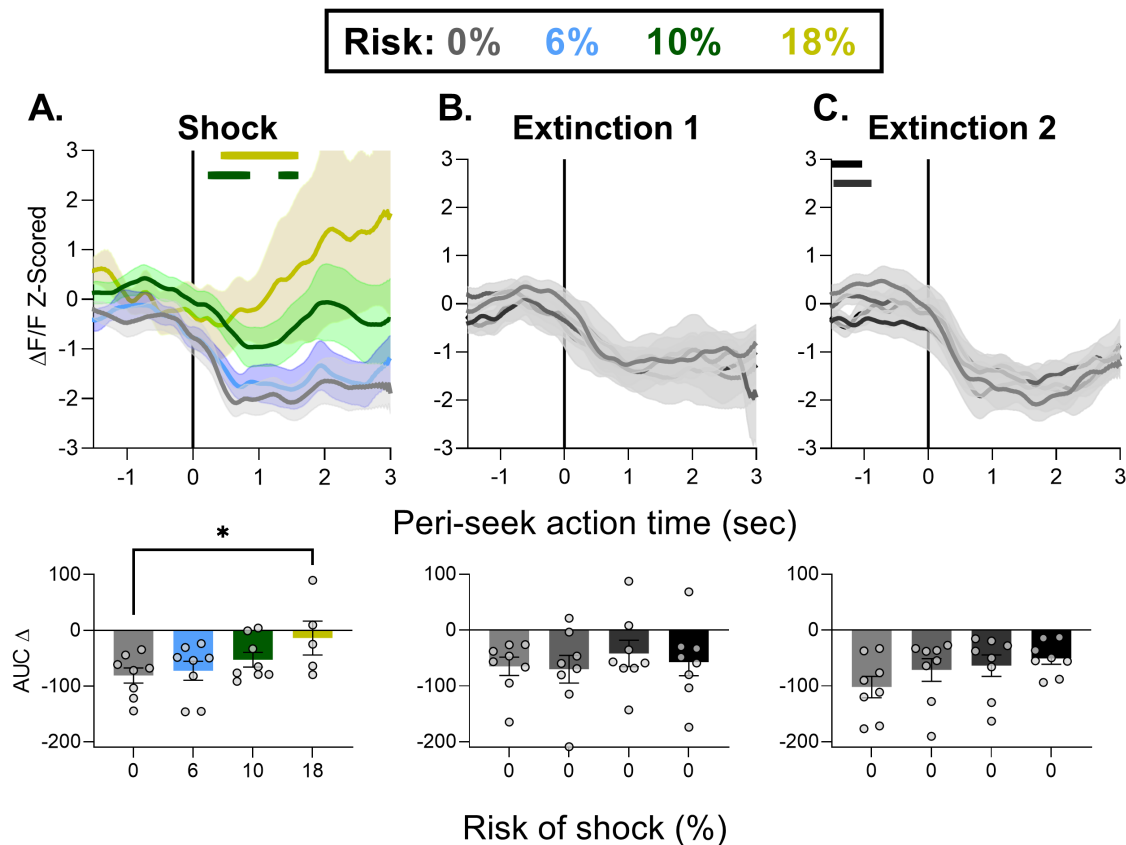


Figure 3.8: Phasic decreases during seek action execution are recovered by extinction. **A.** When probabilistic punishment contingencies were present we observed attenuation of phasic decreases at the time of seek action encoding for 10-18% risk. **B-C.** When the probabilistic punishment contingency was removed, action encoding returned to phasic decreases at the time of action execution. Solid lines indicate significant differences from the first 0% risk block. \*  $p = .039$ , one-tailed t-test - uncorrected.  $n = 6-8$ .

## Discussion

Similar to our results in [Chapter 2](#) we observed distinct patterns of behavior during the learning of probabilistic punishment. Behavior generally was resistant to punishment at low risk before the suppressive effects of punishment became more gradual and appeared earlier after behavior became stable (i.e. the PPT was learned). Recording of neural activity in the PL-mPFC during the PPT revealed that risky action encoding changed with learning of punishment probability and that changes in punishment resistance over learning were associated with these changes in phasic PL-mPFC neuronal activity. We also observed no learning related changes in PL-mPFC encoding of the safe take actions nor punishment. These findings highlight a novel role for the PL-mPFC in the tracking of actions as they become conflicted with anxiogenic contingencies.

### A PPT for fiber photometry recording

Due to restrictions in recording neural activity in behaving animals we adapted the PPT to make the task shorter in length and to allow greater separation between task events. We found markedly similar patterns of task learning compared to PPT utilized in [Chapter 2](#). We observed that in the first session punishment contingencies were overgeneralized to the take action. However after 5-8 sessions of training, behavior became stable and suppression was specific to the seek action. Patterns of punishment resistance also mirrored that of the full task, with decreases in behavior appearing earlier after learning than in the first session. Lastly, we replicated our observed sex differences in the PPT. Females showed increased sensitivity to punishment risk compared to males, which mirrors risk taking patterns seen in other studies ([Orsini et al., 2016](#); [Orsini & Setlow, 2017](#)). These findings emphasize that learned probabilistic punishment procedures are robust and powerful methods to assess this mode of anxiety.

### The PL-mPFC adapts its response to learning action-outcome contingencies

Localized lesions and manipulations of neuronal activity have demonstrated that learning of action-outcome associations involves the PL-mPFC ([Balleine & Dickinson, 1998](#); [Ostlund & Balleine, 2005](#)). Electrophysiological recordings during instrumental learning show that this learning is expressed at a dynamic level throughout the PFC by emergence of a phasic response during action execution ([Del Arco et al., 2017](#); [Sturman & Moghaddam, 2011](#)). Moreover, while the adaptive response of individual neurons is both inhibitory and excitatory, the net population response following action execution is largely inhibitory ([Homayoun & Moghaddam, 2009](#); [Mulder et al., 2003](#)). After learning, phasic response of PL-mPFC neurons during action execution is flexible and changes with learning of new rules about outcome contingencies ([Del Arco et al., 2017](#); [Mulder et al., 2003](#); [Simon et al., 2015](#)). Given these studies, and that PL-mPFC is implicated in fear conditioning and other models of punishment representation ([Corcoran & Quirk, 2007](#); [Park & Moghaddam, 2017b](#)), we had hypothesized that learning of punishment probability is, in part, represented in PL-mPFC. Fiber photometry was used to assess changes in population activity because it allows for evaluation of PL-mPFC encoding of shock during learning.

The inhibitory response during peri-peek action periods of the no-shock blocks was consistent with previous unit recordings during action execution in various instrumental goal-directed tasks ([Hong et al., 2019](#); [Simon et al., 2015](#)) suggesting that our output measure reflects phasic neuronal activity. These inhibitory responses may represent disengagement of prefrontal cortical regions when motor actions become automatic or well learned ([Kupferschmidt et al., 2017](#);

Sturman & Moghaddam, 2011; Wu et al., 2004). This interpretation is further supported by our FR1 data, whereby utilization of the same fiber photometric approach revealed that peri-action phasic decreases emerge after instrumental actions are well learned.

We observed a significant reduction in this peri-*seek* action phasic response as punishment risk was learned. Importantly, this change in neuronal activity, similar to the change in behavior, was selective to the *seek* action. Further these attenuations subsided after the punishment contingency was removed, stressing these encoding changes were due to punishment contingencies and not experience with the *seek-take* chain schedule in general. Responses to events that were not associated with risk, i.e., *take* action and reward delivery, did not significantly change with learning, strengthening the notion that PL-mPFC ensembles are selectively encoding learning of punishment risk. Despite sex differences in this task, this change in PL-mPFC activity was not different depending on sex. Rather PL-mPFC encoding changes were predictive of individual differences in punishment resistance between pre and post PPT learning. Taken together, this is a novel learning role for the PL-mPFC and is consistent with its proposed role in mediating punishment related decision making after learning (Friedman et al., 2015; Orsini et al., 2018).

Further studies are needed to establish the neuronal basis of the reduced inhibitory response in calcium activity seen during PPT learning. One possible mechanism is changes in the recruitment of inhibitory interneurons, which then influence the activity of the excitatory pyramidal cells. Another possibility is changes in the recruitment of neuromodulators such as DA and NE, which generally inhibit the firing rate of spontaneously active neurons. DA and NE projections to the mPFC are sensitive to stress and anxiety provoking contexts (Deutch et al., 1990; Morilak et al., 2005; Pezze & Feldon, 2004). While these modulators generally do not produce overt excitatory or inhibitory responses on their target cells, they may influence ongoing responses.

## **PL-mPFC response to footshock is learning independent**

The excitatory response to footshock was consistent with previous studies showing that PFC responds strongly to stressors by increasing glutamate release (Moghaddam, 1993) and very recent studies where footshock produced an increase in the immediate early gene *c-fos* and neural calcium activity (Pascoli et al., 2015; Vander Weele et al., 2018). While it has been proposed that mPFC may adapt and desensitize its response to known stressors (McKlveen et al., 2015), we did not observe an overt reduction in phasic response to the footshock suggesting that any PL-mPFC mediated learning of probabilistic punishment in this task may be unrelated to adaptation to pain perception. It is, however, important to consider that population level activity measured in fiber photometry may arise through a variety of processes. For example, while no change in population level response may indicate a stable response of a brain region, it may also reflect a bidirectional change in both excitatory and inhibitory responses. Consequently, future studies with cell-specific and functional manipulations will advance our understanding of punishment learning. Regardless we failed to observe any correlation between changes in punishment encoding and changes in PPT behavior. Thus while the PL-mPFC encodes punishment it may generally represent punishment detection. However when the same footshock was given in a different context unconditionally, the response of the PL-mPFC was smaller in magnitude. Thus while such processing appears unrelated to learned punishment contingencies, footshock may be differentially encoded based on the context it is received (i.e. contingent vs. non-contingent).

## Conclusions

The mPFC is a critical node in the context of stress responsiveness, goal driven behavior, and fear and anxiety. These experiments indicate that the PL-mPFC selectively changes its response to risky actions as conflict contingencies are learned, suggesting this region may subserve learning of this form of anxiety by signaling information relevant to detect anxiogenic contingencies. Future studies may wish to parse the role of the PL-mPFC by comparison to other brain regions and manipulations of neural activity time-locked to risky action encoding periods.

The next chapter will add additional characterization to the role of the PL-mPFC in the learning of anxiogenic contingencies. This will be done by recording neural calcium activity in a conflict task already well characterized by electrophysiology. This allows for comparison of population signals to each other across these two distinct, but complementary, approaches. It will also investigate if anxiolytic treatment with diazepam influences action-related or punishment encoding in the PL-mPFC. Lastly, these studies will also present data from the ventral tegmental area, a key brain DA nucleus, to understand how neuromodulatory systems could mediate learned anxiety.

# Chapter 4

## PL-mPFC and VTA Encoding During Probabilistic Punishment: Diazepam Treatment and Comparison to Electrophysiology

In preparation as: Jacobs, D. S., Allen, M. C., Park, J., & Moghaddam, B. (In prep). **Encoding of instrumental action and punishment in the rodent prefrontal cortex and ventral tegmental area: Effects of learning and diazepam**

### Abstract

We utilized a previously characterized punishment risk task (PRT) to address how rodent PL-mPFC and VTA fiber photometry recordings relate to electrophysiological approaches. We also assessed the outstanding question of whether anxiolytic treatment with diazepam alters PL-mPFC action encoding under probabilistic punishment. Fiber photometry was used to measure pan-neural calcium activity in PL-mPFC and VTA in adult male and female rats. We find that selective suppression of male and female behavior developed after 2-3 sessions of exposure to the PRT. This change, or learning, was accompanied by a reduction of phasic neural activity in PL-mPFC and an upward shift in VTA activity, primarily during the peri-action period. Footshock produced a robust activation of neural activity in PL-mPFC and VTA that remained consistent in magnitude after learning. Diazepam did not change the phasic neural response of PL-mPFC or VTA to the footshock nor did it influence PL-mPFC responses to task events. Diazepam did, however, significantly and selectively produce a peri-action ramping response in the VTA and enhanced correlative VTA-mPFC activity. These findings characterize the adaptive neural responses of PL-mPFC and VTA during the learning of anxiogenic contingencies that are independent from the aversive experience itself. This may indicate that some of the anxiolytic properties of diazepam are not due to alterations in PL-mPFC encoding but rather by potentiating VTA action encoding.

**Key Abbreviations:** PRT- Punishment Risk Task, mPFC-medial prefrontal cortex, VTA-ventral tegmental area, DA-dopamine

### Introduction

Despite decades of research, neural mechanisms of anxiety remain poorly understood and the prevalence of anxiety continues to rise (Sartori & Singewald, 2019; Twenge & Joiner, 2020).

Studies into the neural underpinnings of anxiety, which assess innate anxiety, have also produced conflicting results in regards to prefrontal involvement (Roberts, 2020). Further these approaches fail to address real-world instances where anxiety develops because ongoing actions are learned to potentially result in an aversive outcome. To address the neural mechanisms underlying this mode of anxiety we utilize behavioral procedures where reward motivated behaviors are learned to conflict with the presence of a threat of harm via a low probability of footshock (see Jacobs & Moghaddam, 2021; Park & Moghaddam, 2017b). These contingencies typically result in behavioral suppression and mirror those used to produce anxiety in human and primate studies (Fischer et al., 2010; Jacobs & Moghaddam, 2020; Schmitz & Grillon, 2012; Vogel et al., 1971).

While the neural effects of anxiety are distributed across several brain regions (see Calhoun & Tye, 2015; McNaughton & Corr, 2004), the prefrontal cortex (PFC) in humans and prelimbic medial prefrontal cortex (PL-mPFC) in rodents is exquisitely sensitive to anxiety (Jacobs & Moghaddam, 2021), as induction of anxiety pharmacologically or through threat of punishment can result in cortical hypoactivity and alter task-related encoding (Balderston, Liu, et al., 2017; Balderston, Vytal, et al., 2017; Eysenck et al., 2007; Holmes & Wellman, 2009; Jacobs & Moghaddam, 2020; Park & Moghaddam, 2017b; Park et al., 2016; Roberts, 2020). In the no shock, predictable shock, non-predictable shock task, learned cues that signal unpredictable shock not only induce changes in PFC activity, but also disrupt PFC dependent behavior. Such findings clarify observations that anxiety taxes PFC executive functioning, producing deficits in cognitive control, neural encoding, and flexible adaptation to probabilistic conditions (Balderston, Liu, et al., 2017; Balderston, Vytal, et al., 2017; Grillon, 2008). The rodent PL-mPFC similarly becomes hypoactive under anxiety and is sensitive to stressful or anxiogenic conditions (Holmes & Wellman, 2009; Park & Moghaddam, 2017a; Radley et al., 2006).

The PL-mPFC is connected with many brain regions implicated in motivated action, fear, and anxiety. Several lines of research have implicated dopaminergic (DA) activity in adapting action strategy under negative outcomes (Broersen et al., 1995; Simon et al., 2011; St. Onge et al., 2011; St. Onge & Floresco, 2009; Verharen et al., 2018). The PL-mPFC is also reciprocally connected with DA nuclei such as the ventral tegmental area (VTA; Hoover & Vertes, 2007; Vertes, 2004), which is known to mediate reward motivated behavior (Schultz, 1998; Watabe-Uchida et al., 2017) and, more recently, in processing aversive outcomes (Cohen et al., 2012; Luo et al., 2018). The VTA sends predominantly DA projections to the PL-mPFC, which produce dramatic effects on PL-mPFC neural activity, local field potentials, as well as changes in motivational state (Lodge, 2011; Lohani et al., 2019; Vertes, 2004). In addition, communication between the VTA and PL-mPFC influences innate anxiety on the elevated plus maze (Gunaydin et al., 2014).

In the context of learned forms of anxiety through threat of harm, nascent research has found mPFC–VTA projections can discriminate punishment under risky conditions (Kim et al., 2017) and a previous report (Park & Moghaddam, 2017b) used single unit recordings in the punishment risk task (PRT) to show that PL-mPFC and VTA neurons adaptively encode actions depending on the presence or absence of a threat of punishment. Though these findings indicate these regions track anxiogenic contingencies, several outstanding questions remain. Do these brain regions adapt their responses to the punishment itself during the initial learning of anxiogenic contingencies? And, does anxiolytic treatment alter neural encoding of punishment, reward, or risky actions in this context?

The present studies utilized fiber photometry to assess how neural population states in the PL-mPFC and VTA encode action-contingent punishment in the PRT as contingencies were learned. Utilizing the PRT was a significant opportunity as it allowed for comparison of population photometry signals to our observations with punishment learning in the PPT and to

single unit responses. While few would claim globular neural calcium represents spiking *per se*, the exact representation of fiber photometry signals are still a matter of debate (Legaria et al., 2021). Thus characterization of similarities and differences across techniques will be informative for this burgeoning technique. Finally, we also assessed what role, if any, the PL-mPFC plays in the effects of treatment with a gold-standard anxiolytic, diazepam.

It was found that both the PL-mPFC and VTA demonstrated relatively similar overall patterns of activity compared to single units in the PRT. Over PRT learning, both regions showed unique patterns of action encoding while responsiveness to punishment was stable. Lastly, anxiolytic treatment selectively enhanced VTA action encoding and enhanced correlated activity between the two regions but did not influence PL-mPFC action encoding.

## Methods

### Subjects

A total of thirteen adult Long-Evans (n=8) and Sprague-Dawley (n=5) rats, pair-housed on a reverse 12 h:12 h light/dark cycle, were used. All experimental procedures and behavioral testing were performed during the rodents' dark (active) cycle. Both males (n=7) and females (n=6) were utilized. Subjects were run in several cohorts and were bred in house (n=8) or obtained from Charles River (n=5). All experimental procedures were approved by the OHSU Institutional Animal Use and Care Committee and were conducted in accordance with National Institutes of Health Guide for the Care and Use of Laboratory Animals.

### Surgery

**Viral Infusion Surgery:** Surgical techniques were outlined in Chapter 3. Briefly, prior to task training, subjects were injected with AAV8-hSyn-GCaMP6s-P2A-tdTomato to allow for pan-neuronal expression of fluorescent calcium indicator GCaMP6s and red fluorophore tdTomato. The coexpression of tdTomato allows for a motion artifact control signal to be used to correct GCaMP signals in noisy environments with rodents (Babayán et al., 2018; Matias et al., 2017; Menegas et al., 2018; Soares et al., 2016). Rats were anesthetized with isoflurane and placed in a stereotaxic apparatus, and injected with virus in the PL-mPFC and contralateral VTA.

**Fiber Implant Surgery:** After allowing at least seven weeks for virus expression, subjects were implanted with an optical fiber aimed at the prelimbic region of the mPFC (AP +3.0, ML  $\pm$  0.6, DV -3.3 mm from dura) and VTA (AP -5.4, ML  $\pm$  0.6, DV -7.5 mm from dura) using surgical procedures outlined in earlier. Subjects were given 1 week to recover from surgery before behavioral testing.

### Initial Training & Punishment Risk Task (PRT)

The PRT follows previously published methods (Chowdhury et al., 2019; Park & Moghaddam, 2017b). Rats were trained to make an instrumental response to receive a 45-mg sugar pellet (BioServe) under fixed ratio one schedule of reinforcement (FR1). The availability of the nose-poke for reinforcement was signaled by a 5-s tone. After at least three FR1 training sessions PRT sessions began. PRT sessions consisted of three blocks of 30 trials each. The action-reward contingency remained constant, with one nose-poke resulting in one sugar pellet. However, the

probability of receiving a punishment (300 ms electrical shock of 0.3 mA) after the FR1 action increased over the blocks (0%, 6%, or 10% in blocks 1, 2 and 3, respectively). To minimize generalization of the action-punishment contingency, blocks were organized in an ascending shock probability with 2-min timeouts between blocks. Punishment trials were pseudo-randomly assigned, with the first shock occurring within the first five trials. All sessions were terminated if not completed in 180 mins.

## Diazepam Treatment

Injectable diazepam (Pfizer/Hospira, Lake Forest, Il.) at a concentration of 5 mg/mL was used. Sterile saline (0.9% NaCl) was used for control injections. Diazepam (2.0 mg/kg) or saline was administered intraperitoneal 5 min prior to operant sessions with all injections given at a volume of  $\leq 1.0$  mL/kg. This dose of diazepam is known to produce anxiolytic effects on rats in the elevated plus maze and was utilized in [Chapter 2](#) (Pellow et al., 1985).

## Fiber Photometry System and Recording Procedures

Similar to [Chapter 3](#), recordings were performed with a commercially available fiber photometry system, Neurophotometrics Model: FP3001 (NPM). Recording was accomplished by providing both 470 nm and 560 nm excitation light through the 400- $\mu$ m core patchcord to the PL-mPFC or VTA for GCaMP6 and tdTomato signals, respectively. Data were recorded using bonsai open source software (Lopes et al., 2015) and timestamps of behavioral events were collected by 5V TTL pulses that were read into an Arduino interfaced with bonsai software.

## Fiber Photometry Analysis

**Peri-event analysis:** As outlined earlier, signals from the 465 (GCaMP6) and 560 (tdTomato) streams were processed in Python (Version 3.7.4) using custom written scripts in accordance with previously published methods (Jacobs & Moghaddam, 2020). Briefly, 465 and 560 streams were low pass filtered at 3 Hz using a butterworth filter and subsequently broken up based on the start and end of a given trial. The 560 signal was fitted to the 465 by a first order polynomial using the least-squares approach and subtracted from 465 signal to yield the change in fluorescent activity ( $\Delta F/F = 465 \text{ signal} - \text{fitted } 560 \text{ signal} / \text{fitted } 560 \text{ signal}$ ). Peri-event z-scores were computed by comparing the  $\Delta F/F$  after the behavioral action to the 4-2 sec baseline  $\Delta F/F$  prior to a given epoch. To investigate differential activity that was seen during punishment administration and during anticipation of punishment, punished (i.e. shock) trials and unpunished trials were separated. Any trials with a z-score value  $> 40$  were excluded. Of the approximately 3,000 trials analyzed this occurred on  $< 1\%$  of trials.

**Time Lagged Cross-Correlation Analysis:** Cross correlation analysis has been used to identify networks from simultaneously measured fiber photometry signals (Sych et al., 2019). For subjects with properly placed fibers in the PL-mPFC and VTA, correlations between photometry signals arising in the VTA and PL-mPFC were calculated for the peri-action, punishment, and peri-food periods using the z-score normalized data. The following equation was used to normalize covariance scores for each time lag to achieve a correlation coefficient between -1 and 1:

$$Coe\!f = Cov / (s^1 * s^2 * n) \tag{4.1}$$

Where  $Cov$  is the covariance from the dot product of the signal for each timepoint,  $s^1$  and  $s^2$  are the standard deviation of the PL-mPFC and VTA streams, respectively, and  $n$  is the number

of samples. An entire cross-correlations function was derived for each trial and epoch.

## Statistical Analysis

Trial completion was measured as the percentage of completed trials (of the 30 possible) for each block, while action latencies were defined as time from cue onset to action execution. Data were assessed through a repeated measures ANOVA or mixed effects model with factors risk block and session and *post-hoc* tests were performed using the bonferroni correction where appropriate. Statistical tests were performed using GraphPad Prism (Version 8) and utilized an  $\alpha$  of .05.

To assess changes in neural activity, we utilized a permutation based approach as outlined in (Jean-Richard-dit-Bressel et al., 2020) using Python (Version 3). An average response for each subject for a given time point in the cue, action, or food delivery period was compared to either the first PRT session or saline. For each time point a null distribution was generated by shuffling the data, randomly selecting the data into two groups, and the mean difference between groups was calculated. This was done 1,000 times for each timepoint and a two-sided p-value was obtained by determining the percentage of times a value in the null distribution of mean differences was greater than or equal to the observed difference in the unshuffled data. To control for multiple comparisons we utilized a consecutive threshold approach based on the 3 Hz lowpass filter window (Jean-Richard-dit-Bressel et al., 2020; Pascoli et al., 2018), where a p value  $< .05$  was required for 13 consecutive samples (i.e.  $>$  the low-pass filter window, 300 msec) to be considered significant.

To assess correlated activity changes as a function of risk or session, we took the peak and confidence interval for the overall cross correlation function. These values were compared by a two-way ANOVA with factors risk and session and utilized a *post-hoc* bonferonni correction. Tests were done using GraphPad Prism (Version 8) and utilized an  $\alpha$  of .05.

## Excluded Data

One rat was excluded from behavioral and photometric analysis for session 3 due to completion of only two trials. Three VTA rats were excluded because fiber placements were too ventral or GCaMP expression was not observed. Several rats did not complete all phases of the experiment due to lost fiber implants, leaving the final sample sizes as  $n=9$  and  $n=7$  for PL-mPFC in learning and diazepam treatment stages, respectively, and  $n=4$  for VTA in learning and diazepam treatment stages.

## Histology and Imaging

Methods for determination of fiber location and viral expression were determined according to the methods outlined in the [Histology and Imaging Section](#) of Chapter 3.

## Results

### Modeling learned anxiety using the probabilistic risk task (PRT)

To assess how global neural activity in the PL-mPFC and VTA changes during anxiety learning, we infected neurons with GCaMP6s using a synapsin promotor and implanted optical fibers in

the PL-mPFC and contralateral VTA (Figure 4.1A, G-H). Fibers were largely confined to the PL-mPFC. After initial FR1 training we then introduced a punishment contingency to the FR1 schedule of reinforcement whereby multiple 30-trial components were each associated with a risk of shock (increasing from 0-10% logarithmically, Figure 4.1B-C.). This model, and other similar approaches, have been validated with by demonstrating that action suppression is specific to risk blocks and sensitive to anxiolytic treatment with diazepam. (Dalterio et al., 1988; Jacobs & Moghaddam, 2020; Park & Moghaddam, 2017b). To inform our previous results we monitored behavior and recorded neural calcium activity during the first three sessions of PRT learning. The punishment contingency resulted in increases in latency to perform the risky action as well as changes in trial completion over learning (Figure 4.1D-E). Action execution was suppressed in the PRT (effect of risk:  $F(1.4,11.2) = 17.6, p < .01$ ) but this effect was greater with learning (risk by session interaction:  $F(2.2,16.03) = 3.98, p = .036$ ). Significant decreases from 0% risk were only observed in Sessions 2 and 3 in the last block (post hoc  $p$  values  $< .023$ ). Learning was also evident because threat of punishment was overgeneralized to food pellet retrieval and inspection of risk blocks in Session 3 indicated this effect decreased over training (two-tailed paired  $t$ -test<sub>Session 1 vs. 3</sub>:  $t(7)=2.38, p = .048$ ; Figure 4.1F).

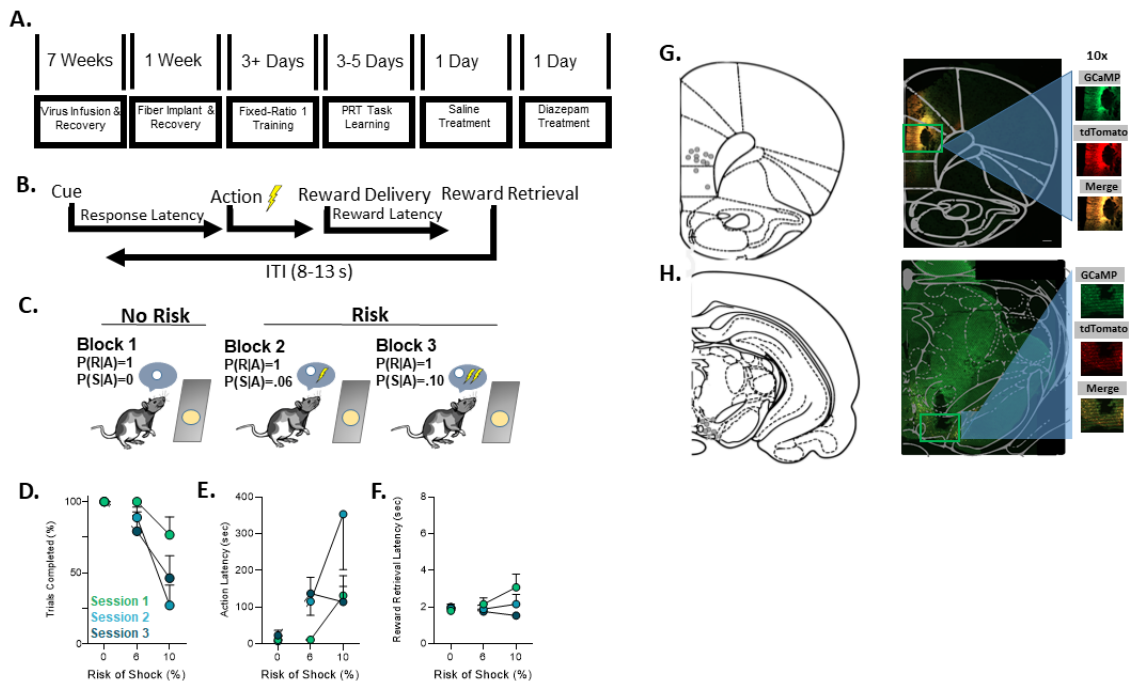


Figure 4.1: Schematic of experimental design and behavior on the PRT. **A.** Timeline of experiment. **B.** Trial structure for the PRT and **C.** the corresponding multi-component schedule used for ascending risk of shock. **D.** Trial completion over the first three session. **E.** Changes in latency to action completion over the first three sessions. **F.** Latency to retrieve the food pellet. **G-H.** Fiber placements and representative images of expression for PL-mPFC and VTA. Grey scale bar = 500  $\mu$ m.  $n = 4-9$  rats.

## Punishment is encoded by the VTA and mPFC over Learning

An important outstanding question is how aversive events which support anxiety, i.e. threat of punishment, are encoded by the brain and how, or if, changes occur with the learning of anxiogenic contingencies. Fiber photometry allowed for assessment of neural encoding of punishment, which was not possible during single unit recording. We observed robust increases in

activity time-locked to the presentation of footshock in both the PL-mPFC and VTA (Figure 4.2A-B). Interestingly these effects did not change with learning or exposure to the shock as the magnitude of increase from footshock was similar across each of the three sessions and the only significant change was seen in the PL-mPFC approximately 1.5 sec after shock (i.e. in the reward delivery period).

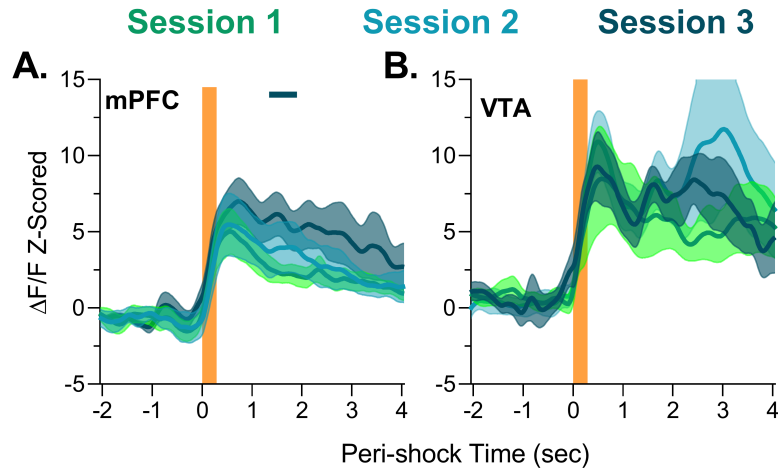


Figure 4.2: Encoding of punishment by VTA and PL-mPFC. **A.** The PL-mPFC demonstrated robust phasic increases in neural activity at the time of shock administration (orange bar) over the first three PRT sessions. **B.** Same as **A** but for the VTA. Solid bars indicate significant differences from Session 1.  $n = 4-9$  rats.

## The PL-mPFC and VTA dynamically encode actions in PRT learning

We further asked if encoding of task events changed in these brain regions before and after learning of the PRT. In the PL-mPFC, evidence for changes in encoding of the tone cue was not observed across any of the sessions. The PL-mPFC demonstrated phasic decreases during the action execution epoch when actions were performed with no risk of punishment (Figure 4.3A). However this phasic decrease was attenuated when a threat of punishment was part of the reinforcement schedule (Figure 4.3B-C) after both two and three sessions of training. Further, encoding for the reward increased with risk of shock in the second session, though this effect dissipated by the third session.

We observed learning dependent encoding of the tone cue in the VTA, which achieved significance in the third session in the highest risk block (Figure 4.3F). The VTA also showed a phasic increase in activity after action execution after learning of threat of punishment, specifically in risk blocks (Figure 4.3E-F). The largest task related response of the VTA was observed after food delivery, which elicited about twice the level of increase compared to tone and action epochs, and was seen over task learning. Collectively these results indicate that both the VTA and PL-mPFC change their encoding of risky actions during the learning of anxiogenic contingencies.

## Diazepam does not alter punishment encoding by the VTA or PL-mPFC

We further sought to determine if anxiolytic treatment changed the encoding of probabilistic punishment by the PL-mPFC and VTA. We administered an anxiolytic dose of diazepam before

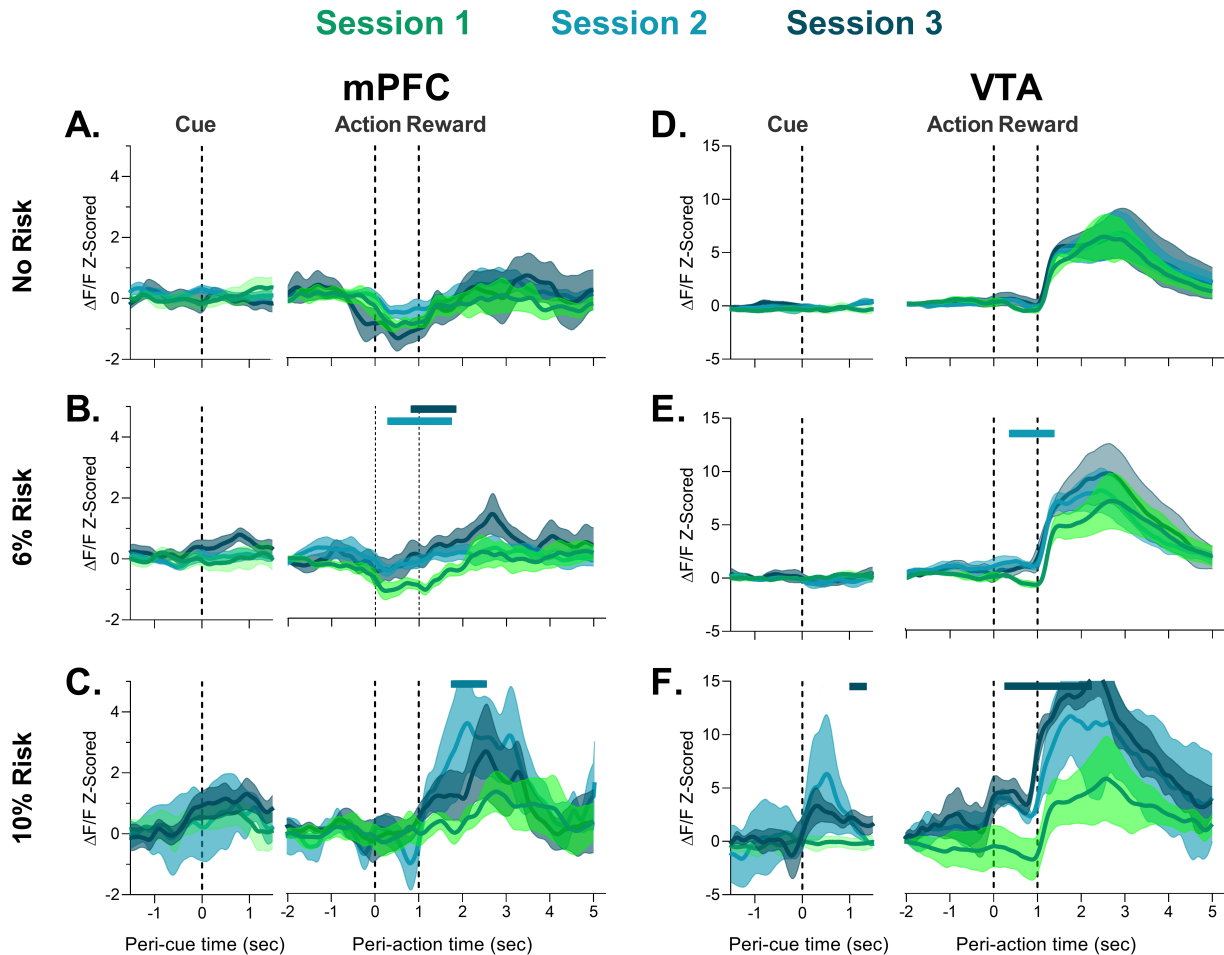


Figure 4.3: Encoding of punishment anticipation by VTA and PL-mPFC during the first three sessions of PRT learning. **A-C.** PL-mPFC encoding of cue, action, and reward delivery for each risk block during the PRT task. **D-F.** VTA encoding of cue, action, and reward delivery for each block during the PRT task. Solid bars indicate significant differences from Session 1, where the color of the bar indicates the different session.  $n = 4-9$  rats.

the PRT which theoretically attenuated states of anxiety but kept contingencies present. Similar to our previous results, diazepam pretreatment did not influence the number of trials completed ( $F$  values  $< 1.1$ ,  $p$  values  $> .35$ ; Figure 4.4A-B). Motoric effects from diazepam were observed in three subjects in the first safe block. However, these effects subsided as action latencies were selectively decreased during risk blocks (Figure 4.4C). Because we were specifically interested in risk versus no risk blocks, and because one subject did not complete all trials, we opted to compare combined risk blocks between saline and diazepam. Individually it was evident that diazepam decreased risky action hesitation (latency) and this was verified statistically (risk by treatment interaction:  $F(1,6)=6.6$ ,  $p = .042$ ) such that diazepam selectively attenuated action latency increases in risk blocks (post hoc  $p$  value =  $.048$ ; Figure 4.4C) but not the no risk block (post hoc  $p$  value =  $.38$ ).

Fiber photometry afforded the possibility to assess if diazepam's anxiolytic effects may be related to changes in processing of aversive events. Thus we assessed trials which resulted in footshock to test the possibility that diazepam could influence processing of punishment in either the PL-mPFC or VTA. Interestingly diazepam had no significant effects on the encoding of the footshock punishment. Both VTA and the PL-mPFC increased neural activity after shock administration at comparable levels to that of saline (Figure 4.4D). These results suggest that while anxiolytic, diazepam does not change the encoding of the anxiogenic stimulus by

the PL-mPFC nor VTA.

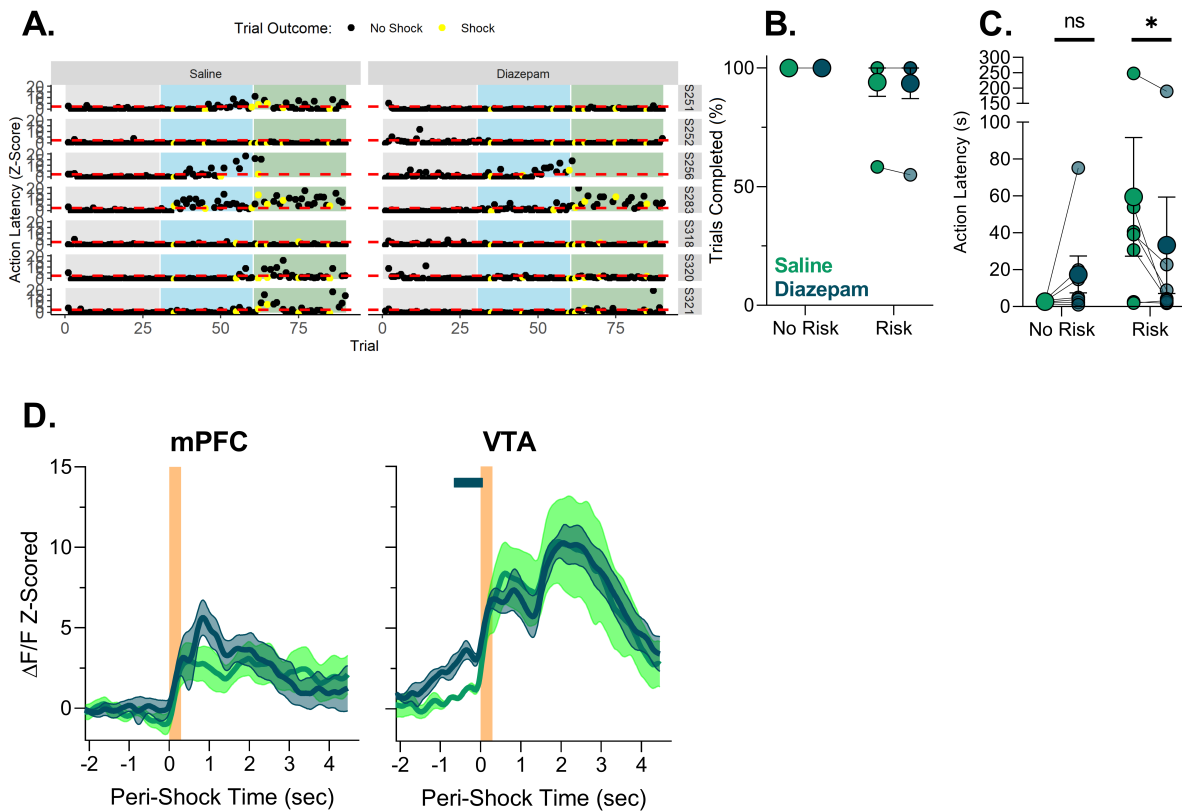


Figure 4.4: Effects of diazepam on PRT behavior and punishment encoding. **A.** Individual subject normalized action latencies over the course of saline and diazepam sessions. Each dot is a trial color-coded by whether a shock was administered on that trial. Trials in risk blocks reflect trials 30+ (i.e. blue and green backgrounds). **B.** Trial completion was unaffected by diazepam. All but one subject completed nearly all trials and that subject showed stable behavior. **C.** Overall action latencies for trials where risk was present or absent. Diazepam significantly and consistently attenuated action latency increases seen from probabilistic punishment. Smaller circles denote individual data points. **D.** Recordings from the PL-mPFC and VTA time-locked to footshock punishment (orange bar). Solid bars above traces indicates a significant deviation from Saline at those timepoints. \* $p < .05$ , ns = not significant.  $n = 4-7$  rats.

## Diazepam changes VTA but not PL-mPFC encoding during action execution

We further asked if diazepam influenced encoding in unpunished trials in the PRT. In the PL-mPFC we observed little change from diazepam treatment, as responses, or lack thereof, to the cue and action execution were not different from saline. We did observe that the population signal was briefly lower around the time of reward delivery following diazepam in the 0% risk block. The signal returned to saline levels within one second after reward delivery. We also further replicated our finding that activity states become more neutral in the PL-mPFC with increased probabilistic punishment (Figure 4.5A-C).

In the VTA, diazepam enhanced activity during the task. This was weakly observed in the cue epoch period at no risk. A more robust and sustained increase in activity was observed

during the peri-action epoch where the VTA developed a phasic increase in activity just prior to action execution after diazepam treatment (Figure 4.5D-E). Reward encoding in the VTA, as evidenced by an increase in activity at the time of food delivery, did not change with diazepam. Taken with the previous findings, these results suggest that an anxiolytic dose of diazepam does not affect encoding of punishment or reward in the PL-mPFC or VTA under anxiogenic contingencies, but does influence VTA activity in the initial approach to execute a risky action.

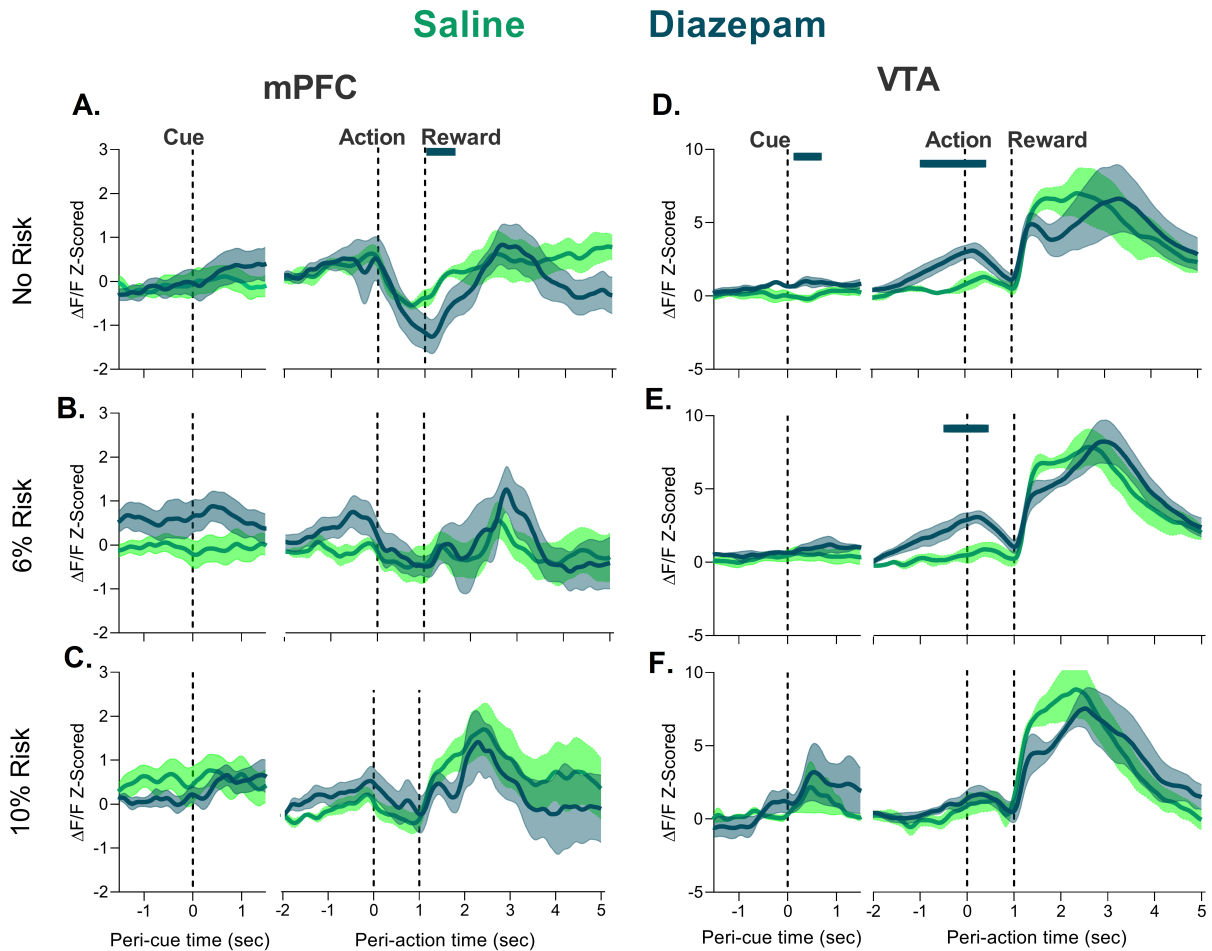


Figure 4.5: Effects of diazepam on action encoding in the PRT in the PL-mPFC (left) and VTA (right). **A-C**. In PL-mPFC, no effect of diazepam was observed during the cue or action epoch in the PL-mPFC, and a small but significant downward shift was seen following treatment early in the food epoch. **D-F**. In VTA, diazepam had little or no effect on neural activity during the cue or reward period. However pre-action activity was enhanced by diazepam, an effect which extended until briefly after action execution. Solid lines above traces indicate significant differences from Saline at those timepoints.  $n = 4-7$  rats.

## Diazepam enhances correlated activity of the PL-mPFC and VTA

Finally, we wondered if diazepam may exert effects on the correlated activity of the PL-mPFC and VTA. Thus we performed a cross correlation analysis for all trials after saline or diazepam treatment for the action and food epochs. For action execution, diazepam transiently increased correlated activity of the PL-mPFC and VTA regions in the safe and 6% risk blocks before activity patterns returned to saline levels in the 10% risk block (Interaction:  $F(2,596) = 7.9$ ,  $p < .01$ ; Figure 4.6A-D). In the food epoch, diazepam produced a consistent increase in correlated

activity across all blocks (Interaction:  $F(2,596) = 9.1$ ,  $p < .01$ ; Figure 4.6E-H). Across all analyses, peak correlations between these two regions generally appeared with no time lag, with the exception of the action period at high risk, where a 0.5 second VTA lead was observed. Finally, while we observed the highest correlated activity during encoding of the footshock, we did not observe any effect of diazepam (Figure A.13). Taken together these results suggest that diazepam enhances correlated activity between the VTA and PL-mPFC during risky action and reward outcome encoding, though this effect is not specific to blocks with risk.

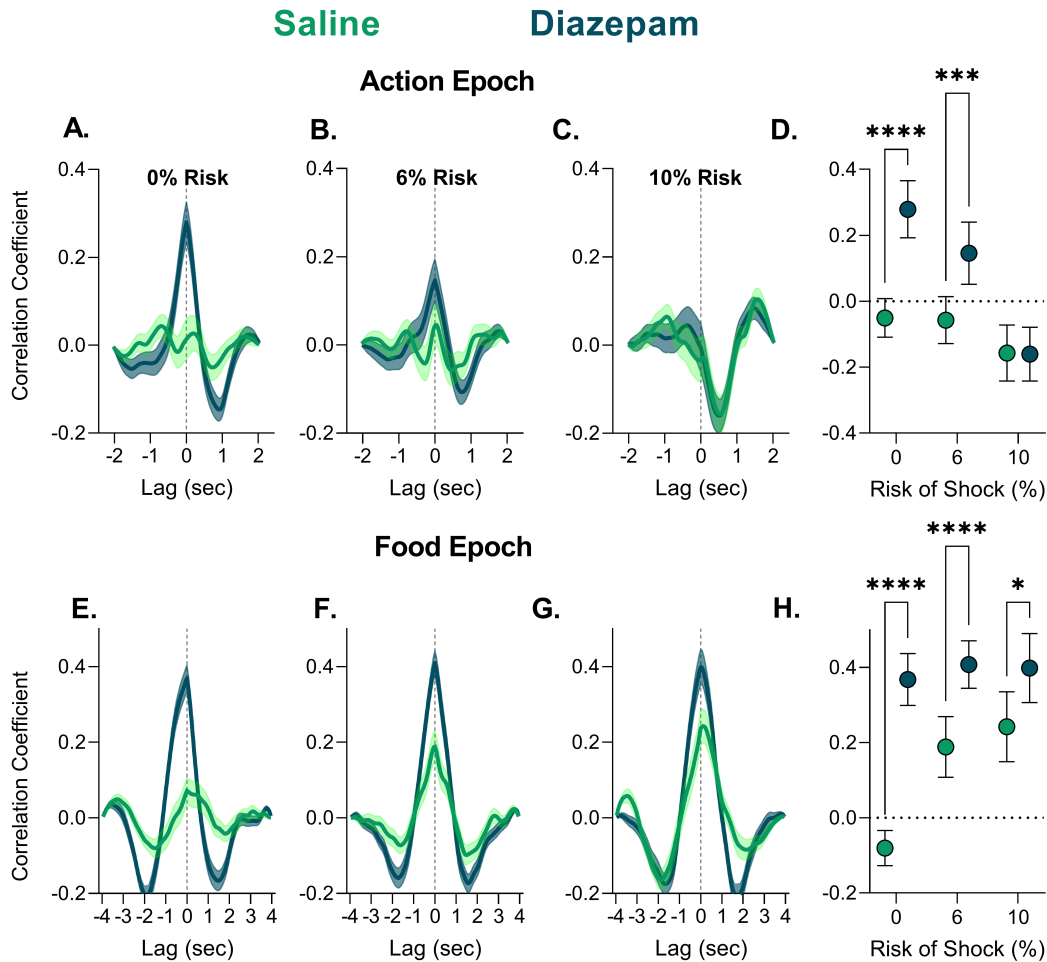


Figure 4.6: Effects of diazepam on correlated activity between the PL-mPFC and VTA during action and food epochs. **A-D.** Correlated activity was enhanced by diazepam treatment in the safe block and the lower risk block. While correlated activity reached its lowest level at the highest risk block, regardless of treatment. **E-H.** Correlated activity was enhanced by diazepam during the food epoch across all blocks. \*  $p < .05$ .  $n = 77-120$  trials from 4 rats.

## Discussion

Adapting behavior in response to reward and punishment is critical for survival. In the real world these outcomes are not independent, as actions executed to obtain something commonly carry some risk of punishment. The risk of punishment is learned over experience, and the perceived risk of punishment can engender anxiety-related states that will bias behavioral action. Previous work has demonstrated that the PL-mPFC and VTA dynamically encode risk of punishment during reward-motivated actions through *in vivo* electrophysiology (Park & Moghaddam, 2017b). The present studies expand on these findings by utilizing fiber photometry to demonstrate that population level signals in both the VTA and PL-mPFC encode punishing outcomes during reward seeking, and maintain sensitivity to punishment through initial learning of punishment contingencies and after anxiolytic treatment with diazepam. Diazepam did not influence PL-mPFC action encoding. Rather diazepam enhanced the pre-action response of the VTA. Taken together these studies inform our understanding of the functional role of these regions in the encoding of actions performed under anxiety and in the context of responsivity to punishment.

### Relation to electrophysiological findings

While few would claim fiber photometry signals reflect spiking seen in single unit recording, photometry is increasingly popular due to its potential for cell and pathway specific measurements and its ability to record over extended periods of time. Thus one aim of the present study was to assess how fiber photometry measurements in the PRT relate to overall unit recordings measured in Park and Moghaddam, 2017b. We observed that PL-mPFC activity became progressively more neutral with risk, while the VTA developed phasic increases at the time of action execution. This finding similarly reflects ordinal patterns of population averages seen from single units and complements the previous finding that neural activity in both regions was significantly influenced by punishment risk during action encoding after task learning (i.e. after three days of task exposure).

Encoding changes of the tone cue were not observed in the PL-mPFC and only observed at the highest risk block in the VTA. Previously, we had not observed a robust single unit responses to the cue in the PL-mPFC but did in the VTA across all blocks. However the risk related VTA response was mixed, depending on if units were putative DA versus non-DA. Thus an important consideration in this data set is that our responses reflect neural activity across all subtypes, and may provide a rationale for the discrepancy seen here. Nevertheless the risk dependent elevation in VTA response to the cue seen here and in Park and Moghaddam, 2017b may suggest the cue gains increased salience with risk.

Finally, similar to the single unit data, the largest observed response was the VTA response to food delivery which has been extensively documented (Park & Moghaddam, 2017b; Watabe-Uchida et al., 2017). Taken together these results indicate that calcium imaging of PL-mPFC and VTA activity through fiber photometry shows similarities to the overall population responses seen from *in vivo* unit recording in this task, particularly when considering our signals were not specific to particular subtypes of neurons.

### Uniform punishment encoding in mPFC and VTA

Learning of the punishment risk contingencies was apparent because the risk of shock was initially overgeneralized to other aspects of task behavior, but became selective for the risky action after three sessions. An important question which fiber photometry is well positioned to

address in regards to the learned suppression of behavior is whether such changes are related to responsivity to the punishment itself. Encoding of the punishment itself did not change in the VTA or PL-mPFC over the learning of this task. This finding reinforces the results of the PL-mPFC during punishment encoding seen in Chapter 3 and adds support to the VTA role in aversion processing (Cohen et al., 2012; Jacobs & Moghaddam, 2020; Lammel et al., 2012; Park & Moghaddam, 2017b).

## **Diazepam does not alter PL-mPFC action or punishment encoding**

Diazepam is a common anxiolytic drug that is used to validate anxiety assays and attenuates the action suppression seen from punishment risk in this task and others (Jacobs & Moghaddam, 2020; Liljequist & Engel, 1984; Park & Moghaddam, 2017b). The mechanism for diazepam's anxiolytic effects are poorly understood, aside from its pharmacological properties (Sartori & Singewald, 2019). One possibility is that diazepam itself attenuates responses to anxiogenic stimuli such as punishments. This idea, however, was not supported by our data, as we saw no attenuation of punishment responsivity in the VTA or PL-mPFC after diazepam.

An alternative explanation is that diazepam enhances responsivity to reward, which would consequently drive reinforced behavior under punishment risk. Again, our results failed to support this explanation, as reward encoding was similar across regions after treatment. Together these findings stress diazepam has little impact on the processing of emotional stimuli itself in these regions, and begs the question of whether its effects extend outside of basic punishment or reward sensitivity.

Changes in action encoding seen in the PL-mPFC with risk were unaffected by diazepam. This finding extends on the work of Chapter 3. While extinguishing punishment contingencies in the prior chapter recovered the phasic decreases seen without risk, lessening states of anxiety with diazepam did not produce such an effect. Collectively this suggests PL-mPFC risky action encoding changes reflect the tracking of anxiogenic contingencies rather than anxiety itself.

## **Diazepam enhances VTA action encoding and VTA-mPFC coactivity**

The main observed effect of diazepam on encoding in the task was seen in the VTA during the action epoch. Diazepam produced a gradual enhancement of neural activity beginning >1 second before action completion in the first two blocks. VTA neurons demonstrate diverse encoding patterns for task-related information (Engelhard et al., 2019) and are sensitive diazepam treatment (Rincón-Cortés et al., 2018; van der Kooij et al., 2018). Our results with diazepam may be illuminated by the observation of so-called “ramping activity” of VTA neurons. This pattern of encoding when seen with single-units has previously been associated with attentional tuning, movement kinetics, and distance to goals (Kremer et al., 2020; Totah et al., 2013). A recent study which elegantly characterized VTA ramps using fiber photometry found that, after learning, these signals reflect interoceptive goals particularly when internal maps, and not external stimuli, are utilized to process reward proximity (Guru et al., 2020).

One possible explanation for the results here is that impending or present anxiety contingencies may render subjects more attentive to stimuli and external conditions rather than their own internal drive towards goal acquisition which ultimately produces a suppression of behavioral response. Thus diazepam's production of VTA ramping activity may be a mechanism to redirect attentional processes to serve goals towards acquiring rewards. This interpretation is also in line with studies which assess the cognitive effects of diazepam in humans, as diazepam has been shown to attenuate vigilant-avoidant patterns of emotional attention to fearful stimuli (Pringle et al., 2016).

It is intriguing that these effects dissipated by the highest risk block, when anxiety is presumably highest. Similarly, we found that an enhancement in peri-action correlated activity between the PL-mPFC and VTA from diazepam also dissipated in the high risk block. One possible explanation for this is due to the metabolism of diazepam. However, this is not likely as most subjects completed the task within 1 hr (Diazepam  $t_{1/2} \approx 1$  hr; Friedman et al., 1986) and we continued to see enhanced correlated activity across all blocks during the food epoch.

Another possibility is that diazepam may only function in such a capacity when threats are distal, such as in block one, or lower in likelihood; and different mechanisms may be utilized in response to greater increases in harm likelihood or in accordance with time on task. The persistent increase in correlated activity during the food epoch may be one such mechanism at play. PFC communication with subcortical drives is critical for motivated behavior and disruption of which is a potential mechanism of anxiety (Balderston, Vytal, et al., 2017; Fujisawa & Buzsáki, 2011; Sartori & Singewald, 2019), and the VTA and dACC containing salience network is attenuated by anxiety in humans (Xu et al., 2019). In regards to reward encoding, rodent VTA projections to the mPFC show enhanced response to reward delivery under probabilistic conditions and can drive behavior away from previously learned cue-reward associations (Ellwood et al., 2017). Lastly, benzodiazepine treatment with midazolam has recently been shown to restore non-prefrontal cortical-subcortical connectivity in healthy humans during acute anxiety (Cornwell et al., 2017). Taken together it is possible that diazepam's restorative effects on behavior require normalization of cortical and subcortical regions across multiple facets of reward motivated processes, an idea which may be addressed through temporally specific causal manipulations.

## Conclusion

Our results indicate that action encoding by PL-mPFC, and VTA, change over exposure to probabilistic punishment contingencies, while punishment and reward encoding *per se* are largely stable. This corroborates our prior PL-mPFC findings in Chapter 3 and single unit data in Park and Moghaddam, 2017b. Diazepam attenuated behavioral suppression without influencing PL-mPFC encoding changes during risky actions. This finding suggest the PL-mPFC action encoding is particularly sensitive to anxiogenic contingencies rather than the state of anxiety alone. We further propose that diazepam's effects may be due to enhancement of VTA action encoding and network level restoration to support task engagement. These findings provide important insight into the effects of learned anxiogenic contingencies on neural processes which are critical for animal survival and may inform our understanding of maladaptive anxiety (Aylward et al., 2019).

The upcoming chapter will return to utilization of the PPT outlined in Chapter 3. This work will utilize the same fiber photometry approach to investigate whether there are overlapping or divergent roles across the rodent PFC in anxiogenic contingency learning by assessing the rodent lateral OFC (LO-OFC) during PPT learning. These recordings were also performed in tandem with PL-mPFC recordings to permit correlation analysis between these subregions during probabilistic punishment learning.

# Chapter 5

## LO-OFC Encoding During Probabilistic Punishment Task Learning

In preparation as: Jacobs, D. S., & Moghaddam, B. (In prep). The orbitofrontal and medial prefrontal cortex differentially encode the learning of probabilistic punishment during reward seeking

### Abstract

The prefrontal cortex (PFC) is implicated in reckless behavior and maladaptive anxiety. Mounting evidence has shown that these regions have distinct and overlapping involvement in the control of behavior. However, little is known about how distinct PFC regions encode behavioral action when conflicted with punishment. Our previous studies demonstrated a role of the PL-mPFC in encoding risky action contingencies. Here we extend these results to the lateral orbitofrontal cortex (LO-OFC) by recording neural calcium activity before and after the acquisition and extinction of probabilistic punishment learning using fiber photometry. We further assessed how correlated activity of these regions changes with punishment learning and extinction using trial-averaged cross correlation analysis. Overall, the LO-OFC showed learning related changes in task encoding but with notable differences compared to the PL-mPFC. While we have previously shown the PL-mPFC adapts to the risky action (i.e. punishment contingency) the LO-OFC adapted to safe actions and punishment itself. These changes in action encoding, as well as disruption of correlated activity, were normalized when punishment contingencies were extinguished. These findings suggests the PL-mPFC and LO-OFC serve complementary roles in learned anxiety during reward seeking.

**Key Abbreviations:** PPT-Probabilistic Punishment Task, PL-mPFC-prelimbic medial prefrontal cortex, LO-OFC-lateral orbitofrontal cortex

### Introduction

In naturalistic settings reward-driven action commonly carries some risk of harm. Navigating such an environment requires processing of reward, punishment, and the interconnection between the two to flexibly adapt reward seeking. In both reckless and anxiety related disorders these processes are disrupted and co-occur with disruption or lesions of the PFC, highlighting that action and threat processing may underlie certain symptoms of multiple psychopathologies (Goldstein & Volkow, 2011; Milad & Rauch, 2007; Moghaddam & Homayoun, 2008; Robinson et al., 2019).

Both the OFC and mPFC subregions of the PFC are implicated in reward-related encoding of actions and outcomes, fear stimuli or contexts, behavioral flexibility, and updating (Panayi & Killcross, 2018; Sarlitto et al., 2018; Schoenbaum et al., 1998; Sierra-Mercado et al., 2011; Stalnaker et al., 2015; Sul et al., 2010; Turner et al., 2021). Differential plasticity in OFC and mPFC neural activity has also been observed. These experiments demonstrated that OFC and mPFC divergently adapt neural activity to drug exposure as well as to encoding actions and outcomes in instrumental contexts (Homayoun & Moghaddam, 2009; Homayoun & Moghaddam, 2006; Simon et al., 2015).

Burgeoning research has begun to characterize how each of these cortical regions may influence and encode action when conflicted with punishment. Inactivation or hypoactivity in the PL-mPFC is associated with perturbed compulsive drug taking in rats (Chen, Yau, et al., 2013). In contrast, hyperactivity in the LO-OFC is associated with higher punishment resistance and compulsive reward seeking (Harada et al., 2019; Pascoli et al., 2015). Pharmacogenetic manipulation of the LO-OFC can exert bidirectional effects depending on whether subjects are risk-averse or risk insensitive (Pascoli et al., 2015; Pascoli et al., 2018) an effect that has similarly been observed with optogenetic stimulation of neurons in the PL-mPFC (Chen, Yau, et al., 2013).

Using the risky decision making task to assess changes in behavior under changing probability of punishment, lesions of the PL-mPFC result in suboptimal adaptation of behavior to punishment risk (Orsini et al., 2018). However lesions of the OFC in the risky decision making task lead to hypersuppression of risk taking (Orsini et al., 2015). These findings are intriguing given the well documented interconnectivity of these regions (Murphy & Deutch, 2018; Vertes, 2004) and two recent influential publications have demonstrated the causal role of either mPFC or OFC striatum projecting pathways in rodent behavioral control under conflict (Friedman et al., 2015; Pascoli et al., 2018). These findings lead to the potential for complementary information being moderated by these regions to support learned approach-avoidance conflict.

No studies have recorded neural activity in the mPFC and OFC to investigate how these two regions may uniquely contribute to reward-driven actions as punishment risk is learned. To begin to address this void we recorded neural activity in the PL-mPFC and contralateral LO-OFC before and after animals learned the probabilistic punishment task (PPT). We then removed the punishment contingency to observe if changes in task encoding would return to baseline. We observe that, unlike the PL-mPFC, the LO-OFC adapted its encoding after safe action execution, without adapting its response to the risky action. The LO-OFC also adapted its responsiveness to punishment after learning in a context specific manner. Lastly, while punishment risk selectively attenuated correlated activity between the PL-mPFC and LO-OFC, extinction of the punishment contingency normalized learning related changes. Together these results suggest the PL-mPFC and LO-OFC demonstrate distinct and complementary processing of action sequences under punishment which may be used by different behavioral systems to orchestrate behavior in approach-avoidance decision making.

## Methods

### Subjects

A total of 11 adult Long-Evans rats, housed on a reverse 12 h:12 h light/dark cycle, were used. Animals were pair housed until implantation of the optical fiber. All experimental procedures and behavioral testing were performed during the rodents' dark (active) cycle. Both males (n=7) and females (n=4) were utilized. Subjects were run in several cohorts and were bred in house.

## Surgery

**Viral Infusion Surgery:** Subjects were injected with AAV8-hSyn-GCaMP6s-P2A-tdTomato (OHSU Vector Core,  $5^{e13}$  ng/mL) to allow for pan-neuronal expression of fluorescent calcium indicator GCaMP6s as well as a non-calcium dependent fluorophore tdTomato. Rats were anesthetized with isoflurane and placed in a stereotaxic apparatus. Following an incision and topical application of lidocaine, craniotomy was performed to lower a 10  $\mu$ L syringe (Hamilton) for virus infusion into the mPFC and OFC. Two injections were made (325 nL/site @ 50 nL/min) at the coordinates AP + 2.8, ML  $\pm$  0.65, DV -2.5 and -3.5 mm (from dura) and AP + 3.0, ML  $\pm$  3.0, DV -3.8 and -4.8 mm (from dura), for the PL-mPFC and LO-OFC respectively, with the most ventral injection always performed first. A microcontroller (World Precision Instruments) was used for the injections. Virus was allowed to diffuse for 5 min after the most ventral injection. The needle was slowly raised and the second injection was performed and allowed 12 min to diffuse. After this the needle was removed, the incision was stapled, and animals were given a 5 mg/kg injection of carprofen subcutaneously.

**Fiber Implant Surgery:** After allowing at least four weeks for virus expression, subjects were implanted with an optical fiber aimed at the PL-mPFC (AP +2.8, ML  $\pm$  0.7, DV -3.3 mm from dura) and LO-OFC (AP +3.0, ML  $\pm$  3.6, DV -5.2 mm from skull at a 7° angle) using the surgical procedures outlined above, with the exception that three additional bore holes were made for three skull screws which surrounded the craniotomy. The optical fiber was slowly lowered and was glued to the skull with light-curing epoxy (Tetric N-flow, Ivoclar Vivadent). Subjects were given 5 mg/kg of carprofen after this procedure and returned to ad libitum food for 5 d before returning to food restriction. Subjects were given 1 week to recover from surgery before behavioral testing.

## Apparatus

An operant chamber (Coulbourn Instruments, PA) was used for behavioral testing. The chamber included two nose poke holes, which could be illuminated, on one wall located 2 cm above a grid floor. The grid floor was connected to a shock generator which delivered footshocks. The food trough was on the opposite wall to the nosepokes and was used to dispense 45 mg sucrose pellets (Bio-Serv) and detect food trough entries. The operant chamber had an opening in the top of the box to permit entry for the recording patchcord. Graphic State software (version 4, Coulbourn Instruments) running on a windows PC was used for programming the task.

### No Shock Baseline Session

As outlined earlier, subjects were trained to make two spatiotemporally distinct successive instrumental responses to receive a 45-mg sugar pellet under a fixed ratio one schedule of reinforcement (FR1). The first action will be referred to as the “seek” action and the second action will be referred to as the “take” action. Completion of the seek action led to a 1.5 sec delay followed by illumination of the take nosepoke. Completion of the take nosepoke led to a 1 sec delay followed by delivery of a 45 mg sucrose pellet into the food trough. A 15 sec intertrial interval began after the subject retrieved the pellet before initiation of a new trial by illumination of the seek nosepoke. Sessions were split into four 12 min blocks separated by a 2 min inter-block interval where all lights were extinguished. Subjects could complete up to 20 trials in each block (i.e. earn 20 reinforcers). In no shock sessions, no risk of shock was present for any action and subjects were given at least four no shock sessions before beginning the probabilistic punishment task.

## Probabilistic Punishment Task (PPT)

The PPT follows previously published methods (Jacobs & Moghaddam, 2020) and training procedures are outlined in Chapter 3. Identical to the no shock sessions, PPT sessions consisted of four blocks of 20 trials each. The take action-reward contingency remained constant. However, the probability of receiving a punishment (300 ms electrical footshock at 0.25 mA) after the seek action increased over the blocks (0%, 6%, 10%, and 18% in blocks 1, 2, 3, and 4, respectively). Ascending punishment risk is commonly used in similar procedures and prevents overgeneralizing of the shock (Park & Moghaddam, 2017b; Simon et al., 2009; St Onge & Floresco, 2010). Seek action execution would always activate the take cue light 1.5 sec after seek action execution. Subjects were required to reach a stability criteria of at least four PPT sessions and demonstrate stability (3 consecutive sessions within 25% of the 3 day mean).

## Extinction of Probabilistic Punishment

Following learning of the PPT, extinction was performed by removing the probabilistic punishment contingency and keeping all other contingencies (see Jacobs & Moghaddam, 2020). If subjects were completely resistant to shock, we increased shock intensity (up to 0.5 mA) to achieve suppression of behavior. Neural activity was recorded in a session prior to extinction and in the two extinction sessions.

## Shock Probe Test

To determine if any learning related changes in shock responsivity were products of shock exposure. We applied the same shock (0.25 mA, 300 msec) in a different context (operant box with no nosepokes or feeder) with a variable 90 sec (60-120 sec) inter-stimulus interval. Subjects were given one session to acclimate to the new context for 10-min. In the next session subjects received seven footshocks. Footshocks were administered after a 5-min habituation period and were not signalled. Shock probe tests were performed after extinction.

## Fiber Photometry System and Recording Procedures

As outlined earlier, recordings were performed with a commercially available fiber photometry system, Tucker-Davis Technologies RZ5. Recording was accomplished by providing both 470 nm and 560 nm excitation light through the 400- $\mu$ m core patchcord to the mPFC or OFC for GCaMP6 and tdTomato signals, respectively. LEDs were sinusoidally modulated at 210 and 330 Hz. GCaMP and tdTomato (500-540 nm and 580-680 nm, respectively) were collected back through the patchcord to dichroic mirrors and bandpass filters within a Doric minicube. Fluorescence was converted to voltage through four femtowatt detectors (Newport 2151). Data were recorded using Synapse software (Tucker-Davis Technologies) and timestamps of behavioral events were collected by 5V TTL pulses that were read into the RZ5 system. Synapse software demodulated fluorescence signals in real time at 1 kHz with a 6-Hz low pass filter. As in Chapter 3, data were further downsampled to 41-Hz using Fourier method.

Neural activity was recorded in a no-shock control session, in the first PPT session (hereafter called Session 1) and after subjects reached the stability criteria for punishment related suppression (hereafter called Learned). If required for extinction, we titrated shock intensity and re-recorded during that shock intensity. This was required for two male subjects. We then recorded during the following two extinction sessions (hereafter referred to as extinction 1 and extinction 2).

## Fiber Photometry Analysis

**Peri-event analysis:** Signals from the 465 (GCaMP6) and 560 (tdTomato) streams were processed in Python (Version 3.7.4) using custom written scripts in accordance with previously published methods (Jacobs & Moghaddam, 2020). Briefly, 465 and 560 streams were low pass filtered at 3 Hz using a butterworth filter and subsequently broken up based on the start and end of a given trial. The 560 signal was fitted to the 465 using a least-squares first order polynomial and subtracted from 465 signal to yield the change in fluorescent activity. The z-score window was 4-2 sec  $\Delta F/F$  prior to a given epoch to understand if changes in the peri-action epoch began before or after action execution.

**Time Lagged Cross-Correlation Analysis:** Similar to Chapter 4, we computed covariance scores by taking the dot product of PL-mPFC and LO-OFC signals across all possible time lags for seek and take action epochs. The same equation was used to normalize covariance scores for each time lag to achieve a correlation coefficient between -1 and 1:

$$Coe\!f = Cov / (s^1 * s^2 * n) \quad (5.1)$$

Where  $Cov$  is the covariance from the dot product of the signal for each timepoint,  $s^1$  and  $s^2$  are the standard deviation of the PL-mPFC and LO-OFC streams, respectively, and  $n$  is the number of samples. An entire cross-correlations function was derived for each trial and epoch (i.e. seek and take).

## Statistical Analysis

### PPT Behavior

Statistical procedures utilized either a two-way ANOVA or mixed-effects model using factors of risk block and session. Tests were done with the Greenhouse-Geisser correction for sphericity violation where appropriate. Post-hoc comparisons were performed using the bonferroni correction. An  $\alpha$  level of .05 was used for all tests. Behavior data files were processed using custom written scripts in Python (version 3.0) and all statistical analyses were performed in GraphPad Prism (Version 8, San Diego, CA).

### Fiber Photometry

To assess changes in neural activity, we first utilized a permutation based approach as outlined in (Jean-Richard-dit-Bressel et al., 2020) using Python (Version 3). An average response for each subject for a given time point in the seek or take action was compared to the corresponding block of the no shock session, or, in the case of extinction data, learned PPT sessions. For each time point a null distribution was generated by shuffling the data, randomly selecting the data into two groups, and determining the difference in means between the two groups. This was done 1,000 times for each timepoint and a two-sided p-value was obtained by determining the percentage of times a value in the null distribution was greater than or equal to the observed difference in the unshuffled data. To control for multiple comparisons we utilized a consecutive threshold approach based on the 3 Hz lowpass filter window (Jean-Richard-dit-Bressel et al., 2020; Pascoli et al., 2018), where a p value  $< .05$  was required for 13 consecutive samples; i.e. the 1/3 second low-pass filter window) to be considered significant.

To investigate if individual differences in learning related changes were associated with action encoding we performed area under the curve (AUC) analysis for epochs identified by

permutation testing. We also correlated AUC derived metrics (either a change score for action execution or 1.5-sec after punishment delivery) with changes in punishment resistance from the first PPT session to the learned PPT session. After verifying no violations in normality with the Shapiro-Wilk test, we performed two-tailed Pearson correlations for punished and unpunished trials or compared AUC values via paired t-test or wilcoxon signed rank test.

To assess correlated activity changes as a function of risk or session, we took the peak and 95% confidence interval for the overall cross correlation function. These values were compared by a two-way ANOVA with factors risk and session followed by *post-hoc* tests with a bonferonni correction. Tests were done using GraphPad Prism (Version 8) and utilized an  $\alpha$  of .05.

## Excluded Data

LO-OFC photometry data from one male and two female subjects were excluded due to the fiber ferrule being too close to permit recording from both PL-mPFC and LO-OFC, complicating their comparison to other subjects. Trials where the optical fiber patch cord fell off during action periods or needed to be reconnected were also excluded.

# Results

## Histology and Behavioral Analysis

Fibers were located largely in the LO-OFC, with one fiber slightly more dorsal in the agranular insular cortex [Figure 5.1](#). These locations are relatable to the location of lesions in lesion studies and electrode placements in single unit studies.

Behavior from these subjects (combined with others) was previously shown in [Chapter 3](#). However upon selecting out only subjects from these studies the same patterns of behavior appear (see [Figure A.14](#)), namely that punishment risk suppresses trial completion and latency increases are only seen for the risky seek action after learning.

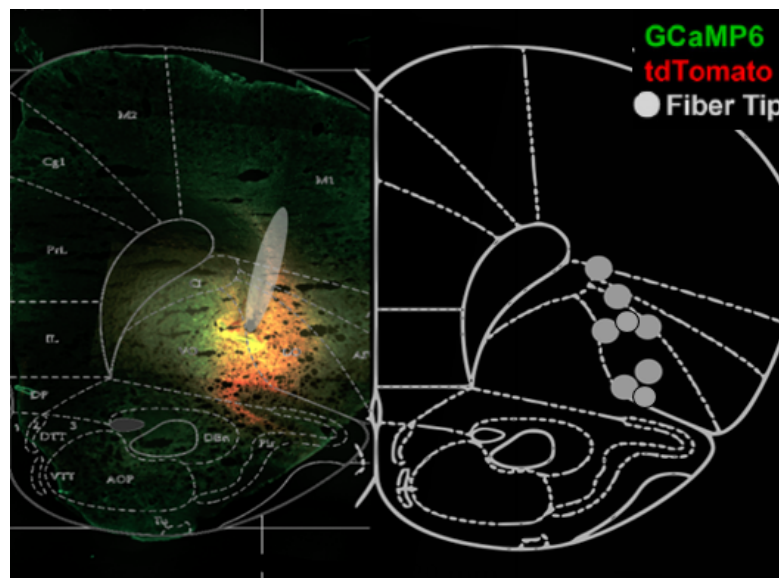


Figure 5.1: Fiber placements (grey circles) and representative coexpression of GCaMP and tdtomato for rats in the current study. Most fibers are positioned in the lateral OFC, with one fiber in the agranular insular cortex, an area also considered in many studies to be part of the OFC (Stalnaker et al., 2015).

## LO-OFC Response to Punishment Changes with Learning

The LO-OFC was responsive to action contingent footshock. In both session 1 and after learning, footshock produced a robust elevation in activity in all risk blocks when compared to the corresponding no shock session (omitted from plot) and thus the average of all footshocks across blocks is shown in Figure 5.2A. In session 1 the response was characterized by a rapid rise and gradual decay, much like that observed in the PL-mPFC before and after learning (see Figure 3.3). However after task learning, the rapid rise in the LO-OFC response was attenuated. To investigate this we determined both the AUC and time to peak ( $t_{\text{peak}}$ ) for the neural response to the footshock. While the AUC was unchanged with learning ( $W=-4$ ,  $p=.84$ ; Figure 5.2B), the time to reach the peak increased after learning ( $t(7)=3.34$ ,  $p=.012$ ; Figure 5.2C). This effect was not observed following reanalysis of PL-mPFC data ( $W=20$ ,  $p=.50$ , Figure A.17).

To see if this effect was merely related to continued experience with footshock itself, we exposed the same animals to a shock probe session where the exact same footshock was utilized but footshocks were unsignaled and in a context with no footshock experience. A significant effect of session was observed when the probe session was included in the analysis (effect of session:  $F(1.4, 9.7)=8.79$ ,  $p=.011$ ; Figure 5.3). Because our hypothesis was already informed by prior analysis we utilized one-tailed *post-hoc* tests. Similar to session 1, response to probe test footshock in the LO-OFC was rapid and followed by a gradual decay. The elevation in  $t_{\text{peak}}$  returned to session 1 values (*post-hoc*  $p=.43$ ) and was significantly less than in the PPT after learning (*post-hoc*  $p=.0425$ ). This suggests that changes in punishment encoding are likely related to learning the context/contingencies which predict the footshock rather than physical desensitization or sensitization to the footshock.

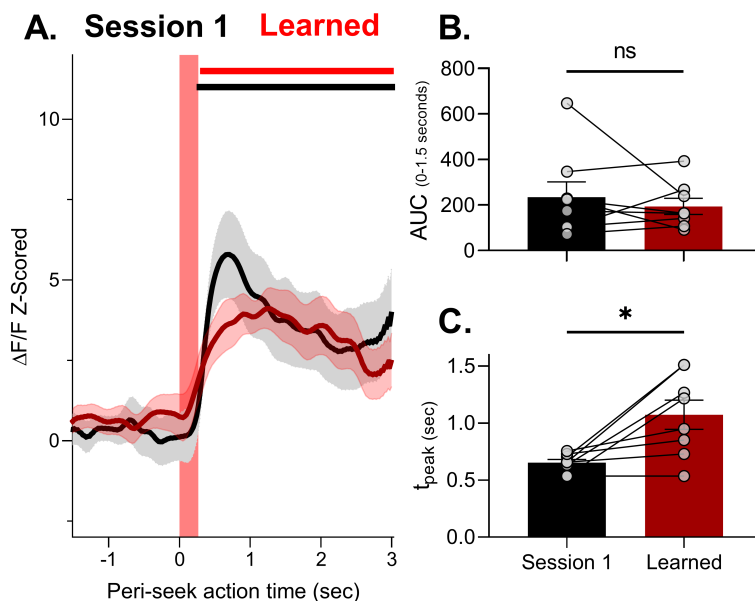


Figure 5.2: Encoding of action contingent footshock punishment (red bar) by the LO-OFC before (black) and after learning (red). **A.** Z-scored response before and after seek actions which resulted in footshock. **B.** AUC of response to footshock before (session 1) and after PPT learning. **C.** Time to reach peak before (session 1) and after PPT learning. \* $p < .05$ , two-tailed t-test, ns= not significant.  $n = 8$  rats.

## LO-OFC encoding of risky actions does not change after probabilistic punishment learning

Permutation based analysis indicated that in no shock sessions there was a significant shift in z-scored activity around the time of the seek action, whereby activity increased both prior to and after action execution with increasing blocks (Figure A.15A-B). To explicitly control for this effect of time in session, we compared the PPT sessions to the corresponding block in the no-shock sessions.

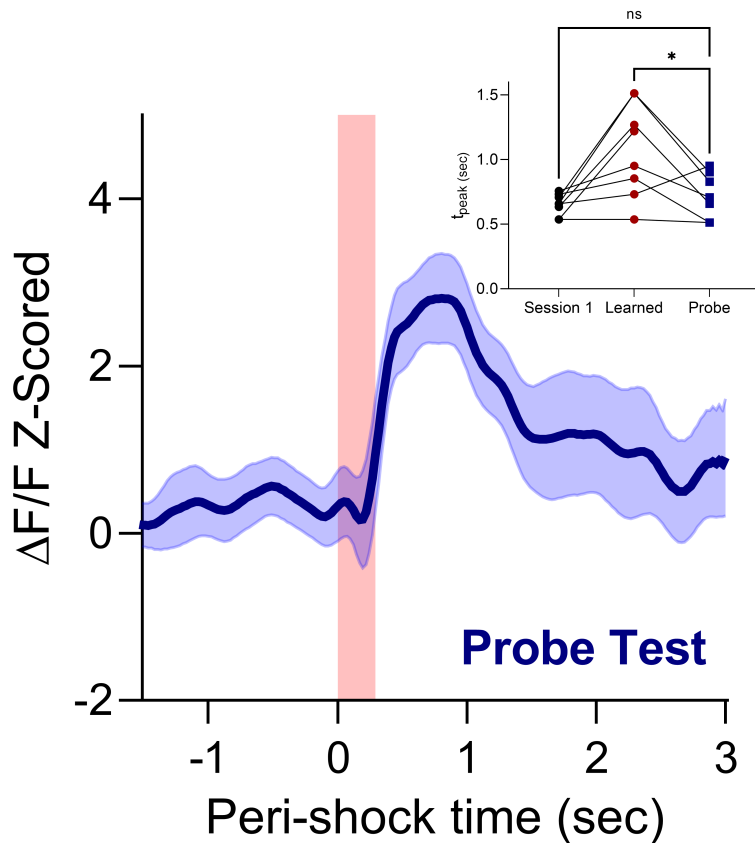


Figure 5.3: LO-OFC response to the footshock (red bar) when given non-contingently in probe sessions. Inset: time to peak for individual subjects. A rapid ( $<1$  sec) time to peak was observed that did not differ from the first PPT session.  $*p < .05$ , one-tailed bonferroni corrected paired t-test, ns= not significant.  $n=7-8$  rats.

No learning related change in response to the risky action was observed when comparing to the no shock session (shaded grey area) during the seek action period (Figure 5.4), though a small but significant difference between session 1 and no shock was observed in the 0% risk block. Furthermore, utilizing the same AUC analysis used for the PL-mPFC in Chapter 3, we found no differences between any of the sessions for change scores in peri-seek action activity (F values  $< 2.82$ , p values  $> .107$ ; Figure 5.4-bottom).

## LO-OFC encoding of safe actions changes after probabilistic punishment learning

Assessment of the take action revealed that take action encoding changed with learning in the peri-action period (Figure 5.5). No differences were seen when no risk of shock was present (0% risk, Figure 5.5A). However, higher levels of activity were observed in the peri-action epoch for risk blocks (Figure 5.5B-D) only after learning (red) and not in the first PPT session (black). By taking the AUC change from pre and post action, a significant phasic increase for the take action was seen for the highest risk block after learning ( $F(1.66,14.98)=9.96$ ,  $p=.0026$ , *post hoc*  $p = .03$ ; Figure 5.5D-middle).

Lastly, while we observed a similar increase in responsiveness to reward delivery after learning at 18% risk this effect was not significantly different from no shock using either permutation or AUC based approaches ( $F(1.46,8.06)=3.15$ ,  $p=.11$ , Figure 5.5D-bottom).

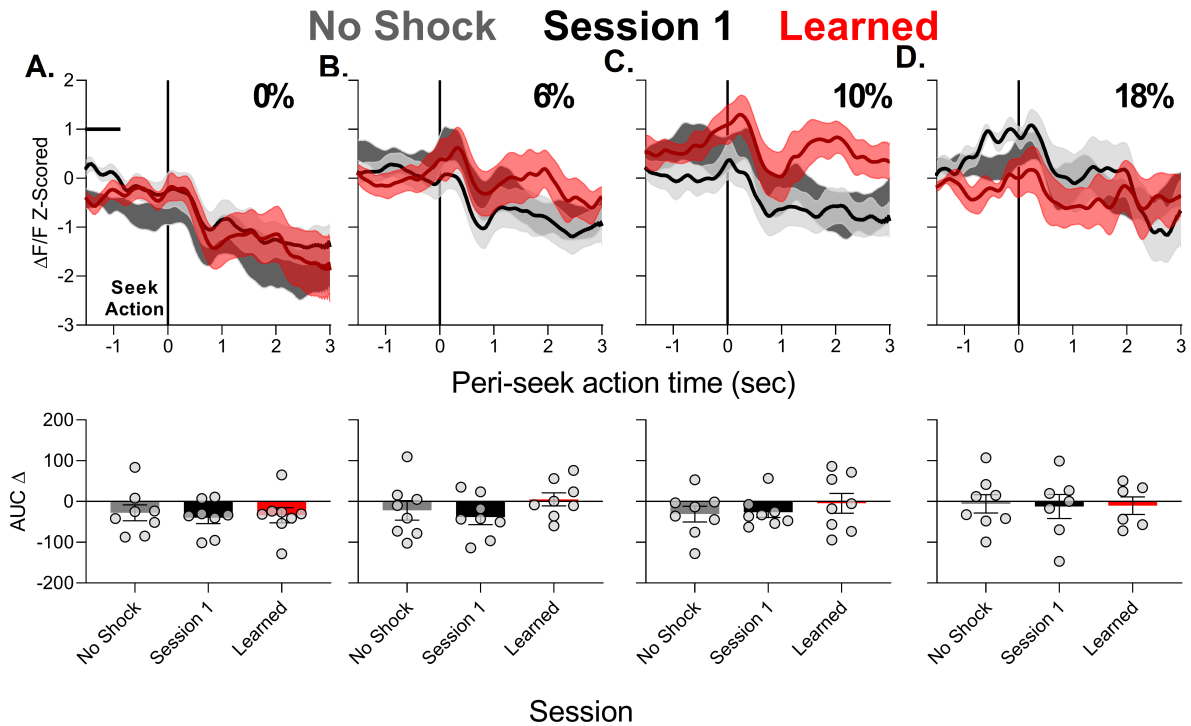


Figure 5.4: Encoding of risky actions (unpunished seek actions) by LO-OFC in session 1 (black) or after PPT learning (red). Risk of shock for each panel is noted in the upper plots (increasing from left to right). **A.** In the first 0% risk block a small transient difference from the no shock (grey) was observed in session 1 (black) but this difference was not present during or after action execution and no peri-action AUC changes in activity were detected. **B-D** When shock risk was present, no change from control was seen in the seek action period for any block or session. Solid lines in upper plots indicates significant difference from no shock. Grey circles represent individual data points in lower plots.  $n = 6-8$  rats.

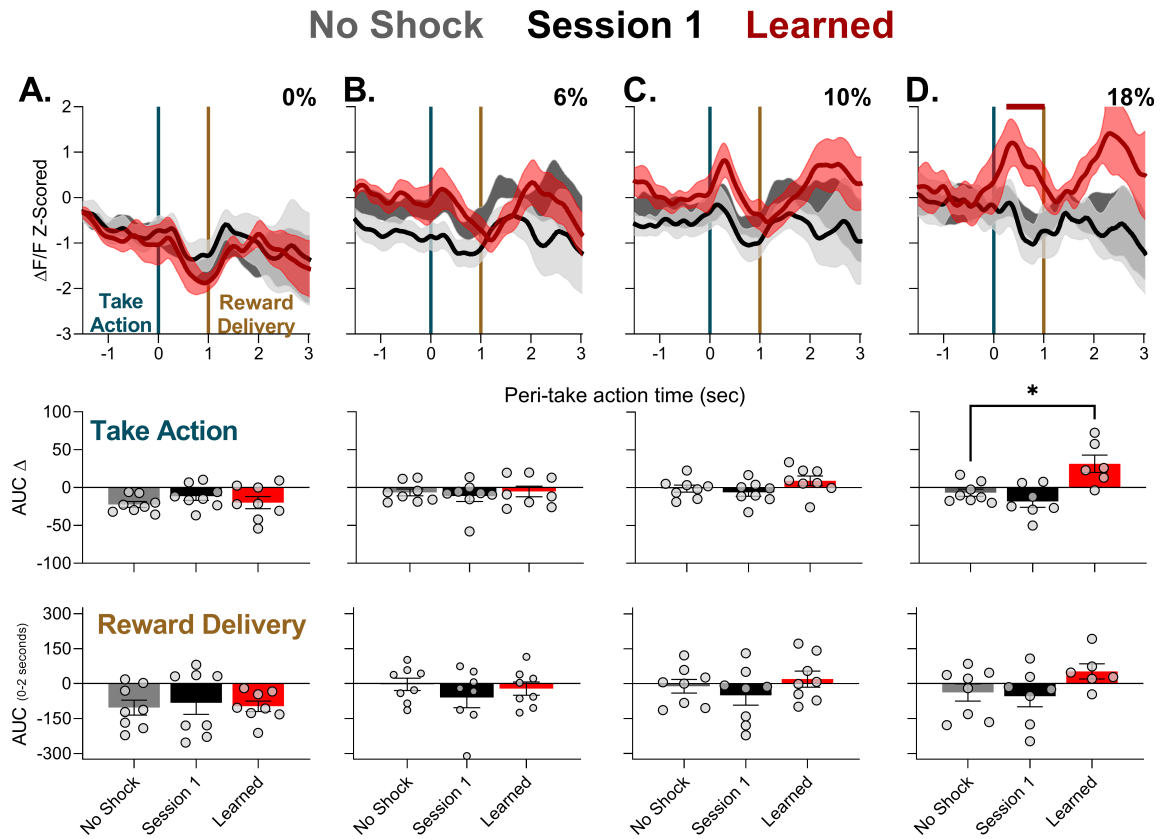


Figure 5.5: Encoding of safe actions (take actions - blue bar) and reward delivery (brown bar at 1-sec) by LO-OFC during PPT learning. Risk of shock for each panel is noted in the upper plots (increasing from left to right). **A.** No encoding changes for the 0% risk block were seen for session 1 (black) or after learning (red) when compared the no shock control (shaded grey trace). **B-D.** After learning, elevations in LO-OFC activity were seen during the take action and, non-significantly, for the reward delivery as risk of shock increased. **D-middle.** Phasic increases to take action execution were seen for all but one subjects at 18% risk after learning. Solid colored lines above traces indicates significant difference from no shock. \*  $p < .05$  *post-hoc* test.  $n = 6-8$  rats.

## LO-OFC related changes are not correlated with sensitivity to punishment

In Chapter 3, we found that learning related changes in PL-mPFC action encoding were correlated with behavioral changes in action suppression over PPT learning. Consequently, we took the LO-OFC measurements that changed with PPT learning and investigated if such changes were related to individual differences in behavior. Surprisingly, while non-zero correlation coefficients were observed for take action changes and the  $t_{\text{peak}}$  for footshock encoding neither of these reached significance ( $p$  values  $> .18$ , two tailed). The strongest association observed was for punishment related changes (Figure 5.6B) where larger increases in latency to reach peak for punishment encoding were associated with more punishment resistance.

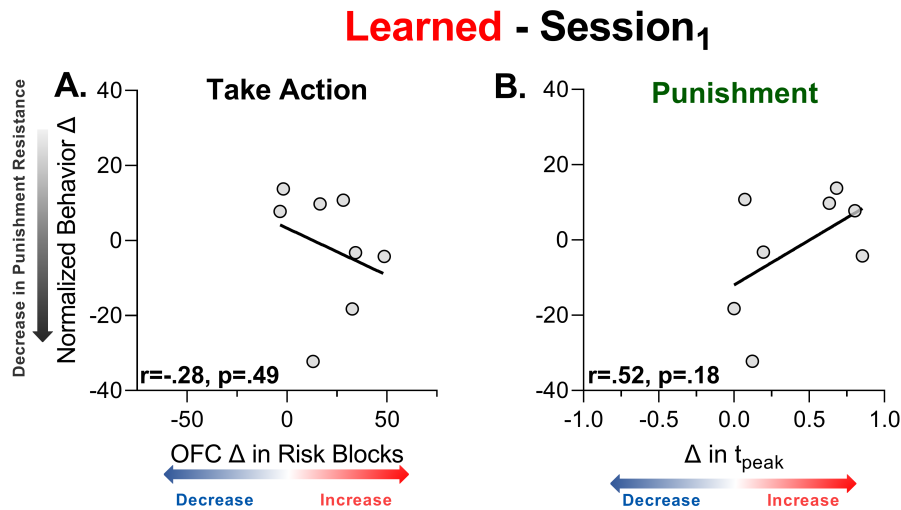


Figure 5.6: Assessment of correlations for individual differences in behavior and LO-OFC encoding changes for safe actions and punishment. **A.** Take action changes were non-significantly negatively associated with increased resistance after learning. **B.** Changes in latency to peak during punishment encoding were non-significantly positively associated with increased resistance.  $n = 8$  rats.

## LO-OFC and PL-mPFC correlated activity during risky actions, but not safe actions, decreases with punishment risk

Because anxiety and anxiogenic contingencies alter cortical synchrony with other brain regions (Park & Moghaddam, 2017b; Sartori & Singewald, 2019), we further applied cross correlation analysis to the neural responses to risky action in animals with fibers in both the PL-mPFC and LO-OFC.

Initially positively correlated activity during the seek action was observed across all blocks in the no shock session (Figure 5.7A). However, punishment risk produced disruptive effects on this pattern of correlated activity ( $F_{\text{interaction}}(6,1473)=6.002, p < .001$ ). As early as the first PPT session, risk of shock decreased correlated activity at the highest risk block compared to no shock sessions (*post hoc*  $p < .001$ ; Figure 5.7B,D). After learning this disruption developed earlier in the 10 and 18% risk blocks (*post hoc*  $p = .031$ ; Figure 5.7C,D). This further suggests that anxiogenic contingencies alter correlated activity during action encoding in cortical regions.

Interestingly when we applied this analysis to the take action epoch we observed a similar positive correlation across blocks in the no shock sessions (Figure 5.8A). However these correla-

tions persisted across blocks when probabilistic punishment was introduced and after learning (F values < 1.41, p values > .20; Figure 5.8B-D).

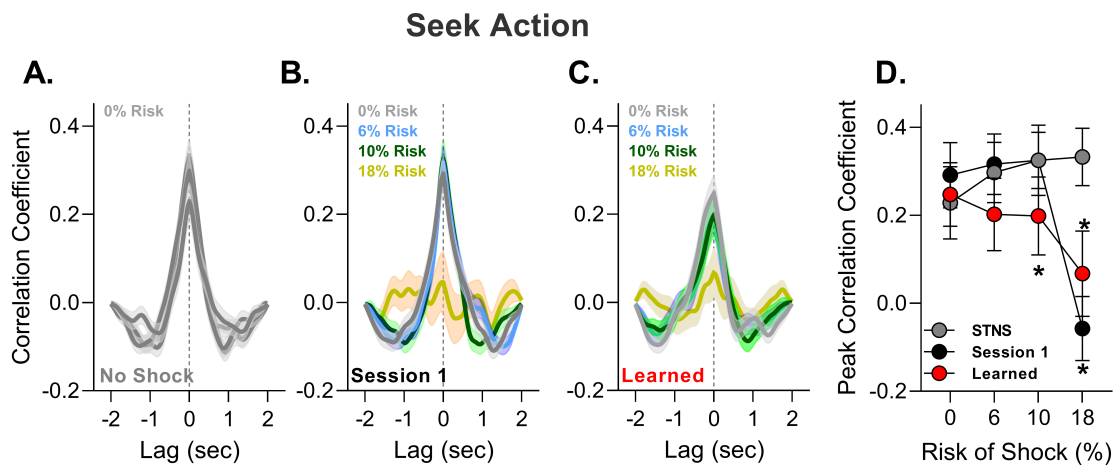


Figure 5.7: Correlated activity of the PL-mPFC and LO-OFC during seek action encoding is disrupted by probabilistic punishment. **A.** When no shock was present, activity was positively correlated with no time lag and, generally, increased over the session. **B.** In the first PPT session, correlated activity was originally similar to the no shock session but was decreased by the last risk block. **C.** After PPT learning, disruptions in correlated activity were seen earlier with risk. **D.** Peak correlated activity and 95% confidence interval for each session and risk block. \* $p < .05$  vs. no shock (STNS).  $n = 53$ -157 trials from 6-8 rats.

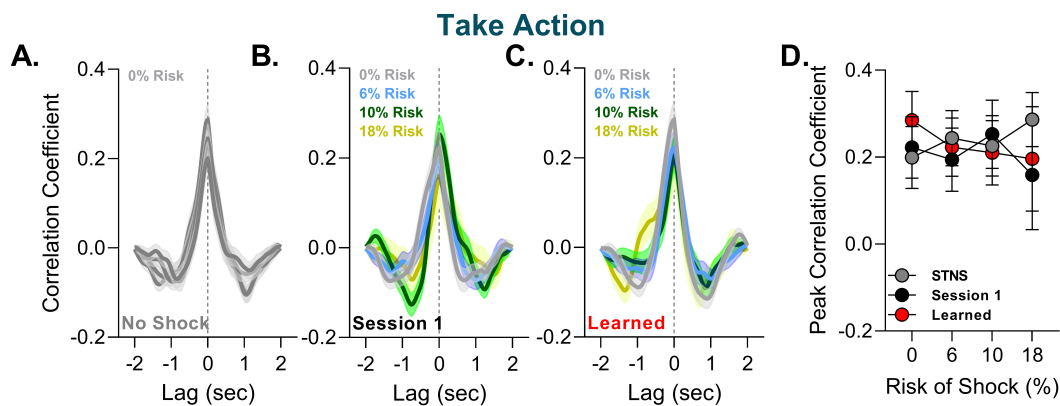


Figure 5.8: Correlated activity of the PL-mPFC and LO-OFC during take action execution. **A.** Activity was positively correlated across blocks during the take action in the no shock session with no time lag. **B-C.** Positive correlations were also observed in the PPT before and after learning across all risk blocks. **D.** Peak correlated activity and 95% confidence interval for each session and risk block.  $n = 53$ -157 trials from 6-8 rats.

## Probabilistic punishment extinction normalizes LO-OFC activity

We then extinguished the probabilistic punishment contingency to ask if learning related changes seen in the LO-OFC would persist even if punishment risk was removed. For the risky seek action we continued to see no change in OFC encoding during the peri-action period (Figure A.16).

However, the elevated phasic response seen after learning for the safe take action dissipated following extinction, an effect that failed to reach significance in extinction session 1 but reached significance in extinction session 2 based on permutation testing. These effects were specific to the 18% risk block (Figure 5.9).

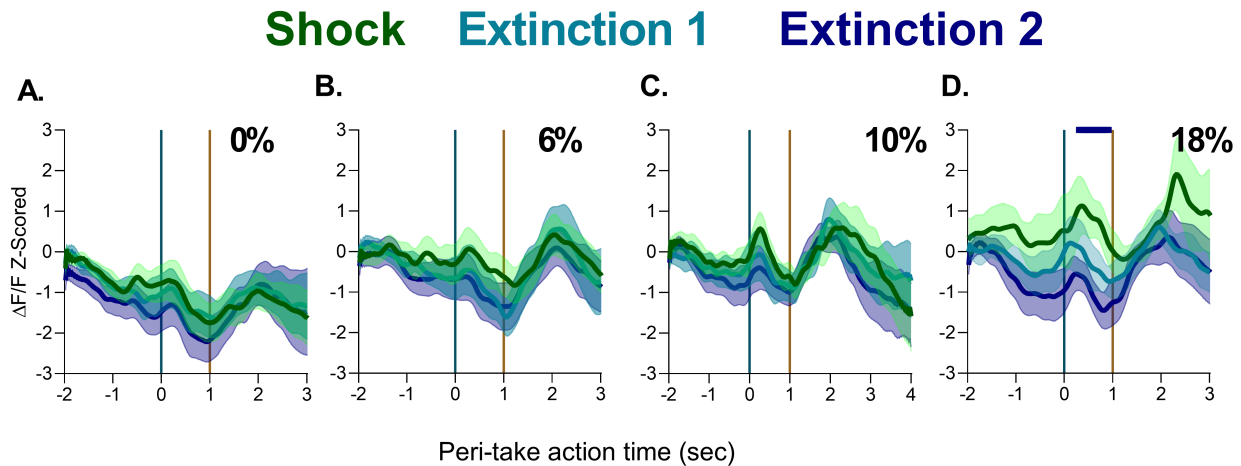


Figure 5.9: Effects of extinction on take action encoding (blue line) and food delivery (brown line). **A-C**. At 0-10% risk (increasing left to right) neither extinction session deviated from activity observed in PPT sessions (green trace). **D**. At 18% risk the elevation in activity at the time of take action execution was attenuated in the second extinction session (purple). Solid colored lines above traces indicates significant difference from shock (i.e. Learned PPT Sessions).  $n = 5-8$  rats.

Lastly we asked if correlated activity between the LO-OFC and PL-mPFC was normalized following extinction of probabilistic punishment. We found that risk related decreases in correlated activity were attenuated following two days of extinction training ( $F_{\text{interaction}}(6,1570)=3.63$ ,  $p = .0014$ ; Figure 5.10A). Specifically, risk related disruptions in correlated activity were normalized by extinction both non-significantly in extinction 1 (*post hoc*  $p = .096$ ) and significantly in extinction 2 (*post hoc*  $p = .032$ ; Figure 5.10B).

For the take action we continued to observe a consistent positive correlation between PL-mPFC and the LO-OFC and these correlations did not change with extinction ( $F$  values  $< 1.4$ ,  $p$  values  $> .21$ ; Figure 5.11A-B).

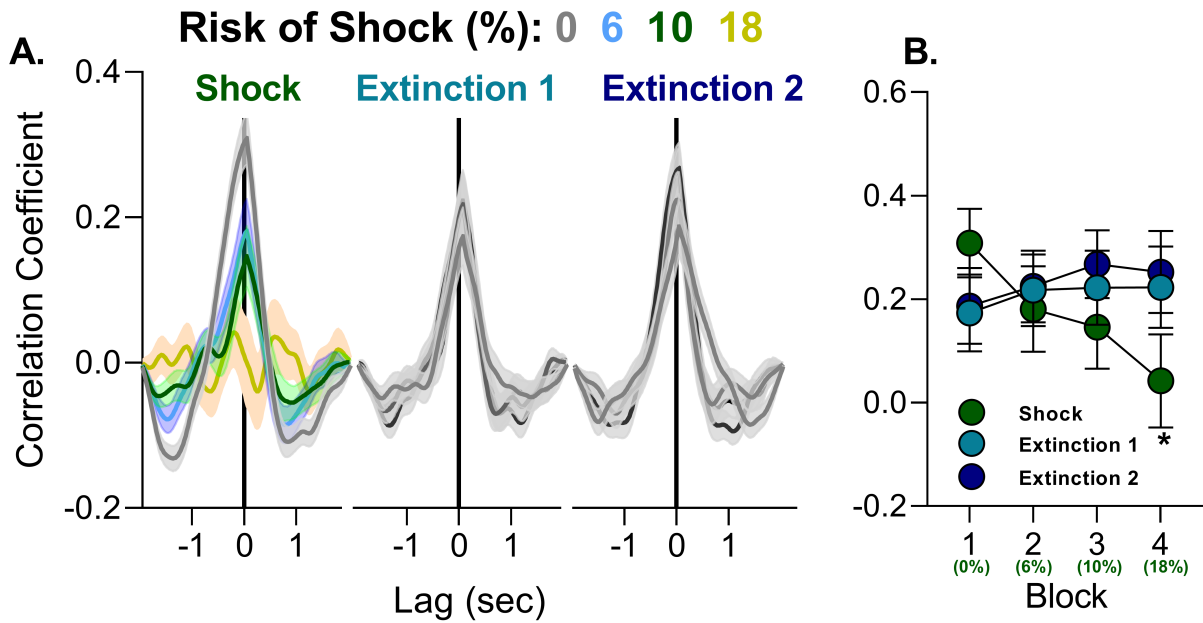


Figure 5.10: Effects of extinction on seek action correlated activity during the PPT (Shock-green) and extinction (blue and purple). **A.** Cross correlation functions demonstrating decreases in correlated activity following risk, and an attenuation of this effect following extinction. **B.** Mean and 95% confidence interval for the peak of the cross correlation function for each block and session. \* $p < .05$  vs. Extinction 2.  $n = 51-158$  trials from 5-8 rats. Extinction sessions have no risk in each block and risk of punishment is denoted in green for the Shock session.

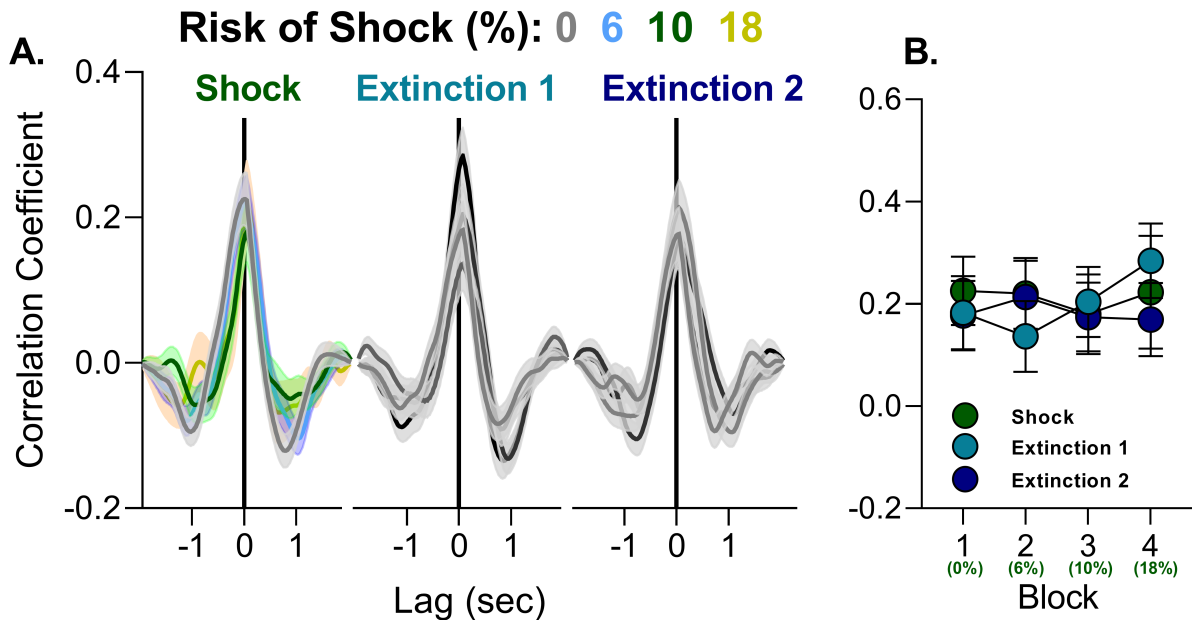


Figure 5.11: Effects of extinction on safe take action correlated activity during the PPT (green) and extinction (blue and purple). **A.** Cross correlation functions demonstrating consistent correlated activity across risk block and extinction. **B.** Mean and 95% confidence interval for the peak of the cross correlation function for each block and session.  $n = 51-158$  trials from 4-8 rats. Extinction sessions have no risk in each block and risk of punishment is denoted in green for the Shock session.

## Discussion

Our work and others have begun to highlight a dynamic role for the PL-mPFC in adapting behavior to probabilistic punishment contingencies (Friedman et al., 2015; Jacobs & Moghaddam, 2020; Orsini et al., 2018). Less is known about the OFC in these processes. So far LO-OFC studies in approach-avoidance conflict have largely been confined to temporally non-specific lesions or global inactivation and have produced conflicting results (Jean-Richard-dit-Bressel & McNally, 2016; Orsini et al., 2015; Turner et al., 2021). Using *in vivo* fiber photometry we show that the LO-OFC adapts its encoding of distinct information in the PPT in relation to the PL-mPFC. Rather than showing learning related changes in encoding of the risky action, the LO-OFC adapted to receipt of punishment itself and to the safe/rewarded action. We also observe that correlated activity between the PL-mPFC and LO-OFC was attenuated by the presence of punishment risk in a learning-independent manner. These findings inform our understanding of the neural diversity in the PFC that supports behavior under risk of punishment, which has applications to learned anxiety and preservative reward seeking.

### A role for the LO-OFC in Approach-Avoidance Conflict

The OFC is known to process outcomes and stimuli to guide behavior (Izquierdo, 2017). Approach-avoidance conflict requires proper processing of reward, punishment, and the overall learning and integration of the underlying punishment contingencies (Gray, 1987; Jean-Richard-dit-Bressel et al., 2019). In the PPT we assess action with and without conflict through the risky seek and safe take actions, respectively. While we did not observe any learning related changes in risky action encoding in the LO-OFC, we did see changes in encoding of the take action when seek action risk was high. This is intriguing because the likelihood of take action producing reward is constant and certain. This suggests a novel role for the LO-OFC in scaling reward producing actions depending on the context they are executed in (safe vs. risky).

Relatedly the dynamic response of the LO-OFC to punishment outcomes from seek actions changed with learning. Punishment encoding was initially characterized by a rapid increase following shock, but became slower and more extended after learning punishment contingencies. It is unlikely these effects were due to shock exposure, because the slowed LO-OFC response to footshock was not observed in a different context with non-contingent footshock even though animals had ample exposure to footshock.

Neither of these effects were observed in the PL-mPFC suggesting the LO-OFC serves a different function in the PPT. One interpretation is that the LO-OFC signals value of reward and punishment. We did not observe any relationship between individual difference in these encoding changes and punishment resistance, however, making this interpretation less likely. An alternative interpretation is that the OFC supports information utilized to produce a cognitive map of the experimental context. The LO-OFC has documented importance in tracking stimuli to support learning in decision making and some theories of OFC function posit the OFC takes learned biologically relevant information to make a map of the task space (Izquierdo, 2017; Stalnaker et al., 2015). Adapting response to predictable rewarded actions and punishment outcomes in a learning and context specific manner would help the animal weighing the current importance, or allow disambiguation, of rewarded actions against those of punishment according to the task space.

## Resolving LO-OFC Roles in Approach-Avoidance

A role for the LO-OFC in task space creation may inform ongoing discrepancies in the OFC literature in relation to punishment sensitivity. When probabilistic punishment is utilized through non-reward, OFC lesions have been observed to produce less sensitivity to punishment (Pais-Vieira et al., 2007; Stopper et al., 2014; Verharen, den Ouden, et al., 2020). This is opposite to the increased punishment sensitivity from LO-OFC lesions in tasks with explicit punishment (Ishikawa et al., 2020) and in the risky decision making task (Orsini et al., 2015).

One consideration is that both of these scenarios require the subject to discriminate between safe and risky conditions to appropriately disambiguate multiple actions and their contingencies. While reward discrimination is unchanged from OFC lesions (Orsini et al., 2015), discrimination capabilities in relation to changing threat probability or conflicting stimuli are disrupted following LO-OFC inactivation (Ray et al., 2018; Verharen et al., 2019). These diverse experimental findings may be rationalized by the interpretation that a key role for the LO-OFC in approach-avoidance conflict is not to encode aversive outcomes or value, but rather to build a model of the learned information to facilitate action schemas for the animal through adapting encoding to outcomes or safe actions (also see Jean-Richard-dit-Bressel & McNally, 2016; Shiba et al., 2016). Though speculative, this role for the OFC in approach-avoidance conflict may explain why OFC damage could enhance or suppress action under punishment as the inability to develop proper schemas could result in heightened resistance to punishment in non-reward scenarios or hyper-suppression during explicit punishment.

Importantly, such information could be utilized by other downstream regions to control behavior. One limitation of our approach is that our LO-OFC signal is global and pathways for behavioral control may be more isolated. Thus an outstanding question will be whether OFC changes in action and punishment encoding are pathway specific, particularly with lower level systems in the approach-avoid decision hierarchy. For example, terminal OFC activity in the DS or selective excitation/inhibition of OFC-DS synapses have been linked with individual differences in preservative reward seeing under punishment (Harada et al., 2019; Pascoli et al., 2018). Further using pathway specific ablation, recent work has shown the OFC sends unique “value” related signals through the BLA and NAc in probabilistic decision making and loss (Groman et al., 2019). Whether such pathways have the same involvement with explicit probabilistic punishment remains to be determined.

## Correlated activity between PL-mPFC and LO-OFC is disrupted by approach-avoidance conflict

Activation of the behavioral inhibition system through approach-avoidance is believed to produce anxiety, which is critical for shifting behavior when punishment is uncertain. This is not without consequence, as network level connectivity of the cortex is augmented by anxiety and can produce deficits in cognitive processes (Balderston, Vytal, et al., 2017; Cornwell et al., 2017; Sartori & Singewald, 2019). We observed that correlated activity between the PL-mPFC and LO-OFC was disrupted by probabilistic punishment. Previous single unit studies and our data in Chapter 4 have implicated probabilistic punishment in suppressing mPFC-VTA correlated activity (Park & Moghaddam, 2017b). Thus, this finding adds another node to the neural systems involved in the mode of anxiety stressed in this dissertation. Interestingly this effect was observed both before and after the task was learned, returned to baseline when punishment probability was removed, and was specific to the risky seek action. This suggests these anxiety-related effects were specific to the presence of punishment producing a state of anxiety during the task but not the learned contingencies specifically. Previous work has show threat of punishment can disrupt network activity in both in generalized anxiety disorder and control

persons (Balderston, Vytal, et al., 2017). Thus the effects of anxiety on network level coactivity could reflect a way in which information processing is disrupted by both learned and unlearned states of anxiety.

## Conclusions

We are just beginning to understand how brain regions relevant for anxiety and compulsive reward seeking change their encoding of rewards and punishment to guide behavior. Taken with my prior work in the PL-mPFC in [Chapter 3](#), these findings stress the LO-OFC has complementary patterns of encoding during probabilistic punishment contingencies. While the PL-mPFC shows learning related encoding changes to the risky contingency, the LO-OFC displayed learning related changes in response to actions toward rewards and punishment itself. Correlated activity between these two regions was disrupted by risk of punishment in a learning independent manner, proposing a mechanism for anxiety to disrupt PFC related processes. These findings add important data for characterization of neural activity patterns in these processes and inform our understanding of why overlapping cortical systems are implicated in anxiety and addictive disorders.

The final chapter of this dissertation will now synthesize the key findings regarding the role of the PL-mPFC and LO-OFC in the context of learned anxiety and behavioral response to probabilistic punishment. Particular attention will be paid to how each PFC subregion may relate to the reinforcement sensitivity theory outlined in the Introduction.

# Chapter 6

## General Discussion

Some sections adapted from: Jacobs, D. S., & Moghaddam, B. (2021). Chapter two - medial prefrontal cortex encoding of stress and anxiety. In A. T. Brockett, L. M. Amarante, M. Laubach, & M. R. Roesch (Eds.), *What does medial frontal cortex signal during behavior? insights from behavioral neurophysiology* (pp. 29–55). Academic Press. <https://doi.org/doi.org/10.1016/bs.irn.2020.11.014>

### Main Findings

The decision to execute or inhibit an action is often driven by conflicting goals of acquiring rewards or avoiding punishments. In the real world, the contingencies between action and reward or punishment are dynamic and situational making learning and adapting behavior in response to learned conflicting contingencies critical for survival. Learned conflict between approach and avoidance can ultimately activate the behavioral inhibition system, which utilizes states of anxiety to inform approach and avoidance strategies. This critical process can become disrupted and may be an impetus for diverse psychopathologies characterized by reckless or anxious-avoidant behaviors. The neural underpinnings which support these processes are diverse and incompletely understood, particularly in regard to the PFC which is well poised to control and inform other brain regions. This dissertation assessed goal motivated action in the context of learned anxiety-related conflict. It further combined this behavioral approach with fiber photometry to assess how PL-mPFC and LO-OFC subregions of the PFC encode action and punishment and are altered by the presence or absence of conflict contingencies.

In Chapter 2, we describe the development and characterization of a probabilistic punishment task (PPT) designed to assess action encoding with and without anxiety. This was done by utilizing a homogeneous chained schedule of reinforcement where the first “seeking” action was risky, because it could probabilistically result in a mild footshock, but deterministically resulted in the ability to perform the second “taking” action which produced food reward. After task learning animals demonstrated behavioral suppression earlier than in the first PPT session and suppression became selective for the risky action. The suppressive effects of probabilistic punishment were also attenuated by anxiolytic treatment. These findings collectively suggest this task engages the behavioral inhibition system and allow us to assess anxiety both before and after the contingencies are learned. We also observed sex differences in punishment sensitivity/risk-taking similar to those seen in humans (Orsini & Setlow, 2017) which have not been consistently documented with innate models of anxiety. Additionally, innate anxiety as assessed via the open field failed to correlate with PPT. This suggests the PPT captures a unique mode of learned action-related anxiety that extends upon more prevalent innate anxiety models.

In Chapter 3, we combine this behavioral approach with *in vivo* calcium imaging to measure neural activity in the PL-mPFC before and after animals learned the PPT. Thus, we could assess whether specific actions (safe vs. risky-anxiogenic) or outcomes (footshock vs. reward) were encoded differently with the learning of risk of punishment. Footshock punishment was represented by large increases in neural activity and these responses did not change with learning. This indicates that the PL-mPFC does not desensitize or stop tracking stressful stimuli, at least over the initial stages of learning. There was also little to no response during execution of the safe/rewarded take action even after learning. Encoding for the seek action was characterized by a phasic decrease in PL-mPFC neural activity in the anxiety-free no-shock session and much of the first PPT session (i.e., before learning). After PPT learning, however, the phasic decrease during the risky seek action was attenuated. After removing the punishment contingencies, these changes returned to pre-punishment phasic decreases. Collectively these findings highlight a novel role for the PL-PFC in the learning of anxiety by selectively changing neural activity patterns for actions with anxiogenic contingencies.

In Chapter 4, we utilized an alternative approach to assess PL-mPFC action encoding under anxiety by utilizing the punishment risk task (PRT) which uses a similar approach to the PPT, but risky and safe actions are not segregated and thus the risky action contains the same “distance” from reward as the take action in the PPT. This task also explicitly uses a tone cue to signal trial initiation which helped us to more carefully assess if the encoding of action related conditioned stimuli are differentially encoded by the mPFC with risk. Though this study also co-assessed neural activity in the VTA, I will omit some of these findings from the discussion to adhere to the focus of this dissertation.

Similar to the data presented in Chapter 3, we observed an attenuation of the phasic decrease during action execution as the probabilistic punishment contingencies were learned. This suggests the learning related changes in PL-mPFC action encoding under anxiety are not influenced by its distance from the reward but, again, whether an action has probabilistic punishment contingencies. No change in PL-mPFC cue encoding was found with PRT learning, suggesting that PRT Pavlovian CS processes which influence action execution were not influenced by the presence of learned anxiety in the PL-mPFC. Overall, these fiber photometry findings mirrored the electrophysiological findings of Park and Moghaddam, 2017b, by showing that of the cue, action, and reward epochs, PL-mPFC neurons were most sensitive to action encoding under risk.

We also used a behavioral pharmacological approach to attempt to parse the role of anxiety states on PL-mPFC action encoding through treatment with the GABA<sub>a</sub> positive allosteric modulator, diazepam. This is a complementary approach to the use of extinction of punishment because anxiety is theoretically mitigated by diazepam but anxiogenic contingencies are still present. Unlike punishment extinction, phasic decreases during risky action execution did not re-emerge with anxiolytic treatment. This indicates the PL-mPFC may be preferentially involved in tracking anxiety related contingencies which support conflict rather than the affective state of anxiety itself.

In Chapter 5 we explored the role of the LO-OFC in approach-avoidance conflict using procedures outlined in Chapter 3. In the first PPT session the LO-OFC showed a rapid increase in activity after footshock punishment. This response became slower after learning but was recovered when footshock was given unpredictably in a novel context. This suggests the LO-OFC adapts its encoding of punishment after learning in a context dependent manner, which may indicate it receives or transmits information about stressful stimuli depending on learned probabilistic contingencies.

Surprisingly, encoding of the risky action did not change with learning, highlighting a deviation from patterns seen with PL-mPFC encoding. LO-OFC encoding of the safe take action,

however, changed with probabilistic punishment learning and returned to baseline upon punishment extinction. This is intriguing because the take action has a certain, rewarded outcome. Taken with the footshock encoding findings, the LO-OFC may play a unique role in disambiguation of punishment and rewarded actions to create a task space without tracking probabilistic punishment contingencies themselves. These findings indicate a point of divergence between the mPFC and OFC in action encoding that could be utilized to inform action schemas.

We also observed that correlated activity decreased with probabilistic punishment between the PL-mPFC and LO-OFC. This effect was specific for the risky seek action but was independent of whether the task was learned. Because this effect was seen across all phases of PPT recording, this may reflect one mechanism by which states of anxiety disrupt cortical processes. We similarly found that diazepam, which theoretically lessens state anxiety while keeping anxiogenic contingencies, enhanced PL-mPFC correlated activity with the VTA in Chapter 4. These findings add to a growing collection of clinical and preclinical data implicating cortical network disruption from states of anxiety (Balderston, Vytal, et al., 2017; Park & Moghaddam, 2017b; Sartori & Singewald, 2019).

## Revisiting the role of the PFC in the behavioral inhibition system

Reinforcement sensitivity theory posits three systems for approach-avoidance conflict: the behavioral activation system, fight-flight-freeze system, and behavioral inhibition system (Gray & McNaughton, 2000). When engaged, the behavioral inhibition system has an important role for conflict detection and in biasing behavioral activation and fight-flight-freeze systems through new and learned information. The PFC role in this process has, at best, been described as “tentative” (Corr, 2013). This dissertation provides evidence for unique roles of the PFC in the behavioral inhibition system and, subsequently, learned anxiety.

Based on our findings that the PL-mPFC adapted to actions with risky contingencies, the PL-mPFC may serve a pivotal role in conflict detection and risk assessment processes of the behavioral inhibition system. Such an interpretation also coincides with more general theories of PL-mPFC function, where the PL-mPFC drives attention to important aspects of the task to properly change behavior (Sharpe & Killcross, 2018). The PL-mPFC is complemented by engagement of LO-OFC. Changes in encoding of punishment and the safe action after learning in LO-OFC may support reward and punishment comparator mechanisms that can be used to update the behavioral inhibition system in accordance to changing conditions within the task. More specifically, the OFC response to punishment and safe actions may help produce a map of the task space to disambiguate actions with unique contingencies and determine the distance of threats.

These roles in conflict detection and task representation would work together not only to process conflict scenarios but also to promote engagement of optimal behavioral choices. If the behavioral inhibition system is not engaged when threat is distant, one may expect maladaptive levels of suppression because of increased fight-flight-freeze system engagement. Alternatively, without proper contingency learning to engage the behavioral inhibition system, this mechanism for control over the behavioral activation system is disrupted and would thus rely on the fight-flight-freeze system to sufficiently attenuate behavioral activation system in times of danger. In summary, reduced engagement of the PFC in learned anxiety contexts may further break down communication in these systems and lead to maladaptive approach or exaggerated avoidance behaviors. This dissertation describes specific functions for the PL-mPFC and LO-OFC to support the behavioral inhibition system and reinforces the role of the PFC as a hub for action control in decision making hierarchies as well as in diverse symptoms seen in mental health disorders.

## Limitations

One limitation of the present studies is that the utilization of fiber photometry means our signal reflects the global activity of large numbers of neurons. Such an approach is more restrictive than single unit approaches where the complexity of single unit activity can permit more sophisticated decoding and correlational analysis (Park et al., 2016). The use of photometry was deliberate in this case as it allowed recording for extended periods of time and of response to footshock itself, and should be considered as a complement, not replacement, for electrophysiological approaches.

We also utilized a synapsin promotor which meant signals were recorded from all neural subtypes. This leaves questions as to whether unique involvement of GABA, glutamate, or monoaminergic activity may play a unique role in the changes in activity presented in Chapters 3-5. Nevertheless, global signals are the frequent output of clinical studies from BOLD signals. Given the novelty of recording neural activity during the behavioral task used here, investigating how these approaches map to clinical endpoints is important.

Fiber photometry data, like many recording techniques, are correlational in nature. We are observing changes in neural activity that co-occur with a behavior of interest. Whether such changes are necessary and sufficient for such behaviors is not rigorously addressed by such an approach. Because methods for parsing whether certain neural substrates are necessary for a behavior have become increasingly temporally resolute (e.g. optogenetics), the findings from recording techniques provided here may illuminate hypothesis driven time-points to target neurons at specific epochs during approach-avoidance conflict.

Lastly we investigated some but not all regions of the PFC in these studies. As outlined in the Introduction, there are several other subregions such as the IL, VO, and MO. Each of these regions is implicated in affective processing or approach-avoidance conflict (Halladay et al., 2020; Shiba et al., 2016). Many of these regions, such as the PL and IL have been suggested to play opposing roles in behavioral processes. Thus these studies are not to be interpreted as a complete picture of the PFC in these processes but a starting point focused on LO-OFC and PL-mPFC subregions.

## Future Directions

Although we provide evidence for a role of the PL-mPFC and LO-OFC in the detection of risky contingencies and punishment, there are still open questions as to what drives encoding changes. Due to the diversity of neural subtypes and input/outputs in these regions, the specific modules for these processes are yet to be determined. One approach could be using Cre-dependent GCaMP or pathway ablation to map how specific pathways may contribute to population level signals seen here. This has been a recent approach which has already yielded novel findings in distinct pathway involvement between the mPFC with approach mechanisms like the NAc or VTA during conflict (Kim et al., 2017) and the OFC with NAc, DS, or BLA (Groman et al., 2019; Pascoli et al., 2018).

There are emerging technologies to parse neuron specific roles in these behaviors through optogenetics and DREADDs in rats. While CaMKII- $\alpha$  neurons have been studied in relation to the mPFC under risky decisions, the development of TH-Cre rat lines and the mDLX enhancer elements allow manipulation of DA/NE and GABA-ergic activity in real time (Ellwood et al., 2017; Passecker et al., 2019). Such studies may wish to target the mPFC during risky actions and the OFC during punishment or take actions after learning to see if these regions have causal effects on anxiety-related behavior if they are overactive.

Lastly, in data presented in Chapters 2-3, consistent with other probabilistic punishment tasks, we found both sex and individual differences in animal behavior. This is an important finding as individual differences in these processes are believed to underlie excessive anxiety and impulsivity seen in psychiatric disorders. Many of these disorders also have sex dependent presentation of symptoms in the human population. Thus use of these tasks and sex as a biological variable (SABV) may yield a more complete picture in relation to using neural processing to understand mental illness. SABV and individual differences analysis is thus an open area for approach-avoidance research and may be an excellent approach to utilize with electrophysiological techniques.

# Bibliography

- Abercrombie, E. D., Keefe, K. A., DiFrischia, D. S., & Zigmond, M. J. (1989). Differential effect of stress on in vivo dopamine release in striatum, nucleus accumbens, and medial frontal cortex. *Journal of neurochemistry*, *52*(5), 1655–1658.
- Adhikari, A., Lerner, T. N., Finkelstein, J., Pak, S., Jennings, J. H., Davidson, T. J., Ferenczi, E., Gunaydin, L. A., Mirzabekov, J. J., Ye, L., Kim, S. Y., Lei, A., & Deisseroth, K. (2015). Basomedial amygdala mediates top-down control of anxiety and fear. *Nature*, *527*(7577), 179–85. <https://doi.org/10.1038/nature15698>
- Adhikari, A., Topiwala, M. A., & Gordon, J. A. (2011). Single units in the medial prefrontal cortex with anxiety-related firing patterns are preferentially influenced by ventral hippocampal activity. *Neuron*, *71*(5), 898–910. <https://doi.org/10.1016/j.neuron.2011.07.027>
- Adhikari, A., Topiwala, M. A., & Gordon, J. A. (2010). Synchronized activity between the ventral hippocampus and the medial prefrontal cortex during anxiety. *Neuron*, *65*(2), 257–269.
- Arinze, I., & Moorman, D. E. (2020). Selective impact of lateral orbitofrontal cortex inactivation on reinstatement of alcohol seeking in male long-evans rats. *Neuropharmacology*, *168*, 108007.
- Arnsten, A. F. (2015). Stress weakens prefrontal networks: Molecular insults to higher cognition. *Nat Neurosci*, *18*(10), 1376–85. <https://doi.org/10.1038/nn.4087>
- Aylward, J., Valton, V., Ahn, W.-Y., Bond, R. L., Dayan, P., Roiser, J. P., & Robinson, O. J. (2019). Altered learning under uncertainty in unmedicated mood and anxiety disorders. *Nature human behaviour*, *3*(10), 1116–1123.
- Azrin, N. H., Holz, W. C., & Hake, D. F. (1963). Fixed-ratio punishment. *J Exp Anal Behav*, *6*, 141–8. <https://doi.org/10.1901/jeab.1963.6-141>
- Babayan, B. M., Uchida, N., & Gershman, S. J. (2018). Belief state representation in the dopamine system. *Nat Commun*, *9*(1), 1891. <https://doi.org/10.1038/s41467-018-04397-0>
- Baeg, E. H., Kim, Y. B., Jang, J., Kim, H. T., Mook-Jung, I., & Jung, M. W. (2001). Fast spiking and regular spiking neural correlates of fear conditioning in the medial prefrontal cortex of the rat. *Cereb Cortex*, *11*(5), 441–51. <https://doi.org/10.1093/cercor/11.5.441>
- Balderston, N. L., Liu, J., Roberson-Nay, R., Ernst, M., & Grillon, C. (2017). The relationship between dlpc activity during unpredictable threat and co(2)-induced panic symptoms. *Transl Psychiatry*, *7*(12), 1266. <https://doi.org/10.1038/s41398-017-0006-5>
- Balderston, N. L., Vytal, K. E., O'Connell, K., Torrissi, S., Letkiewicz, A., Ernst, M., & Grillon, C. (2017). Anxiety patients show reduced working memory related dlpc activation during safety and threat. *Depress Anxiety*, *34*(1), 25–36. <https://doi.org/10.1002/da.22518>
- Bale, T. L., Abel, T., Akil, H., Carlezon Jr, W. A., Moghaddam, B., Nestler, E. J., Ressler, K. J., & Thompson, S. M. (2019). The critical importance of basic animal research for neuropsychiatric disorders. *Neuropsychopharmacology*, *44*(8), 1349–1353.
- Balleine, B. W., & Dickinson, A. (1998). Goal-directed instrumental action: Contingency and incentive learning and their cortical substrates. *Neuropharmacology*, *37*(4-5), 407–419.
- Barker, J. M., Glen, W. B., Linsenhardt, D. N., Lapsch, C. C., & Chandler, L. J. (2017). Habitual behavior is mediated by a shift in response-outcome encoding by infralimbic cortex. *Eneuro*, *4*(6).
- Barreiros, I. V., Panayi, M. C., & Walton, M. E. (2021). Organization of afferents along the anterior–posterior and medial–lateral axes of the rat orbitofrontal cortex. *Neuroscience*, *460*, 53–68. <https://doi.org/https://doi.org/10.1016/j.neuroscience.2021.02.017>

- Basten, U., Stelzel, C., & Fiebach, C. J. (2011). Trait anxiety modulates the neural efficiency of inhibitory control. *J Cogn Neurosci*, *23*(10), 3132–45. [https://doi.org/10.1162/jocn\\_a\\_00003](https://doi.org/10.1162/jocn_a_00003)
- Basten, U., Stelzel, C., & Fiebach, C. J. (2012). Trait anxiety and the neural efficiency of manipulation in working memory. *Cogn Affect Behav Neurosci*, *12*(3), 571–88. <https://doi.org/10.3758/s13415-012-0100-3>
- Baxter, M. G., Parker, A., Lindner, C. C., Izquierdo, A. D., & Murray, E. A. (2000). Control of response selection by reinforcer value requires interaction of amygdala and orbital prefrontal cortex. *Journal of Neuroscience*, *20*(11), 4311–4319.
- Bechara, A., Dolan, S., & Hinds, A. (2002). Decision-making and addiction (part ii): Myopia for the future or hypersensitivity to reward? *Neuropsychologia*, *40*(10), 1690–705. [https://doi.org/10.1016/s0028-3932\(02\)00016-7](https://doi.org/10.1016/s0028-3932(02)00016-7)
- Becker, J. B., & Chartoff, E. (2019). Sex differences in neural mechanisms mediating reward and addiction. *Neuropsychopharmacology*, *44*(1), 166–183. <https://doi.org/10.1038/s41386-018-0125-6>
- Bi, L.-L., Wang, J., Luo, Z.-Y., Chen, S.-P., Geng, F., Chen, Y.-h., Li, S.-J., Yuan, C.-h., Lin, S., & Gao, T.-M. (2013). Enhanced excitability in the infralimbic cortex produces anxiety-like behaviors. *Neuropharmacology*, *72*, 148–156.
- Birrell, J. M., & Brown, V. J. (2000). Medial frontal cortex mediates perceptual attentional set shifting in the rat. *J Neurosci*, *20*(11), 4320–4. <https://doi.org/10.1523/jneurosci.20-11-04320.2000>
- Bishop, S. J. (2009). Trait anxiety and impoverished prefrontal control of attention. *Nature neuroscience*, *12*(1), 92–98.
- Bishop, S. J., Duncan, J., & Lawrence, A. D. (2004). State anxiety modulation of the amygdala response to unattended threat-related stimuli. *Journal of Neuroscience*, *24*(46), 10364–10368.
- Bissiere, S., McAllister, K. H., Olpe, H.-R., & Cryan, J. F. (2006). The rostral anterior cingulate cortex modulates depression but not anxiety-related behaviour in the rat. *Behavioural brain research*, *175*(1), 195–199.
- Brodkin, J., Busse, C., Sukoff, S. J., & Varney, M. A. (2002). Anxiolytic-like activity of the mglur5 antagonist mpep: A comparison with diazepam and buspirone. *Pharmacology Biochemistry and Behavior*, *73*(2), 359–366.
- Broersen, L., Heinsbroek, R., De Bruin, J., Laan, J.-B., Joosten, R., & Olivier, B. (1995). Local pharmacological manipulations of prefrontal dopamine affect conflict behaviour in rats. *Behavioural Pharmacology*.
- Burgos-Robles, A., Vidal-Gonzalez, I., & Quirk, G. J. (2009). Sustained conditioned responses in prelimbic prefrontal neurons are correlated with fear expression and extinction failure. *J Neurosci*, *29*(26), 8474–82. <https://doi.org/10.1523/jneurosci.0378-09.2009>
- Caballero, J. P., Scarpa, G. B., Remage-Healey, L., & Moorman, D. E. (2019). Differential effects of dorsal and ventral medial prefrontal cortex inactivation during natural reward seeking, extinction, and cue-induced reinstatement. *Eneuro*, *6*(5).
- Calhoun, G. G., & Tye, K. M. (2015). Resolving the neural circuits of anxiety. *Nature neuroscience*, *18*(10), 1394–1404.
- Campeau, S., Dolan, D., Akil, H., & Watson, S. J. (2002). C-fos mRNA induction in acute and chronic audiogenic stress: Possible role of the orbitofrontal cortex in habituation. *Stress*, *5*(2), 121–130.
- Capriles, N., Rodaros, D., Sorge, R. E., & Stewart, J. (2003). A role for the prefrontal cortex in stress-and cocaine-induced reinstatement of cocaine seeking in rats. *Psychopharmacology*, *168*(1), 66–74.

- Capuzzo, G., & Floresco, S. B. (2020). Prelimbic and infralimbic prefrontal regulation of active and inhibitory avoidance and reward-seeking. *J Neurosci*, *40*(24), 4773–4787. <https://doi.org/10.1523/jneurosci.0414-20.2020>
- Cardinal, R. N., & Howes, N. J. (2005). Effects of lesions of the nucleus accumbens core on choice between small certain rewards and large uncertain rewards in rats. *BMC neuroscience*, *6*(1), 1–19.
- Carlén, M. (2017). What constitutes the prefrontal cortex? *Science*, *358*(6362), 478–482.
- Cerqueira, J. J., Mailliet, F., Almeida, O. F., Jay, T. M., & Sousa, N. (2007). The prefrontal cortex as a key target of the maladaptive response to stress. *J Neurosci*, *27*(11), 2781–7. <https://doi.org/10.1523/jneurosci.4372-06.2007>
- Chang, C. H., Berke, J. D., & Maren, S. (2010). Single-unit activity in the medial prefrontal cortex during immediate and delayed extinction of fear in rats. *PLoS One*, *5*(8), e11971. <https://doi.org/10.1371/journal.pone.0011971>
- Chang, Y.-H., Liu, S.-W., & Chang, C.-h. (2018). Pharmacological activation of the lateral orbitofrontal cortex on regulation of learned fear and extinction. *Neurobiology of learning and memory*, *148*, 30–37.
- Chen, B. T., Yau, H. J., Hatch, C., Kusumoto-Yoshida, I., Cho, S. L., Hopf, F. W., & Bonci, A. (2013). Rescuing cocaine-induced prefrontal cortex hypoactivity prevents compulsive cocaine seeking. *Nature*, *496*(7445), 359–62. <https://doi.org/10.1038/nature12024>
- Chen, T.-W., Wardill, T. J., Sun, Y., Pulver, S. R., Renninger, S. L., Baohan, A., Schreiter, E. R., Kerr, R. A., Orger, M. B., Jayaraman, V., et al. (2013). Ultrasensitive fluorescent proteins for imaging neuronal activity. *Nature*, *499*(7458), 295–300.
- Chowdhury, T. G., Wallin-Miller, K. G., Rear, A. A., Park, J., Diaz, V., Simon, N. W., & Moghaddam, B. (2019). Sex differences in reward-and punishment-guided actions. *Cognitive, Affective, & Behavioral Neuroscience*, *19*(6), 1404–1417.
- Chudasama, Y., Passeti, F., Rhodes, S., Lopian, D., Desai, A., & Robbins, T. (2003). Dissociable aspects of performance on the 5-choice serial reaction time task following lesions of the dorsal anterior cingulate, infralimbic and orbitofrontal cortex in the rat: Differential effects on selectivity, impulsivity and compulsivity. *Behavioural brain research*, *146*(1-2), 105–119.
- Cohen, J. Y., Haesler, S., Vong, L., Lowell, B. B., & Uchida, N. (2012). Neuron-type-specific signals for reward and punishment in the ventral tegmental area. *nature*, *482*(7383), 85–88.
- Collins, G. T., & Woods, J. H. (2007). Drug and reinforcement history as determinants of the response-maintaining effects of quinpirole in the rat. *Journal of Pharmacology and Experimental Therapeutics*, *323*(2), 599–605.
- Compton, R. J. (2003). The interface between emotion and attention: A review of evidence from psychology and neuroscience. *Behavioral and cognitive neuroscience reviews*, *2*(2), 115–129.
- Cook, S. C., & Wellman, C. L. (2004). Chronic stress alters dendritic morphology in rat medial prefrontal cortex. *Journal of neurobiology*, *60*(2), 236–248.
- Cooper, S. E., Goings, S. P., Kim, J. Y., & Wood, R. I. (2014). Testosterone enhances risk tolerance without altering motor impulsivity in male rats. *Psychoneuroendocrinology*, *40*, 201–12. <https://doi.org/10.1016/j.psyneuen.2013.11.017>
- Corcoran, K. A., & Quirk, G. J. (2007). Activity in prelimbic cortex is necessary for the expression of learned, but not innate, fears. *J Neurosci*, *27*(4), 840–4. <https://doi.org/10.1523/jneurosci.5327-06.2007>
- Cornwell, B. R., Garrido, M. I., Overstreet, C., Pine, D. S., & Grillon, C. (2017). The unpredictable brain under threat: A neurocomputational account of anxious hypervigilance [Computational Psychiatry]. *Biological Psychiatry*, *82*(6), 447–454. <https://doi.org/https://doi.org/10.1016/j.biopsych.2017.06.031>

- Corr, P. J. (2004). Reinforcement sensitivity theory and personality. *Neuroscience & Biobehavioral Reviews*, 28(3), 317–332.
- Corr, P. J. (2010). Automatic and controlled processes in behavioural control: Implications for personality psychology. *European Journal of Personality*, 24(5), 376–403.
- Corr, P. J. (2013). Approach and avoidance behaviour: Multiple systems and their interactions. *Emotion Review*, 5(3), 285–290.
- Courtin, J., Chaudun, F., Rozeske, R. R., Karalis, N., Gonzalez-Campo, C., Wurtz, H., Abdi, A., Baufreton, J., Bienvenu, T. C., & Herry, C. (2014). Prefrontal parvalbumin interneurons shape neuronal activity to drive fear expression. *Nature*, 505(7481), 92–6. <https://doi.org/10.1038/nature12755>
- Coutureau, E., & Killcross, S. (2003). Inactivation of the infralimbic prefrontal cortex reinstates goal-directed responding in overtrained rats. *Behavioural brain research*, 146(1-2), 167–174.
- Crawley, J. N., Ninan, P. T., Pickar, D., Chrousos, G. P., Linnoila, M., Skolnick, P., & Paul, S. M. (1985). Neuropharmacological antagonism of the beta-carboline-induced “anxiety” response in rhesus monkeys. *J Neurosci*, 5(2), 477–85. <https://doi.org/10.1523/jneurosci.05-02-00477.1985>
- Dalterio, S., Wayner, M., Geller, I., & Hartmann, R. (1988). Ethanol and diazepam interactions on conflict behavior in rats. *Alcohol*, 5(6), 471–476.
- Daviu, N., Bruchas, M. R., Moghaddam, B., Sandi, C., & Beyeler, A. (2019). Neurobiological links between stress and anxiety. *Neurobiology of stress*, 11, 100191.
- Del Arco, A., Park, J., Wood, J., Kim, Y., & Moghaddam, B. (2017). Adaptive encoding of outcome prediction by prefrontal cortex ensembles supports behavioral flexibility. *J Neurosci*, 37(35), 8363–8373. <https://doi.org/10.1523/jneurosci.0450-17.2017>
- Deutch, A. Y., Clark, W. A., & Roth, R. H. (1990). Prefrontal cortical dopamine depletion enhances the responsiveness of mesolimbic dopamine neurons to stress. *Brain research*, 521(1-2), 311–315.
- Diehl, M. M., Bravo-Rivera, C., Rodriguez-Romaguera, J., Pagan-Rivera, P. A., Burgos-Robles, A., Roman-Ortiz, C., & Quirk, G. J. (2018). Active avoidance requires inhibitory signaling in the rodent prelimbic prefrontal cortex. *Elife*, 7. <https://doi.org/10.7554/eLife.34657>
- Do-Monte, F. H., Manzano-Nieves, G., Quiñones-Laracuente, K., Ramos-Medina, L., & Quirk, G. J. (2015). Revisiting the role of infralimbic cortex in fear extinction with optogenetics. *J Neurosci*, 35(8), 3607–15. <https://doi.org/10.1523/jneurosci.3137-14.2015>
- Dorow, R. (1987). Fg 7142 and its anxiety-inducing effects in humans. *Br J Clin Pharmacol*, 23(6), 781–2.
- Ellwood, I. T., Patel, T., Wadia, V., Lee, A. T., Liptak, A. T., Bender, K. J., & Sohal, V. S. (2017). Tonic or phasic stimulation of dopaminergic projections to prefrontal cortex causes mice to maintain or deviate from previously learned behavioral strategies. *Journal of Neuroscience*, 37(35), 8315–8329.
- Engelhard, B., Finkelstein, J., Cox, J., Fleming, W., Jang, H. J., Ornelas, S., Koay, S. A., Thiberge, S. Y., Daw, N. D., Tank, D. W., et al. (2019). Specialized coding of sensory, motor and cognitive variables in vta dopamine neurons. *Nature*, 570(7762), 509–513.
- Ersche, K. D., Gillan, C. M., Jones, P. S., Williams, G. B., Ward, L. H., Luijten, M., de Wit, S., Sahakian, B. J., Bullmore, E. T., & Robbins, T. W. (2016). Carrots and sticks fail to change behavior in cocaine addiction. *Science*, 352(6292), 1468–1471.
- Eysenck, M. W., Derakshan, N., Santos, R., & Calvo, M. G. (2007). Anxiety and cognitive performance: Attentional control theory. *Emotion*, 7(2), 336–53. <https://doi.org/10.1037/1528-3542.7.2.336>

- Finlay, J., Zigmond, M., & Abercrombie, E. (1995). Increased dopamine and norepinephrine release in medial prefrontal cortex induced by acute and chronic stress: Effects of diazepam. *Neuroscience*, *64*(3), 619–628.
- Fischer, B. D., Licata, S. C., Edwankar, R. V., Wang, Z.-J., Huang, S., He, X., Yu, J., Zhou, H., Johnson, E. M., Cook, J. M., Furtmüller, R., Ramerstorfer, J., Sieghart, W., Roth, B. L., Majumder, S., & Rowlett, J. K. (2010). Anxiolytic-like effects of 8-acetylene imidazobenzodiazepines in a rhesus monkey conflict procedure. *Neuropharmacology*, *59*(7), 612–618. <https://doi.org/https://doi.org/10.1016/j.neuropharm.2010.08.011>
- Floresco, S. B., Block, A. E., & Maric, T. (2008). Inactivation of the medial prefrontal cortex of the rat impairs strategy set-shifting, but not reversal learning, using a novel, automated procedure. *Behavioural brain research*, *190*(1), 85–96.
- Floresco, S. B., Magyar, O., Ghods-Sharifi, S., Vexelman, C., & Maric, T. (2006). Multiple dopamine receptor subtypes in the medial prefrontal cortex of the rat regulate set-shifting. *Neuropsychopharmacology*, *31*(2), 297–309.
- Floresco, S. B., & Whelan, J. M. (2009). Perturbations in different forms of cost/benefit decision making induced by repeated amphetamine exposure. *Psychopharmacology*, *205*(2), 189–201.
- Fox, M. A., French, H. T., LaPorte, J. L., Blackler, A. R., & Murphy, D. L. (2010). The serotonin 5-HT<sub>2A</sub> receptor agonist tcb-2: A behavioral and neurophysiological analysis. *Psychopharmacology*, *212*(1), 13–23.
- Friedman, A., Homma, D., Bloem, B., Gibb, L. G., Amemori, K. I., Hu, D., Delcasso, S., Truong, T. F., Yang, J., Hood, A. S., Mikofalvy, K. A., Beck, D. W., Nguyen, N., Nelson, E. D., Toro Arana, S. E., Vorder Bruegge, R. H., Goosens, K. A., & Graybiel, A. M. (2017). Chronic stress alters striosome-circuit dynamics, leading to aberrant decision-making. *Cell*, *171*(5), 1191–1205.e28. <https://doi.org/10.1016/j.cell.2017.10.017>
- Friedman, A., Homma, D., Gibb, L. G., Amemori, K., Rubin, S. J., Hood, A. S., Riad, M. H., & Graybiel, A. M. (2015). A corticostriatal path targeting striosomes controls decision-making under conflict. *Cell*, *161*(6), 1320–33. <https://doi.org/10.1016/j.cell.2015.04.049>
- Friedman, H., Abernethy, D. R., Greenblatt, D. J., & Shader, R. I. (1986). The pharmacokinetics of diazepam and desmethyldiazepam in rat brain and plasma. *Psychopharmacology*, *88*(3), 267–270.
- Fujisawa, S., & Buzsáki, G. (2011). A 4 hz oscillation adaptively synchronizes prefrontal, vta, and hippocampal activities. *Neuron*, *72*(1), 153–165.
- Furuyashiki, T., & Gallagher, M. (2007). Neural encoding in the orbitofrontal cortex related to goal-directed behavior. *Annals of the New York Academy of Sciences*, *1121*(1), 193–215.
- Furuyashiki, T., Holland, P. C., & Gallagher, M. (2008). Rat orbitofrontal cortex separately encodes response and outcome information during performance of goal-directed behavior. *Journal of Neuroscience*, *28*(19), 5127–5138.
- Fuster, J. M. (2001). The prefrontal cortex—an update: Time is of the essence. *Neuron*, *30*(2), 319–33. [https://doi.org/10.1016/s0896-6273\(01\)00285-9](https://doi.org/10.1016/s0896-6273(01)00285-9)
- Fuster, J. (2015). *The prefrontal cortex*. Academic Press.
- Fuster, J. M. (2000). Prefrontal neurons in networks of executive memory. *Brain research bulletin*, *52*(5), 331–336.
- Gabriel, D. B., Freels, T. G., Setlow, B., & Simon, N. W. (2019). Risky decision-making is associated with impulsive action and sensitivity to first-time nicotine exposure. *Behavioural brain research*, *359*, 579–588.
- Gallagher, M., McMahan, R. W., & Schoenbaum, G. (1999). Orbitofrontal cortex and representation of incentive value in associative learning. *Journal of Neuroscience*, *19*(15), 6610–6614.

- Geller, I., & Seifter, J. (1960). The effects of meprobamate, barbiturates, d-amphetamine and promazine on experimentally induced conflict in the rat. *Psychopharmacologia*, *1*(6), 482–492. <https://doi.org/10.1007/BF00429273>
- Glover, L. R., McFadden, K. M., Bjorni, M., Smith, S. R., Rovero, N. G., Oreizi-Esfahani, S., Yoshida, T., Postle, A. F., Nonaka, M., Halladay, L. R., et al. (2020). A prefrontal-bed nucleus of the stria terminalis circuit limits fear to uncertain threat. *Elife*, *9*, e60812.
- Goldstein, R. Z., & Volkow, N. D. (2011). Dysfunction of the prefrontal cortex in addiction: Neuroimaging findings and clinical implications. *Nature reviews neuroscience*, *12*(11), 652–669.
- Goode, T. D., Ressler, R. L., Acca, G. M., Miles, O. W., & Maren, S. (2019). Bed nucleus of the stria terminalis regulates fear to unpredictable threat signals. *Elife*, *8*, e46525.
- Gourley, S. L., & Taylor, J. R. (2016). Going and stopping: Dichotomies in behavioral control by the prefrontal cortex. *Nat Neurosci*, *19*(6), 656–664. <https://doi.org/10.1038/nn.4275>
- Gray, J., & Smith, P. (1969). An arousal-decision model for partial reinforcement and discrimination learning in rm gilbert & ns sutherland (eds.), animal discrimination learning.
- Gray, J., & McNaughton, N. (2000). *The neuropsychology of anxiety* (2nd ed.). Oxford University Press.
- Gray, J. A. (1982). The neuropsychology of anxiety: An enquiry into the functions of the septo-hippocampal system. *Behavioral and brain sciences*, *5*(3), 469–484.
- Gray, J. A. (1987). Perspectives on anxiety and impulsivity: A commentary.
- Green, T. A., Baracz, S. J., Everett, N. A., Robinson, K. J., & Cornish, J. L. (2020). Differential effects of gaba a receptor activation in the prelimbic and orbitofrontal cortices on anxiety. *Psychopharmacology*, *237*(11), 3237–3247.
- Gremel, C. M., & Costa, R. M. (2013). Orbitofrontal and striatal circuits dynamically encode the shift between goal-directed and habitual actions. *Nature communications*, *4*(1), 1–12.
- Grillon, C. (2008). Models and mechanisms of anxiety: Evidence from startle studies. *Psychopharmacology (Berl)*, *199*(3), 421–37. <https://doi.org/10.1007/s00213-007-1019-1>
- Grillon, C., Pine, D. S., Lissek, S., Rabin, S., Bonne, O., & Vythilingam, M. (2009). Increased anxiety during anticipation of unpredictable aversive stimuli in posttraumatic stress disorder but not in generalized anxiety disorder. *Biol Psychiatry*, *66*(1), 47–53. <https://doi.org/10.1016/j.biopsych.2008.12.028>
- Groman, S. M., Keistler, C., Keip, A. J., Hammarlund, E., DiLeone, R. J., Pittenger, C., Lee, D., & Taylor, J. R. (2019). Orbitofrontal circuits control multiple reinforcement-learning processes. *Neuron*, *103*(4), 734–746.
- Gruene, T. M., Flick, K., Stefano, A., Shea, S. D., & Shansky, R. M. (2015). Sexually divergent expression of active and passive conditioned fear responses in rats. *Elife*, *4*. <https://doi.org/10.7554/eLife.11352>
- Gunaydin, L. A., Grosenick, L., Finkelstein, J. C., Kauvar, I. V., Fenno, L. E., Adhikari, A., Lammel, S., Mirzabekov, J. J., Airan, R. D., Zalocusky, K. A., et al. (2014). Natural neural projection dynamics underlying social behavior. *Cell*, *157*(7), 1535–1551.
- Guru, A., Seo, C., Post, R. J., Kullakanda, D. S., Schaffer, J. A., & Warden, M. R. (2020). Ramping activity in midbrain dopamine neurons signifies the use of a cognitive map. *BioRxiv*.
- Halladay, L. R., Kocharian, A., Piantadosi, P. T., Authement, M. E., Lieberman, A. G., Spitz, N. A., Coden, K., Glover, L. R., Costa, V. D., Alvarez, V. A., & Holmes, A. (2020). Prefrontal regulation of punished ethanol self-administration. *Biol Psychiatry*, *87*(11), 967–978. <https://doi.org/10.1016/j.biopsych.2019.10.030>
- Han, H. J., Jung, W. H., Yun, J. Y., Park, J. W., Cho, K. K., Hur, J. W., Shin, N. Y., Lee, T. Y., & Kwon, J. S. (2016). Disruption of effective connectivity from the dorsolateral prefrontal cortex to the orbitofrontal cortex by negative emotional distraction in

- obsessive-compulsive disorder. *Psychol Med*, 46(5), 921–32. <https://doi.org/10.1017/S0033291715002391>
- Harada, M., Hiver, A., Pascoli, V., & Lüscher, C. (2019). Cortico-striatal synaptic plasticity underlying compulsive reward seeking. *bioRxiv*, 789495.
- Hardung, S., Epple, R., Jäckel, Z., Eriksson, D., Uran, C., Senn, V., Gibor, L., Yizhar, O., & Diester, I. (2017). A functional gradient in the rodent prefrontal cortex supports behavioral inhibition. *Current Biology*, 27(4), 549–555.
- Hart, A. S., Rutledge, R. B., Glimcher, P. W., & Phillips, P. E. (2014). Phasic dopamine release in the rat nucleus accumbens symmetrically encodes a reward prediction error term. *Journal of Neuroscience*, 34(3), 698–704.
- Hartley, C. A., & Phelps, E. A. (2012). Anxiety and decision-making. *Biol Psychiatry*, 72(2), 113–8. <https://doi.org/10.1016/j.biopsych.2011.12.027>
- Hesselgrave, N., Troppoli, T. A., Wulff, A. B., Cole, A. B., & Thompson, S. M. (2021). Harnessing psilocybin: Antidepressant-like behavioral and synaptic actions of psilocybin are independent of 5-HT<sub>2R</sub> activation in mice. *Proceedings of the National Academy of Sciences*, 118(17).
- Holmes, A., & Wellman, C. L. (2009). Stress-induced prefrontal reorganization and executive dysfunction in rodents. *Neurosci Biobehav Rev*, 33(6), 773–83. <https://doi.org/10.1016/j.neubiorev.2008.11.005>
- Homayoun, H., & Moghaddam, B. (2009). Differential representation of pavlovian-instrumental transfer by prefrontal cortex subregions and striatum. *Eur J Neurosci*, 29(7), 1461–76. <https://doi.org/10.1111/j.1460-9568.2009.06679.x>
- Homayoun, H., & Moghaddam, B. (2006). Progression of cellular adaptations in medial prefrontal and orbitofrontal cortex in response to repeated amphetamine. *Journal of Neuroscience*, 26(31), 8025–8039.
- Hong, D. D., Huang, W. Q., Ji, A. A., Yang, S. S., Xu, H., Sun, K. Y., Cao, A., Gao, W. J., Zhou, N., & Yu, P. (2019). Neurons in rat orbitofrontal cortex and medial prefrontal cortex exhibit distinct responses in reward and strategy-update in a risk-based decision-making task. *Metab Brain Dis*, 34(2), 417–429. <https://doi.org/10.1007/s11011-018-0360-x>
- Hoover, W. B., & Vertes, R. P. (2007). Anatomical analysis of afferent projections to the medial prefrontal cortex in the rat. *Brain Struct Funct*, 212(2), 149–79. <https://doi.org/10.1007/s00429-007-0150-4>
- Hoover, W. B., & Vertes, R. P. (2011). Projections of the medial orbital and ventral orbital cortex in the rat. *Journal of Comparative Neurology*, 519(18), 3766–3801.
- Hsieh, H.-T., & Chang, C.-h. (2020). Activation of medial orbitofrontal cortex abolishes fear extinction and interferes with fear expression in rats. *Neurobiology of learning and memory*, 169, 107170.
- Ishikawa, J., Sakurai, Y., Ishikawa, A., & Mitsushima, D. (2020). Contribution of the prefrontal cortex and basolateral amygdala to behavioral decision-making under reward/punishment conflict. *Psychopharmacology*, 237(3), 639–654.
- Izquierdo, A. (2017). Functional heterogeneity within rat orbitofrontal cortex in reward learning and decision making. *Journal of Neuroscience*, 37(44), 10529–10540.
- Izquierdo, A., & Murray, E. A. (2005). Opposing effects of amygdala and orbital prefrontal cortex lesions on the extinction of instrumental responding in macaque monkeys. *European Journal of Neuroscience*, 22(9), 2341–2346.
- Izquierdo, A., Suda, R. K., & Murray, E. A. (2004). Bilateral orbital prefrontal cortex lesions in rhesus monkeys disrupt choices guided by both reward value and reward contingency. *Journal of Neuroscience*, 24(34), 7540–7548.
- Jacobs, D. S., & Moghaddam, B. (2020). Prefrontal cortex representation of learning of punishment probability during reward-motivated actions. *J Neurosci*, 40(26), 5063–5077. <https://doi.org/10.1523/jneurosci.0310-20.2020>

- Jacobs, D. S., Allen, M. C., Park, J., & Moghaddam, B. (In prep). Encoding of instrumental action and punishment in the rodent prefrontal cortex and ventral tegmental area: Effects of learning and diazepam.
- Jacobs, D. S., & Moghaddam, B. (2021). Chapter two - medial prefrontal cortex encoding of stress and anxiety. In A. T. Brockett, L. M. Amarante, M. Laubach, & M. R. Roesch (Eds.), *What does medial frontal cortex signal during behavior? insights from behavioral neurophysiology* (pp. 29–55). Academic Press. <https://doi.org/10.1016/bs.irn.2020.11.014>
- Jacobs, D. S., & Moghaddam, B. (In prep). The orbitofrontal and medial prefrontal cortex differentially encode the learning of probabilistic punishment during reward seeking.
- Jean-Richard-dit-Bressel, P., Clifford, C. W., & McNally, G. P. (2020). Analyzing event-related transients: Confidence intervals, permutation tests, and consecutive thresholds. *Frontiers in molecular neuroscience*, *13*, 14.
- Jean-Richard-Dit-Bressel, P., Killcross, S., & McNally, G. P. (2018). Behavioral and neurobiological mechanisms of punishment: Implications for psychiatric disorders. *Neuropsychopharmacology*, *43*(8), 1639–1650.
- Jean-Richard-dit-Bressel, P., Ma, C., Bradfield, L. A., Killcross, S., & McNally, G. P. (2019). Punishment insensitivity emerges from impaired contingency detection, not aversion insensitivity or reward dominance. *Elife*, *8*, e52765.
- Jean-Richard-dit-Bressel, P., & McNally, G. P. (2016). Lateral, not medial, prefrontal cortex contributes to punishment and aversive instrumental learning. *Learning & memory*, *23*(11), 607–617.
- Jett, J. D., & Morilak, D. A. (2013). Too much of a good thing: Blocking noradrenergic facilitation in medial prefrontal cortex prevents the detrimental effects of chronic stress on cognition. *Neuropsychopharmacology*, *38*(4), 585–595.
- Johansen, J. P., Cain, C. K., Ostroff, L. E., & LeDoux, J. E. (2011). Molecular mechanisms of fear learning and memory. *Cell*, *147*(3), 509–24. <https://doi.org/10.1016/j.cell.2011.10.009>
- Johnson, M. W., & Griffiths, R. R. (2017). Potential therapeutic effects of psilocybin. *Neurotherapeutics*, *14*(3), 734–740.
- Kesner, R. P., & Churchwell, J. C. (2011). An analysis of rat prefrontal cortex in mediating executive function. *Neurobiology of learning and memory*, *96*(3), 417–431.
- Killcross, S., & Coutureau, E. (2003). Coordination of actions and habits in the medial prefrontal cortex of rats. *Cereb Cortex*, *13*(4), 400–8. <https://doi.org/10.1093/cercor/13.4.400>
- Kim, C. K., Ye, L., Jennings, J. H., Pichamoorthy, N., Tang, D. D., Yoo, A. W., Ramakrishnan, C., & Deisseroth, K. (2017). Molecular and circuit-dynamical identification of top-down neural mechanisms for restraint of reward seeking. *Cell*, *170*(5), 1013–1027.e14. <https://doi.org/10.1016/j.cell.2017.07.020>
- Kim, J. J., Lee, H. J., Welday, A. C., Song, E., Cho, J., Sharp, P. E., Jung, M. W., & Blair, H. T. (2007). Stress-induced alterations in hippocampal plasticity, place cells, and spatial memory. *Proc Natl Acad Sci U S A*, *104*(46), 18297–302. <https://doi.org/10.1073/pnas.0708644104>
- Kremer, Y., Flakowski, J., Rohner, C., & Lüscher, C. (2020). Context-dependent multiplexing by individual vta dopamine neurons. *Journal of Neuroscience*, *40*(39), 7489–7509. <https://doi.org/10.1523/JNEUROSCI.0502-20.2020>
- Kumar, S., Black, S. J., Hultman, R., Szabo, S. T., DeMaio, K. D., Du, J., Katz, B. M., Feng, G., Covington, 3., H. E., & Dzirasa, K. (2013). Cortical control of affective networks. *J Neurosci*, *33*(3), 1116–29. <https://doi.org/10.1523/jneurosci.0092-12.2013>
- Kuniishi, H., Ichisaka, S., Matsuda, S., Futora, E., Harada, R., & Hata, Y. (2017). Chronic inactivation of the orbitofrontal cortex increases anxiety-like behavior and impulsive

- aggression, but decreases depression-like behavior in rats. *Frontiers in behavioral neuroscience*, *10*, 250.
- Kupferschmidt, D. A., Juczewski, K., Cui, G., Johnson, K. A., & Lovinger, D. M. (2017). Parallel, but dissociable, processing in discrete corticostriatal inputs encodes skill learning. *Neuron*, *96*(2), 476–489.e5. <https://doi.org/10.1016/j.neuron.2017.09.040>
- Lacroix, L., Broersen, L., Weiner, I., & Feldon, J. (1998). The effects of excitotoxic lesion of the medial prefrontal cortex on latent inhibition, prepulse inhibition, food hoarding, elevated plus maze, active avoidance and locomotor activity in the rat. *Neuroscience*, *84*(2), 431–442.
- Lacroix, L., Spinelli, S., Heidbreder, C. A., & Feldon, J. (2000). Differential role of the medial and lateral prefrontal cortices in fear and anxiety. *Behavioral neuroscience*, *114*(6), 1119.
- Lammel, S., Lim, B. K., Ran, C., Huang, K. W., Betley, M. J., Tye, K. M., Deisseroth, K., & Malenka, R. C. (2012). Input-specific control of reward and aversion in the ventral tegmental area. *Nature*, *491*(7423), 212–217.
- Lammel, S., Tye, K., & Warden, M. (2014). Progress in understanding mood disorders: Optogenetic dissection of neural circuits. *Genes, Brain and Behavior*, *13*(1), 38–51.
- Laubach, M., Amarante, L. M., Swanson, K., & White, S. R. (2018). What, if anything, is rodent prefrontal cortex? *eNeuro*, *5*(5). <https://doi.org/10.1523/eneuro.0315-18.2018>
- Legaria, A. A., Licholai, J. A., & Kravitz, A. (2021). Fiber photometry does not reflect spiking activity in the striatum. *bioRxiv*.
- Lezak, K. R., Missig, G., & Carlezon, J., W. A. (2017). Behavioral methods to study anxiety in rodents. *Dialogues Clin Neurosci*, *19*(2), 181–191.
- Likhtik, E., Stujenske, J. M., Topiwala, M. A., Harris, A. Z., & Gordon, J. A. (2014). Prefrontal entrainment of amygdala activity signals safety in learned fear and innate anxiety. *Nature neuroscience*, *17*(1), 106–113.
- Liljequist, S., & Engel, J. A. (1984). The effects of gaba and benzodiazepine receptor antagonists on the anti-conflict actions of diazepam or ethanol. *Pharmacology Biochemistry and Behavior*, *21*(4), 521–525.
- Liston, C., Miller, M. M., Goldwater, D. S., Radley, J. J., Rocher, A. B., Hof, P. R., Morrison, J. H., & McEwen, B. S. (2006). Stress-induced alterations in prefrontal cortical dendritic morphology predict selective impairments in perceptual attentional set-shifting. *J Neurosci*, *26*(30), 7870–4. <https://doi.org/10.1523/jneurosci.1184-06.2006>
- Lodge, D. J. (2011). The medial prefrontal and orbitofrontal cortices differentially regulate dopamine system function. *Neuropsychopharmacology*, *36*(6), 1227–36. <https://doi.org/10.1038/npp.2011.7>
- Loewke, A. C., Minerva, A. R., Nelson, A. B., Kreitzer, A. C., & Gunaydin, L. A. (2021). Frontostriatal projections regulate innate avoidance behavior. *Journal of Neuroscience*, *41*(25), 5487–5501.
- Lohani, S., Martig, A. K., Deisseroth, K., Witten, I. B., & Moghaddam, B. (2019). Dopamine modulation of prefrontal cortex activity is manifold and operates at multiple temporal and spatial scales. *Cell reports*, *27*(1), 99–114.
- Lopes, G., Bonacchi, N., Frazão, J., Neto, J. P., Atallah, B. V., Soares, S., Moreira, L., Matias, S., Itskov, P. M., Correia, P. A., et al. (2015). Bonsai: An event-based framework for processing and controlling data streams. *Frontiers in neuroinformatics*, *9*, 7.
- Luo, R., Uematsu, A., Weitemier, A., Aquili, L., Koivumaa, J., McHugh, T. J., & Johansen, J. P. (2018). A dopaminergic switch for fear to safety transitions. *Nature communications*, *9*(1), 1–11.
- Matias, S., Lottem, E., Dugue, G. P., & Mainen, Z. F. (2017). Activity patterns of serotonin neurons underlying cognitive flexibility. *Elife*, *6*. <https://doi.org/10.7554/eLife.20552>

- McDannald, M. A., Esber, G. R., Wegener, M. A., Wied, H. M., Liu, T.-L., Stalnaker, T. A., Jones, J. L., Trageser, J., & Schoenbaum, G. (2014). Orbitofrontal neurons acquire responses to ‘valueless’ pavlovian cues during unblocking. *Elife*, *3*, e02653.
- McEwen, B. S., & Morrison, J. H. (2013). The brain on stress: Vulnerability and plasticity of the prefrontal cortex over the life course. *Neuron*, *79*(1), 16–29. <https://doi.org/10.1016/j.neuron.2013.06.028>
- McEwen, B. S., Bowles, N. P., Gray, J. D., Hill, M. N., Hunter, R. G., Karatsoreos, I. N., & Nasca, C. (2015). Mechanisms of stress in the brain. *Nature neuroscience*, *18*(10), 1353–1363.
- McEwen, B. S., Nasca, C., & Gray, J. D. (2016). Stress effects on neuronal structure: Hippocampus, amygdala, and prefrontal cortex. *Neuropsychopharmacology*, *41*(1), 3–23.
- McFarland, K., Davidge, S. B., Lapish, C. C., & Kalivas, P. W. (2004). Limbic and motor circuitry underlying footshock-induced reinstatement of cocaine-seeking behavior. *Journal of Neuroscience*, *24*(7), 1551–1560.
- McKlveen, J. M., Moloney, R. D., Scheimann, J. R., Myers, B., & Herman, J. P. (2019). “Braking” the prefrontal cortex: The role of glucocorticoids and interneurons in stress adaptation and pathology. *Biol Psychiatry*, *86*(9), 669–681. <https://doi.org/10.1016/j.biopsych.2019.04.032>
- McKlveen, J. M., Myers, B., & Herman, J. P. (2015). The medial prefrontal cortex: Coordinator of autonomic, neuroendocrine and behavioural responses to stress. *J Neuroendocrinol*, *27*(6), 446–56. <https://doi.org/10.1111/jne.12272>
- McKlveen, J. M., Morano, R. L., Fitzgerald, M., Zoubovsky, S., Cassella, S. N., Scheimann, J. R., Ghosal, S., Mahbod, P., Packard, B. A., & Myers, B. (2016). Chronic stress increases prefrontal inhibition: A mechanism for stress-induced prefrontal dysfunction. *Biological psychiatry*, *80*(10), 754–764.
- McNaughton, N., & Corr, P. J. (2004). A two-dimensional neuropsychology of defense: Fear/anxiety and defensive distance [Festschrift in Honour of Jeffrey Gray - Issue 1: Anxiety and Neuroticism]. *Neuroscience Biobehavioral Reviews*, *28*(3), 285–305. <https://doi.org/https://doi.org/10.1016/j.neubiorev.2004.03.005>
- Menegas, W., Akiti, K., Amo, R., Uchida, N., & Watabe-Uchida, M. (2018). Dopamine neurons projecting to the posterior striatum reinforce avoidance of threatening stimuli. *Nat Neurosci*, *21*(10), 1421–1430. <https://doi.org/10.1038/s41593-018-0222-1>
- Milad, M. R., & Quirk, G. J. (2002). Neurons in medial prefrontal cortex signal memory for fear extinction. *Nature*, *420*(6911), 70–4. <https://doi.org/10.1038/nature01138>
- Milad, M. R., & Rauch, S. L. (2007). The role of the orbitofrontal cortex in anxiety disorders. *Annals of the New York Academy of Sciences*, *1121*(1), 546–561.
- Miller, E. K. (2000). The prefrontal cortex and cognitive control. *Nature reviews neuroscience*, *1*(1), 59–65.
- Miller, N. (1944). Experimental studies of conflict. In J. M. Hunt (Ed.), *Personality and the behavioral disorders* (pp. 431–465). Ronald Press.
- Mitchell, M. R., Vokes, C. M., Blankenship, A. L., Simon, N. W., & Setlow, B. (2011). Effects of acute administration of nicotine, amphetamine, diazepam, morphine, and ethanol on risky decision-making in rats. *Psychopharmacology*, *218*(4), 703–712.
- Mizoguchi, K., Yuzurihara, M., Ishige, A., Sasaki, H., Chui, D. H., & Tabira, T. (2000). Chronic stress induces impairment of spatial working memory because of prefrontal dopaminergic dysfunction. *J Neurosci*, *20*(4), 1568–74. <https://doi.org/10.1523/jneurosci.20-04-01568.2000>
- Mochcovitch, M. D., da Rocha Freire, R. C., Garcia, R. F., & Nardi, A. E. (2014). A systematic review of fmri studies in generalized anxiety disorder: Evaluating its neural and cognitive basis. *Journal of affective disorders*, *167*, 336–342.

- Moghaddam, B. (1993). Stress preferentially increases extraneuronal levels of excitatory amino acids in the prefrontal cortex: Comparison to hippocampus and basal ganglia. *J Neurochem*, *60*(5), 1650–7. <https://doi.org/10.1111/j.1471-4159.1993.tb13387.x>
- Moghaddam, B., & Homayoun, H. (2008). Divergent plasticity of prefrontal cortex networks. *Neuropsychopharmacology*, *33*(1), 42–55.
- Morilak, D. A., Barrera, G., Echevarria, D. J., Garcia, A. S., Hernandez, A., Ma, S., & Petre, C. O. (2005). Role of brain norepinephrine in the behavioral response to stress. *Prog Neuropsychopharmacol Biol Psychiatry*, *29*(8), 1214–24. <https://doi.org/10.1016/j.pnpbp.2005.08.007>
- Morrow, B. A., Elsworth, J. D., Lee, E. J., & Roth, R. H. (2000). Divergent effects of putative anxiolytics on stress-induced fos expression in the mesoprefrontal system of the rat. *Synapse*, *36*(2), 143–154.
- Moscarello, J. M., & LeDoux, J. E. (2013). Active avoidance learning requires prefrontal suppression of amygdala-mediated defensive reactions. *J Neurosci*, *33*(9), 3815–23. <https://doi.org/10.1523/jneurosci.2596-12.2013>
- Mulder, A. B., Nordquist, R. E., Orgüt, O., & Pennartz, C. M. (2003). Learning-related changes in response patterns of prefrontal neurons during instrumental conditioning. *Behav Brain Res*, *146*(1-2), 77–88. <https://doi.org/10.1016/j.bbr.2003.09.016>
- Murphy, B. L., Arnsten, A. F., Jentsch, J. D., & Roth, R. H. (1996). Dopamine and spatial working memory in rats and monkeys: Pharmacological reversal of stress-induced impairment. *Journal of Neuroscience*, *16*(23), 7768–7775.
- Murphy, M. J., & Deutch, A. Y. (2018). Organization of afferents to the orbitofrontal cortex in the rat. *Journal of Comparative Neurology*, *526*(9), 1498–1526.
- Mychasiuk, R., Muhammad, A., & Kolb, B. (2016). Chronic stress induces persistent changes in global dna methylation and gene expression in the medial prefrontal cortex, orbitofrontal cortex, and hippocampus. *Neuroscience*, *322*, 489–499.
- Naqvi, N., Shiv, B., & Bechara, A. (2006). The role of emotion in decision making: A cognitive neuroscience perspective. *Current directions in psychological science*, *15*(5), 260–264.
- Nichols, D. E. (2016). Psychedelics. *Pharmacological reviews*, *68*(2), 264–355.
- Olson, E. A., Kaiser, R. H., Pizzagalli, D. A., Rauch, S. L., & Rosso, I. M. (2019). Regional prefrontal resting-state functional connectivity in posttraumatic stress disorder. *Biol Psychiatry Cogn Neurosci Neuroimaging*, *4*(4), 390–398. <https://doi.org/10.1016/j.bpsc.2018.09.012>
- Öngür, D., & Price, J. L. (2000). The organization of networks within the orbital and medial prefrontal cortex of rats, monkeys and humans. *Cerebral cortex*, *10*(3), 206–219.
- Orsini, C. A., Heshmati, S. C., Garman, T. S., Wall, S. C., Bizon, J. L., & Setlow, B. (2018). Contributions of medial prefrontal cortex to decision making involving risk of punishment. *Neuropharmacology*, *139*, 205–216. <https://doi.org/10.1016/j.neuropharm.2018.07.018>
- Orsini, C. A., Willis, M. L., Gilbert, R. J., Bizon, J. L., & Setlow, B. (2016). Sex differences in a rat model of risky decision making. *Behav Neurosci*, *130*(1), 50–61. <https://doi.org/10.1037/bne0000111>
- Orsini, C. A., & Setlow, B. (2017). Sex differences in animal models of decision making. *Journal of neuroscience research*, *95*(1-2), 260–269.
- Orsini, C. A., Trotta, R. T., Bizon, J. L., & Setlow, B. (2015). Dissociable roles for the basolateral amygdala and orbitofrontal cortex in decision-making under risk of punishment. *Journal of Neuroscience*, *35*(4), 1368–1379.
- Ostlund, S. B., & Balleine, B. W. (2005). Lesions of medial prefrontal cortex disrupt the acquisition but not the expression of goal-directed learning. *J Neurosci*, *25*(34), 7763–70. <https://doi.org/10.1523/jneurosci.1921-05.2005>

- Ostlund, S. B., & Balleine, B. W. (2007). Orbitofrontal cortex mediates outcome encoding in pavlovian but not instrumental conditioning. *Journal of Neuroscience*, *27*(18), 4819–4825.
- Ostrander, M. M., Richtand, N. M., & Herman, J. P. (2003). Stress and amphetamine induce fos expression in medial prefrontal cortex neurons containing glucocorticoid receptors. *Brain research*, *990*(1-2), 209–214.
- Padilla-Coreano, N., Bolkan, S. S., Pierce, G. M., Blackman, D. R., Hardin, W. D., Garcia-Garcia, A. L., Spellman, T. J., & Gordon, J. A. (2016). Direct ventral hippocampal-prefrontal input is required for anxiety-related neural activity and behavior. *Neuron*, *89*(4), 857–866.
- Padilla-Coreano, N., Canetta, S., Mikofsky, R. M., Alway, E., Passecker, J., Myroshnychenko, M. V., Garcia-Garcia, A. L., Warren, R., Teboul, E., Blackman, D. R., et al. (2019). Hippocampal-prefrontal theta transmission regulates avoidance behavior. *Neuron*, *104*(3), 601–610.
- Pais-Vieira, M., Lima, D., & Galhardo, V. (2007). Orbitofrontal cortex lesions disrupt risk assessment in a novel serial decision-making task for rats. *Neuroscience*, *145*(1), 225–231.
- Panayi, M. C., & Killcross, S. (2018). Functional heterogeneity within the rodent lateral orbitofrontal cortex dissociates outcome devaluation and reversal learning deficits. *Elife*, *7*, e37357.
- Park, J., & Moghaddam, B. (2017a). Impact of anxiety on prefrontal cortex encoding of cognitive flexibility. *Neuroscience*, *345*, 193–202. <https://doi.org/10.1016/j.neuroscience.2016.06.013>
- Park, J., & Moghaddam, B. (2017b). Risk of punishment influences discrete and coordinated encoding of reward-guided actions by prefrontal cortex and vta neurons. *Elife*, *6*. <https://doi.org/10.7554/eLife.30056>
- Park, J., Wood, J., Bondi, C., Del Arco, A., & Moghaddam, B. (2016). Anxiety evokes hypofrontality and disrupts rule-relevant encoding by dorsomedial prefrontal cortex neurons. *J Neurosci*, *36*(11), 3322–35. <https://doi.org/10.1523/jneurosci.4250-15.2016>
- Pascoli, V., Terrier, J., Hiver, A., & Lüscher, C. (2015). Sufficiency of mesolimbic dopamine neuron stimulation for the progression to addiction. *Neuron*, *88*(5), 1054–1066. <https://doi.org/10.1016/j.neuron.2015.10.017>
- Pascoli, V., Hiver, A., Van Zessen, R., Loureiro, M., Achargui, R., Harada, M., Flakowski, J., & Lüscher, C. (2018). Stochastic synaptic plasticity underlying compulsion in a model of addiction. *Nature*, *564*(7736), 366–371.
- Passecker, J., Mikus, N., Malagon-Vina, H., Anner, P., Dimidschstein, J., Fishell, G., Dorffner, G., & Klausberger, T. (2019). Activity of prefrontal neurons predict future choices during gambling. *Neuron*, *101*(1), 152–164.
- Pati, S., Sood, A., Mukhopadhyay, S., & Vaidya, V. A. (2018). Acute pharmacogenetic activation of medial prefrontal cortex excitatory neurons regulates anxiety-like behaviour. *Journal of biosciences*, *43*(1), 85–95.
- Paxinos, G., & Watson, C. (1998). A stereotaxic atlas of the rat brain. *New York: Academic*.
- Pelloux, Y., Everitt, B. J., & Dickinson, A. (2007). Compulsive drug seeking by rats under punishment: Effects of drug taking history. *Psychopharmacology (Berl)*, *194*(1), 127–37. <https://doi.org/10.1007/s00213-007-0805-0>
- Pelloux, Y., Murray, J. E., & Everitt, B. J. (2015). Differential vulnerability to the punishment of cocaine related behaviours: Effects of locus of punishment, cocaine taking history and alternative reinforcer availability. *Psychopharmacology (Berl)*, *232*(1), 125–34. <https://doi.org/10.1007/s00213-014-3648-5>

- Pellow, S., & File, S. E. (1986). Anxiolytic and anxiogenic drug effects on exploratory activity in an elevated plus-maze: A novel test of anxiety in the rat. *Pharmacol Biochem Behav*, *24*(3), 525–9. [https://doi.org/10.1016/0091-3057\(86\)90552-6](https://doi.org/10.1016/0091-3057(86)90552-6)
- Pellow, S., Chopin, P., File, S. E., & Briley, M. (1985). Validation of open: Closed arm entries in an elevated plus-maze as a measure of anxiety in the rat. *Journal of neuroscience methods*, *14*(3), 149–167.
- Peters, J., LaLumiere, R. T., & Kalivas, P. W. (2008). Infralimbic prefrontal cortex is responsible for inhibiting cocaine seeking in extinguished rats. *Journal of Neuroscience*, *28*(23), 6046–6053.
- Pezze, M. A., & Feldon, J. (2004). Mesolimbic dopaminergic pathways in fear conditioning. *Prog Neurobiol*, *74*(5), 301–20. <https://doi.org/10.1016/j.pneurobio.2004.09.004>
- Pickens, C. L., Saddoris, M. P., Gallagher, M., & Holland, P. C. (2005). Orbitofrontal lesions impair use of cue-outcome associations in a devaluation task. *Behavioral neuroscience*, *119*(1), 317.
- Pickens, C. L., Saddoris, M. P., Setlow, B., Gallagher, M., Holland, P. C., & Schoenbaum, G. (2003). Different roles for orbitofrontal cortex and basolateral amygdala in a reinforcer devaluation task. *Journal of Neuroscience*, *23*(35), 11078–11084.
- Pizzagalli, D. A., Oakes, T. R., Fox, A. S., Chung, M. K., Larson, C. L., Abercrombie, H. C., Schaefer, S. M., Benca, R. M., & Davidson, R. J. (2004). Functional but not structural subgenual prefrontal cortex abnormalities in melancholia. *Mol Psychiatry*, *9*(4), 325, 393–405. <https://doi.org/10.1038/sj.mp.4001501>
- Porcelli, A. J., Cruz, D., Wenberg, K., Patterson, M. D., Biswal, B. B., & Rypma, B. (2008). The effects of acute stress on human prefrontal working memory systems. *Physiol Behav*, *95*(3), 282–9. <https://doi.org/10.1016/j.physbeh.2008.04.027>
- Preuss, T. M. (1995). Do rats have prefrontal cortex? the rose-woolsey-akert program reconsidered. *J Cogn Neurosci*, *7*(1), 1–24. <https://doi.org/10.1162/jocn.1995.7.1.1>
- Pringle, A., Warren, M., Gottwald, J., Cowen, P., & Harmer, C. (2016). Cognitive mechanisms of diazepam administration: A healthy volunteer model of emotional processing. *Psychopharmacology*, *233*(12), 2221–2228.
- Quirk, G. J., Russo, G. K., Barron, J. L., & Lebron, K. (2000). The role of ventromedial prefrontal cortex in the recovery of extinguished fear. *J Neurosci*, *20*(16), 6225–31. <https://doi.org/10.1523/jneurosci.20-16-06225.2000>
- Radley, J. J., Rocher, A. B., Miller, M., Janssen, W. G., Liston, C., Hof, P. R., McEwen, B. S., & Morrison, J. H. (2006). Repeated stress induces dendritic spine loss in the rat medial prefrontal cortex. *Cereb Cortex*, *16*(3), 313–20. <https://doi.org/10.1093/cercor/bhi104>
- Ray, M. H., Hanlon, E., & McDannald, M. A. (2018). Lateral orbitofrontal cortex partitions mechanisms for fear regulation and alcohol consumption. *PloS one*, *13*(6), e0198043.
- Resstel, L., Souza, R., & Guimaraes, F. (2008). Anxiolytic-like effects induced by medial prefrontal cortex inhibition in rats submitted to the Vogel conflict test. *Physiology behavior*, *93*(1-2), 200–205.
- Rhodes, S. E., & Murray, E. A. (2013). Differential effects of amygdala, orbital prefrontal cortex, and prelimbic cortex lesions on goal-directed behavior in rhesus macaques. *Journal of Neuroscience*, *33*(8), 3380–3389.
- Richardson, N. R., & Roberts, D. C. (1996). Progressive ratio schedules in drug self-administration studies in rats: A method to evaluate reinforcing efficacy. *Journal of neuroscience methods*, *66*(1), 1–11.
- Rincón-Cortés, M., Gagnon, K. G., Dollish, H. K., & Grace, A. A. (2018). Diazepam reverses increased anxiety-like behavior, social behavior deficit, and dopamine dysregulation following withdrawal from acute amphetamine. *Neuropsychopharmacology*, *43*(12), 2418–2425.

- Roberts, A. C. (2020). Prefrontal regulation of threat-elicited behaviors: A pathway to translation. *Annu Rev Psychol*, *71*, 357–387. <https://doi.org/10.1146/annurev-psych-010419-050905>
- Roberts, A. C., & Clarke, H. F. (2019). Why we need nonhuman primates to study the role of ventromedial prefrontal cortex in the regulation of threat-and reward-elicited responses. *Proceedings of the National Academy of Sciences*, *116*(52), 26297–26304.
- Robinson, O. J., Pike, A. C., Cornwell, B., & Grillon, C. (2019). The translational neural circuitry of anxiety. *Journal of Neurology, Neurosurgery & Psychiatry*, *90*(12), 1353–1360.
- Rodriguez-Romaguera, J., Greenberg, B. D., Rasmussen, S. A., & Quirk, G. J. (2016). An avoidance-based rodent model of exposure with response prevention therapy for obsessive-compulsive disorder. *Biological psychiatry*, *80*(7), 534–540.
- Rose, J. E., & Woolsey, C. N. (1948). Structure and relations of limbic cortex and anterior thalamic nuclei in rabbit and cat. *Journal of Comparative Neurology*, *89*(3), 279–347.
- Rushworth, M. F., & Owen, M., A. (1998). The functional organization of the lateral frontal cortex: Conjecture or conjuncture in the electrophysiology literature? *Trends Cogn Sci*, *2*(2), 46–53. [https://doi.org/10.1016/s1364-6613\(98\)01127-9](https://doi.org/10.1016/s1364-6613(98)01127-9)
- Ryghula, R., Clarke, H. F., Cardinal, R. N., Cockcroft, G. J., Xia, J., Dalley, J. W., Robbins, T. W., & Roberts, A. C. (2015). Role of central serotonin in anticipation of rewarding and punishing outcomes: Effects of selective amygdala or orbitofrontal 5-HT depletion. *Cerebral cortex*, *25*(9), 3064–3076.
- Sarlitto, M. C., Foilb, A. R., & Christianson, J. P. (2018). Inactivation of the ventrolateral orbitofrontal cortex impairs flexible use of safety signals. *Neuroscience*, *379*, 350–358.
- Sartori, S. B., & Singewald, N. (2019). Novel pharmacological targets in drug development for the treatment of anxiety and anxiety-related disorders. *Pharmacology Therapeutics*, *204*, 107402. <https://doi.org/https://doi.org/10.1016/j.pharmthera.2019.107402>
- Schmitz, A., & Grillon, C. (2012). Assessing fear and anxiety in humans using the threat of predictable and unpredictable aversive events (the npu-threat test). *Nat Protoc*, *7*(3), 527–32. <https://doi.org/10.1038/nprot.2012.001>
- Schoenbaum, G., Chiba, A. A., & Gallagher, M. (1998). Orbitofrontal cortex and basolateral amygdala encode expected outcomes during learning. *Nature neuroscience*, *1*(2), 155–159.
- Schoenbaum, G., Nugent, S. L., Saddoris, M. P., & Setlow, B. (2002). Orbitofrontal lesions in rats impair reversal but not acquisition of go, no-go odor discriminations. *Neuroreport*, *13*(6), 885–890.
- Schoenbaum, G., & Roesch, M. (2005). Orbitofrontal cortex, associative learning, and expectancies. *Neuron*, *47*(5), 633–636.
- Schoenbaum, G., Roesch, M. R., Stalnaker, T. A., & Takahashi, Y. K. (2009). A new perspective on the role of the orbitofrontal cortex in adaptive behaviour. *Nature Reviews Neuroscience*, *10*(12), 885–892.
- Schultz, W. (1998). Predictive reward signal of dopamine neurons. *Journal of neurophysiology*, *80*(1), 1–27.
- Schultz, W. (2016). Dopamine reward prediction error coding. *Dialogues in clinical neuroscience*, *18*(1), 23.
- Schwabe, L., & Wolf, O. T. (2011). Stress-induced modulation of instrumental behavior: From goal-directed to habitual control of action. *Behavioural brain research*, *219*(2), 321–328.
- Sebaugh, J., & McCray, P. (2003). Defining the linear portion of a sigmoid-shaped curve: Bend points. *Pharmaceutical Statistics: The Journal of Applied Statistics in the Pharmaceutical Industry*, *2*(3), 167–174.

- Shah, A. A., & Treit, D. (2003). Excitotoxic lesions of the medial prefrontal cortex attenuate fear responses in the elevated-plus maze, social interaction and shock probe burying tests. *Brain research*, *969*(1-2), 183–194.
- Sharpe, M. J., & Killcross, S. (2015). The prelimbic cortex directs attention toward predictive cues during fear learning. *Learning & Memory*, *22*(6), 289–293.
- Sharpe, M. J., & Killcross, S. (2018). Modulation of attention and action in the medial prefrontal cortex of rats. *Psychological review*, *125*(5), 822.
- Shiba, Y., Santangelo, A. M., & Roberts, A. C. (2016). Beyond the medial regions of prefrontal cortex in the regulation of fear and anxiety. *Frontiers in systems neuroscience*, *10*, 12.
- Shih, C.-W., & Chang, C.-h. (2021). Medial or lateral orbitofrontal cortex activation during fear extinction differentially regulates fear renewal. *Behavioural Brain Research*, 113412.
- Shimizu, H., Kumasaka, Y., Tanaka, H., Hirose, A., & Nakamura, M. (1992). Anticonflict action of tandospirone in a modified geller-seifter conflict test in rats. *The Japanese Journal of Pharmacology*, *58*(3), 283–289.
- Sierra-Mercado, D., Padilla-Coreano, N., & Quirk, G. J. (2011). Dissociable roles of prelimbic and infralimbic cortices, ventral hippocampus, and basolateral amygdala in the expression and extinction of conditioned fear. *Neuropsychopharmacology*, *36*(2), 529–38. <https://doi.org/10.1038/npp.2010.184>
- Simon, N. W., Gilbert, R. J., Mayse, J. D., Bizon, J. L., & Setlow, B. (2009). Balancing risk and reward: A rat model of risky decision making. *Neuropsychopharmacology*, *34*(10), 2208–17. <https://doi.org/10.1038/npp.2009.48>
- Simon, N. W., Wood, J., & Moghaddam, B. (2015). Action-outcome relationships are represented differently by medial prefrontal and orbitofrontal cortex neurons during action execution. *J Neurophysiol*, *114*(6), 3374–85. <https://doi.org/10.1152/jn.00884.2015>
- Simon, N. W., Montgomery, K. S., Beas, B. S., Mitchell, M. R., LaSarge, C. L., Mendez, I. A., Banuelos, C., Vokes, C. M., Taylor, A. B., Haberman, R. P., et al. (2011). Dopaminergic modulation of risky decision-making. *Journal of Neuroscience*, *31*(48), 17460–17470.
- Soares, S., Atallah, B. V., & Paton, J. J. (2016). Midbrain dopamine neurons control judgment of time. *Science*, *354*(6317), 1273–1277. <https://doi.org/10.1126/science.aah5234>
- Söderpalm, B., & Engel, J. (1988). Biphasic effects of clonidine on conflict behavior: Involvement of different alpha-adrenoceptors. *Pharmacology Biochemistry and Behavior*, *30*(2), 471–477.
- Sotres-Bayon, F., Sierra-Mercado, D., Pardilla-Delgado, E., & Quirk, G. J. (2012). Gating of fear in prelimbic cortex by hippocampal and amygdala inputs. *Neuron*, *76*(4), 804–812.
- Spellman, T., Svei, M., Kaminsky, J., Manzano-Nieves, G., & Liston, C. (2021). Prefrontal deep projection neurons enable cognitive flexibility via persistent feedback monitoring. *Cell*, *184*(10), 2750–2766.
- St Onge, J. R., & Floresco, S. B. (2010). Prefrontal cortical contribution to risk-based decision making. *Cereb Cortex*, *20*(8), 1816–28. <https://doi.org/10.1093/cercor/bhp250>
- St. Onge, J. R., Abhari, H., & Floresco, S. B. (2011). Dissociable contributions by prefrontal d1 and d2 receptors to risk-based decision making. *Journal of Neuroscience*, *31*(23), 8625–8633.
- St. Onge, J. R., & Floresco, S. B. (2009). Dopaminergic modulation of risk-based decision making. *Neuropsychopharmacology*, *34*(3), 681–697.
- Stalnaker, T. A., Cooch, N. K., & Schoenbaum, G. (2015). What the orbitofrontal cortex does not do. *Nature neuroscience*, *18*(5), 620–627.
- Stefani, M. R., & Moghaddam, B. (2005). Systemic and prefrontal cortical nmda receptor blockade differentially affect discrimination learning and set-shift ability in rats. *Behavioral neuroscience*, *119*(2), 420.

- Stern, C., Do Monte, F., Gazarini, L., Carobrez, A., & Bertoglio, L. (2010). Activity in prelimbic cortex is required for adjusting the anxiety response level during the elevated plus-maze retest. *Neuroscience*, *170*(1), 214–222.
- Stopper, C. M., Green, E. B., & Floresco, S. B. (2014). Selective involvement by the medial orbitofrontal cortex in biasing risky, but not impulsive, choice. *Cerebral cortex*, *24*(1), 154–162.
- Sturman, D. A., & Moghaddam, B. (2011). Reduced neuronal inhibition and coordination of adolescent prefrontal cortex during motivated behavior. *J Neurosci*, *31*(4), 1471–8. <https://doi.org/10.1523/jneurosci.4210-10.2011>
- Sul, J. H., Kim, H., Huh, N., Lee, D., & Jung, M. W. (2010). Distinct roles of rodent orbitofrontal and medial prefrontal cortex in decision making. *Neuron*, *66*(3), 449–460.
- Suzuki, S., Saitoh, A., Ohashi, M., Yamada, M., Oka, J.-I., & Yamada, M. (2016). The infralimbic and prelimbic medial prefrontal cortices have differential functions in the expression of anxiety-like behaviors in mice. *Behavioural Brain Research*, *304*, 120–124.
- Sych, Y., Chernysheva, M., Sumanovski, L. T., & Helmchen, F. (2019). High-density multi-fiber photometry for studying large-scale brain circuit dynamics. *Nature methods*, *16*(6), 553–560.
- Torregrassa, M. M., Quinn, J. J., & Taylor, J. R. (2008). Impulsivity, compulsivity, and habit: The role of orbitofrontal cortex revisited. *Biological psychiatry*, *63*(3), 253–255.
- Totah, N. K., Kim, Y., & Moghaddam, B. (2013). Distinct prestimulus and poststimulus activation of vta neurons correlates with stimulus detection. *Journal of neurophysiology*, *110*(1), 75–85.
- Turner, K. M., Balleine, B. W., & Bradfield, L. A. (2021). Does disrupting the orbitofrontal cortex alter sensitivity to punishment? a potential mechanism of compulsivity. *Behavioral Neuroscience*, *135*(2), 174.
- Twenge, J. M., & Joiner, T. E. (2020). US census bureau-assessed prevalence of anxiety and depressive symptoms in 2019 and during the 2020 covid-19 pandemic. *Depression and anxiety*, *37*(10), 954–956.
- van den Bos, R., Homberg, J., & de Visser, L. (2013). A critical review of sex differences in decision-making tasks: Focus on the iowa gambling task. *Behavioural brain research*, *238*, 95–108.
- van der Kooij, M. A., Hollis, F., Lozano, L., Zalachoras, I., Abad, S., Zanoletti, O., Grosse, J., De Suduiraut, I. G., Canto, C., & Sandi, C. (2018). Diazepam actions in the vta enhance social dominance and mitochondrial function in the nucleus accumbens by activation of dopamine d1 receptors. *Molecular psychiatry*, *23*(3), 569–578.
- Vander Weele, C. M., Siciliano, C. A., Matthews, G. A., Namburi, P., Izadmehr, E. M., Espinel, I. C., Nieh, E. H., Schut, E. H., Padilla-Coreano, N., Burgos-Robles, A., et al. (2018). Dopamine enhances signal-to-noise ratio in cortical-brainstem encoding of aversive stimuli. *Nature*, *563*(7731), 397–401.
- Vanderschuren, L. J., Minnaard, A. M., Smeets, J. A., & Lesscher, H. M. (2017). Punishment models of addictive behavior. *Current opinion in behavioral sciences*, *13*, 77–84.
- Verharen, J. P. H., van den Heuvel, M. W., Luijendijk, M., Vanderschuren, L., & Adan, R. A. H. (2019). Corticolimbic mechanisms of behavioral inhibition under threat of punishment. *J Neurosci*, *39*(22), 4353–4364. <https://doi.org/10.1523/jneurosci.2814-18.2019>
- Verharen, J. P., De Jong, J. W., Roelofs, T. J., Huffels, C. F., Van Zessen, R., Luijendijk, M. C., Hamelink, R., Willuhn, I., Den Ouden, H. E., Van Der Plasse, G., et al. (2018). A neuronal mechanism underlying decision-making deficits during hyperdopaminergic states. *Nature communications*, *9*(1), 1–15.
- Verharen, J. P., den Ouden, H. E., Adan, R. A., & Vanderschuren, L. J. (2020). Modulation of value-based decision making behavior by subregions of the rat prefrontal cortex. *Psychopharmacology*, 1–14.

- Verharen, J. P., Luijendijk, M. C., Vanderschuren, L. J., & Adan, R. A. (2020). Dopaminergic contributions to behavioral control under threat of punishment in rats. *Psychopharmacology*, *237*(6), 1769–1782.
- Vertes, R. P. (2004). Differential projections of the infralimbic and prelimbic cortex in the rat. *Synapse*, *51*(1), 32–58. <https://doi.org/10.1002/syn.10279>
- Vogel, J. R., Beer, B., & Clody, D. E. (1971). A simple and reliable conflict procedure for testing anti-anxiety agents. *Psychopharmacologia*, *21*(1), 1–7. <https://doi.org/10.1007/BF00403989>
- Volkow, N. D., Fowler, J. S., & Wang, G. J. (2003). The addicted human brain: Insights from imaging studies. *J Clin Invest*, *111*(10), 1444–51. <https://doi.org/10.1172/jci18533>
- Wager, T. D., Davidson, M. L., Hughes, B. L., Lindquist, M. A., & Ochsner, K. N. (2008). Prefrontal-subcortical pathways mediating successful emotion regulation. *Neuron*, *59*(6), 1037–1050.
- Walker, D. L., Toufexis, D. J., & Davis, M. (2003). Role of the bed nucleus of the stria terminalis versus the amygdala in fear, stress, and anxiety. *European journal of pharmacology*, *463*(1-3), 199–216.
- Wallis, J. D. (2012). Cross-species studies of orbitofrontal cortex and value-based decision-making. *Nature neuroscience*, *15*(1), 13–19.
- Walton, M. E., Behrens, T. E., Buckley, M. J., Rudebeck, P. H., & Rushworth, M. F. (2010). Separable learning systems in the macaque brain and the role of orbitofrontal cortex in contingent learning. *Neuron*, *65*(6), 927–939.
- Watabe-Uchida, M., Eshel, N., & Uchida, N. (2017). Neural circuitry of reward prediction error [PMID: 28441114]. *Annual Review of Neuroscience*, *40*(1), 373–394. <https://doi.org/10.1146/annurev-neuro-072116-031109>
- Weinshenker, D., & Schroeder, J. P. (2007). There and back again: A tale of norepinephrine and drug addiction. *Neuropsychopharmacology*, *32*(7), 1433–1451.
- Wikenheiser, A. M., Gardner, M. P., Mueller, L. E., & Schoenbaum, G. (2021). Spatial representations in rat orbitofrontal cortex. *Journal of Neuroscience*.
- Winter, J., Rice, K., Amorosi, D., & Rabin, R. (2007). Psilocybin-induced stimulus control in the rat. *Pharmacology Biochemistry and Behavior*, *87*(4), 472–480.
- Wu, T., Kansaku, K., & Hallett, M. (2004). How self-initiated memorized movements become automatic: A functional mri study. *Journal of neurophysiology*, *91*(4), 1690–1698.
- Xu, J., Van Dam, N. T., Feng, C., Luo, Y., Ai, H., Gu, R., & Xu, P. (2019). Anxious brain networks: A coordinate-based activation likelihood estimation meta-analysis of resting-state functional connectivity studies in anxiety. *Neuroscience Biobehavioral Reviews*, *96*, 21–30. <https://doi.org/https://doi.org/10.1016/j.neubiorev.2018.11.005>
- Yuen, E. Y., Wei, J., Liu, W., Zhong, P., Li, X., & Yan, Z. (2012). Repeated stress causes cognitive impairment by suppressing glutamate receptor expression and function in prefrontal cortex. *Neuron*, *73*(5), 962–77. <https://doi.org/10.1016/j.neuron.2011.12.033>
- Zelinski, E. L., Hong, N. S., Tyndall, A. V., Halsall, B., & McDonald, R. J. (2010). Prefrontal cortical contributions during discriminative fear conditioning, extinction, and spontaneous recovery in rats. *Experimental brain research*, *203*(2), 285–297.
- Zimmermann, K. S., Li, C.-c., Rainnie, D. G., Ressler, K. J., & Gourley, S. L. (2018). Memory retention involves the ventrolateral orbitofrontal cortex: Comparison with the basolateral amygdala. *Neuropsychopharmacology*, *43*(2), 373–383.
- Zimmermann, K. S., Yamin, J. A., Rainnie, D. G., Ressler, K. J., & Gourley, S. L. (2017). Connections of the mouse orbitofrontal cortex and regulation of goal-directed action selection by brain-derived neurotrophic factor. *Biological psychiatry*, *81*(4), 366–377.

# Appendix A

## Supplemental Figures

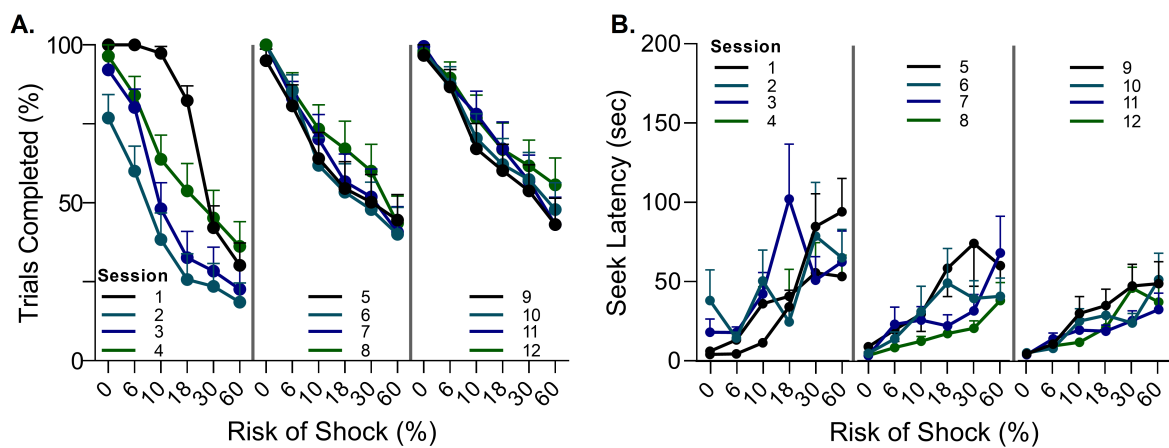


Figure A.1: Demonstration of stable PPT performance over learning. **A.** Decreases in trial completion with risk were initially variable on a day to day basis, but stabilized after about 5 sessions. **B.** Seek latency increases were consistent and were selective to risk blocks after 5 sessions. Line and symbol color indicates session number for each section of the plot. [Back to Chapter 2 results.](#)

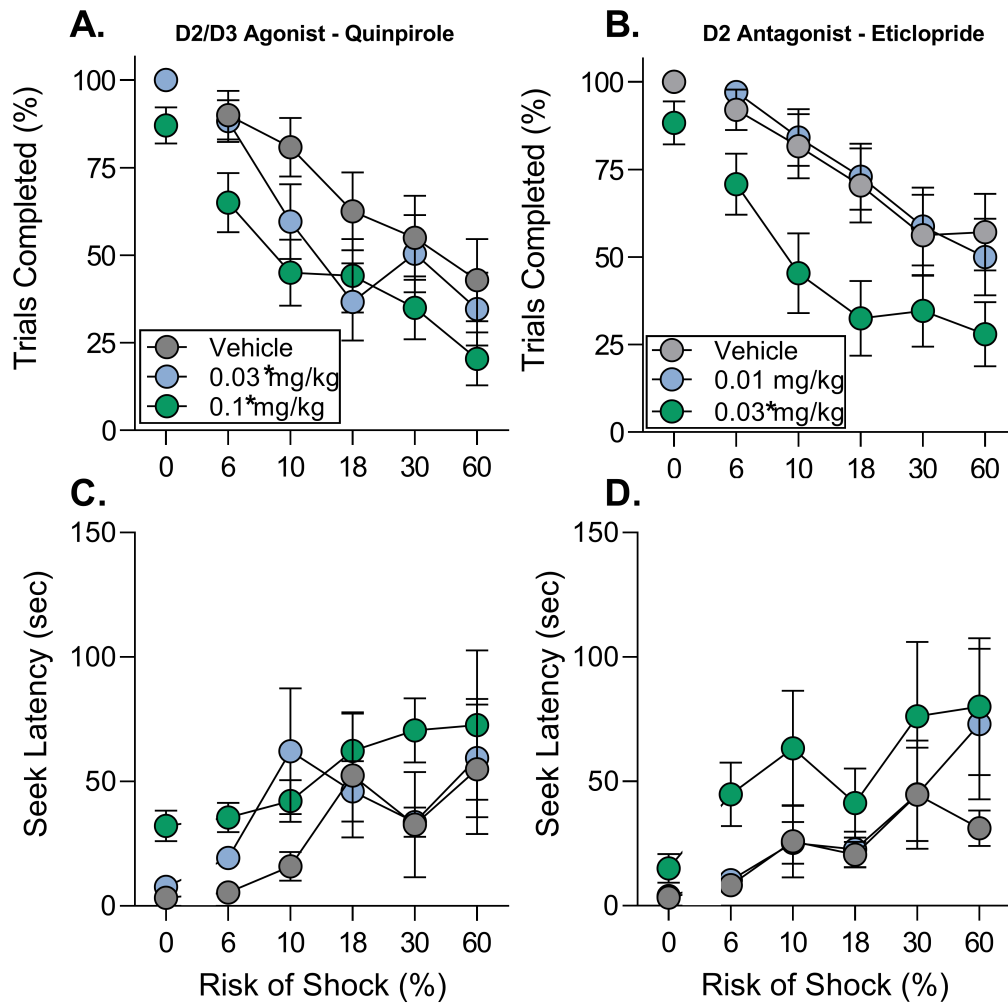


Figure A.2: Dopamine D2 receptor ligands increase punishment sensitivity in the PPT but also produce non-selective effects. **A,C.** Effects of D2/D3 agonist quinpirole on trial completion and seek latency. **B,D.** Effects of D2 antagonist eticlopride on trial completion and seek latency. \*  $p < .05$  vs vehicle. [Back to Chapter 2 results.](#)

## 0.25 mA Shock

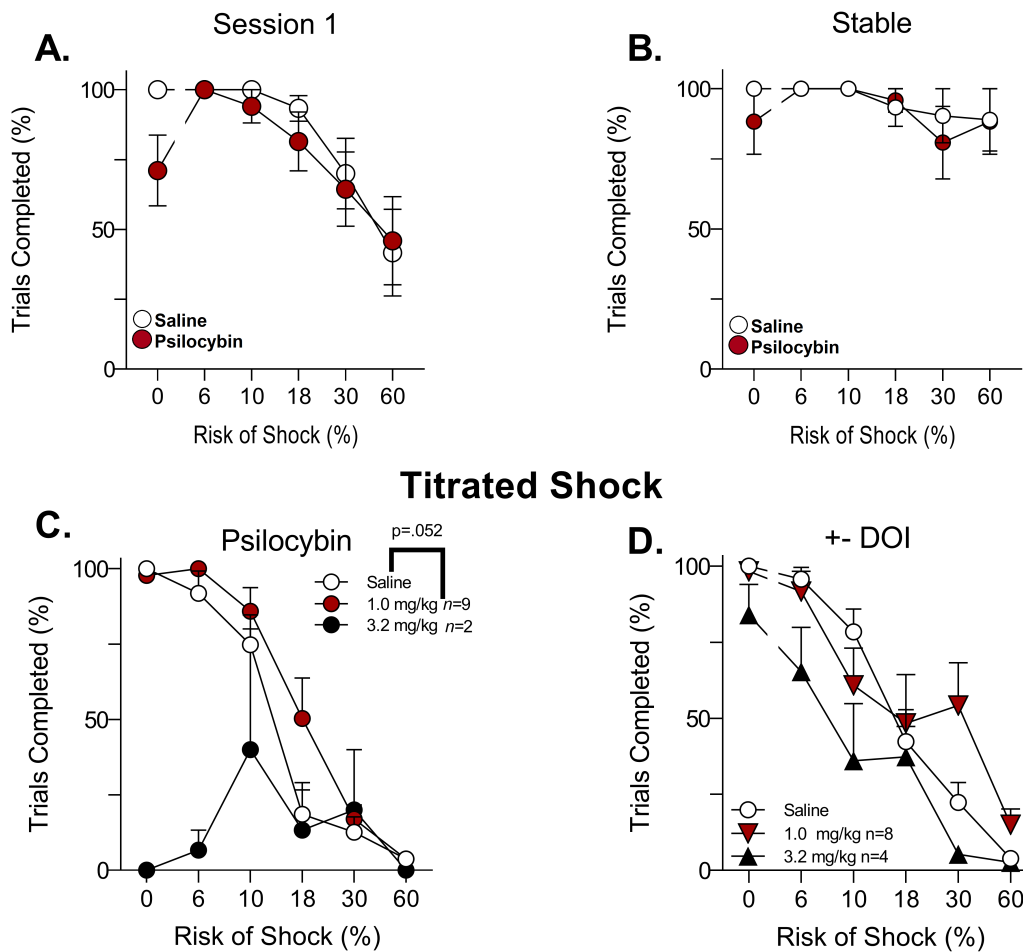


Figure A.3: **A-B.** Psilocybin (1.0 mg/kg; red circles) failed to alter behavior during risk blocks when administered before or after PPT learning at a standard 0.25 mA footshock intensity. **C.** After titrating shock intensity to prevent ceiling effects we observed a modest increase in punishment resistance after psilocybin treatment. Robust behavioral disruption was observed with a 1/2 log unit higher dose. **D.**  $\pm$ -DOI failed to significantly alter PPT behavior at 1 mg/kg and generally disrupted behavior at 3.2 mg/kg. [Back to Chapter 2 results.](#)

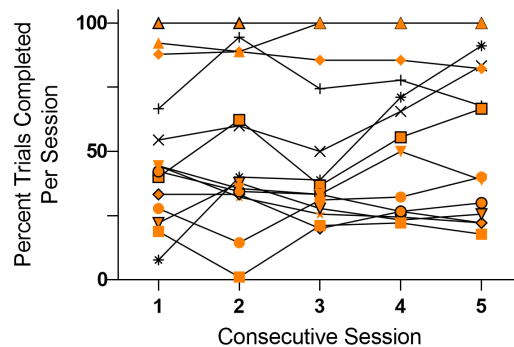


Figure A.4: Female behavior was generally stable over the five stable sessions in the PPT, suggesting behavior did not vary with estrous cycles (4 days). [Back to Chapter 2 results.](#)

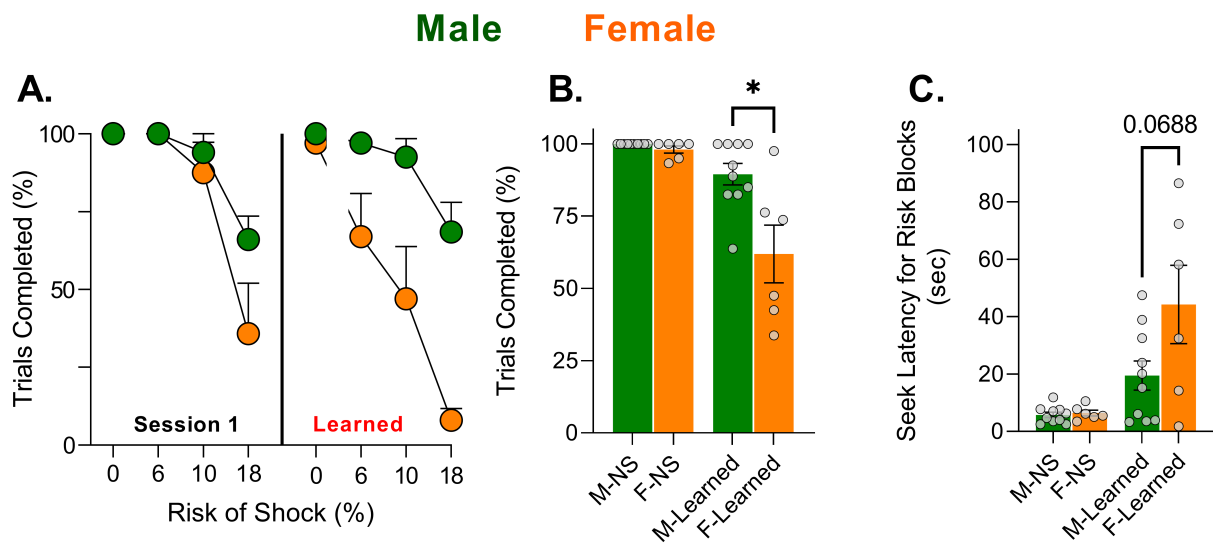


Figure A.5: Sex difference were also observed in the fiber photometry version of the PPT. **A.-B.** Trial completion was similar between males and females in no shock (NS) sessions and session 1. After learning females showed greater decreases in behavior with punishment risk. Averages for NS and learned sessions can be seen in **B.** **C.** Increases in seek latency during risk mirrored sex differences in the full task, but did not reach significance.  $n=6-10/\text{sex}$ , \*  $p<.05$ . M=Male, F=Female. [Back to Chapter 3 results.](#)

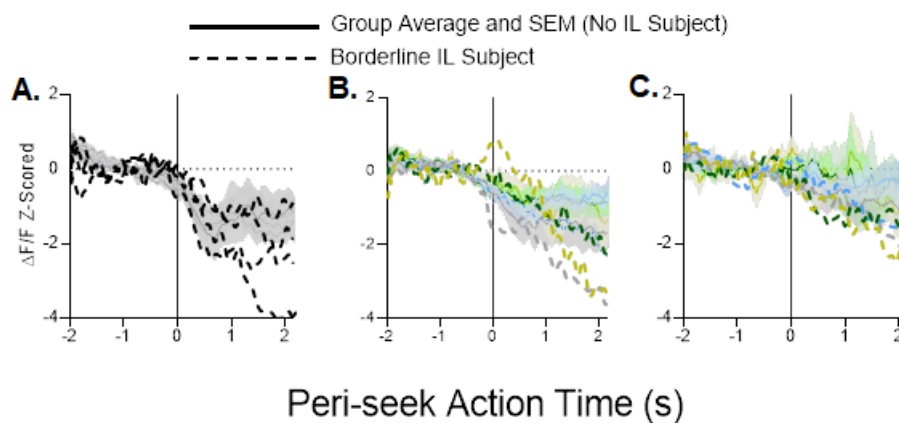


Figure A.6: the rat from PL-mPFC studies in Chapter 3 with borderline IL fiber placement generally showed similar patterns of seek action encoding in the no shock session **A**, session one **B**, and after learning **C**. [Back to Chapter 3 results.](#)

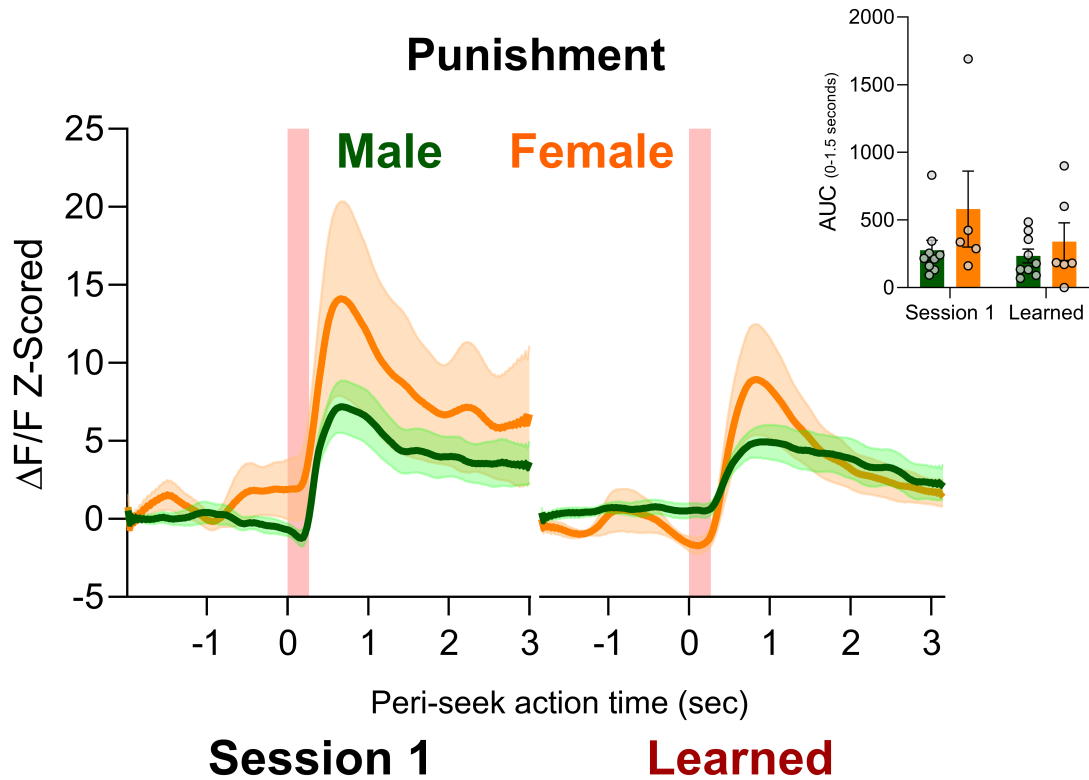


Figure A.7: Both males and females showed robust increases in PL-mPFC neural activity following action contingent footshock (red bar) before (left) and after (right) PPT learning. Inset: AUC calculations for the footshock period (0-1.5 sec after action execution) did not indicate significant differences. [Back to Chapter 3 results.](#)

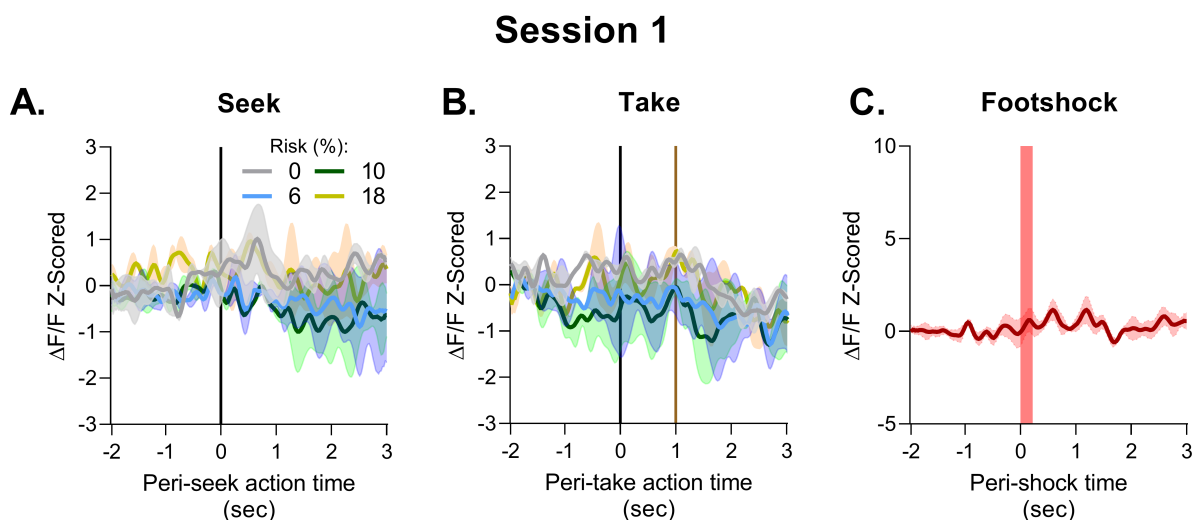


Figure A.8: Recording from GFP only rats during a single PPT session. **A.** Rats with GFP did not show phasic decreases during the seek action for any block. **B-C.** Take action and footshock responsivity were not observed in GFP rats. n=2, red bar= footshock administration. [Back to Chapter 3 results.](#)

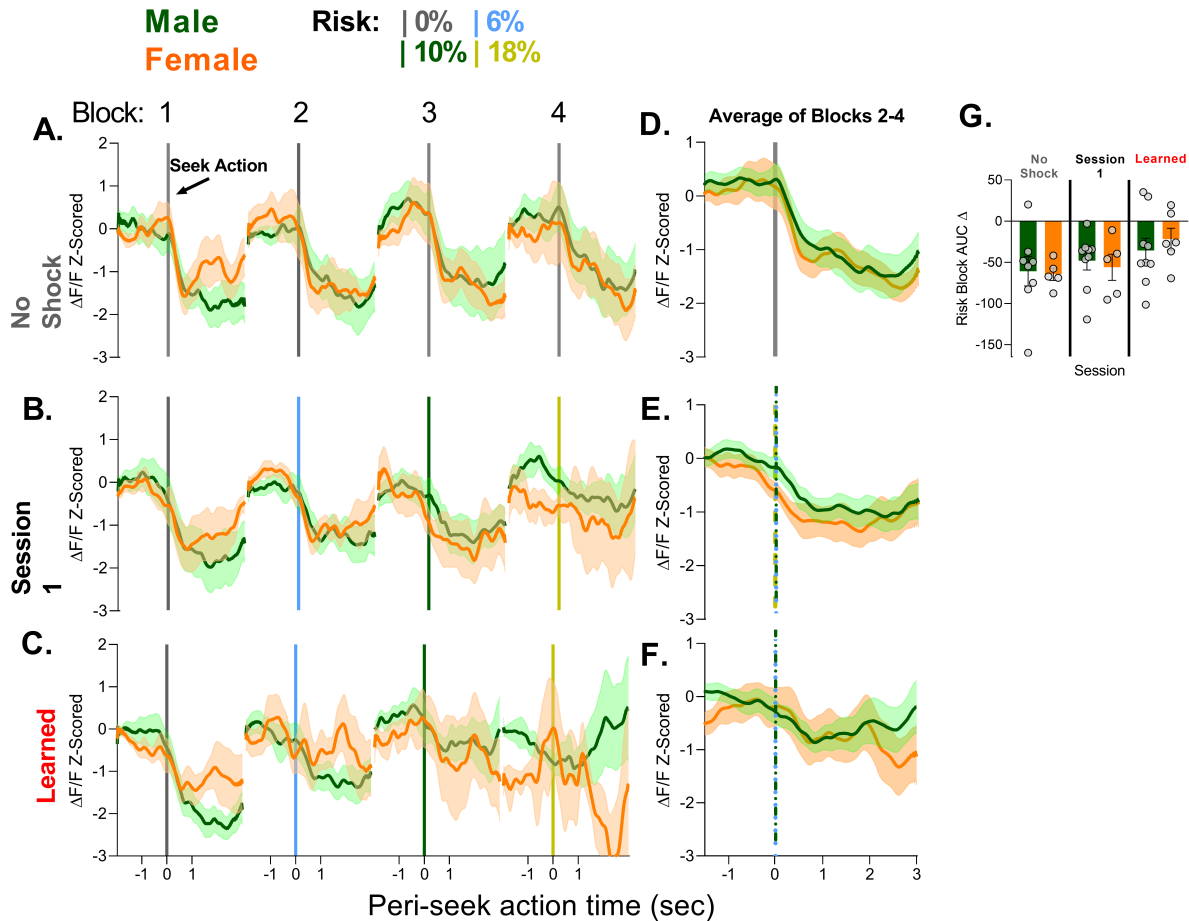


Figure A.9: Sex differences are not seen in PPT PL-mPFC seek action encoding. **A-C.** Both sexes demonstrated an attenuation of the phasic decrease seen during no-shock sessions after task learning. **D-F.** The average of blocks 2-4, i.e. the risk blocks for session 1 and learned demonstrate this difference and the corresponding AUCs are provided in **G**. No significant differences between sexes were detected via paired t-test.  $n=6-9$ -sex, vertical lines=seek action, circles indicate individual subjects. [Back to Chapter 3 results.](#)

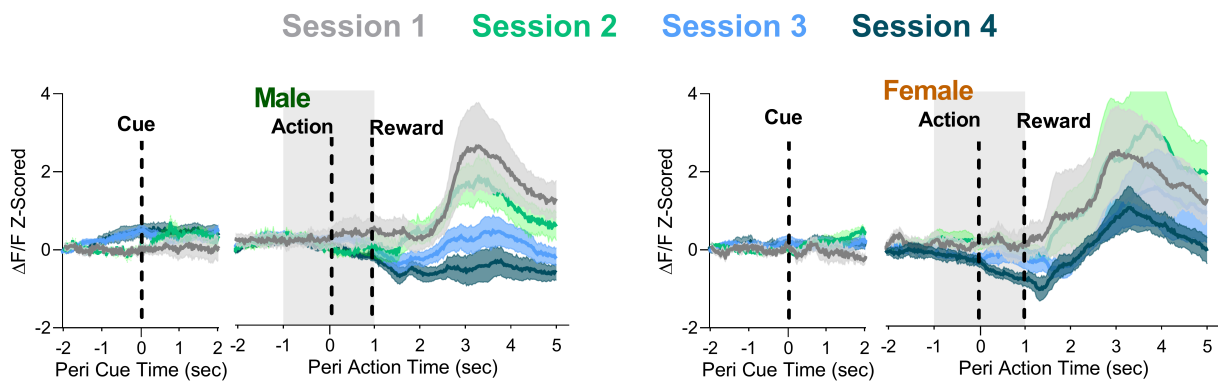


Figure A.10: Both male and female rats demonstrate the emergence of phasic decreases after learning FR1 nosepoke actions with no punishment.  $n=5-8$ /sex. [Back to Chapter 3 results.](#)

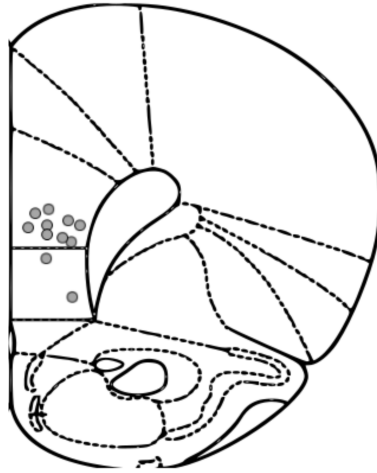


Figure A.11: Location of mPFC fiber placements for FR1 learning studies. Dots reflect the most ventral fiber tip. [Back to Chapter 3 results.](#)

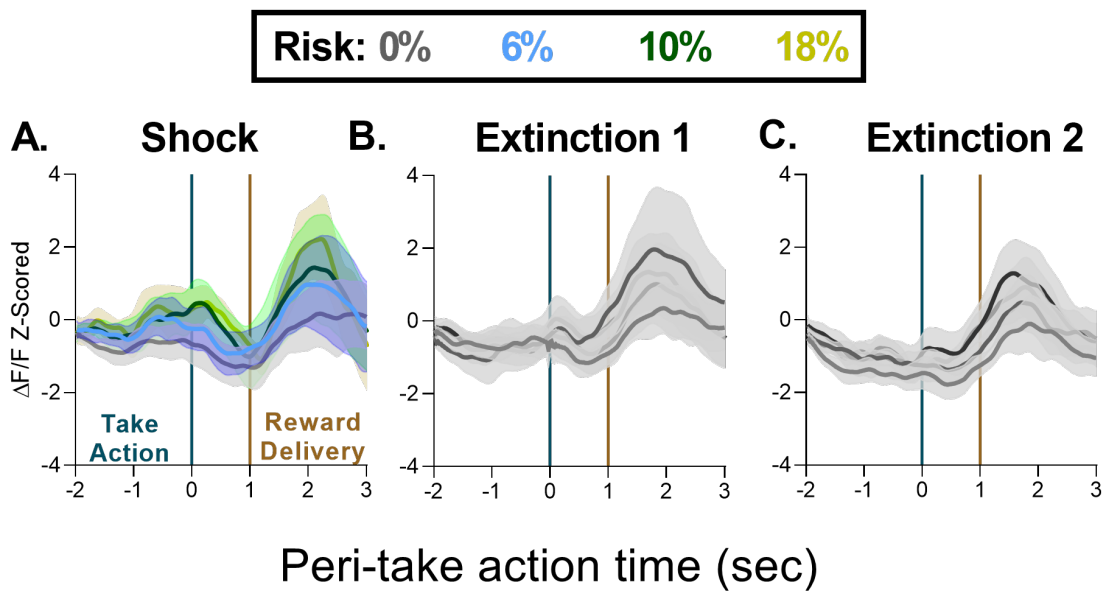


Figure A.12: PL-mPFC activity in the take epoch before and during probabilistic punishment extinction. **A.** No significant risk-block related changes in the safe take action were observed. **B-C.** The same pattern of activity was observed when punishment contingencies were extinguished. Shades of grey indicate different blocks.  $n = 6-8$  rats. [Back to Chapter 3 results.](#)

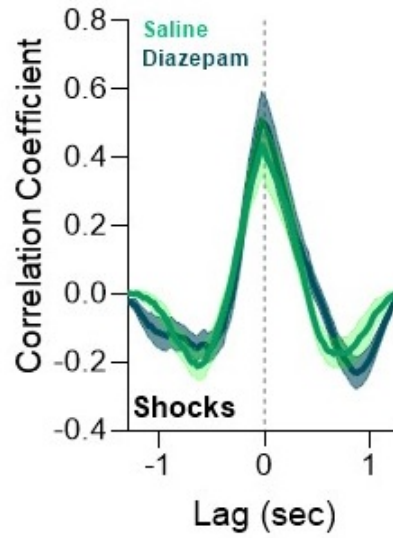


Figure A.13: Diazepam failed to impact positive correlations between the PL-mPFC and VTA during footshock administration. [Back to Chapter 4 results.](#)

Table A.1: Subject Ages through fiber photometry experiments with PPT

Subject(Sex)	Virus Age	Fiber Age	Session 1 Age	Session 5-8 Age	Experiment
S4(F)	25	70	88	97	mPFC
S5(F)	26	97	120	125	mPFC
S14(M)	25	70	88	97	mPFC
S15(M)	26	98	119	123	mPFC
S18(F)	46	99	116	121	mPFC/OFC
S19(F)	50	99	117	122	mPFC/OFC
S20(M)	53	95	117	121	mPFC/OFC
S152(M)	57	95	117	124	mPFC (Excluded)
S3(M)	47	69	89	93	mPFC/OFC
S17(M)	48	69	89	94	mPFC/OFC
S427(M)	61	102	117	121	mPFC/OFC
S428(M)	61	102	117	122	mPFC/OFC
SC41(F)	46	71	87	93	mPFC/OFC
SC42(F)	46	71	86	92	mPFC/OFC
SC41(M)	47	72	86	92	mPFC/OFC
SC42(M)	47	72	86	93	mPFC/OFC
GFP1(M)	50	78	95	102	mPFC (GFP)
GFP2(M)	50	78	95	102	mPFC (GFP)

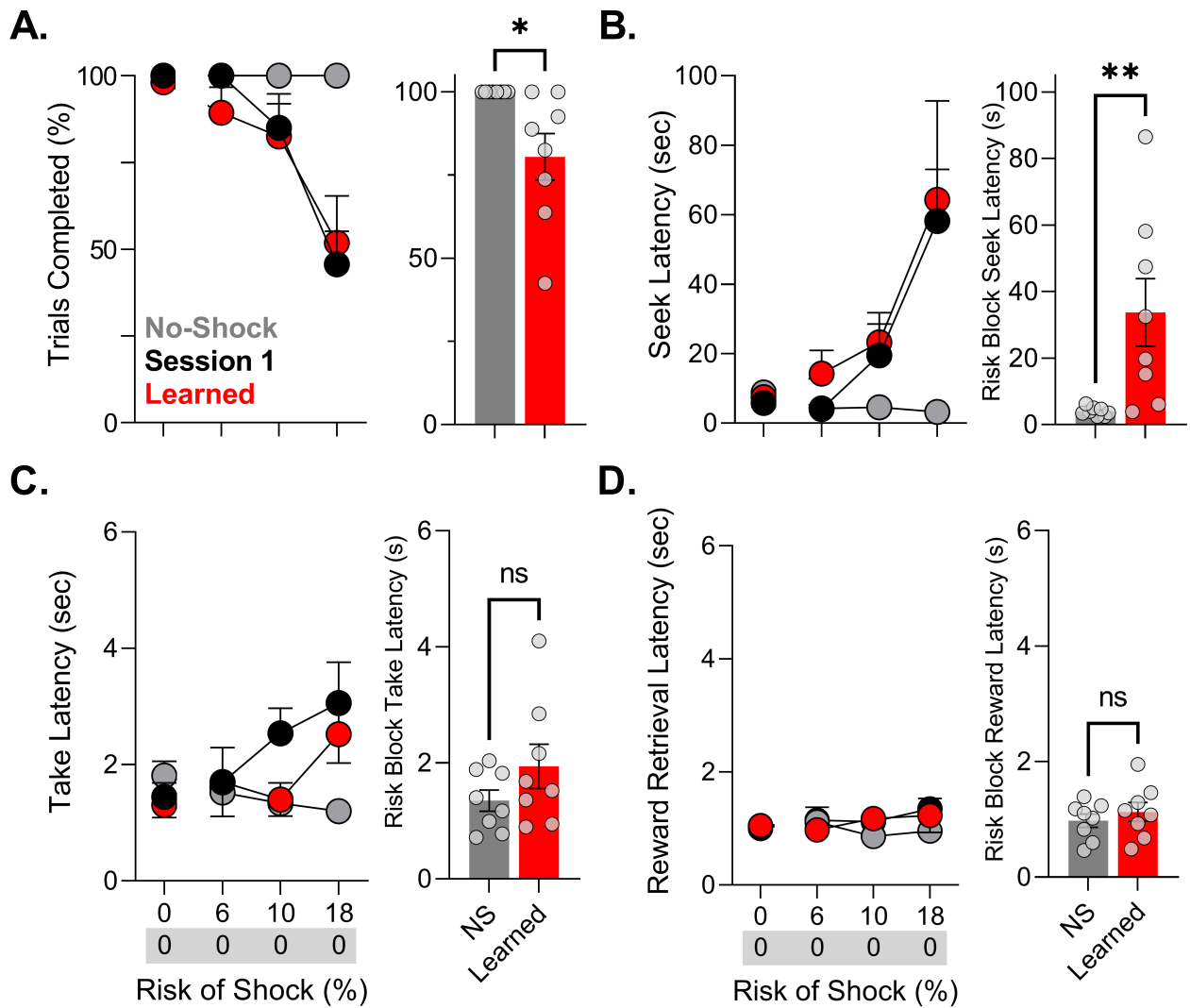


Figure A.14: Patterns of PPT learning in the OFC cohort utilized in Chapter 5 were reflective of the behavior of the all subjects presented in Chapter 3. **A-B.** Risk of shock produced selective suppression of risky actions after 5-8 sessions of learning. **C-D.** Take action and reward retrieval latency did not increase significantly in risk blocks after PPT learning. \*  $p < .05$ , NS= no-shock, ns= not significant,  $n=8$ . [Back to Chapter 5 results.](#)

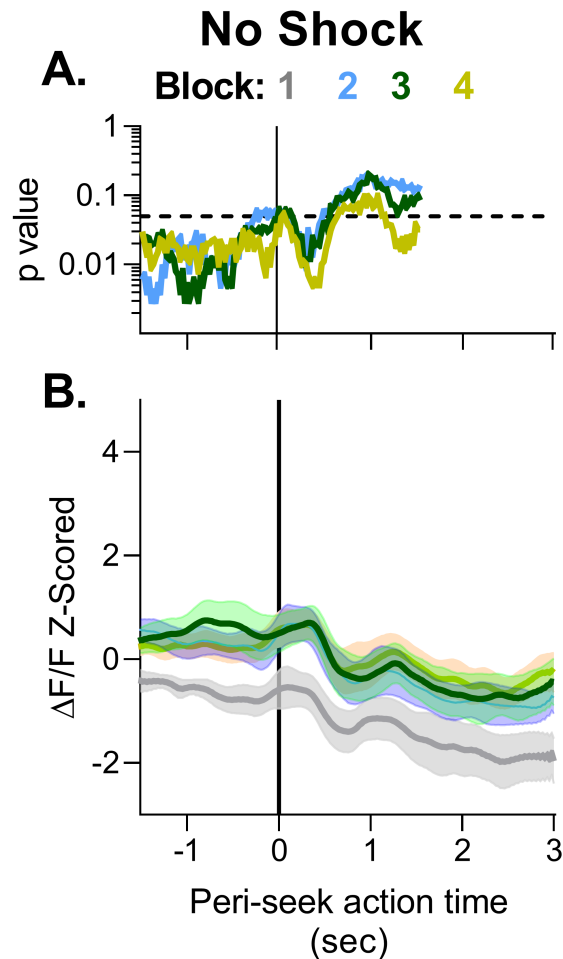


Figure A.15: LO-OFC activity in peri-seek action periods varied significantly with block in no shock sessions. Activity was generally lower in block 1 both before and after action. For this reason we opted to compare PPT sessions to the corresponding block of the no shock session for statistical tests rather than the 0% risk block for the LO-OFC. **A.** Plot of permutation test p-values for the data in **B** color-coded by block number. **B.** Plot of z-scored peri-action activity for the seek action in each block.  $n = 8$  rats. [Back to Chapter 5 results.](#)

Table A.2: Subjects utilized in fiber photometry experiments with FR1 and PRT

Subject(Sex)	Strain	Experiment
263(M)	Long-evans	mPFC
264(M)	Long-evans	mPFC
251(M)	Sprague-dawley	mPFC/VTA
252(M)	Sprague-dawley	mPFC/VTA
256(F)	Sprague-dawley	mPFC/VTA
257(F)	Sprague-dawley	mPFC
282(F)	Sprague-dawley	mPFC
283(F)	Long-evans	mPFC
284(F)	Long-evans	mPFC/VTA
318(M)	Long-evans	mPFC
319(M)	Long-evans	mPFC/VTA
320(M)	Long-evans	mPFC/VTA
321(M)	Long-evans	mPFC

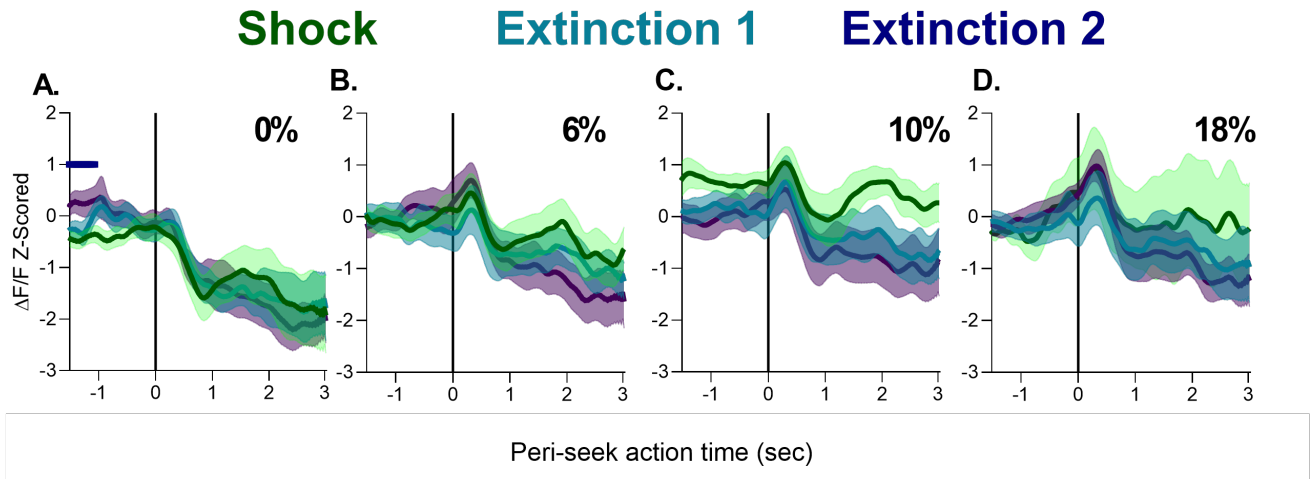


Figure A.16: LO-OFC encoding of the seek action did not change with punishment risk extinction when compared to encoding during the PPT (Shock-green). Solid line is a significant difference between extinction 2 and Shock sessions which was > 1 sec before action. n=6-8. [Back to Chapter 5 results.](#)

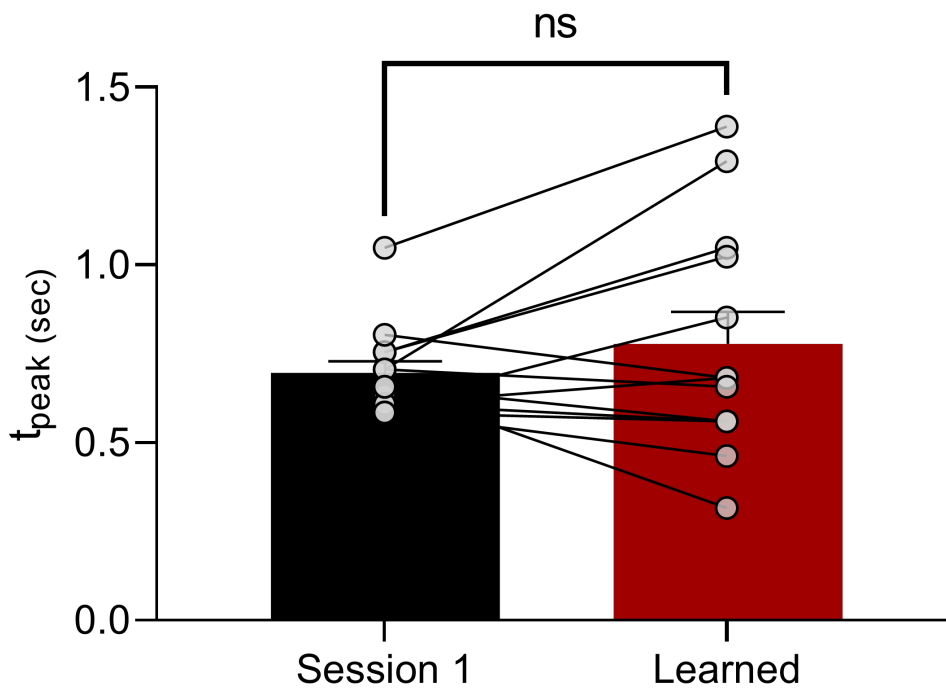


Figure A.17: PL-mPFC time to reach peak does not change with learning. ns=not significant, Wilcoxon test, n=13-14. [Back to Chapter 5 results.](#)

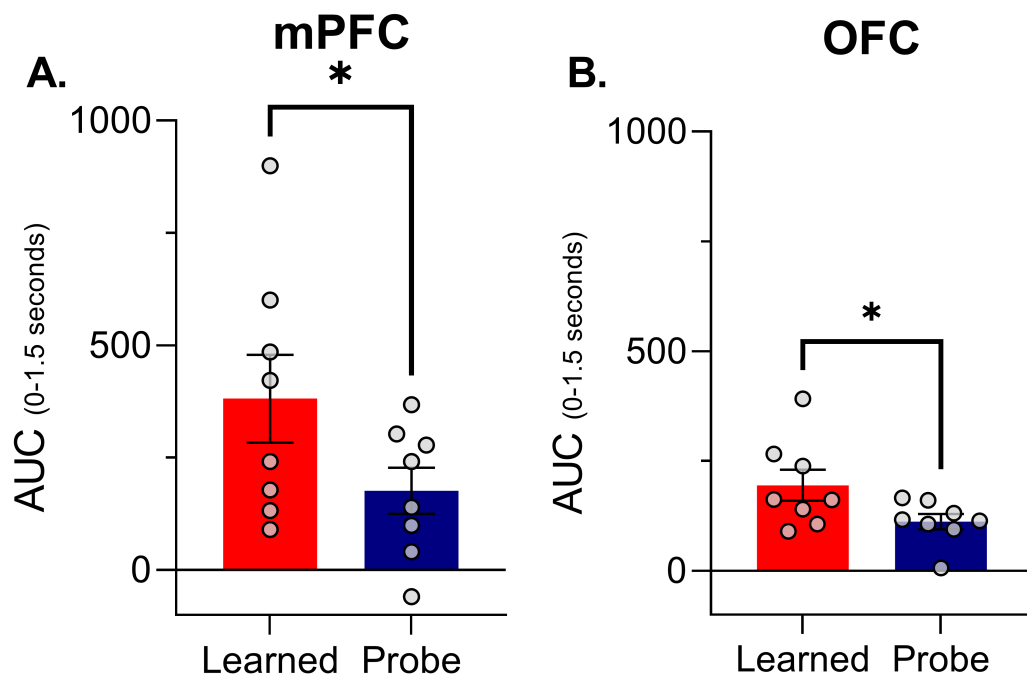
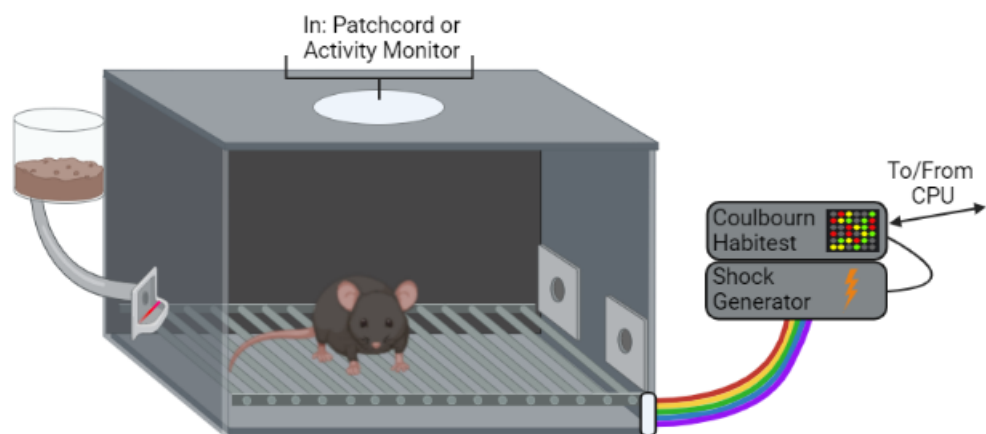


Figure A.18: Response to the footshock was greater following action contingent footshock in the PPT (Learned-red) compared to non-contingent footshock in probe sessions (blue). \* $p < .05$ , paired t-test.  $n=7-8$ . [Back to Chapter 3 results.](#) or [Back to Chapter 5 results.](#)

# Appendix B

## Instrument Setup



Created in [BioRender.com](https://www.biorender.com) 

Figure B.1: Schematic of Operant Box For Behavioral Experiments.

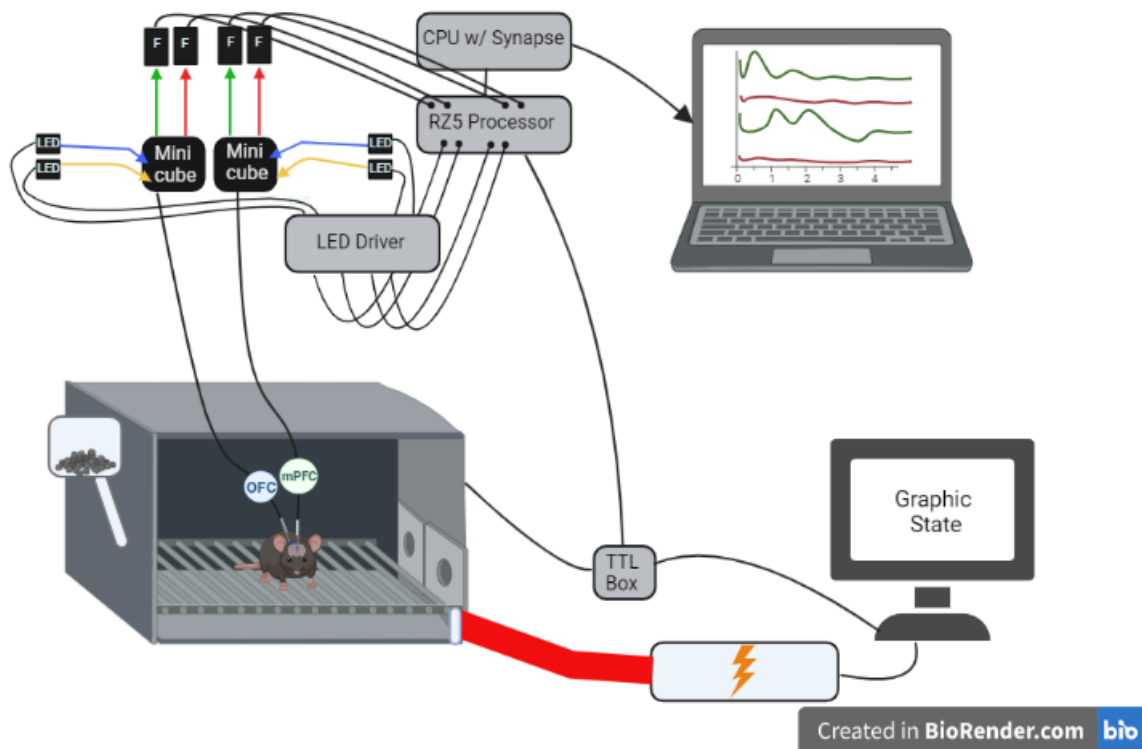


Figure B.2: Schematic of equipment for recording neural activity during operant behavior. Note: NPM system uses similar setup but the operant box is interfaced with an Arduino to timestamp behavioral events and NPM system is interfaced with Bonsai software.

## Software

Much of the software used for this dissertation is free and open source. Code written for analyses is or will be reposted online in GitHub.

### Behavioral and photometry acquisition



By Lopes et al., [2015](#) |Version 2.3.1 |Open Source |For Control Camera Images in Photometry and Arduino Interfacing

### Graphic State

By Coulbourn Instruments |Version 3, 4 |For Control of Coulbourn Habitest Environment

### Synapse

By Tucker-Davis Technologies |Version 90 |For Control and Demodulation of Photometry Signals with RZ5

### Data analysis and Graphing



Open Source Language Run through Anaconda |Version 3+ |For processing, analyzing, and graphing photometry and behavioral data



Open Source Statistics Run through RStudio |Version 4 |For analyzing and graphing photometry data

### Graphpad Prism

By Graphpad |Version 7,8 |For low level analysis, statistics, and graphing

### Dissertation Compilation



Open Source Typesetter |For dissertation compilation

### Code Repository



[Dave Jacobs Personal Repo](#)  
[Moghaddam Lab Repo](#)